NORTHERN ILLINOIS UNIVERSITY

College of Engineering and Engineering Technology

# Senior Design Book

APRIL 23, 2021

# WELCOME!

On behalf of the faculty, staff, and students of Northern Illinois University's College of Engineering and Engineering Technology (CEET), I am extremely delighted to welcome you to our Senior Design Demonstration Day. CEET is hosting this event to recognize the accomplishments of our engineering and engineering technology seniors and to showcase their project demonstrations. This brochure of abstracts represents the design projects they have been working on all year.

The Senior Design Program is the pinnacle learning experience in an engineering student's undergraduate education and represents the hallmark of success for seniors. Under the mentorship of faculty and industry professionals, the Senior Design Program engages students in a meaningful experience by bringing together concepts and principles learned in the engineering curricula, extending theories to practical application, and ultimately culminating in the construction of a prototype and/or process. In this program, an emphasis is placed on learning the design process within the framework of a design team, while a particular focus in the design experience is placed on the creation of products that can be commercialized or put into practical use to improve an industrial process. The experience students gain is comprehensive and reflects all aspects of engineering design and industry practice, including how professionals communicate ideas, how intellectual property impacts day-to-day engineering operations, and how ethics influences engineering decisions. Problem solving for open-ended complex and, sometimes, an incompletely defined system, is the ultimate challenge faced within this experience and, in its a successful completion, the design is often viewed as a student's first professional achievement.

If you have questions about any of our degrees, and/or programs in the College of Engineering and Engineering Technology, please feel free to contact me directly.

Sincerely,

Donald R. Peterson, Ph.D.
Dean and Professor of Mechanical Engineering


NIU

# Project List and Table of Contents


| TEAM# Page # | PROJECT TITLE | STUDENT TEAM | TEACHING ASSISTANT | Faculty Mentor(s) | DEPT(S) | SPONSOR |
|---|---|---|---|---|---|---|
| Tech 1 Page 9 | MTH Leak Detection | Gilbert Bounchaleunsouk, Devin Breske, Nicholas Cascio, Dianiso Dorsey, Levi Hensley | | Charles Ruetsche | Engineering Technology | MTH |
| Tech 2 Page 10 | X-Y Table | Paul Aguada, Wayne Huffman, Jacob Hall, Mark Crisostomo | | William Mills, Kevin Martin | Engineering Technology | Faculty |
| ISYE 1 Page 12 | Paragon Medical: Improving Metrology Calibration Frequency and Traceability | Christopher Aguirre, Jan Gonzalez, Jennifer Oduwole | Marieantoinette Calash | Niechen Chen, Ph.D. and Christine Nguyen, Ph.D. | Industrial and Systems Engineering | Paragon Medical |
| ISYE 2 Page 14 | Maximizing Therapy Order Throughput by Improving a Hospital Scheduling Process | Madalynn Derro, Makenzie Kuzmanic | Marieantoinette Calash | Christine Nguyen, Ph.D. | Industrial and Systems Engineering | Faculty |
| ISYE 3 Page 16 | Minimization of Trucker Idle Time and Transportation Cost in Container Delivery | Krystal Diaz, Alexis Koch, Matt Slouka | Marieantoinette Calash | Christine Nguyen, Ph.D. | Industrial and Systems Engineering | Faculty |
| ISYE 4 Page 18 | Designing a 3D Printed Catalyst Carrier That Maximizes Reaction Yield | Dominque Beck, Moosa Obaidullah, Justin Santiago | Marieantoinette Calash | Niechen Chen, Ph.D. | Industrial and Systems Engineering | Dr. Douglas Klumpp, Department of Chemistry and Biochemistry |
| ISYE 5 Page 20 | Design and Evaluation of Patient Transfer Device | Mohammed Aburmishan, Mohammed Rahat Anwar, Varun Thandy | Marieantoinette Calash | Jaejin Hwang, Ph.D. | Industrial and Systems Engineering | Jaejin Hwang, Ph.D. |
| Int'l Page 22 | AI-Based Camera: Integrated Speech Recognition and Emotion Detection | K. Anupama Satya Sai Lakshmi, Keerthi A. M., Prasanthi V, Sai Dhruthi Varna K, K. Sudarsana Reddy | | Mansour Tahernezhadi | Electrical Engineering | Mansour Tahernezhadi |
| Team 01 Page 24 | Carbon Fiber Monocoque Chassis Redesign | Lauren Marie Bangert, Todd Edward Durham, Matthew Lawrence McCoy | Aayush Patel | Nicholas Pohlman | Mechanical Engineering | Student Proposed |
| Team 02 Page 26 | Novel Audiometer Calibration Device | Papa A Boaheng, Nana Adusei Poku Jr, Nicolas Ivory Rancher | Alex Wills | Mansour Tahernezhadi | Mechanical Engineering, Electrical Engineering | Audiology, CHHS |
| Team 03 Page 28 | Non-Invasive Glucometer to Continuously Monitor Blood Glucose Levels and Alert Abnormalities in Real-Time | Kyle Steven Butle, Dhakshenan Pushparajan, Joaquin Emilio Rodarte | Alex Wills | Venu Korampally | Biomedical Engineering | Student Proposed |
| Team 04 Page 31 | Acoustic Emissions and Phenological Acoustics Monitoring System | Theresa Li, Esteban Molina Hoyos, Charles Henry West | Aayush Patel | Lichuan Liu | Mechanical Engineering, Electric | Morton Arboretum |
| Team 05 Page 34 | Rock Valley Roasters | Luke Patrick Freeman, Andrew Lee Hastings, Ryan Alden Sievert | Sonali Rawat | Ghazi Malkawi | Mechanical Engineering | Student Proposed |

| TEAM #/ Page | PROJECT TITLE | STUDENT TEAM | TEACHING ASSISTANT | Faculty Mentor(s) | DEPT(S) | SPONSOR |
|---|---|---|---|---|---|---|
| Team 06 Page 36 | Adaptive fishing rod and reel for individuals with disabilities | James Lloyd Breithaupt, Juan Daniel Gomez Ayala, Gregory Thomas Perkins | Sonali Rawat | Don Zinger | Electrical Engineering | Student Proposed |
| Team 07 Page 38 | Design of a Pyrolysis System with Temperature and Oxygen Sensors to Recover Liquid Fuel from LDPE | Daniel John Rotta Jr, David N Street, Carson James Wallace | Aayush Patel | John Shelton | Mechanical Engineering | Biological Sciences, CLAS |
| Team 08 Page 40 | Ergonomically Designed Folding Chair to Promote Correct Spinal Alignment | Mark Clifford Boesen Jr, Alejandro Garcia, Anthony Michael Lazzerini | Sonali Rawat | Ghazi Malkawi | Mechanical Engineering | Student Proposed |
| Team 09 Page 42 | Soil Analysis Unit | Matthew Richard Kennett, Clare Frances Keough, Griffin Matthew Schroeder, Hayden James Tillhof | Sonali Rawat | Sachit Butail | Mechanical Engineering, Electrical Engineering | Student Proposed |
| Team 10 Page 44 | Remote Control of Laser Parts | Peter James Coffell, Erick Joseph Koenig, Teofanes Patrick Ruiz | Ian Gilmour | Stanislav Baturin | Mechanical Engineering, Electrical Engineering | ANL |
| Team 11 Page 47 | Miniature, Unnoticeable, Lightweight, Hearing Aid | Selina Cervantes, Pedro Hernandez Jr, Rakshil R Soni | Sandhaya Chapagain | Mohamad Moghimi | Biomedical Engineering, Electrical Engineering | Faculty |
| Team 12 Page 49 | Automated Window System | Kevin Kruse, Brandon Howe, Edward Parker | German Ibarra | Don Zinger | Mechanical Engineering, Electrical Engineering | Student Proposed |
| Team 13 Page 51 | 2 Degree of Freedom Lab Helicopter System | Jonathan Cepeda, Vijaysinh B Rana, Ryan Thomas Tuohy | German Ibarra | Hasan Ferdowsi | Mechanical Engineering, Electrical Engineering | Faculty |
| Team 14 Page 53 | IoT-Based Patient Monitoring Device | Matthew Ryan Baldwin, Tyler Dieter, Matthew Eric Lowe | Alex Wills | Ji-Chul Ryu/Pradip Majumdar | Mechanical Engineering | Faculty |
| Team 15 Page 55 | Self-locomotive Spherical Rolling Robot for Social Interaction | Nicholas P Feliciano, Daniel Patrick O'Dette, Mitch Oliver Wehner | Aayush Patel | Ji-Chul Ryu | Mechanical Engineering | Faculty |
| Team 16 Page 57 | Phase III Electric Vehicle (EV) | Edgar Rolando Rodriguez, Angelica Elizabeth Rodriguez, Leon Seun | Sonali Rawat | Don Zinger | Mechanical Engineering, Electrical Engineering | Faculty |
| Team 17 Page 59 | Wearable Device for Detection of COVID-19 and Tracking Symptoms | Courtney Dinae Bradley, Noelle Ashten Maire, Kyle White | Aayush Patel | Mohamad Moghimi | Biomedical Engineering, Electrical Engineering | Faculty |
| Team 18 Page 61 | Intelligent Square Stepping Exercise Mat | Dominique Husani Johnson, Kristopher Kudla, Neal Devin Tailor | Amin RoostaeeHosseinAbadi | Mansoor Alam | Mechanical Engineering, Electrical Engineering | Kinesiology and Phys. Ed, CED |
| Team 19 Page 63 | Design of a Noninvasive Ventilator Enabled by Non-thermal Plasma for Inactivation of Airborne Viruses | Jabreel Baig, Bhvani Nakum, William Gabriel Schoepke | Sandhaya Chapagain | Eric Monsu Lee | Mechanical Engineering, Electrical Engineering | Faculty |

| TEAM #/Page | PROJECT TITLE | STUDENT TEAM | TEACHING ASSISTANT | Faculty Mentor(s) | DEPT(S) | SPONSOR |
|---|---|---|---|---|---|---|
| Team 20 Page 65 | Industrial Wash Process Six Sigma | Samuel Francis Fisher, Gunnar James Verace, Elijah James Wartgow | Sandhaya Chapagain | Ghazi Malkawi | Mechanical Engineering | Parker Hannifin |
| Team 21 Page 67 | Sewage Sampling for COVID Testing | Omar Antonio Roman-Sanchez, Kevin Michael Simms, Spencer Marcus Simpson | Aayush Patel | John Shelton | Mechanical Engineering | Kishwaukee Water Reclamation District |
| Team 22 Page 69 | Argonne Wakefield Accelerator Laser Phase Feedback Control System Design | Hailah Saleh Aljarboua, Saif M Nasir, Peter Mike Solomon,Ata Urrab | Sonali Rawat | Stanislav Baturin | Electrical Engineering | ANL |
| Team 23 Page 71 | Carbon Dioxide Sensor Array for the ISS | Zahra Abbas, Susanna Margaret Eschbach, Joseph Kenneth Gehant | Alex Wills | Bendito Fonseca | Electrical Engineering | JPL |
| Team 24 Page 73 | Foldable Gantry Crane Project | Deep Ashvin Babaria, Manavkumar Harshadkumar Patel, Dhruv Vijaykumar Thakkar | Ian Gilmour | Ting Xia | Mechanical Engineering | Faculty |
| Team 25 Page 75 | Smart End Effector for 6-DOF robot | Victor H Aguado, Adam Henry Cotton, Jakob Dylan Furgat | Amin RoostaeeHosseinAbadi | YJ Lin | Mechanical Engineering, Electrical Engineering | Faculty |
| Team 26 Page 77 | Remote Piloted Aerial Vehicle for Cenote Water Sampling | Noah James Reid, Jacob Anthony Sampson, Matthew Arthur Sebek | German Ibarra | Sachit Butail | Mechanical Engineering, Electrical Engineering | Environment, Sustainability, and Energy, CLAS |
| Team 27 Page 79 | Wahl Clippers Testing | Zackery Taylor Joy, William John Lee, Michael William Pavlick | German Ibarra | Abul Azad | Mechanical Engineering | Wahl Clipper |
| Team 28 Page 81 | An Energy -Saving Smart Window System | Kevin William Bottorff, Lucas Maxwell Enser, Ivan Gomez | Alex Wills | YJ Lin | Mechanical Engineering, Electrical Engineering | Faculty |
| Team 29 Page 83 | LEGO Bricks Sorting Machine | William Michael Dumoulin, Rachel Mary Dumoulin, Oscar Miguel Ramirez | Amin RoostaeeHosseinAbadi | Veysel Demir | Mechanical Engineering | Faculty |
| Team 30 Page 85 | Ball Nut Ball Bearing Injection System | Stephen Louis Dodd, Shannon Bernadette Duffy, Anthony David Ward | Sandhaya Chapagain | YJ Lin | Mechanical Engineering | Rockford Ball and Screw |
| Team 31 Page 87 | Design of a Human Assisted Robotic Platform for Monitoring Round Goby in Lake Michigan | Robert Werner Heck, Max William Kubale, Hayley Nicole Mellin | Alex Wills | Sachit Butail | Mechanical Engineering | Faculty |
| Team 32 Page 89 | Integration of a NAO robot with an autonomous mobile platform, phase II | Bryce Jacob Papke, Dylan Leon Russom, Adam Bradley Spear | Ian Gilmour | Donald Peterson | Mechanical engineering, Electrical Engineering | Faculty |
| Team 33 Page 91 | Integrated wearable feedback device for human walking | Haley Taylor Hoppe, Nathan Gene Moser, Nathan Jeffery Tom | Sonali Rawat | Mohamad Moghimi | Mechanical Engineering, Electrical Engineering | Kinesiology and Phys. Ed, CED |

| TEAM #/Page | PROJECT TITLE | STUDENT TEAM | TEACHING ASSISTANT | Faculty Mentor(s) | DEPT(S) | SPONSOR |
|---|---|---|---|---|---|---|
| Team 34<br><br>Page 96 | CNC Handheld Operator Station | Kenneth Allen Braswell, Tserendemberel Gantulga, Eucario Raul Matos Sulbaran | Alex Wills | Niechen Chen | Mechanical Engineering, Electrical Engineering | Bourn & Koch |
| Team 35 Page 100 | Design of Berimbau Instrument | Michael Joseph Abukhader, Matthew J Hasto, Clayton Lee Smith | German Ibarra | Hasan Ferdowsi | Mechanical Engineering | Percussion Studies, CVPA |
| Team 36 age 102 | Design of a Human Assisted Robotic Platform for Automated Sampling Waterflea Population in Nearshore Regions | Sarah Nichole Kenkel, Leonardo Lopez Jr, Dakota James Rivard | Alex Wills | Sachit Butail | Mechanical Engineering, Electrical Engineering | Faculty |
| Team 37 age 105 | A Wearable Wireless Video/Audio Recording System for Livestreaming Undergraduate Engineering Labs | Harsh Satishkumar Gandhi, Alec Bernard Krabbe, Jacob Michael Witecha | Amin RoostaeeHosseinAbadi | Venu Korampally | Electrical Engineering | Faculty |
| Team 38 Page 107 | Noninvasive, Wireless Chargers for Implantable Devices and Epidermal Electronics ms | Natalia Dmitruk, James Raymond Jersey, Karla Esmeralda Perez Lopez | Aayush Patel | Mohamad Moghimi | Biomedical Engineering, Electrical Engineering | Faculty |
| Team 39 Page 109 | PLC-Based Vibration Signature Analysis | Dexter Dixon Kling, Riley Edward Plock, Ryan Shaw | Ian Gilmour | Donald Peterson | Mechanical Engineering | Omron |
| Team 40 Page 112 | Automated Edge Rounding of Steel Sheets | Noah Campbell Adams, Blake Charles Buccola, Zachary David McNamara | Ian Gilmour | Jenn-Terng Gau | Mechanical Engineering | CST Industries |
| Team 41 Page 114 | Fluid Powered Vehicle Challenge | Pawel Andrzej Jakubczyk, Joshua Michael Rogers, Thomas Patrick Stewart | Sandhaya Chapagain | Dr Ghazi Malkawi | Mechanical Engineering | Faculty |
| Team 42 Page 116 | Candy Worx Belt Coater Automated Belt Cleaner | Robert Eric Ciavarella, Timothy Patrick Cullinan, Christopher Edward Schmidt | Amin RoostaeeHosseinAbadi | Bobby Sinko | Mechanical Engineering | Candy Worx |
| Team 43 Page 118 | Spell Vision (Ver 2) | Nicholas Jackson Emerson, Carlos Maldonado, Ethan Charles Taylor | Ian Gilmour | Ting Xia | Electrical Engineering | Faculty |
| Team 44 Page 120 | Photography System for Persons with Physical Differences | Daniel Avila, Daisy Hernandez, Malak Zayed | German Ibarra | Ting Xia | Mechanical Engineering, Electrical Engineering | Art and Design Education, CVPA |
| Team 45 Page 123 | Drone Enabled Sensing & Monitering of Tree Canopies | Justin Christopher Holder, Elijah Paul Kues, Colhane William Peterson | German Ibarra | Sachit Butail | Mechanical Engineering, | Morton Arboretum |
| Team 46 Page 125 | Design of the Phase-Change Induced Active Cooling (PCIAC) Systems for Efficient Thermal Management of Battery Systems for the Electrical Vechicle Applications | Abbas Alaidroos, Scott M Chavez, Daniel Skurski | Alex Wills | Kyu Taek Cho | Mechanical Engineering | Faculty |

| TEAM #/Page | PROJECT TITLE | STUDENT TEAM | TEACHING ASSISTANT | Faculty Mentor(s) | DEPT(S) | SPONSOR |
|---|---|---|---|---|---|---|
| Team 47 Page 127 | Fluid Powered Vehicle Challenge | Jason Alan Fidder, Trey Paul Fry, Grant Alan Heckel | Sandhaya Chapagain | Dr Ghazi Malkawi | Mechanical Engineering | Faculty |
| Team 48 Page 129 | Battery Storage Stack Design with an Intelligent IoT-based Active Cooling System | Eric Charles Holmes, Iris Starbuck Johnson, Nolan J Magsamen | Amin RoostaeeHosseinAbadi | Pradip Majumdar | Mechanical Engineering, Electrical Engineering | Faculty |
| Team 49 Page 131 | Design of Warm Units For PIP-II Linac | Kyle Riley Kendziora, Antonio Silva, Mindi Carol Zimmerman | Sandhaya Chapagain | Nicholas Pohlman | Mechanical Engineering | Student Proposed |
| Team 50 Page 133 | Query-by-Humming | David Mark Goldberg, Benjamin Peter Leonard, Nathan Douglas McDonald | Sandhaya Chapagain | Dr Bendito Fonseca | Electrical Engineering | Faculty |
| Team 51 Page 135 | Mechanical Forging for the Construction of a Standardized Steelpan Instrument | Gabriel Gandara, Nicholas Grimes, Josefina Buan | Aayush Patel Patel | Jenn-Terng Gau | Mechanical Engineering, Electrical Engineering | CSA Steelband, CVPA |
| Team 52 Page 137 | Robotic Human Nose Simulator | Jacob Taylor Martinez, Joseph Anthony Panzica, James Casey Vonderhaar | Ian Gilmour | Donald Peterson/Angela Dixon | Biomedical Engineering, Mechanical Engineering | Faculty |
| Team 53 Page 139 | Active Noise Control For Automobiles | Raul V Hernandez Guzman, Ed Atkinson Mims, Fernando Angel Olmedo | German Ibarra | Lichuan Liu | Mechanical Engineering | Faculty |
| Team 54 Page 141 | Cost Effective Bead Resin Unloader | Israel Lopez Lazaro, Michael Rizzo, Andrew James Rowe | Sonali Rawat | Bobby Sinko | Mechanical Engineering | Student Proposed |
| Team 55 Page 143 | Brain Impact Sensor | James Arnold Carratt III, Yeshua Y Chacha Gonzalez, Mackenzie Ray Little | German Ibarra | Venu Korampally | Biomedical Engineering, Mechanical Engineering | Pizur Financial Group |
| Team 56 Page 145 | Precise Temperature Control of a Laser Room at the Argonne Wakefield Accelerator | Cornelio Ibarra Jr, Merrick Edward McNames, Konnor Drake Parrish | Amin | Stanislav Baturin | Electrical Engineering | ANL |
| Team 57 Page 147 | SecuriBot: Low-Cost Autonomous Sentinel Robot | Michael Ronald Brons, Jerrel C Grays, Daniel Craig Ingalsbe | Ian Gilmour | Donald Peterson | Mechanical Engineering, Electrical Engineering | Donald Peterson |
| Team 58 Page 149 | Device for High Strain Rate Deformation Research and Experiments | Lee Russell Bowen, Joshua Tyler Clark, Joie Marie Vittetow | Aayush Patel | Jenn-Terng Gau | Mechanical Engineering | Faculty |
| Team 59 Pg151 | Autonomous Vehicle with Automatic Lane Following | Antaruo Mama, Meng Fan Shi, Liam John Soraghan | Ian Gilmour | Hasan Ferdowsi | Mechanical Engineering | Faculty |
| Team 60 Page 153 | Low Friction Feeder of Enhanced Specular Reflector Material for CMS Detector | Anthony Edward Antoine, Brandyn Alexander Jay, Joshua Song | Amin RoostaeeHosseinAbadi | Nicholas Pohlman/Iman Salehinia | Mechanical Engineering, Electrical Engineering | Faculty |
| Team 61 Page 155 | Development of a Heart Rate Monitoring System (Part II) | Teef Saad Alobaidan, Jordan Reshad Drumgoole, Jonathan Fajardo Schrum, Zachary Christopher Wagner | Sandhaya Chapagain | Lichuan Liu | Mechanical Engineering | Faculty |

MTH Leak detection Team

Tech 478

4/19/2021

## Abstract

**MTH Pumps** is a commercial and industrial pump manufacturer based in Plano, IL. Our Senior design group was tasked with improving a leak detection system for pump housings for MTH Pumps. Their current system is inefficient and unreliable.

Some components for our project were provided by MTH while others needed to be sourced by our group. All materials were funded by MTH.

Our group's design demonstrates a proof of concept which utilizes a Decay type leak detection system. We paired this new testing method with PLC automation and pneumatic control. Additionally, our revised system provides a quantifiable result as well as simple LED light indicators. Lastly, we verified the accuracy of the testing procedure by monitoring the results of known passing and failing parts provided by MTH pumps.

Our system, when compared to the current, will more efficiently identify leaks and limit operator interaction, therefore reducing waste in the workplace.

# *Vertical Farm Automatic X-Y Table*

Jacob Hall, Wayne Huffman, Mark Crisostomo, and Paul Aguda
Northern Illinois University, College of Engineering and Engineering Technology,
Department of Engineering Technology
Still Gym 203
DeKalb, IL 60115

***Abstract*— Vertical farms help feed the growing global population and undo the environmental damage caused by conventional agriculture [1]. While there are many benefits from vertical farming, it is vital to ensure that vertical farms enable food production in a safe, efficient, and clean way. The Engineering Technology building (Still Gym) at Northern Illinois University holds a vertical farm in their BEEEAM (Building, Energy, Efficiency, Ergonomics, and Management) Lab. To ensure that each plant at the NIU vertical farm is healthy, a Raspberry Pi controlled X-Y positioning table will be integrated within the existing vertical farm. The X-Y table will have the ability to traverse the 2ft by 4ft area (growing tub area) using belt-driven movement. The table will contain specific sensors used to collect data from microgreens grown.**

## I. Introduction

Vertical farming is experiencing a growth in interest due to many factors including the reduction of useable agricultural space and the ability to set up farms in smaller areas. In the NIU BEEAM Lab, the vertical farm grow tables have seen many advancements in recent years, however, due to COVID-19, some of the processes were automated [1]. It was determined that automated measuring and scanning capabilities were also needed.

### *Impacts of an Automated measuring system*

Having an automated system in place will allow the user to run scans with a wide variety of cameras and sensors across the entire table. Right now, these scans are being done by hand. The goal of automation is to run scans along with the lighting cycles, which are already automated.

## II. Components and Functions

### *Device Functions*

The XY table will have two primary modes. The main use will be a continuous scan on a pre-determined path across the grow tubs below. The other will be a point scan, where the user will input a specific point and the table will move to that location.

### *Electrical Components*

- NEMA 17 Stepper Motor
- TB6560 3A Motor Controller
- 1.4 GHz 63-bit quad core Raspberry Pi 3B+
- Hinge Roller Lever Micro Switches 3 Pins
- Plastic Enclosure

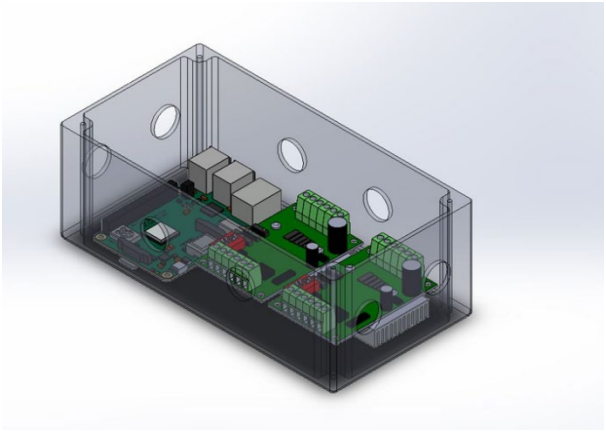

Figure 1 Enclosure with Raspberry Pi and motor Controllers

The image above is a representation of what the enclosure would look like with the Raspberry Pi (RPi) and stepper motor controllers inside of it. The RPi will send a signal to the motor controllers using the GPIO pins. This will enable the controllers to send the appropriate amperage to the stepper motors to move the table. Figure 2 below outlines the wiring of the electrical components.

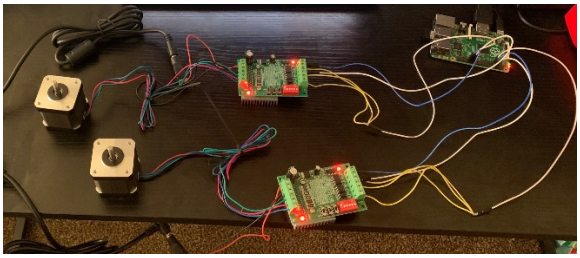

Figure 2 Wiring of electrical components

### *Structural Components*

- 8020 Aluminum Extrude
- Sleeve Bearing
- Timing Belt
- Sensor Mount

The table was designed using the H-bot belt design [3]. Using the single belt approach reduced the footprint of the moving components because both motors were fixed on the ends of the suspended rails. A rendering of this can be seen in figure 3.

Figure 3 XY table with belt and rack mounts

## III.

## IV. Metrics and Equations

For the table to move properly, the minimum torque required was calculated using equations from Oriental Motor. These calculations are seen here:

*Torque Calculations* [2]

$$T_L = \frac{F}{2\pi\eta} \times \frac{\pi D}{i} = \frac{FD}{2\eta i}$$

$$T_L = \frac{31.392N * 0.162m}{2 * 0.93 * 1}$$

$$T_L = 0.273Nm$$

η = efficiency of belt
μ = Coefficient of friction
$i$ = gear ratio
$F$ = Force
$F_A$ = Applied Force
$D$ = Diameter of pulley
$T_L$ = Torque load
$m$ = Mass of moving parts
$g$ = Gravity

$$F = F_A + mg(sin\theta + \mu cos\theta)$$

$$F = 0N + 10kg * 9.81m/s^2(sin0 + 0.32cos0)$$

$$F = 31.392N$$

*Results*

From these calculations, the motor selected was the NEMA 17 Stepper Motor. The specific motor chosen is 0.44 N*m each. Having two motors to move one belt nets a total torque applied of 0.88 N*m, roughly 3 times the minimum torque required. The motor takes 400 steps to complete one revolution (0.9° step angle). The circumference of each pulley is 50.89mm, or about 2 inches. Each step will move the table approximately 1/200 inches. This will keep the table accurate and ensure repeatability when carrying the various sensors.

## V. Conclusions

Creating an easy to assemble XY table will allow the BEEAM Lab vertical farm to add in automated sensing and scanning of the plants. The exact sensors being used are currently being researched by another team. Future improvements identified include adding various safety features. These include end caps on the end of the extruded aluminum. Also, there is potential to flip the assembly to point up, and with proper code adjustments and a z-axis, the table can act as a goniophotometer to measure the lighting in the system at any point within the grow tubs in the farm [4].

*Figures*

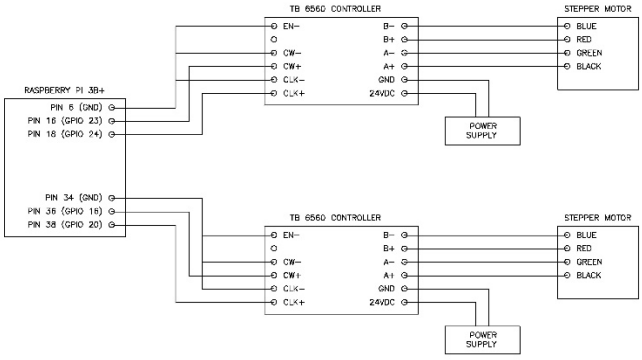


Figure 4 Wiring Schematic


## Acknowledgments

Dr. Kevin Martin
Dr. Theodore Hogan
Dr. William Mills


## References


[1] Cuevas, Brandon, Thomas O'Donnell, and Alex Koenen. "Indoor Vertical Farming." Northern Illinois University, 2019. Print.

[2] Belt Actuator Sizing Tool. www.orientalmotor.com/motor-sizing/beltActuator-sizing.html.

[3] Sollmann, Klaus, Musa Jouaneh, and David Lavender. "Dynamic Modeling of a Two Axes, Parallel, H-Frame Type Xy-Positioning System." IEEE/ASME Transactions on Mechatronics 15 (2010): 11. Print.

[4] Merriam-Webster. (n.d.). Goniophotometer. In Merriam-Webster.com dictionary. Retrieved April 7, 2021, from https://www.merriam-webster.com/dictionary/goniophotometer

[5] Hall, J., Huffman, W., Crisostomo, M., & Aguada, P. (2021). *X-Y Table* Northern Illinois University

# Improving Metrology Calibration Frequency and Traceability

Jan W. Gonzalez, Jennifer Oduwole, Chrisopher Aguirre
Department of Industrial and Systems Engineering
Northern Illinois University
Dekalb, IL USA

***Abstract* — For this project, Paragon Medical, a medical component manufacturer in Bloomindale, Illinois, reached out to Northern Illinois for a team of students to assist in improving the Q/C and Metrology department gage calibration frequency and traceability. The team conducted reliability analysis to determine whether 250 tool uses before validation of gages is sustainable and can be revised to a data driven value to minimize calibrations conducted daily. Concurrently times studies and various 5S+1 audits were conducted in order to improve standardization of set ups for in process inspections of various parts made by Paragon Medical as well as reducing the set up time it takes to set up Coordinate Measuring Machines. Another area of focus is the editing and creation of work instructions to assist in training for current and future employees. With improvements in work instructions, employees will be able to confidently conduct calibrations of the various measuring machines available at Paragon Medical.**

***Keywords-5S, Reliability Anlaysis, Work Instructions, Process Improvement, Time Studies***

## I. INTRODUCTION

Paragon is split into several departments, grouped by smaller, more distinct "cells". The focus of this project was centered on the Quality Control Lab department. The cell primary affected will be the Coordinate Measuring Machine area (CMM). The Quality Control Lab has been operating without data to support many of the process flows.

Employees were uncertain of the calibration frequency for gauges, whether it is a batch size of 250 pcs or 1000 pcs (depending on gauge type). There also seemed to be difficulty amongst the operators to keep track of the number of times a pin was used during the manufacturing of a part. They had trouble identifying how often to calibrate the gauge.

The Keyence, OGP, Hawk, and Zeiss CMM calibration work instructions needed validation to ensure that they meet the standard practices provided by vendors. We also applied 5S to various parts of the department such as the CMM setup as well as fixture and probe storage. The contractor will be responsible for developing and documenting a labeling system to assist in effective traceability of pin/ plug/ thread gages and other areas of the Metrology department.

## II. OBJECTIVES

### A. *Validate gauge calibration frequency*

- Analyzed tool wear and calibration dimensions.
- Improved calibration tracking and counts.

### B. *Improve CMM set-up time*

- Created work instructions to improve calibration times and reliability.
- Developed standardized process for CMM inspections.

### C. *Improve metrology and Q/C lab*

- Maximized storage for less used fixtures and probes based on used frequency.
- Implemented identification system to fixtures and have a set-up guide to eliminate set-up guess work.

## III. CURRENT STATE

In order to improve the quality of the Metrology department's calibration frequency and traceability, the team conducted the following methods:

### A. *Data Analysis*

The team observed the current state of the system. A process flow chart was created by the team to completely explains the current state. This can be seen in *Figure 1* below.

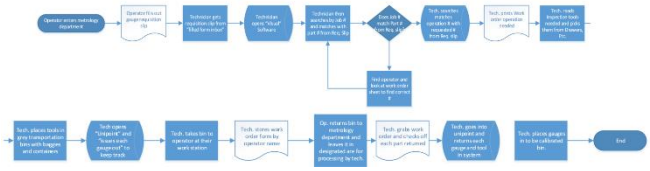

*Figure 1: Process Flow Chart*

### B. *Live Training*

The team shadowed the inspections department to analyze the true current practices for calibrating the CMM machines, and documented the process flow for a single artifact that was calibrated respectively with either the OGP, Keyence, Hawk, and Zeiss machines. Instructions on potential risks were also documented.

### C. *Data Collection*

To validate the 250-pc threshold for calibration, data was collected using Omega Cube and Unipoint. The Unipoint software provided annual, historical data for inspection records from 06/2014-06/2020. Unipoint contained calibration record. Past work orders were used to evaluate the number of uses. The team obtained the original work instructions for each CMM machine. The Zeiss machine did

not have any available work instructions and needed work instructions constructed.

### *D. 5S+1: Probes and Fixtures*

Currently, the fixture and probe storage were not fully utilized. We can establish an organizational system based on the frequency of use and ease of access. The cabinets were used for probes and fixtures that are less commonly used or required a more unique set up requirement. Each CMM station had its own set of probes and had a storage carousel to store their respective probes. However, the stations lacked labeling and organization for all the equipment at the station. The current time it takes for a metrology technician to set up a CMM and run their "in process" set-up is 20 minutes. Using 5S+1 Methodology, the team can reduce the time it takes for them to perform the task and save Paragon Medical money.

## IV. Deliverables and Conclusion

### *A. Validation of Calibration frequency*

Data about tool wear and number of uses from Unipoint and Omega Cube was needed to use Minitab to conduct a reliability analysis. Every calibration conducted is recorded. The relevant information were the nominal dimensions, actual dimensions, tolerances for each specific tool being inspected and finally a pass or fail based on tolerance specifications of each part. We focused on the "0-80" thread gage, which had the most historical data points in both systems. We collected previous work orders that used the "0-80" Gage. There were ~16,000 uses for the tool with about 5 points of failure due to wear or damaged and chipped threads.

This thread gage required 100% inspection which meant every unit made with this thread gage for inspection was checked. The only thing that the tool use count didn't contain was the amount of uses for final inspection. Only in process parts were inspected and recorded. But for final inspection they were inspected but the tool use is not recorded. To account for this there are two approaches: (1) remove missing data points and conduct the reliability analysis, (2) fill in missing data with an average of production rate and actual number of days between each missing point. In Minitab, we performed both approaches.

Both approaches show that increasing the tool use count from 250 uses between validations to 500 has about 83% chance of survival for approach 1 and 92% of survival for approach 2. We can reduce the number of calibrations needed between parts and reduce the time spent calibrating each day.

Table 1: Survival probabilities for approach 1

| | | 95.0% Normal CI | |
|---|---|---|---|
| Time | Probability | Lower | Upper |
| 250 | 0.934950 | 0.825149 | 0.981792 |
| 500 | 0.836660 | 0.666836 | 0.937048 |
| 750 | 0.748285 | 0.522537 | 0.900023 |
| 1000 | 0.672900 | 0.406521 | 0.871261 |

Table 2: Survival probabilities for approach 2

| | | 95.0% Normal CI | |
|---|---|---|---|
| Time | Probability | Lower | Upper |
| 250 | 0.946223 | 0.877569 | 0.976875 |
| 500 | 0.922839 | 0.841753 | 0.963261 |
| 750 | 0.904925 | 0.813790 | 0.952717 |
| 1000 | 0.889896 | 0.789670 | 0.944005 |

It is strongly recommended to continue to perform reliability analysis with the collection of more data points.

### *B. Work Instructions*

The updated work instructions for Keyence, OGP, and Hawk machines could improve calibration times and reliability. Lower-level calibration instructions, mitigation measures, images, and set up instructions that reflect Paragon's current practices were added. The Zeiss work instructions' first revision was verified. We recommended that the company transition from hard copy work instructions to an electronic database that is easily accessible to operators. The continuous application of 5S should also apply to work instructions. These efforts will guarantee continuous improvement in calibration flow and reliability.

### *C. 5S+1: Probes and Fixtures*

While implementing 5S+1, the team standardized the process by minimizing time searching for equipment and decluttered the CMM station. A picture displaying all the contents inside of the storage cabinets was attached on the outside of door. This will help the technician find what they need before opening the door. Additionally, the team added labels to the carousel storages and gave each probe a designated home. This reduces the time it takes for each technician to locate the probes that they need. It also declutters the workstation so that efficient work can be performed. The racks under the CMM station tables stored less frequently used fixtures. A 5S+1 audit sheet was created that allows the metrology team to track their progress, while making abnormalities easily recognizable. The team conducted a 5S+1 Workshop to introduce the concepts of 5S+1 and how to implement in the future.

Finally, a time study was conducted a final time to determine the updated time it takes a technician to execute an "in process" set-up. The updated time it took the technician was 7 minutes, which reduced the original time by 13 minutes. A cost analysis was performed, and it saved the company $21 per each "in process" set-up.


## Acknowledgment

Special thanks to the Paragon team for sponsoring the project and the support from the faculty: Brad Reinke, Pete Anetsberger, Rudy Bautista, Cecilia, and others. The team would like to also acknowledge the department of Industrial and Systems Engineering for their guidance and support of the project: Dr. Hwang, Dr. Gary Chen, Dr. Nguyen, Dr. Niechen Chen, and Dr. Damodaran.

# Maximizing Therapy Appointments by Improving a Hospital Scheduling Process

Madalynn Derro, Makenzie Kuzmanic
Department of Industrial and Systems Engineering
College of Engineering and Engineering Technology
Dekalb, IL
Z1818355@students.niu.edu, Z1847633@students.niu.edu

***Abstract*—A hospital in the Northern Illinois region was finding complications with handing the scheduling of the number of patients that are coming into a clinic. This hospital asked the Department of Industrial and Systems Engineering at Northern Illinois University to help find ways to maximize the throughput of patients within a process of physical therapy (PT) and occupational therapy (OT) evaluations and follow-up appointments by improving the scheduling techniques. This project resulted in small, proposed improvements as well as a scheduling tool deliverable that the hospital will be able to use to cut down on scheduling time.**

***Keywords- physical therapy, occupational therapy, data analysis, simulation, improvements, utilization, scheduling***

## I. Introduction

In the hospital environment, patients come for a service that initiates the need from a doctor for post care treatment. This project focused on inpatient physical and occupational therapy. A doctor initiated an order for a patient in their electronic system for the corresponding therapy. There was only a manual scheduling process that is creating a backlog of patients that are not being seen in a timely manner. A patient stay for inpatient therapy care can includes an evaluation appointment where the therapist determined whether the patient needed follow-up appointment(s) before being discharged. At any appointment, it was possible that patients missed appointments or were not ready for the therapy. When scheduling patients, evaluations were a priority over follow-up appointments.

## II. Problem Statement

This hospital is experiencing issues with patients having long stays due to staff members abusing the priorities of evaluations and labeling follow-up appointments incorrectly to push patients through the system. Since the scheduler is to create the morning schedule based off of what patients need to be seen first, there is becoming a backlog of patients since the scheduling employee is only allotted one hour for scheduling and can only plan up until lunch of the same day. This is causing a lot of patients to wait in the system for longer than necessary since the scheduling process is so inefficient.

## III. Objectives

The objectives of this project include:

- Created a current state simulation that mimics the current process at the hospital.
- Developed and analyzed improvement scenarios
- Created a scheduling tool to assist the manual process

## IV. Current State Process

At the current time, the hospital's patients went through a similar process no matter if the appointment type is Physical Therapy (PT) or Occupational Therapy (OT). Figure 1 shows that the after the patients see the doctor, the doctor initiated the order for therapy. Once the order was created, each patient had an evaluation with a therapist that then determined the number of follow-ups, if needed, the patient had to attend before being discharged and end the order.

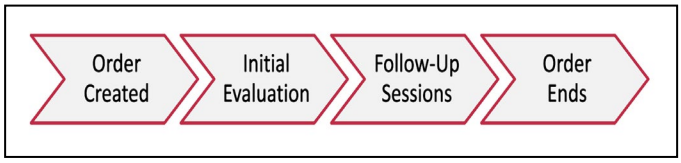


Figure 1. General Patient Process

Each order corresponds to one patient. A patient always had an evaluation appointment but the number of follow-ups varied based on the type of care needed.

## V. Hospitals Data Analysis

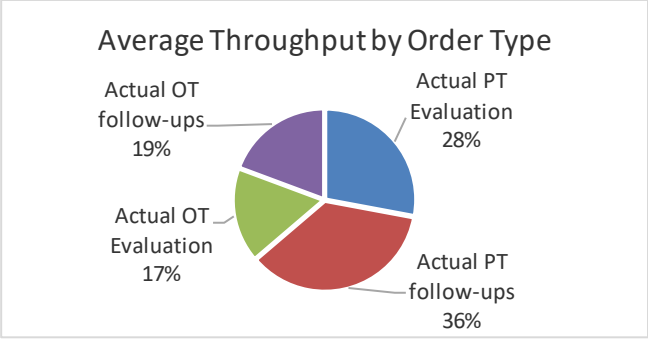


Figure 2. Average Throughput by Order Type

The hospital supplied the team with one year worth of data of PT and OT order records that included the order creation date and time, the order end date and time, the type of appointment, if the patient had an evaluation, and how many follow-ups were needed. One month worth of data contained a break-down of appointment types as well as evaluation and follow-ups statistics that allowed the team to create an accurate simulation of the process. Figure 2 shows the

breakdown analysis from the empirical data of average order types for one month. From the given data, the team found trends and calculated the average time between order creations (interarrival times), and average time a patient spends in the system. This information was required for the creation of a simulation of the process (See figure 3) to help analyze the current state and improvements.

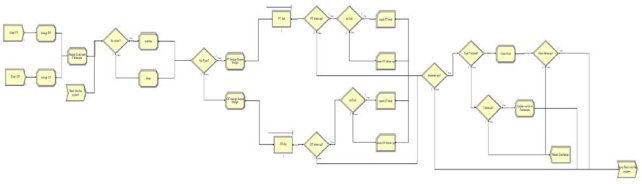

Figure 3. Overview of Simulation

## VI. Future Improvement Proposals

The team created and implemented two changes into the current state simulation that were meant to improve the patient's experience. The first improvement proposed having a dedicated set of workers specifically for evaluations. Since the hospital received multiple new evaluation appointments a day, this could help make sure patients are seen in a timely manner. The second improvement investigated the time in-between patients' appointments to help patients get seen sooner. This improvement used a weighted priority rule that put the patients who haven't been seen in a long time in a higher queue position. This improvement decreased the cycle time and patients were able to leave sooner.

## VII. Results

The first improvement was tested against the current state simulation to see how this affected the hospital's process. This change did not make a huge impact since it created a trade-off scenario where if more evaluations were seen, less follow-ups were seen. This improvement did increase the overall throughput of patients in the system, however there was insufficient statistical evidence this improvement would be warranted to adoption into the current scheduling process.

The second improvement saw a similar trade-off between increasing/decreasing evaluations at the expense of follow-up appointments. This improvement allows the cycle time to decrease and have patients leave the system faster. Although it does not increase throughput, it allows the team to see that the simulation can be used to test possible ideas before making drastic changes in real life where the company could lose time or money to see that the changes did not help.

## VIII. Economic Analysis

An understanding that was established before beginning this project is that the hospital is currently understaffed. Since a simulation was created, it allowed the team show the possible outcomes of hiring more individuals. The team was able to run the possibilities of adding more staffed therapists to see how much profit will be made. The state average of PT appointments was $187.50 and OT appointments was $225. The team assumed the staff members earned an annual pay of $80,000 for PTs and $52,000 for OTs. Table 1 shows a breakdown of the profit earned by adding additional PT Staff therapists which also resulted in additional patients being seen. Table 2 shows the same analysis for OTs.

Table 1: Potential Profit for Increasing Number of PT

| PT Therapist | 10 | 11 | 12 | 13 | 14 |
|---|---|---|---|---|---|
| PT Appointments Seen | 3078 | 3382 | 3679 | 3996 | 4320 |
| Monetary Value | $ 577,106 | $ 634,041 | $ 689,803 | $ 749,222 | $ 810,000 |
| Average PT cost | $ 66,667 | $ 73,333 | $ 80,000 | $ 86,667 | $ 93,333 |
| Profit | $ 510,440 | $ 560,707 | $ 609,803 | $ 662,555 | $ 716,667 |

Table 2: Potential Profit for Increasing Number of OT

| OT Therapists | 6 | 7 | 8 | 9 | 10 |
|---|---|---|---|---|---|
| OT Appointments Seen | 1850 | 2152 | 2456 | 2769 | 3079 |
| Monetary Value | $ 416,171 | $ 484,155 | $ 552,679 | $ 622,958 | $ 692,865 |
| Average OT Cost | $ 26,000 | $ 30,333 | $ 34,667 | $ 39,000 | $ 43,333 |
| Profit | $ 390,171 | $ 453,822 | $ 518,012 | $ 583,958 | $ 649,532 |

Using the proposed scheduling tool, or Access Database, the individual in charge of scheduling will be able to cut the time spent by 50%. By estimating the hourly wage of a nurse tech at $20 an hour, scheduling for 1 hour a day, we estimate a yearly savings of $3,360 if the scheduler is used.

## IX. Conclusion

The Access Database was created to aid in the manual evaluations or appointments. The Access database scheduling tool may help to automate a manual, non-value-added process. By adding more staff therapists, the hospital will increase the number of therapy orders completed. Since the hospital is using evaluations as a priority, there needs to be a way to improve the system in a way that the employees can work with.


## Acknowledgment

The project team would like to thank the Northern Illinois University Department of Industrial and Systems Engineering faculty. Special thanks to Dr. Christine Nguyen and Dr. Purush Damodaran for their advisement and service as liaisons between the hospital group and the project team.


## References


[1] NSPE. "Code of Ethics." Code of Ethics | National Society of Professional Engineers, www.nspe.org/resources/ethics/code-ethics?gclid=Cj0KCQjwpdqDBhCSARIsAEUJ0hPWmvfmaqmKwWJoWa6JGQ7lkGZuInK1iRw8najRdj0ekn4XzvTjRZ8aAo_cEALw_wcB. J. Clerk Maxwell, A Treatise on Electricity and Magnetism, 3rd ed., vol. 2. Oxford: Clarendon, 1892, pp.68–73.

[2] "How Much Does Occupational Therapy Cost?" CostHelper, health.costhelper.com/occupational-therapy.html.

[3] "2021 Physical Therapy Costs: Sessions With & Without Insurance." Thervo, thervo.com/costs/physical-therapy-cost#:~:text=The%20average%20cost%20of%20physical,of%20injury%20and%20treatment%20received

# Minimization of Trucker Idle Time and Transportation Cost in Container Delivery

Alexis Koch, Krystal Diaz, Matt Slouka
Department of Industrial & Systems Engineering
Northern Illinois University
DeKalb, IL, USA

*Abstract*— **For any manufacturing company, they need to ship out their products to other companies or their consumers. In some cases, companies use third-party logistic (3PL) companies to transport their product. This can help companies get their product to where they need to go within a given time frame. This project focused on a furniture company that outsources to a logistics company to ship their products to customers. The trucking company has containers to transport any product. The furniture company does not have the resources they need to deliver their product to their customers. Thus, the trucking company takes the furniture products and deliver them to the respective customers. Currently, a trucker will deliver the product to the customer and waits until the customer unloads the product out of the shipping container. There can be extended periods of time the trucker will have to wait. The longer the wait times, the slower it is for the furniture products to arrive at the customer locations. To limit the idle time and transportation cost, this project aims to analyze and determine if a new policy can decrease the idle times and transportation cost.**

***Keywords- Optimization, Python, Tranportation cost, Idle time***

## I. INTRODUCTION

A furniture company needed to deliver full containers, with furniture, to their customer locations. However, the furniture company did not have the necessary resources to carry out their own deliveries. Consequently, they outsourced to a third party logistics company that will provide the furniture company with trucks, truckers, and containers to fulfill their demand. In the current policy, the truckers are assigned a number of containers to deliver to different customers. In each delivery, the trucker must wait for the container to be fully emptied by the customer at the customer site before taking the empty container back to the depot. Then the furniture company loads the containers with product for future deliveries. However, a major issue is the amount of time it took for customers to unload their containers. It varied and could take longer than an hour just to unload a container. Therefore, truckers waiting for this to be done was non-value added time where the trucker literally waited. The team investigated and came up with a new policy to help minimize the wait time and utilize the truckers more efficiently.

## II. PROJECT DESCRIPTION AND SCOPE

In this project, the team focused on developing a new transportation policy for the trucking company. The main concerns included the amount of time it took the truckers to transport a container from the depot to the customer location and back. In addition, the team focused on minimizing the amount of time the trucker waits for the customer to unload the truck. The project does not include the way the product is package nor the way it is loaded in the container. Finally, the composition of the merchandise stored in the container was not in the scope of the project. The scope of the project included only changes in transportation policy related to the transportation time and idle time, and the number of rental containers required.

## III. PROJECT OBJECTIVES

### *A. The Idle Time*

There are two objectives that project focused on. Since the idle time is an important component in the project, the team will focus on minimizing the total idle time of the trucker at each customer location. This will let the team show how much time truckers spent executing the current policy versus the proposed policy.

### *B. The Cost of Transportation*

The second objective was to minimize the cost of transporting full and empty containers. The logistics company is the company that delivers the product within the containers. The containers are a critical resource for logistics company and the furniture company. The truckers took the container from the depot to the respective furniture customer and returned it once the task is finished. The more time truckers wait for the customer to finish unloading, the more delay time existed and potentially cost would increase. In order to minimize the idle time, the cost needs to be minimized as well.

## IV. CURRENT STATE

The current state was modeled as an integer linear programming optimization model. The objective function was to minimize the number of rental containers required, the total transportation cost and the total number of truckers needed. The constraints were to (1) ensure the truckers did not work more than their available time, (2) meet demand and allow for early delivery of containers, and (3) nonnegativity constraints.

## V. PROPOSED POLICY

The proposed policy was designed to address the high wait time in the current policy. The proposed policy allowed the trucker to drop the container off at the customer location and then leave to make other deliveries and pickups. Therefore, the wait time of the trucker in the system is removed. Since containers were dropped off, truckers must return to pick them up on another day. This also introduced situations where the trucker would drive with no container attached. As a result, the total rental cost of the containers

will increase, since the truckers will handle more containers and containers are being left at the customer locations for them to unload in their own time. The proposed state is an integer programming problem, similar to the current state. The optimization model was solved using Python and IBM ILOG CPLEX solver with the packages docplex, cplex, pandas, openpyxl, and numpy packages.

### A. Equations

Eq. 1 was the objective function, stating to minimize the transportation cost of full containers, empty containers and no containers, and the number of truckers needed. Eq. 2 limited the number of hours a trucker can work. Eq. 3 ensured truckers left and returned to the depot. Eq. 4 was a flow balance constraint for containers at all locations. Eq 5-7 made sure demand was satisfied and allowed for early demand delivery. Eq. 8 stated that dropped off containers are ready for pickup the next day, and eq 9-10 were the number of containers left at any location that must be emptied by the next day.

*Minimize*

$$\sum_{t\in T}\sum_{v\in V}\sum_{i\in L}\sum_{j\in L}\left(c^R\left(w_{vijt}+x_{vijt}\right)+c^F s_{ij}w_{vijt}+c^E s_{ij}x_{vijt}+c^N s_{ij}y_{vijt}\right)+\sum_{t\in T}\sum_{v\in V}Z_{vt} \quad (1)$$

*Subject to*

$$\sum_{i\in L}\sum_{j\in L} r_{ij}\left(w_{vijt}+x_{vijt}+y_{vijt}\right)\le K^M z_{vt},\ \forall t\in T,\ v\in V \quad (2)$$

$$\sum_{i\in L}\sum_{j\in L} r_{ij}+x_{vi0t}+y_{vi0t}=\sum_{j\in L} w_{v0jt}+y_{v0jt},\ \forall t\in T \quad (3)$$

$$\sum_{v\in V}\sum_{j\in L} y_{vijt}+w_{v0it}=\sum_{v\in V} x_{vi0t}+\sum_{j\in L} y_{vijt}+I_{it},\ \forall i\in L, t\in T \quad (4)$$

$$\sum_{V\in V} w_{vit}\ge f_{it},\ \forall i\in L,\ t\in T \quad (5)$$

$$f_{i1}=d_{i1},\ \forall i\in L,\ t\in T \quad (6)$$

$$f_{it}=f_{it-1}+d_{it}-\sum_{V\in V} w_{v,0,i,t-1},\ \forall i\in L,\ t\in T \quad (7)$$

$$\sum_{v\in V} x_{vi0t}\ge I_{i,t-1},\forall i\in L \quad (8)$$

$$I_{i1}=\sum_{v\in V}-x_{vi0t}+w_{v0i1},\forall i\in L \quad (9)$$

$$I_{it}=I_{i,t-1}+\sum_{v\in V}-x_{vi0t}+w_{v0it},\forall i\in L, t\in 2\ldots|T| \quad (10)$$

## VI. Results and Conclusions

The optimization program was set up to perform 20 different random instances of a scenario. 4 scenarios were created for testing. The "Near" scenarios were where the network of customer locations was nearby the depot. It was tested with 5 locations and 10 locations. The same was done for a "Far" scenario, where the network created customer location located further away. The parameters of the problem (i.e. cost to transport a full container, rental cost) were arbitrarily determined. The rental cost, travel cost, and total truckers were compared between the current state and proposed state. The first cost associated with the system is the rental cost, which was higher in every situation of the proposed policy. This is an obvious difference since the truckers can now drop the container off, which allows for the truckers to handle other deliveries and drop-offs. This also increased the logistics company's ability to move more containers since truckers weren't idle and waiting for a container to be unloaded. The total transport cost of the proposed state is 1.5% to 4% lower in all scenarios of the proposed policy. The number of truckers used in the system was reduced by 28% to 60% in the proposed policy.

With the reduction of truckers involved and the reduction of transport cost, the proposed policy is less costly than the current state to ship the containers to the customers. Furthermore, the proposed policy is more time-efficient than the current state, which means more containers can be shipped per day, which increases the revenue of the logistics company. The Logistics company is paid per container delivered therefore an increase in delivery rate is a direct increase to revenue.

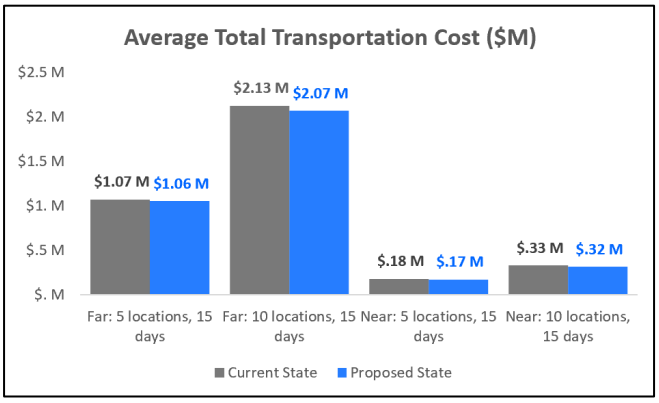


Figure 1. Average Total Transportation Cost

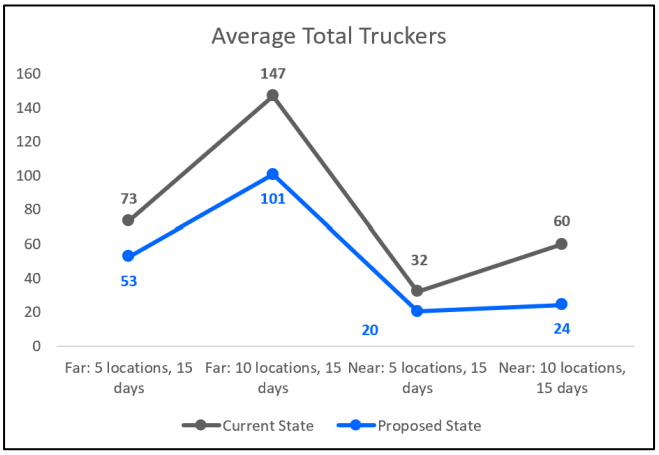


Figure 2. Average Total Truckers


## Acknowledgment

The team would like to thank Northern Illinois University Department of Engineering and Engineering Technology. In addition, the Department of Industrial and Systems Engineering Faculty. Special thanks to Dr. Christine Nguyen for all her immense help and support throughout this project.

# Designing a 3D Printed Catalyst Carrier That Maximizes Reaction Yield

Justin Santiago, Dominque Beck, Moosa Obaidullah
Department of Industrial & Systems Engineering
Northern Illinois University
DeKalb, IL, USA
Z1819598@students.niu.edu, Z1833555@students.niu.edu, Z1868150@students.niu.edu

***Abstract*—A catalyst is a substance that increases a certain chemical reaction rate. However, the currently used catalyst in its normal geometrical form cannot guarantee high single-pass reaction yield. Northern Illinois University's Department of Chemistry and Biochemistry worked with the Department of Industrial and Systems Engineering to optimize the catalyst geometry through design and manufacturing catalyst carriers which is then converted into catalyst. This catalyst carrier has high internal surface area that can facilitate a high reaction yield. Multiple iterations of designs were created in search for an better design that can increase reaction yield but still allowed the carrier to be printed properly and efficiently. These catalyst carriers were then converted to catalysts and their reaction yield was tested.**

***Keywords- catalyst carrier, catalyst, surface area, reaction yield.***

## I. INTRODUCTION

Northern Illinois University's Department of Chemistry and Biochemistry required a catalyst that will allow them to have a high single-pass reaction yield when 2 chemicals are reacted. Our team was tasked with designing and 3D printing a catalyst carrier that would be able to facilitate this high reaction yield. The catalyst carrier has to meet specific dimensions that can be seen in Figure 1. The interior mesh was the focus of our design. The team's approach to maximize the reaction yield is to increase the interior surface area of the catalyst carrier while maintaining proper liquid flow through it. A lattice structure was determined to be the best way to implement a high surface area into the catalyst carrier's design. A lattice structure is commonly composed of repetitive cellular unit geometries. These lattice structures can output a high surface area when working with limited space.

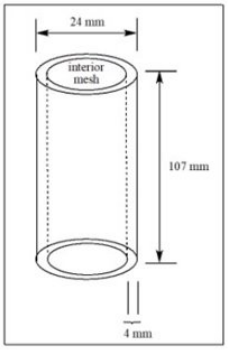

Figure 1. Catalyst Dimensions

The printing method that the team used is an additive manufacturing method known as fused deposition modeling(FDM). Once the catalyst carrier had been 3D printed it is converted into catalyst by treating it with a chemical solution. Once it had been converted, a second chemical solution would be flow through the converted catalyst and the reaction yield would be measured. Reaction yield is the percentage of particles in the solution that completed the reaction.

## II. METHODOLOGY

The first step to 3D printing the catalyst carrier was to create a design in CAD. The team used Solidworks as our software for this task. The next step would be to import the design into CAM. The team used PrusaSlicer software for this task. This software would allow us to choose printing parameters such as the material used to print, the layer height and the nozzle width. The layer height was .15 *mm*, and the nozzle diameter of the printer was .25 *mm*. This software can than output a G-code which are specific instructions the 3D printer will use to print the catalyst carrier. For this catalyst carrier material, the team used Acrylonitrile Butadiene Styrene(ABS) which is a thermoplastic polymer. This styrene molecule can be sulfonated when treated in sulfonic acid solution, which allows our catalyst carrier printed in ABS to be converted into a polystyrene sulfonate catalyst. The catalyst carrier was then treated in sulfonic acid for several hours and can be seen in Figure 2.


Figure 2. Converted Catalyst

Once the catalyst had been fully converted, chloroform solution was then flowed through it. The amount of chloroform that reacts with the catalyst is our reaction yield. Our first iteration of designs failed in allowing the liquid solution to properly flow through after been converted into catalyst. It was learned that after treated in sulfonic acid, there were slight expansions in the catalyst carrier material, and there is possibly a second time expansion during the catalytic reaction when chloroform solution flows through the catalyst. The initial catalyst carrier was designed with too small feature dimensions, so that after the expansion, this causes difficulties to allow the solution to properly flow through the catalyst carrier. In the second iteration, the team designed experiments to find the expansion ratios of catalyst carrier from as-printed geometry to after converted into a catalyst,

and to after reacted with the chloroform. Using the found expansion ratios, an updated design was then created for the second iteration.

## III. CAD Designs

The team created six designs in the first iterations of design, the interior mesh of these designs were lattice structures with geometries of circles, squares, hexagons, triangle, and crosses in a linear and circular pattern. The main metric measured in these designs was interior surface area. The surface areas for the designs can be seen below.

TABLE 1. SURFACE AREA PER DESIGN

| Design | Surface Area ($mm^2$) |
|---|---|
| Circle Design | 33,823 |
| Square Design | 37,560 |
| Cross (linear) Design | 33,547 |
| Cross (circular) Design | 30,370 |
| Triangle Design | 53,245 |
| Hexagon Design | 39,842 |

An example of our designs can be seen in figure 3, this design was circle design, it was created by making a circle with a diameter of 1.2 *mm* and a spacing of 0.5 *mm.* this circle was then repeated over and over and created the lattice type structure.

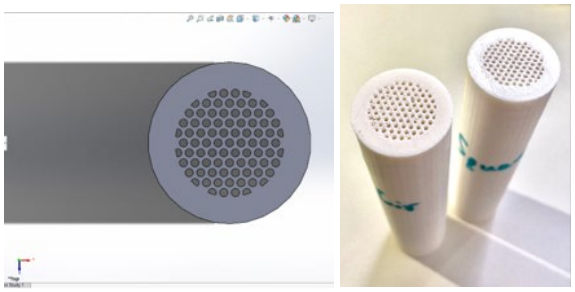

Figure 3. Circle CAD image and 3D Printed design

## IV. Expansion Ratio Testing

To find the expansion ratio for our catalyst we printed small catalysts that could print very quickly, and we could measure the dimensions of the catalyst before experimentation and after. These small catalysts or "coupons" were printed on small base and were of two shapes, squares and circles. The squares had three side lengths chosen which consisted of 7, 8 and 9 *mm*. The circle coupons had three diameters chosen which as well consisted of 8, 9, and 10 *mm*. They both had a three wall thicknesses of 0.5, 1, and 1.5 *mm*. A total of 18 coupons were printed and experimented on. An example of a coupon design can be seen in figure 4 below. This circle coupon had a diameter of 10 *mm* and a wall thickness of 0.5 *mm*.

Figure 4. Circle coupon

After the 18 coupons were printed the dimensions of each were measured carefully using a caliper. The dimensions were measure 3 times from different areas of the coupon and then averaged together, this was to ensure that the dimension was correct and the overall variance was reduced. The coupons were then soaked in sulfonic acid and the remeasured. The team found that there was approximately a 1.66% increase in the dimensions. These coupons were then soaked in chloroform, the team found a 2.22% expansion rate. In total the team found a 4% expansion ratio.

## V. Results and Conclusion

Using the total expansion ratio and feedback from Northern Illinois University chemistry department the team was able to create a final updated design which can be seen in figure 5. A small lip was added to the end of the design so that the catalyst carrier could be converted easily. This design had a significantly reduced surface area of only 27,233 $mm^2$. The surface area of the part needed to be reduced for the catalyst carrier to print and experiment successfully. This catalyst carrier had a reaction yield of approximately 20%. The experimentation is ongoing, and the Chemistry department does not expect to finish till late June of 2021.

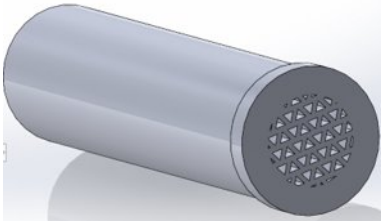

Figure 5 – Final Design


## Acknowledgment

The team would like to thank Northern Illinois University's Chemistry and Biochemistry Department and Industrial and Systems Engineering Department for giving us the opportunity to work on this project A special thanks to Dr. Niechen Chen for guiding us through the difficult aspects of designing the catalyst carrier and to Dr. Douglas Klumpp for conducting a majority of the experimentation.

# Design and Evaluation of Patient Transfer Device

Mohammed Rahat Anwar, Varun Thandy, Mohammed Aburmishan
Department of Industrial and Systems Engineering
Northern Illinois University
Dekalb, IL, USA
Z1831321@students.niu.edu, Z1853360@students.niu.edu, Z1856673@students.niu.edu

***Abstract*— The project aims to design, assemble, and evaluate a patient transfer device within the budget of $200. The objective was to reduce lower back stress on healthcare workers through the implementation of a new device. The device was then evaluated using 3D Static Strength Prediction Program(3DSSPP) and Rapid Entire Body Assessment (REBA). REBA showed posture results to be reduced by half when compared to devices like pivot disc, sliding board. 3DSSPP predicted the lower back compression for the 50$^{th}$ percentile male to be 469 pounds and the 50$^{th}$ percentile female to be 333 pounds. A significant decrease in low back stress was found with our prototype in comparison to devices requiring manual lifting.***

***Keywords-TRANSFER DEVICE, 3DSSPP, REBA, AUTOCAD***

## I. INTRODUCTION

Patient transfer devices are mechanical or electromechanical apparatuses that help move patients with upper or lower disabilities or a combination of both. These transfer devices help to reduce stress on major body extremities for the operator while ensuring a safe transition for patients to and from set locations. Devices include but are not limited to sliding board, pivot disc and E-Tac turner a turn aid device with standing support. Transfers can happen over a range of places like hospitals, clinics or can take place in private households. However, current devices in the market lack the features to reduce physical stress for healthcare workers.

## II. PROBLEM DESCRIPTION

Nurses and healthcare workers are prone to work-related lower back and shoulder injuries due to frequent cycles of manual patient transfers. Patient transfer devices are not widely used in hospitals for constraints such as cost, space and set up time. Studies show that a majority of lower back pain or musculoskeletal disorders for healthcare workers comes from manual transfer of patients and are increasing at a rate of 8.8% every year. Incorrect posture like bending, stoop lifting over repeated cycles are the main driving factors of the problems.

## III. PROJECT OBJECTIVES

The aim of our project is to design, build, and evaluate an easy-to-use and portable patient transfer device within a budget of $200. The project team aims to reduce the lower back stress of healthcare workers and improve the adoption rate of a low-cost, high-quality patient transfer device.

## IV. METHODS

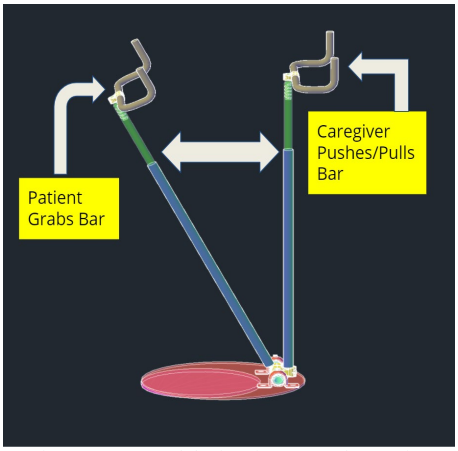


Figure 1. 3D Model of Patient Transfer Device

### *A. Design*

The team had to research existing products in the market to find devices with the best functionality and cost closer to the allocated budget. The pivot disc, sliding board and the E-TAC turner were benchmarked. Multiple sketches were made from which the best functionality was used on the final design. The final 3D modeled design was made using AUTOCAD 2021 (Computer Aided Design).

- Detailed drawings to show dimensions, tooling requirements, materials, and quantity needed were created for design and assembly.
- Prototype device consists of rotation disc on the bottom followed with bearings in housing that hold the lifting mechanism for the device. The handlebar has a spring subassembly providing an initial momentum towards patients.

- Anthropometric static data were used for the seating height, foot length and the center of wrist grip length for the targeted population.

### B. *Analysis of Transfer Tasks*

3D Static Strength Prediction Program: Spinal compression forces and distribution of the center of gravity for the four different tasks were to be determined using 3DSSPP.

Rapid Entire Body Assessment (REBA): REBA assessment worksheet as well as the Ergo Plus software to assess the body during transfers. Load, coupling, movement, and body posture were the primary focuses when analyzing the transfer.

Figure 2. Transfer with Prototype Device

### C. *Design of Experiment*

Two experiments were set up and conducted for this project. The first was the procedure to collect the average push/pull force required to lift the patient for the prototype. Jackson Evaluation Strength System (J.E.S.S) was utilized to measure the average force. A second experiment was set up to understand the usability of manual transfer against transfers done using the prototype. Test subjects were Northern Illinois University students, and the transfers were performed by a qualified nurse.

## V. RESULTS

Static images and video recordings demonstrating transfers done using sliding board, pivot disc and prototype allowed the team to implement two work measurements. The team utilized 3D Static Strength Prediction Program (3DSSPP) and the Rapid Entire Body Assessment (REBA) tool.

### A. *3DSSPP RESULTS*

The humanoid in 3DSSPP software was modified to mimic the posture of the nurse using the prototype. The hand loads were at 25.6 pounds for each hand, and this was determined from the Jackson Evaluation Strength System (J.E.S.S). As shown in Figure 3, the predicted lower back compression forces for both male and female using prototype was significantly lower than the predicted lower back compression for the two other device.

### B. *REBA*

REBA score portrays the level of risk the body would be under during the associated task. Inputting the proper postures and angles into the program, a REBA score of five is outputted. This score indicates a level of medium risk with the associated patient transfer. When in comparison with the sliding board and the pivot disc, both received a higher score of 10. This score represents a high level of risk and in need of implemented change. Results predict our device reduced the level of Musculoskeletal disorder risk by 50%.

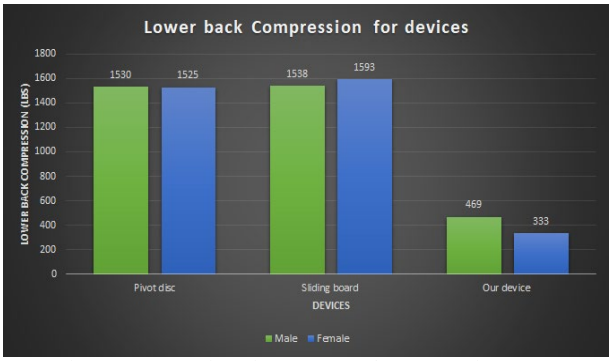


Figure 3. Comparison for Lower Back Compression Force

## VI. COST ANALYSIS

Washington State Ergonomics Cost Benefit Calculator was used to estimate the predicted saving if the prototype was implemented. The model took inputs such as engineering costs, posture data and effectiveness of the solution. Predicted results indicate $4500 saved annually, 40% reduction in injury claims and 4 months payback period for one device.

## VII. CONCLUSION

The team accomplished designing, prototyping, and evaluating our device within the budget constraints of $200. The team successfully utilized two work measurements to analyze the associated tasks involved in patient transfers. Predications involving correct implementation and adoption of this prototype reduced spinal compression forces and work-injury related costs for the healthcare industry.


## ACKNOWLEDGEMENT

The team would like to thank the Department of Industrial and Systems Engineering. Our faculty advisor Dr. Jaejin Hwang. A special thanks to Dr. Christine Nguyen and Dr Purushothaman Damodaran. We would also like to thank Mike Reynolds and the members of the Northern Illinois University Manufacturing Lab.

# AI-Based Camera: Integrated Speech Recognition and Emotion Detection

K. Anupama Satya Sai Lakshmi, Keerthi A. M., Prasanthi V, Sai Dhruthi Varna K, K. Sudarsana Reddy
Visiting Students, Amrita University, India

***Abstract*— In the current scenario, Artificial Intelligence is emphasizing the development of intelligent machines. Considering the frequent use of web camera applications, there is a need for an enhanced and automated version of the application. Emotion Recognition also plays a crucial role in daily lives. An integrated solution of speech detection with the camera application is a great duo and handy to the user as well. In this paper, we present a method for accessing the camera to take an image and perform image processing using pre-trained voice commands. Additionally, the model also predicts the emotion of the user and produces speech output of the emotion recognized.**

## I. Introduction

Recently, the use of automated devices has been increasing significantly. These days the usage of cameras is made often and there are difficulties in accessing the device directly. In this paper, our main focus is to create a user-friendly solution for accessing cameras using speech commands. This paper is a solution to joint-level speech and facial recognition for a PC with a webcam. For developing this system, the main challenge is integrating speech and face recognition as one system [1].

For Speech Recognition, the first task is to extract the features from the given speech phrase input followed by a neural network model. Mel Frequency Cepstral Coefficients (MFCC) is one of the highly efficient speech feature extraction techniques for automatic speech recognition. Its benefits include superior tolerance of noise, better capability for distinction, and simple calculation [1]

For Face Recognition, based on the speech input given to the system it performs various activities like clicking a picture followed by image enhancements or recognizing emotion [2]. If a user wants to detect emotion, then the model has to detect the face first using a Haar cascade filter. Haar Cascade classifier is widely used for applications that involve object detection. This classifier needs a large number of positive and negative images for training. It makes specific targets by examining all the features present in an image. After the face recognition, emotion is detected using a Neural network model.

The input to the proposed model is a set of 8 predefined keywords. The dataset has 34,568 one-second utterances of 7 short words- ON, ONE, TWO, THREE, FOUR, FIVE, SIX. These keywords are predicted using the keyword spotting technique. Each keyword is assigned to click a picture automatically using the webcam followed by different post-image processing techniques and emotion recognition. The keywords are assigned to automated functions like - turning on a camera and clicking a picture, RGB filter, Black &White filter, Auto-adjustment of Brightness and Contrast, Zoom In, Zoom Out, Emotion Recognition.

## II. Methodology

### A. Input

A large number of speech and face samples are used in this paper. In this case, around 21,264 images are used to cover all the possible facial features. The number of speech samples is 34,568 one-second utterances of 8 short words collected from thousands of people. The speech phrases are used as input to the proposed model. Fig. 1 shows the flowchart of the proposed model.

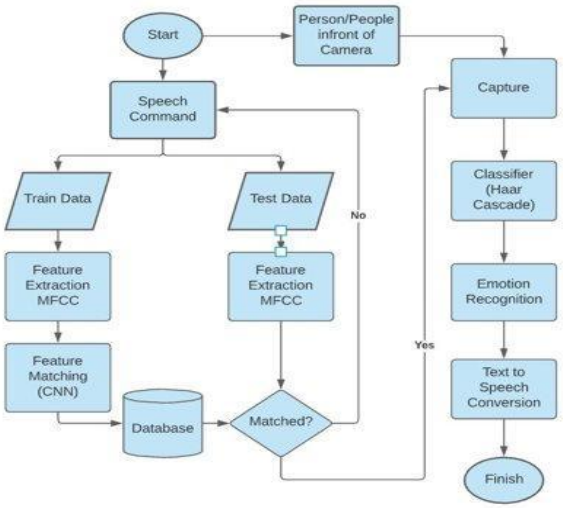


***Fig. 1 Flowchart for the proposed idea.***

### B. Speech Recognition

A Convolutional Neural Network model is built for speech recognition using TensorFlow and Keras frameworks. Firstly, the speech data set is split into train and test data in the ratio of 80:20. The train and test data features are extracted using the Mel Frequency Cepstral Coefficients (MFCC) technique. The training data features are fed to the 3 layered convolutional neural networks and trained for 40 epochs. Later, A training speech keyword by a user is given as the input to the model. The model uses Keyword Spotting Identifier to predict the test speech input. Once the speech input is recognized, the model captures the image of the person and performs post image processing techniques and emotion recognition according to the assigned function to a keyword.

### C. Face Recognition

From the flowchart in Fig.1, it can be depicted that once the keyword is recognized, this model captures the image using an integrated webcam. JavaScript is used to access the webcam. If the speech command “ON” is given, then a

picture clicked. In case if other speech commands like numbers between one to six are given then the clicked picture would be further processed. The post-processing techniques focused in this work are finding emotion and applying filters and basic camera operations to the taken image.

The functions performed by this model for the corresponding keyword inputs are listed as follows-“ONE” - RGB filter; “TWO” - Black and white filter; “THREE” - Auto-adjustment of Brightness and Contrast filter; “FOUR” - Zoom in; “FIVE” - Zoom out; “SIX” - Emotion Recognition

Emotion Recognition is done using CNN. The conventional layers used for the emotion recognition model are five. The activation function used is “Relu” and a batch size of 32. The learning rate and epochs are 0.001 and 100 respectively. The final recognized real-time emotion [2] is then produced in the form of speech. Upon detecting the emotion, the model is designed to give a speech output of the recognized emotion. In the emotion recognition model, the face of a person would be detected using Haar Cascade Classifier and that face would be given as an input to the CNN model. To train and test the CNN model we split the available data set in a 90:10 ratio. We use a large part of the data set for training and the rest for testing. This model outputs recognized emotion in the form of text. This text would be converted to speech. The final output would be a speech indicating the emotion of a person in the taken image.

## III. Results and Discussions

*(a) ONE-RGB filter* *(b) TWO- B&W filter*

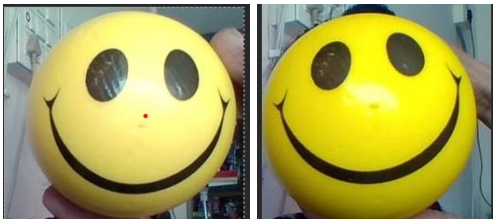

*(c) THREE- Auto-adjusted filter*

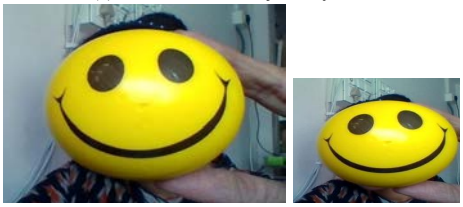

*(d) FOUR- Zoom-in* *(e) FIVE-Zoom-out*

***Fig. 2. Filter output images (a) RGB filter (b) B&W filter (c) Comparison of clicked image and Auto-adjusted filter image (d) Zoom-in filter (e) Zoom out filter.***

Fig.2, shows the output of different speech commands when used. The speech recognition model achieves an accuracy of 94%. Emotional recognition, the other image post-processing technique has been done using CNN model by training the model using three emotions from the Data set. Happy, sad, neutral are three emotional datasets that are used for training the model. Fig. 3 shows the percentage of emotion indicated by the model. It can be inferred that the input image to the model being happy and the model predicted it perfectly with 100% index respectively. Table 1 shows the numerical analysis of the emotion recognition model.

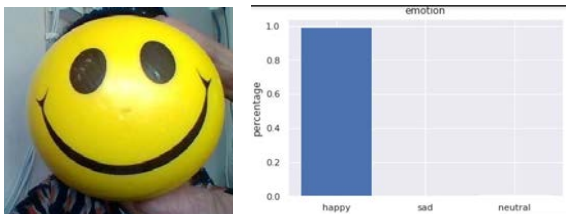


***Fig. 3. Percentage of the emotion of the image.***

TABLE I. ANALYSIS OF EMOTION RECOGNITION MODEL

| **Emotion** | ***Training samples total*** | ***Testing samples total*** | ***Number of correctly classified images*** | ***Sensitivity*** | ***Accuracy*** |
|---|---|---|---|---|---|
| Happy | 8090 | 899 | 824 | $\frac{824}{899} = 0.92$ | $\frac{1670}{2127} = 0.785$ |
| Sad | 5469 | 608 | 400 | $\frac{400}{608} = 0.66$ | |
| Neutral | 5578 | 620 | 446 | $\frac{446}{620} = 0.72$ | |

## IV. Conclusion & Future Work

### A. Conclusion

Concluding, we have developed a camera application that operates on speech commands. Automatic speech recognition helps to click images and apply five post-processing image techniques and emotion recognition. The model recognizes three different emotions namely happy, sad and neutral with an accuracy of 78.7 %. This model can also be used in a variety of real-time applications.

### B. Future Work

To increase the accuracy of the emotion detection model by improving the sensitivity of sad and neutral emotions in the model by extracting special features.

## V. Acknowledgement

The authors would like to thank Dr Mansour Tahernezhadi from the department of electrical engineering for his technical and moral support throughout the project.

## VI. References

[1] H. Alshamsi, V. Kepuska, H. Alshamsi and H. Meng, "Automated Facial Expression and Speech Emotion Recognition App Development on Smart Phones using Cloud Computing," 2018 IEEE 9th Annual Information Technology, Electronics and Mobile Communication Conference (IEMCON), Vancouver, BC, Canada, 2018, pp. 730-738, DOI: 10.1109/IEMCON.2018.8614831.

[2] B. T. Nguyen, M. H. Trinh, T. V. Phan and H. D. Nguyen, "An efficient real-time emotion detection using camera and facial landmarks," 2017 Seventh International Conference on Information Science and Technology (ICIST), Da Nang, Vietnam, 2017, pp. 251-255, DOI: 10.1109/ICIST.2017.7926765.

# Carbon Fiber Monocoque Chassis Redesign

Team 1

Lauren Bangert, Todd Durham, Matthew McCoy
Team Members
NIU Supermileage
Northern Illinois University
DeKalb, IL
niusupermileage@gmail.com

Prof. Nicholas A. Pohlman, PhD
David J. Schroeder, PhD
Advisors
Northern Illinois University
DeKalb, IL

**In recent years, the automotive industry has focused on decreasing the carbon footprint caused by fuel emissions. The Supermileage Team is an SAE affiliated club at NIU that designs, fabricates, and competes internationally for the most fuel-efficient vehicle in order to address this problem and reduce their carbon footprint. The goal of the carbon fiber monocoque chassis redesign was to develop a new vehicle that increases fuel efficiency through weight optimization and aerodynamics in order to achieve 2,000 mpg, which would beat the team's current record of 1,888 mpg. The vehicle's aerodynamics and weight were optimized through iterative CAD designs and simulated in ANSYS Fluent CFD. Due to time constraints of making such a large mold at a sponsoring company, the vehicle will be fabricated after the semester concludes. With the optimized design selected, the fabrication will consist of five negative molds made from high-density foam including the top half, bottom half, two front wheel fairings, and the rear hatch. The negative molds will allow for carbon-fiber layers to have a smooth exterior surface using the resin infusion (vacuum bagging) process. For the core strength, the carbon fiber shell will be attached to a Nomex sandwich core. Nomex panels consist of Aramid honeycomb laminated with carbon fiber sheets on each side allowing for exceptional shear transfer and strength. The overall combination of the carbon fiber shell and Nomex panel, along with intermediary layers such as CNC machined foam core, will allow for a successful carbon fiber monocoque chassis.**

***Keywords - Ansys Fluent; carbon fiber; CFD; monocoque; Nomex honeycomb sandwich panel; resin infusion;supermileage***

## I. INTRODUCTION

It is known that the primary contributors to energy loss after the powertrain in supermileage vehicles are rolling resistance and drag force [1]. The carbon fiber monocoque chassis redesign addresses both of these issues in-depth by focusing on the exterior shell of the car to address aerodynamic drag and sideload. Additionally, the estimated weight reduction from designing a fully composite body is expected to reduce rolling resistance through a 28% body weight reduction and an 11% overall weight reduction.

The carbon fiber monocoque redesign spans a wide range of mechanical engineering foci including CAD, parametric design studies using computational fluid dynamics and finite element analysis, and design for intricate yet feasible mold fabrication. The new vehicle design maintains compatibility with Supermileage subsystems in addition to focusing on reducing the overall size of the vehicle, decreasing the coefficient of drag, minimizing weight, increasing driver visibility, and maintaining a high degree of safety.

This project also allows the team to integrate past design considerations that were not physically allowable in the old vehicle chassis, such as increased turning radius and wider tires and rims for reduced rolling resistance. Furthermore, the monocoque redesign allows for future proofing of the vehicle such that other subsystems can be implemented when needed. Overall, the carbon fiber monocoque chassis redesign provides the Supermileage team the ability to implement changes that minimize energy losses for nearly all subsystems.

## II. SUMMARY OF DESIGNS

The final carbon fiber monocoque chassis design follows a specific set of criteria set forth by the NIU Supermileage Team as well as the competitions attended, including SAE Supermileage and the Shell Eco-Marathon. The Shell Eco-Marathon competition requirements include vehicle dimensions such as maximum height (1000 mm), minimum track width (500 mm), wheelbase (1000 mm), height-to-track width ratio ( < 1.25), maximum width (1300 mm), maximum length (3500 mm), and maximum weight (140 kg) [2].

Following the aforementioned requirement, it was decided that three approaches should be used to design the vehicle. The first is a recreation of the vehicle geometry that the team has used since 2010 due to its previous success and ability to accommodate all of the current vehicle's subsystems. The second is a design that is influenced by the PAC-Car II from ETH Zurich, which was the world's most fuel-efficient vehicle from 2007-2018 [3]. This design takes the general airfoil profile and top profile of the PAC-Car II and modifies the critical areas needed to accommodate Supermileage's current subsystems. Design two acts more as an intermediary step between the current body and the desired body design. The third design is a combination of the current Supermileage vehicle and the PAC-Car II geometries to create the most optimal body.

| Design 1 | Design 2 | Design 3 |
|---|---|---|

***Figure 1:*** *Alternative vehicle design overviews*

All three designs were analyzed using Ansys Fluent (computational fluid dynamics simulations) to estimate the aerodynamic properties of each design (**Figure 2**). This analysis method consisted of importing the geometry into Ansys, processing the geometry into a mesh, and solving the computation problems constrained within boundary conditions to determine the fluid responses as the car is moving. The overall element size of the meshes were between 2–3 cm with between 4–4.5 million cells per mesh. The simulations used the Shear Stress Transport (SST) k-ω with an inlet velocity of 25 mph and ran for 250 iterations to reach a convergence of at least $10^{-6}$. In addition to the simulations, each design was evaluated on the basis of footprint, weight, ground clearance, wheel fairing size, nose cone geometry, and tail design. From these categories, Design Three was selected.


***Figure 2:*** *Ansys Fluent CFD analysis of Design 3*

## III. Fabrication

*Material Selection*

The main shape of the vehicle will be created by 3k 2x2 twill weave carbon fiber infused with high strength infusion epoxy. Attached to the shell will be a CNC machined piece of Rohacell 31 IG-F high strength-to-weight ratio foam. Attached to the foam will be a 1.5" thick Nomex honeycomb panel in which all subassemblies will mount to. A portion of the CNC machined foam can be seen in **Figure 3** below.

***Figure 3:*** *CNC machined Rohacell 31 IG-F foam*

The entire vehicle stack-up can be seen in **Figure 4**, in which the carbon fiber shell is cyan/transparent, with the machined foam in red and Nomex in black stacked on top.

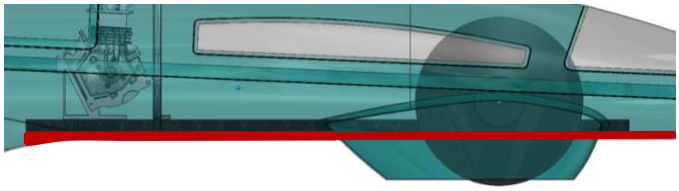

***Figure 4:*** *Vehicle material stack-up (side view)*

An aluminum tubing roll hoop and firewall was also created to protect the driver from the engine and transmission systems. All components will be attached to the Nomex panel through the use of custom 6061-T6 AL potted inserts. These inserts are designed to allow for high strength epoxy to flow around them when inserted into the Nomex panel, creating an extremely durable mounting location. The potted inserts and firewall can be seen in **Figure 5**.

***Figure 5:*** *Potted insert (left) and firewall (right)*

## IV. Results and Discussion

The entire vehicle CAD can be seen in **Figure 6**. The turning radius has improved from 32 ft to 24 ft (20% improvement), the center of gravity is 2 inches lower, the frontal cross-sectional area was reduced by 15%, the side cross-sectional area was reduced by 3%, the body weight was reduced by 28% and overall weight by 11%. Many features were added such as removable wheel fairings in case of damage, lip and groove mating features for all joining surfaces of the body, and a high level of modularity such that all internal subsystems can be redesigned if desired.

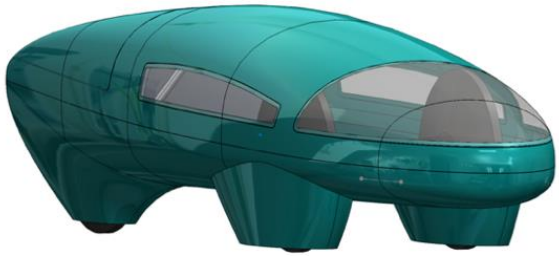

***Figure 6:*** *Full carbon fiber monocoque vehicle*

The overall vehicle redesign was successfully finished along with the desired outcomes including aerodynamic geometry improvement and weight reduction. While the mold timeline change did not allow for final fabrication of the vehicle during the semester, the team has prepared for final delivery of the molds and fabrication of the body after the conclusion of the senior design course. Future body fabrication will allow for confirmation of estimates.

## V. References

[1] P. Grady, G. Chen, S. Verma, A. Marellapudi, and N. Hotz, "A Study of Energy Losses in the World's Most Fuel Efficient Vehicle," in *2019 IEEE Vehicle Power and Propulsion Conference (VPPC)*, Oct. 2019, pp. 1–6, doi: 10.1109/VPPC46532.2019.8952212.

[2] N. Koch, "Shell Eco-Marathon 2021 Official Rules Chapter I," Shell Global, The Hague, 2021.

[3] Webmaster, "PAC-Car II - World Record," ETH Zurich, 2005.

## VI. Acknowledgments

Dr. Pohlman and Dr. Schroeder for their constant support. Mash Angolkar and Mitchel O'Day for securing montetary and in-kind sponsorship at Navistar. Jaimi Smith for his time and design expertise to allow for successful mold design and fabrication at Navistar. Chris Sorich, Bill Popek, and others for mold fabrication at Navistar. Mike Reynolds, Jeremy Peters, and Greg Kleinprinz for their support in the NIU Machine Shop. Joey Cross, Thomas Corbett, and Josh Helsper for additional support in archived Supermileage information and design/simulation advice.

# *Novel Audiometer Calibration Device*

Nana Poku *(Author)* , Papa Adu-Boaheng *(Author)*, Nicolas Rancher *(Author)*
Northern Illinois University Engineering Building
NIU - CEET
DeKalb, IL
Z1649873@students.niu.edu

***Abstract—*** *Technology has become of key importance in the betterment and care of human lives. With that being the case technology must be accurate and precise, due to the risk of error and possible harm those errors could cause. In the audiology field a design of a novel audio device comprised of a microphone and coupling apparatus was designed to be more cost efficient and simplistic to calibrate audiometers to their necessary specifications. The device will capture the audio signal of the audiometer, and process information to the graphical user interface programmed with features to analyze acoustics from the audiometer in real time. Features to display the frequency, sound level, and distortions will be necessary to accurately calibrate the device and determine necessary repairs.*

## I. INTRODUCTION:

The development of a Novel Audiometer Calibration device is no simple task. The goal above all things here is to make a: cost effective, condense user friendly audio calibration device. The idea is to downsize a relatively cumbersome assembly, and replace it with our simpler easier to use prototype. Another main goal to achieve here, is cost. The cost of some of the components that current audiologist use is fairly expensive. Cost can be mitigated using a (3-dimensional) 3-D printer. There are 3 main components that are the parameters when selecting. There is the software section, this will act as the sound level meter to produce a sound, while also being able to record the sound as well. The next portion will be the hardware, a (Micro-Electro-Mechanical System) MEMS. This is a fairly expensive device. Lastly, there is the coupler. The coupler will allow repeatable, consistent data in a controlled environment so that when measurements are taken, the data will be repeatable. The coupler will act as a housing unit for the hardware. Together there will be a device that will allow repeatable measurements, to calibrate circumaural headphones.

## II. OBJECTIVE:

The proposed project is comprised of a microphone coupler to insulate the microphone, a MEMS microphone and amplifier unit to receive audio signals, a USB-Soundcard to convert audio signals to digital signal to communicate the device. The device provides information to the program for real-time analysis. The program allows the device to show sound amplitudes by receiving the audio at sample rate of 44100 Hz, reading chunks by the determined variable $(1024 * x)$. In testing the determined chunks read was 8192 $(1024 * 4)$ chunks. The device displays an amplitude read in decibels over time plot streaming information from the device. The device displays a second screen to show the frequency response in a constant stream utilizing the same stream of the audio and converting the linear device using the Discrete Fourier Transform/Fast Fourier Transform of the audio signal. The frequency response graph allows amplitudes of incoming frequencies to be analyzed by the user. Other important features implemented is the live RMS level of the current max sound level, frequency displayed, and the harmonic distortions.

## III. COUPLER APPARATUS:

The coupler has the purpose of allowing the sound to be propagated in a controlled environment. Allowing repeatable, isolated results. Cavities take the shape of a distances mimicking the tympanic membrane, and the ear canal. The coupler also accounts for the necessary pressure that is acquired from headphones compressing on the ears. More specifically over the ears, these are a common headphone that the coupler was designed to calibrate for. The most common are supra-aural, circumaural, and hearing aids. Depending on the type of hearing device that is being calibrated, specific couplers are then used to calibrate. 2 (Cubic centimeter) cc designated for hearing aids. While 6 (cubic centimeter) cc is designated for bigger headphones such as; supra-aural (sits on ear), and circumaural (sits over the ear).

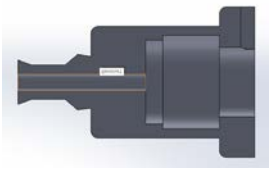

Sectional view of 2-cc

Sectional view of 6-cc

## IV. MICROPHONE AND AMPLIFIER:

The microphone used in the coupler system is a High AOP Analog MEMS microphone, the purpose is to have an affordable microphone that can receive the outputs of the audiometer. The microphone is coupled with a wide dynamic range, a high harmonic distortion, a ± 1 sensitivity, and a high signal to noise ratio. These functions will aid in the microphone's ability to filter out any unwanted noise. The amplifier is Low-Noise, High Performance Audio Preamplifier which is used to strengthen the signal of the

microphone's output so that the software can easily receive the signal.

## V. SOFTWARE:

The method to design the program and capture the audio information was designed in the Python programming language. The program utilizes various Python open-source libraries to make the program functional. The program is comprised of multiple sound analysis algorithms for proper audio processing, and displaying the real-time views of the signals, and information received from the processed signals.

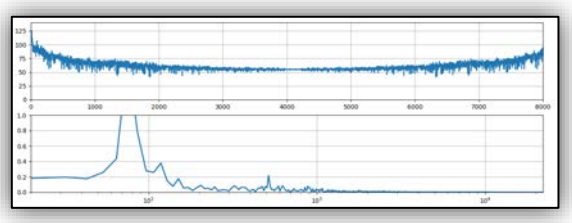

Figure 1.) Display of Novel Audiometer Calibration Device graphical user interface displaying live amplitude and frequency plots.

## VI. CONCLUSION:

The purpose of the Novel Audiometer Calibration Device is to reduce cost, repeatedly allow for a controlled environment to measure the headphones and hearing aid. While making sure to have a computer replace some of the more expensive components in the standard calibration process done by audiologist. With the goal of the project, unnecessary expensive components will not be needed. While also making sure to be portable and easy to use. There are a total of 3 sections that will make up the entire project. These sections are; the coupler a physical device that will allow for the sound to propagate through, in a controlled environment to mimic how over the ear headphones (Circumaural and Supra-aural). Another important section is the software as well. The software will allow real-time data of; frequencies, signal envelopes, sound level, and harmonic distortion. Lastly, we have the microphone which receives the audio that will be outputted from the sound level meter. We have replaced the need of a Sound Level Meter commonly called an (SML). With a standard computer or laptop. All of these components come together and will allow for audiologist to be able to calibrate systems, with ease in terms of transportation, and lowering the overall cost on the standard system.

## ACKNOWLEDGMENT

Mansour Tahernezhadi (faculty advisor), Alexander Willis (Teaching Assistant), King Chung (Client), and College of Engineering and Engineering Technology (CEET)

## REFERENCES

Smith, Steven W. The Scientist and Engineer's Guide to Digital Signal Processing. San Diego, California: California Technical Publishing, 1997.

American National Standard (1973) American national standard method for coupler calibration of earphones. ANSI S3.7-1973 - rev. 1986

International Electrotechniczl Commission (2009) IEC 60318-1 : 2009 Human Simulators of Human head and Ear fir Circumaural and Supra-aural earphones

Aspects of hearing aid fitting procedures 2010 the Netherlands, Thesis: Erasmus University Rotterdam

# Portable Photoplethysmography Sensor: Precursor to Noninvasive Blood Glucose Concentration Measurement

[1]Dhakshanan Pushparajan, [2]Kyle Butler, [3]Joaquin Rodarte
Biomedical Engineering[1,2,3]
Northern Illinois University
DeKalb, IL, USA
[1]Z1814545@students.niu.edu, [2]Z1822842@students.niu.edu, [3]Z1721585@students.niu.edu

***Abstract*— Currently the most accurate and easily accessible method to check the blood glucose levels is to prick the finger for blood samples. This method is painful and unpleasant as multiple finger pricks may be required for adequate blood supply for the detection unit. There is also a chance of infections occurring with the current method and the long-term costs are very high. This project is aimed to create a photoplethysmography (PPG) device to be further used for blood glucose monitoring that will mitigate the issues that arise due to the current methods. The primary objective is to create a non-invasive sensor that would ensure accurate monitoring of a PPG signal. The secondary objective was to relate the features of the PPG signals to estimate blood glucose levels however was not able to be done due to covid-19 restrictions at this time. Due to this the project involved generating a low-cost PPG sensor and to extract the features related to the signal that was acquired.**

***Keywords-component; PPG signal, Glucose, Non-Invasive***

## I. INTRODUCTION

The development of this instrument based on Photoplethysmography technology will revolutionize blood glucose detection. As current methods are expensive, messy, and generally unsanitary, this is not an ideal method for test for blood glucose levels. Currently, the most accurate and easily accessible method to check the blood glucose levels is to prick the finger for blood samples. This method is painful and might require the individual to prick their finger multiple times to ensure adequate blood is supplied to the device. Also, as the finger is being pricked, there is a chance for infections to occur if the needle is not sanitized. Infections can also occur at the prick site if the needles penetrate too deep in the skin and wound does not heal in a timely manner. Furthermore, an individual is required check his or her blood sugar levels multiple times a day to ensure proper steps can be taken which leads to a high quantity of needles and testing strips being required. Diabetes test strips cost on average of $50 a month and can cost up to $100 a month. Needles also need to be regularly replaced adding to that relatively high monthly cost. Due to this, the long-term monetary cost for the current method is very high. However, with the proposed non-invasive blood glucometer, users will have access to a cheaper and more sanitary method that can consistently deliver accurate results.

## II. PURPOSE

The goal of this project is to decrease the need to invasively find blood glucose levels and create a cheap, accurate, and more healthy way to read those levels from a PPG signal. This project is aimed to create a PPG device to be further used for blood glucose monitoring that will mitigate the issues that arise due to the current methods. The primary objective is to create a non-invasive sensor that would ensure accurate monitoring of a PPG signal to be later used for blood glucose monitoring.

## III. MATERIALS AND METHODS

Designing the circuit that would be used to generate a PPG signal was researched intensely to determine what would provide the best results. The schematic of the circuit used is shown below.

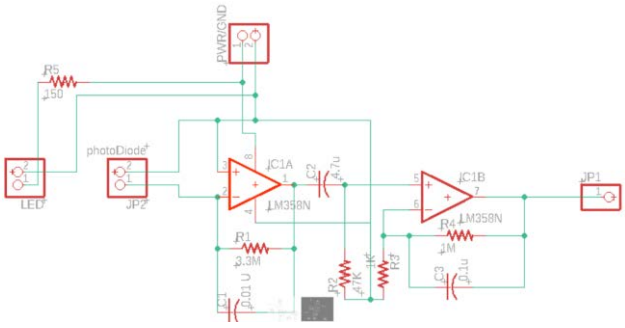


Figure 1: CIRCUIT SCHEMATIC

This circuit is a combination of using a high pass filter and a low pass filter to provide frequencies above .48 Hz and below 4.98 Hz. The average heart beats between frequencies of 1-2 Hz. Using that we determined what would be the best cut off frequencies to use to filter out unwanted noise from the signal. The circuit is composed of:

- Five Resistors
  - One 150Ω
  - One 1KΩ
  - One 47KΩ

    - One 330KΩ
    - One 1MΩ
- Two .1µ Farad Capacitors
- One 4.7µ Farad Capacitor
- One LM358 Operational Amplifier
- One NONIN Finger Probe

The NONIN finger probe is composed of an LED light that emits wavelengths around 940 nm to probably pass through the finger to a photodiode installed within the probe.

The casing that was used for this project was made in SolidWorks and 3d printed. The size of this casing is 150mm (length) x 80mm (width) x 80 mm (height). The material used for the casing was polylactic acid due to its durability and strength.

Figure 2 : IMPLEMENTATION OF SYSTEM

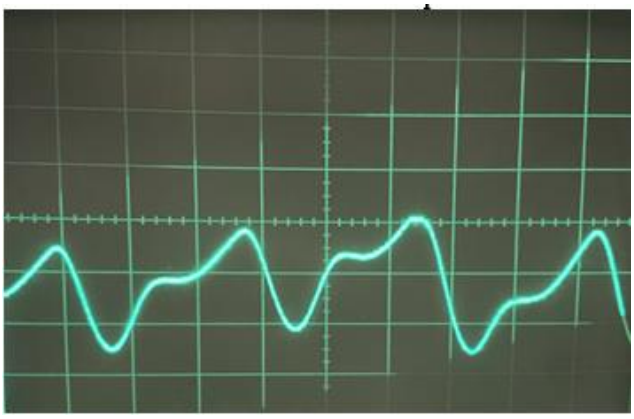

Figure 3: RAW PPG DATA. VOLTAGE VS. TIME

## IV. ANALYSIS AND DISCUSSION

The raw data obtained from the PPG sensor is shown below. This comes directly from the circuit before being processed through the MATLAB code. The signal that is shown in Figure 1, shows the diastolic arch coming before the systolic arch. Once the signal is processed through an Arduino UNO, the signal will be shown correctly through MATLAB. Once this data is digitally filtered, features will be extracted to develop patterns throughout that will analyze the PPG for future development of blood glucose concentrations.

### *A. Data Acquisition*

The data is acquired by an Arduino Uno and is processed in a MATLAB script. 500 samples are collected and stored in a 500x1 matrix file. This file is then used for extracting features that can be used to determine blood glucose levels non-invasively like finding the average waveform, the beats per minute, the width at various heights of the peak, and the peak to peak distance. The sections below will highlight the results of the MATLAB script with sample data

### *B. Averaging*

The MATLAB script takes all the PPG waveforms and segments them into individual pulsatile waveforms and averages all the waveforms into a single waveform for increasing the accuracy of the feature extraction functions.

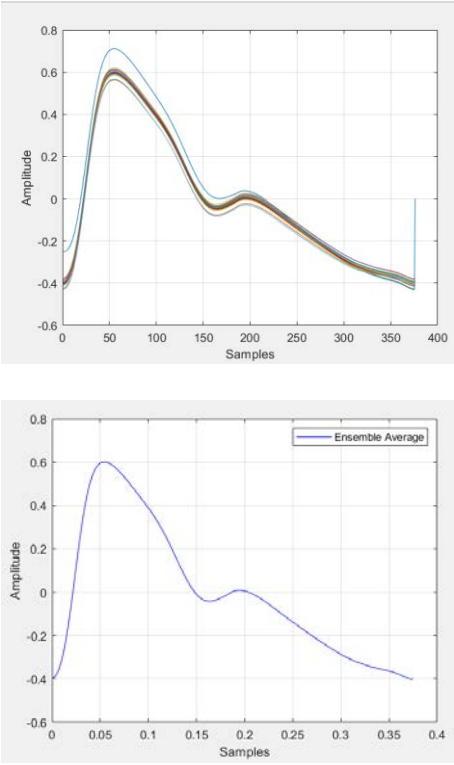


Figure 4a (top): SEGMENTED WAVEFORMS PLACED ON TOP OF EACH OTHER
Figure 4b (bottom): SINGULAR WAVEFORM

### C. *Calculating Beats per Minute*

To calculate the beats per minute (BPM), the total number of peaks found in the 500 sample is recorded. Then this value is divided by the signal duration to find the pulse rate. This is a key factor to identifying blood glucose levels as it allows the machine learning algorithm another artifact to track to increase the accuracy of the model.

### D. *Peak Width*

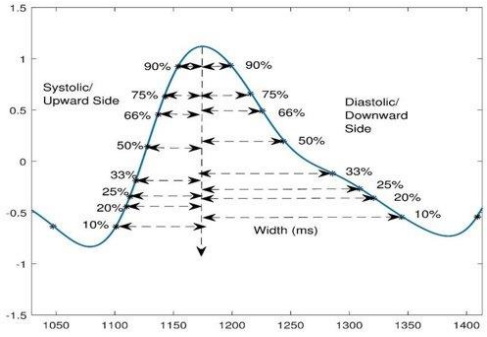


Figure 5: PEAK WIDTH

The peak width allows for extracting more accurate information of the pulsatile waveform as any baseline shift is ignored. This ensures that features that is fed into any machine learning algorithm is as accurate as possible and closely related to just the PPG signal rather than any variations that may arise. These variables could be the user's arm movement, the baseline signal of the user, and the powerline shift of the adapter. This feature also creates a more accurate picture of any changes in the pulsatile volume (aka blood flow) which can be due to changes in blood glucose concentrations.

### E. *Peak to Peak Distance*

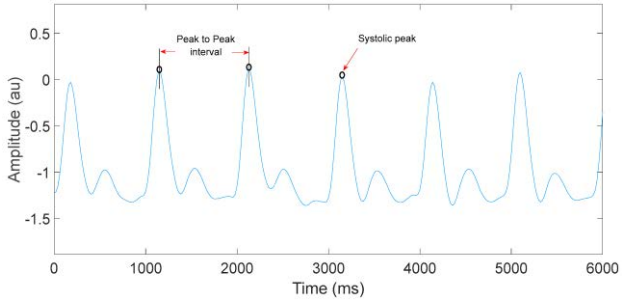


Figure 6: PEAK TO PEAK DISTANCE

The peak to peak interval is an important feature to store as variations in peak to peak voltage of photoplethysmography signals are closely related to changes in pulsatile volume. This allows the machine learning algorithm to have another feature that is closely related to direct changes in the flow of blood. This helps create a more accurate model and strengthen the connection between PPG waveforms and variations in blood glucose concentrations.

## V. CONCLUSION

This project provides a cheap and accurate measurement of a PPG signal generated through the index finger. The features extracted allow for future pattern recognition to develop measurements for blood glucose concentration and many other possibilities.


## ACKNOWLEDGMENT

We would like to express gratitude to Dr. Venumadhav Korampally for guiding us in the right path throughout this project. We would like to express thanks to Dr. Elizabeth Gaillard for allowing us to use her lab and helping throughout the biology related components. We would also like to thank Instructor Edward Miguel for guiding us through the electrical components necessary for this device to work and for supplying us with additional parts that we could not obtain without his expertise.


## REFERENCES


[1] A. Alwosheel, A.G. Alasaad, (May 2016). Heart rate variability estimation in Photoplethysomgraphy signals using Bayesian learning approach. Center of excellence in telecommunication Applications Riyadh-Saudi Arabia. https://www.researchgate.net/publication/303027808_Heart_rate_variability_estimation_in_Photoplethysmography_signals_using_Bayesian_learning_approach#fullTextFileContent

[2] Center for Devices and Radiological Health. (n.d.). Blood Glucose Monitoring Devices Retrieved December 02, 2020, from https://www.fda.gov/medical-devices/vitro-diagnostics/blood-glucose-monitoring-devices

[3] Chen, J., Wu, L., Pan, T., Xie, J., & Chen, H. (2010). A quantification method of glucose in aqueous solution by FTIR/ATR spectroscopy. 2010 Seventh International Conference on Fuzzy Systems and Knowledge Discovery. https://doi.org/10.1109/fskd.2010.5569754

[4] Goodarzi, M., Saeys, W. (2015). Selection of the most informative near infrared spectroscopy wavebands for continuous glucose monitoring in human serum.

[5] Julian, E.S., Prawiroredjo, K., Tjahjadi, G. (2017). "The Model of near infrared sensor output voltage as a function of glucose concentration in solution," 2017 15th International Conference on Quality in Research *(QiR) : International Symposium on Electrical and Computer Engineering*, Nusa Dua, 2017, pp. 146-149, doi: 10.1109/QIR.2017.8168471

[6] R-B. (2012, September 12). A DIY Photoplethysmographic Sensor for Measuring Heart Rate. Retrieved from http://embedded-lab.com/blog/introducing-easy-pulse-a-diy-photoplethysmographic-sensor-for-measuring-heart-rate

# Acoustic Emissions Tree Monitoring System

Esteban Molina-Hoyos, Theresa Li, Charles West
College of Engineering and Engineering Technology
Northern Illinois University
DeKalb, IL United States

***Abstract*—Trees play an essential role of providing oxygen and taking in the increasing carbon dioxide in the atmosphere. They can live thousands of years, but their lives can be cut short due to unexplained circumstances. The Morton Arboretum's Center for Tree Science speculates that acoustic emissions (AE) can help resolve these mysteries by detailing and quantifying the stress waves inside a tree to better understand the health and well-being of trees. For this goal, an electrical circuit and accompanying mechanical housings were designed to support an AE sensor. The AE sensor system was tested in Northern Illinois University's Digital Signal Processing Lab's anechoic chamber. During testing, the system recorded three distinct responses from each mode of testing. While the device displayed an ability to serve as a platform to collect AE readings, improvements to the mechanical housing for eventual long-term deployment and expansions to the circuit to support more detailed data collection methods can be made.**

***Keywords- Acoustic Emissions; Tree; Tree Health***

## I. INTRODUCTION

Acoustic emission is a phenomenon of radiation of acoustic waves in solids that occurs when materials undergo irreversible changes in its internal structure, be it elastic and plastic deformation [1]. For such irreversible changes to occur, the material must be subjected to external forces. It is this mechanical loading that produces structural changes that generate local sources of acoustic waves [1]. Waves generated as a part of AE are of interest in structural health monitoring and quality control. When monitoring AE during testing, it is possible to detect, locate, and characterize the damage done to the object under study. AE testing has been widely applied and studied in the industrial field, through concrete and metallic structures, metallic pressure vessels, pipelines, and composite aircraft structures, among many others [1].

Despite AE testing being prevalent in a plethora of industries, little research has been done in its application on living structures. Within the scope of this investigation, AE testing is ought to be done in two ways: actively and passively. Active AE testing involves an external force controlled by the system being applied to the tree and then studying its response. Passive AE testing involves listening to the structure and its response to naturally occurring stimuli. As part of passive testing, it is theoretically possible to listen to the tree as it undergoes its phenological processes through the developed AE system.

An AE platform would allow researchers to monitor the structural health of trees and provides an opportunity to study physiological processes, such as growth or sap flow, from a new angle. Doing so could provide better insight on internal structural changes as the tree ages and record data on its change through environmental occurrences. With more information, the client seeks to better monitor their older trees and address any health or structural issues as they arise. Similarly, it has relevance in studying physiological processes within the tree, such as plant-water relations or growth. This information will also assist in the management and development of their trees and their environment. Outside of the inner workings of plant life, the acoustic study of trees at Morton Arboretum presents the opportunity to study and measure trees' effectiveness as sound barriers to mitigate noise pollution from highways, industry, or other sources.

## II. METHODS AND MATERIALS

This client hopes for the device to be deployed on older maple and pine trees as they are the most common for them and are more likely to fail due to structural defects, which could pose a threat to their surroundings [2]. While it is desired to have a modular platform with multiple sensors collecting data simultaneously, only the acoustic emission sensor is utilized in the current design. Despite this shortcoming, the design still has the capability to be modular, where other ecological sensors can be added to the circuit with no little to no loss of function. In a typical usage case, this device would be deployed outdoors during Illinois' springtime for at least one week at a time.

A 3-D printed electrical housing protects the electronics. When deployed on a tree, the electrical housing is secured by an adjustable strap that wraps around the tree trunk. This adjustable strap loops through the rectangular cutout in the bottom half of the housing and holds the device against the testing platform. One strap in the center of the bottom housing is not sufficient to hold the system tight against the testing platform.

*Figure 2. Electrical Housing*

Inside the housing contains the circuit for the device. It is made up of a battery, switch, power rail, voltage step down converter, and microcontroller.

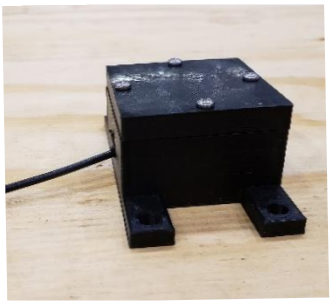

*Figure 3. AE Sensor Housing*

Connected to the microcontroller is the AE sensor that is external to the electrical housing. It is attached to a nail in the crevasse of the tree in its own separate housing. Because the AE sensor is a sensitive device, sound-dampening insulation lining the walls of the AE housing help insulate it from any unwanted noise coming from the environment.

## III. Results and Discussion

Once the microcontroller was set up to take data from the AE sensor, testing began with developing three test cases. It was decided that the AE sensor would be tested with no input response, a knocking input response, and a water flow input response. The primary interest is in the water flow response as this is the client's priority goal. The knocking response and no input response are cases to verify the AE sensor is functional. Next in the process was determining where would be the best location to test. After performing general analyze in an indoor environment and outdoor environment, it was discovered that the AE sensor is quite sensitive to everyday vibrations, like speech. Because of this, further testing was performed in the anechoic chamber. The results of this are shown in Figures 3, 4, and 5.

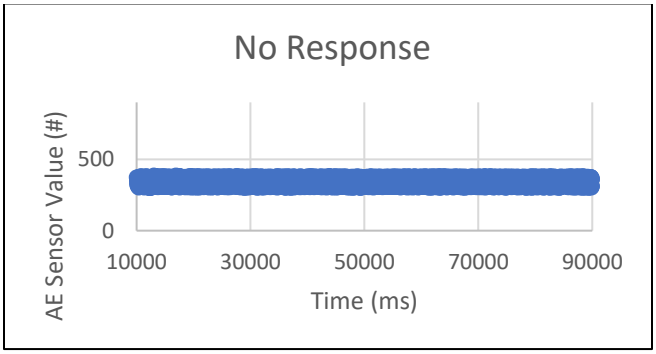


*Figure 3. AE Data Collection with No Input Response*

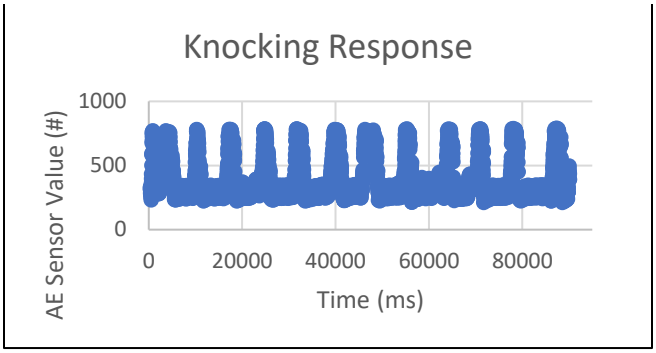


*Figure 4. AE Data Collection with Knocking Input Response*

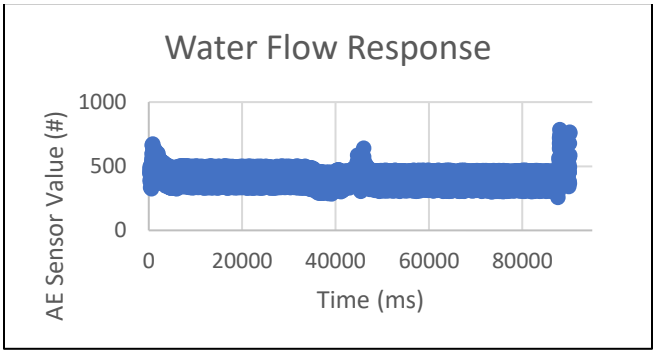


*Figure 5. AE Data Collection with Water Flow Input Response*

## IV. Conclusion

Overall, a baseline acoustic emission platform was built that would be the future gateway to expansions upon the system. There are remaining improvements that could be done before being deployed in the field. With that, a future goal is to improve the modularity and usefulness by adding additional sensors. Another would be to filter out unwanted noise from the AE sensor data when deployed outdoors especially.


## Acknowledgment

The group would like to give a special thanks to The Morton Arboretum's Center for Tree Science for giving us the opportunity to work on this project, especially Colby Borchetta and Chuck Cannon of The Morton Arboretum. The group would also like to thank our teaching assistant, Aayush Patel, and faculty advisor, Dr. Lichuan Liu, for supporting us throughout the whole process and giving us insight on the data collection portion of the project. The group also thanks the University Honors Program for supporting the project development. Lastly, the team would like to thank College of Engineering and Engineering Technology for their helpful resources and overall support.


## References


[1] "What is Acoustic Emission Testing? A definitive Guide," *twi-global.org*, [Online]. Available: http://www.twi-global.com/technical-knowledge/faqs/acoustic-emission-testing. [Accessed Oct. 23, 2020].

[2] I. Takefum and O. Masayasu, "Detection of xylem cavitation in field-grown pine trees using the acoustic emission technique," *Ecological Research*, vol. 7, Dec., pp.391-395, 1992

# Single Drum Coffee Roaster

R. Sievert, L. Freeman, A. Hastings
College of Engineering
Northern Illinois University
DeKalb, Illinois

***Abstract*—The goal of this project is to design and implement a low cost, effective coffee roaster with an innovative design of combining the heating and cooling drums into a one-piece design. This one-piece design will save material, bringing down the overall manufacturing cost and market price. Added is a touchscreen as the user interface that allows the user to set roasting cycle, followed by a cooling cycle while also numerically and graphically displaying roasting data.**

## I. Introduction

Coffee roasting dates back centuries from the early stages using simple pans held over a fire in the 15th century, evolving into commercial roasters used in the 19th century throughout the world. Throughout the 20th century, especially in the later half, coffee-houses were springing up and people were enjoying specialty coffee. At this point these coffee shops necessitated the specialty coffee roasting business [1]. Modern day coffee roasters help provide the necessary volume needed in most coffee shops. There are many varieties of coffee and several stages to the roast allowing for different flavor notes and strengths. Such examples of coffee roasts are New England Roast, City Roast, Vienna Roast, and French Roast.

The coffee roasting market is growing as people's need for coffee increases, especially special brews. The industry is valued at $533 Million in 2020, with an expected increase to $816 Million by the end of 2026. That is an increase of just over 50% in six years. This growth will require an increase of coffee houses and coffee roasters [2]. The goal of this project is to build a more economical coffee roaster to roast up to 10 lbs. of coffee per batch. The current price for comparable coffee roasters is in the $8k to $12k+ price range. The goal is to cut the final assembly and materials cost and therefore the market price by upwards of 30%, by cooling in the same drum that the coffee is roasted in. Undercutting the current competition within the marketplace. Currently, there are many types and sizes of two chamber bean roasters. The market is saturated with this style and at this price point. Having a single drum, that will roast the beans and cool them in the same chamber, will allow entrepreneurs entry into the market with a lower price point coffee roaster. Rock Valley Roasters innovative design that sets it apart from other commercial sized coffee roasters is the single drum design, seen in Figure 1 below. The design implements a modern look and techniques to achieve the perfect user-friendly coffee roasting experience at a much more affordable rate.

## II. Materials and Methods

The process of roasting coffee starts at the hopper. Raw coffee beans are loaded into a stainless-steel hopper which is seen in Figure 1. 304 Stainless Steel is used in any area with contact to the coffee beans per FDA guidelines. The hopper is attached to front door of the Drum Assembly. The beans fall through a gate which leads to the drum. The stainless-steel drum unit is a key portion of Rock Valley Roasters design that sets it apart from other competitors. The heating and cooling of the coffee beans is done within this singular drum. The Paddle Assembly, pictured in Figure 2, is mounted inside the drum assembly. The paddles rotate on a shaft pressed into bearings which are bolted to the ends of the Drum Assembly. The paddle then rotates the raw beans inside the drum. The drum, paddle, and hooper assemblies are mounted on 80/20 aluminum which provides a sturdy, modular frame.

Fig. 1. Rock Valley Roaster Design

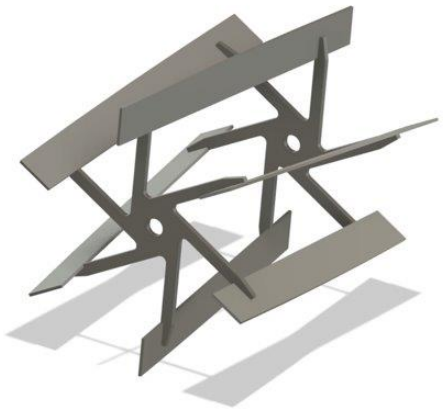

Fig. 2. Rock Valley Roaster Paddle Design

Hot air will be forced into the drum. With correct rotation speed the beans will fall into the stream of hot air, ensuring even cooking throughout the batch. Once the cooking is complete, cool air will be forced into the drum for cooling. The heat will be forced out of the unit with a positive stream of new cool air.

The user interface is a touch screen control allowing the user to control RPM and temperature set points. This interface allows easy control of important factors to roast.

## III. Manufacturing Discussion

There are a lot of components to the coffee roaster. Some of the components are off the shelf and some must be manufactured. The off the shelf parts should integrate with other parts of the system quite nicely. The manufactured components tend to raise the complexity of the build. Linking the drive unit and paddle will be a tight tolerance. A greater constraint is the tolerance in allow radial deflection between the paddle shaft and the bearing in the front and rear of the drum. There can be very a little run-out between the paddles and wall of the drum. Tolerance in manufacturing plays a big role in the cost manufacturing, and that goes for this project. Quality bearings must be used to minimalize radial run-out.

## IV. Conclusions

Rock Valley Roaster's innovative design of a single drum coffee roaster will create a change in the market. The all-in-one system with touch control will allow users to provide a quality product to their customers. As much as this system is designed for coffee houses, this system can be used for your do-it-yourself for coffee connoisseur. This will allow people to provide an independent coffee that cannot be purchased from your local store or coffee house. These people then can share their coffee with friends and family.

The desire for coffee will continue to grow as new generations grow to become coffee drinkers. These coffee houses will require coffee roasters. Young entrepreneurs have a tough time entering the market due to the high cost of ownership in new business. Our project will help new entrepreneurs enter this market by allowing them to afford a low-cost quality coffee roaster. The coffee roaster must be easy to use and set up for novice coffee roasters to make a quality product.

## ACKNOWLEDGMENT

The Team would like to thank Dr. Ghazi Malkawi for the patience and guidance.

The Team would like to recognize the efforts of Sonali Rawat for keeping the team in line, especially for beating the team over the head with "Formatting, Formatting, Formatting!"

Ryan would like to acknowledge Eileen Newcomer's saintly patience during this whole senior design process.

The Team would like to acknowledge Michael Lawson for the Python tutelage and always picking up the phone for conceptual support.

The Team would like to acknowledge Dana Sievert, thank-you for advising on electrical ideas the Team had and for helping to solve any issues that were had in LTSpice.

Luke would like to acknowledge Lars Freeman for always pushing to think outside the box when designing parts. And always bouncing ideas off of, on how to go about a particular problem and its manufacturing capabilities.

The Team would like to acknowledge Jeff Goode's expert welding knowledge and guidance.

## References

[1] Ebrahim, M. (2020, May 27). Python GUI examples (Tkinter Tutorial). Retrieved November 18, 2020, from https://likegeeks.com/python-gui-examples-tkinter-tutorial/

[2] Ltd, M. (n.d.). Coffee Roaster Market Growth, Size, Share, Trends and Forecast to 2025. Retrieved November 18, 2020, from https://www.marketdataforecast.com/market-reports/coffee-roaster-market

# Adaptive Fishing Rod and Reel for Disabled Individuals

J. Breithaupt, G. Perkins, and J. Gomez
College of Engineering and Engineering Technology
Department of Electrical Engineering, Northern Illinois University
1425 West Lincoln Hwy.
Dekalb, IL 60115

## I. Abstract

Team 6 has proposed, developed, and produced a proof-of concept prototype for a novel adaptive fishing rod and reel retrofit device that allows persons of varied degrees of disability to participate in sportfishing in a manner that is congruent with their normally abled peers. Bait casting style fishing reels and rods are a mainstay within fishing arsenals of many individuals in North America. Due to their inherent construction, they are unwieldy, or at times, impossible for differently abled fisherman to use as their design hinges on two-handed operation. In response, a retrofit device was created such that people experiencing total inability to use one hand and/or arm may now use bait casting equipment in a manner that emulates the experience had by those with full use of both hands and arms.

## II. Introduction

The team underwent experimentation to set appropriate human input parameters and subsequent output power needs. Advanced electrical power storage devices and motors were sourced to provide a modular device that is the first of such devices to provide variable speed retrieve capabilities to the user. Likewise, electrical, and mechanical design features allow the user to operate the device while utilizing all the features of the fishing rod and reel in a safe and ergonomic manner.

## III. Material and Methods

The objective of the project was to be able to create a device that would facilitate the task of fishing for individuals with limited mobility with one arm. The main challenge from the project was to retrofit a device into an existing fishing reel. This was achieved by using multiple off the shelf products to be able to create a proof of concept. The major components of the assembly are displayed in (Fig 1) of the high-level block diagram.

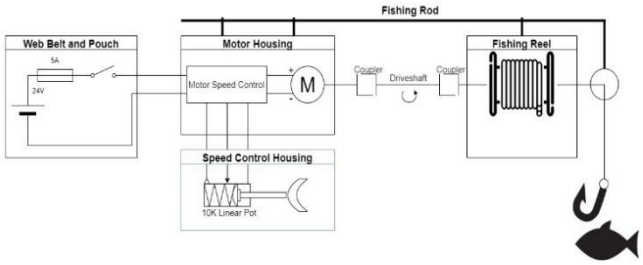


Fig 1. High Level Block Diagram

### A. Brushless motor

The main challenge when the project was started was being able to find an appropriate motor for the intended use of the fishing rod. To meet the appropriate specifications that where needed for driving the fishing reel; two tests were performed on the fishing reel to meet these specifications. The first test was testing the torque need to engage the fishing reel drag. Testing the fishing reel drag was done by using a torque wrench and reading the value at where the torque wrench would engage the drag setting. The result was 2.71 Nm, and this torque was used to narrow done the motor selection. The second test was done to find an equivalent rpm that a normal user could perform on the reel. Measuring reel speed was measured by counting the revolutions as the wheel was spun by hand. The average speed result from the test was 170 revolutions per minute. After the test was performed, we narrowed down the motor selection to a motor that would be able to hit the desired specification such as 2.7Nm and have at max rpm of 200. Additionally, the brushless dc motor we used was able to fit the desired specification and it included an integrated board (Fig 2) that would allow the user to run the motor without additional hardware development.

Fig 2. Interior of Brushless DC Motor w/Transistors

### B. Pontentiometer

Being able to control the speed of reeling in a line is an important process of being able to fish since fishing is not only the equipment but technique as well. When the motor arrived, the team noticed that the board included an integrated potentiometer (Fig 3). The placement of the potentiometer was problematic, and the style of potentiometer was not ideal for fishing. The team was able to find an equivalent potentiometer that was in a style of a spring-loaded plunger that was attached to the board via external cables. This was ideal because it would allow for the potentiometer to be placed in a more ideal position and create a trigger system that when let go, it would turn off the motor.

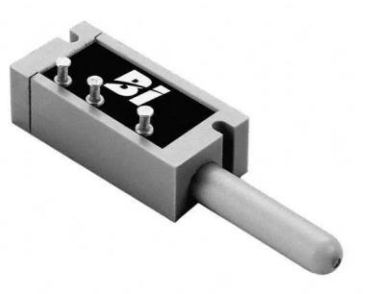

Fig 3. Spring Loaded Potentiometer

### *C. Flexible drive shaft*

The flexible drive shaft is one of the most important parts of the build it allows for the motor to be placed in a more ideal location, while allowing it to still be connected to the reel. The team went with a DeWalt flexible drive shaft since the drive shaft has the moving components enclosed, this allows to minimize danger to a user. The only drawback that a future revision would be is finding a drive shaft that would still be shielded but be much lighter in weight.

### *D. Couplers*

To be able to attach the motors and fishing reel to the flexible drive shaft, couplers are needed. The team decided to go with two aluminum set screws couplers. One of the couplers was treaded to attach to the fishing rod handle screw was. For a future revision getting a stronger material would be advised.

### *E. Batteries and safety switch*

For ease of use for a potential user the team decided to go with a battery that would be found at almost any store. We went with a 24v, 4 Amp hour battery. This battery was able to match the motor specification. To attach to the motor, we used an adapter that would convert the three prong leads from the battery into just a two lead that would simply attach into the motor. During construction, the team notice a potential hazard with the battery, and it was decided to add a switch that would be able to power off the board while switching battery. This switch was attached with a fuse that would protect the board from potential hazard.

### *F. Battery Pouch*

While the team was in the initial phases of discussion on the project one of the things that was discussed is where would the battery be attached. It was designed to reduce weight on the rod itself, a better location to place the battery would be in a case. The team was able to find a military style belt pouch that would allow the user to insert the battery in it and to rest the fishing rod on top of it while in operation.

### *G. Case*

The case is what hold the whole project together. The case was design to house the motor board, the motor and hold the rod on top of it. For testing purposes, a 3d printed case was designed and printed that allowed for a friction fitted motor and a retrofitted rod that was secured with a house clamp. Despite the case not being build out of the strongest material it is able to withstand the torque outputted from the motor. Additionally, a case was design that transform the potentiometer into a trigger, which worked out great. For future revision stronger material and some revisions are needed to accommodate the board.

## IV. DISCUSSION AND RESULTS

Upon completion of the project, the Adaptive Fishing Rod and Reel for Disabled Individuals successfully pulled a weight of 5lbs over 50 yards. The device's design successfully incorporated a variable speed retrieval system, which is the first incorporated in this type of product. Design and construction of the device lends itself to easy use as it properly orients the user's hand to the device. Along with successful testing of the prototype, the parts making up the assembly are low cost and easily sourced.

## V. CONCLUSIONS

The device described here within should act as a basis for which a manufacturable product may be further developed for this niche in the adaptive fishing market. This prototype suffices as proof that advanced, electric motors and respective control circuitry are economically available, off-the-shelf battery options are easily procured, and capable technologies exist to produce the mechanical drivetrain parts and covers to facilitate a venture to produce this product within the sportfishing marketspace. In this, greater development may be taken to produce casements, user controls, and an appropriate drive shaft mechanism to be feasible for large scale manufacturing activities.

Upon initial design and assembly, it is apparent that the product could be produced a price point that is both economically advantageous for a company operating within the fishing market and could be provided to the consumer at a price point that allows for a great deal of inclusion for the target population. Furthermore, the adaptive fishing rod and reel retrofit device would allow far greater inclusion of individuals within these sportfishing communities and provide recreational and therapeutic opportunities not currently available to several hundred thousand differently abled people on the continent of North America.


## ACKNOWLEDGMENT

This project was largely made possible as a result of the overall organizational support of Northern Illinois University's College of Engineering and Engineering Technology. A special thank you is extended to Dr. Donald Zinger for his oversight as the primary staff advisor and Sonali Rawat as the acting graduate assistant to the project. Furthermore, the team would like to thank Dr. Staci Connery, PT and Dr. Mary O'Rourke-Perkins, OT for their expert medical consultation in the realms of their respective professional practices.

# Sustainable Energy - Pyrolysis of Low Density Polyethylene

D. Rotta, D. Street, C. Wallace
Department of Mechanical Engineering
Northern Illinois University
Dekalb, IL 60115

***Abstract* - With global plastic production growing at an unprecedented rate, plastic waste pollution is continuously growing, causing threats to wildlife, and increasing greenhouse gas emissions. The development of an electric-powered pyrolysis system that converts plastic waste to liquid fuel presents a promising solution to this problem, and an incentive to collect plastic waste that is so abundant in the environment. The proposed system is modular, benchtop scaled, and able to be powered by renewable energy sources. The system also provides a base for further implementation with other existing refining technologies such as fractionation. Furthermore, it creates an economic incentive to collect plastic waste in the environment, as it provides an efficient and reliable way to convert it into usable fuel.**

## I. Introduction

According to PLOS ONE, 351x10^6 metric tonnes of plastic was produced in 2015 [1]. Of that plastic approximately 90% goes unrecycled. Pyrolysis, the thermal decomposition of a material at high temperatures, presents a way to harness energy from waste plastic. By pyrolyzing low-density polyethylene (LDPE), energy can be extracted from the plastic in the form of shorter length hydrocarbons. LDPE, $(C2H4)_n$, is the most used packaging material globally and is resistant to biodegrading, making it an appropriate plastic to study due to its significant negative environmental impact. Hydrocarbons from LDPE can be condensed and used in a similar fashion to hydrocarbons produced in a standard oil refining process. Hydrocarbons come in a vast assortment of lengths, with only chains of lengths 14-20 carbons corresponding to diesel. Vapor from the pyrolyzed LDPE is sorted through zone heating such that only hydrocarbons that are diesel length are recovered. Once passed through these zones, the diesel-like hydrocarbons are cooled in a condenser, converting the vapor into liquid fuel. Plastic-to-fuel technology such as this system is proven to reduce greenhouse gas emissions and fossil fuel use.

## II. System Components and Methods

### A. *Experimental Process*

LDPE is loaded into the furnace where it will eventually vaporize from high temperatures provided by electric heating. The vapor will then pass through the reactive distillation column where a chemical reaction occurs, altering the chemical composition of the vaporized feedstock. Finally, the vapor passes through a condenser where diesel like fluid is yielded.

### B. *Furnace*

The furnace is carbon steel pipe with a dome shaped bottom. There is a pressure release valve that doubles as an inlet for purging. The top of the furnace is flat plate with 3 holes: one for a Type K thermocouple for temperature monitoring, one for an agitator that stirs plastic within the furnace, and one for an outlet that transports plastic vapor from the furnace to the RDC. To minimize heat loss, the furnace is wrapped in a layer of fiberglass wrap. Additionally, a fiberglass insulated sheet metal cylinder encloses the furnace.

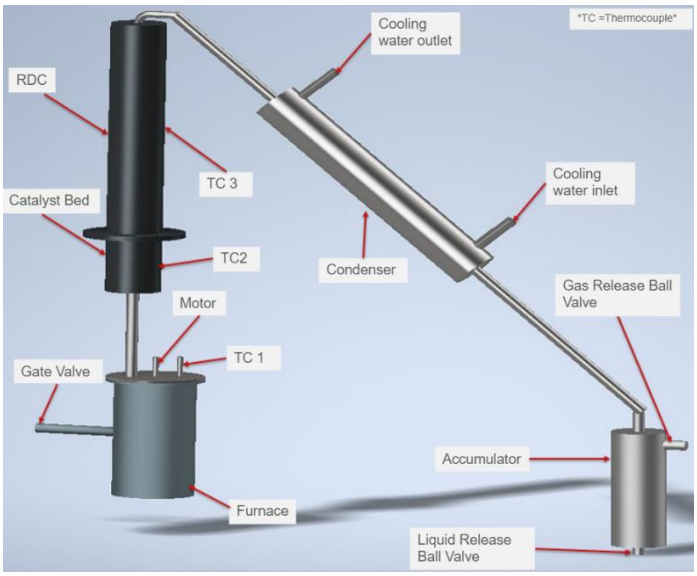


*Figure 1: 3D Model of System*

### C. *Reactive Distillation Column (RDC)*

The RDC is composed of two flanged, carbon steel pipes with endcaps welded at the opposite ends. The flanged pipes allow users to disassemble the RDC to clean interior walls as well as add or remove the catalyst bed. There are two heating zones within this component. One located at the catalyst bed and the other towards the top of the RDC.

### D. *Condenser*

A water-cooled condenser is used to condense yielded product. It utilizes room temperature water from a large container, and a pond pump to control the flow of water.

E. *Accumulator*

The accumulator acts as a collection vessel for yielded liquid as well as a pressure release for uncondensed vapors. There are two ball valves used to control the outgoing flow of these two fluids.

## III. Data

Data that is collected is composed of both thermal and chemical behavior data. Initially, thermal testing of the components was conducted, monitoring temperature using thermocouples to observe the general behavior of the furnace and RDC. In any case, heating a steel vessel externally requires heat transfer analysis. To do this, one would use the following equation to get an estimate of the power needs for one hour of heating to achieve a certain internal surface temperature.

$$KW = \frac{W_t * C_{px} * \Delta T}{3412} * (h) \quad (1)$$

Here, KW is the kilowatt amount needed for the process. $W_t$ is the weight of the material being heated by conduction heating, $C_{px}$ is the specific heat of the material, $\Delta T$ is the temperature difference from start of process to the end, and $h$ is the time in hours of the process. 3412 is the conversion factor to go from BTU/lb*°F to KWh. Figure 2 shows the trend of thermal behavior for the furnace and RDC, where figure 3 shows the thermal gradient of the furnace.

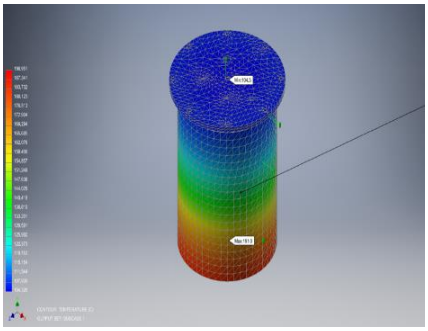

*Figure 2: Thermal Gradient of Furnace*

Temperature data from Type K thermocouples displays a relatively constant, yet down trending heating rate for the furnace. The reactive distillation column settles at two distinct temperature zones separated by approximately 30C. The temperature difference of the RDC is crucial for isolating heavier than diesel hydrocarbon fractions that have a higher boiling point than diesel. As the vapor passes up into the RDC, heavier fractions will see a progressively lower temperature along the height of the RDC and condense inside. These fractions fall back into the furnace, where the diesel fractions will continue in vapor form to be condensed.

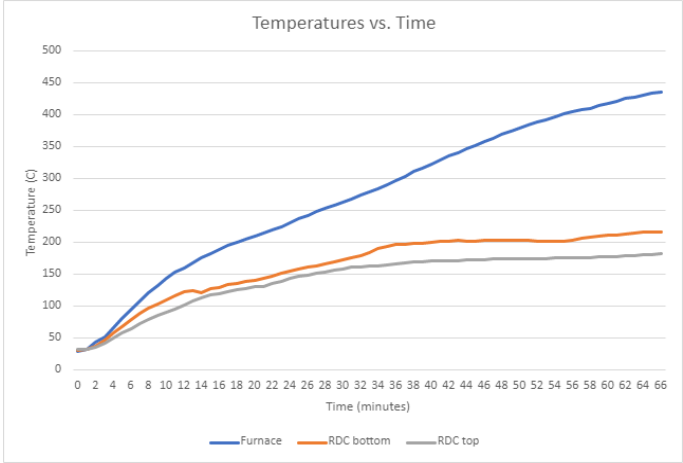


*Figure 3: Heating Rates per Minute*

When considering the efficiency of the system, standard mass balance was used. The volume of the input was recorded and compared to the recovered volume from the outlet of the accumulator. Ideally ratio would be 1, however inefficiencies of the system such as leaks within welds and pipe connections allow for some vapor to escape. The following formula describes this relation:

$$RP = \frac{v_f}{v_i} \quad (2)$$

where RP is the recovery percentage of liquid product, $v_i$ is the initial volume of the feedstock, and $v_f$ is the final collected liquid volume. Expected RP is within the 20%- 45% range, based on trial data. In the case of LDPE, using the average density of the LDPE and weight of the feedstock is sufficient to calculate volume, initially.

## IV. Conclusion

The data collected from test runs using water as feedstock proves that the system exceeds required temperatures for this process to occur, but also shows that the system is capable of vaporizing and condensing a substance in a closed environment. Based on thermal behavior of the system, it can be inferred that feedstocks with higher boiling points can be processed in the pyrolysis system.


## Acknowledgment

Without advice from Dr. John Shelton, Dr. Scott Grayburn, help with fabrication from Mike Reynolds, Jeremy Peters, Greg Kleinprinz, and help from Dr. Douglas Klumpp of the Chemistry Department this project could not have been accomplished.


## References


[1] S. Royer, S. Ferron, S. Wilson, D. Karl (2018). "Production of methane and ethylene form plastic in the environment." Plos One, 13(8): e0200574. https://doi.org/10.1371/journal.pone.0200574

# *Ergonomically Designed Folding Chair to Promote Correct Spinal Alignment*

A. Lazzerini, M. Boesen, A. Garcia
Team #8 Mechanical Engineering
Northern Illinois University
DeKalb, USA
Z1805147@students.niu.edu
Z1858762@students.niu.edu
Z1860161@students.niu.edu

***Abstract*—The purpose of this project was to alter the position of the common folding chair. This chair is catered to the comfort of the spine while sitting. Many common folding chairs have a slight inclined seat angle with the horizontal. This project increased the seat angle as well as the back rest angle. A comfortable rocking chair position was applied to the folding chair. A novel implementation of a telescoping back rest system was added to allow each user to adjust for their own comfortability.**

***Keywords- folding chiar, angle, anterior pelvic tilt, steel, welding***

## I. INTRODUCTION

Estimates say that up to 85% of men and 75% of women suffer from a condition called "Anterior Pelvic Tilt" [1]. Many Americans have developed bad posture due to sitting for many hours of the day at work and at home. Workers are using chairs that while comfortable, are not optimal for the human body in terms of posture and ergonomics. The common workplace and the advancement of technology has led to many people sitting hunched over staring at a computer screen for most of the workday without moving. This can have major ill side effects on the human body. This phenomenon has gotten so bad that it is recommended that workers take a break every hour from sitting and stand up, walk around to help stretch and work their unused muscles. Standing desks are an alternative to seated desks and are becoming more popular to promote better posture. Sitting for extended periods of time can lead to the weakening of the glute muscles and tightening of the hip flexors. When the hip flexors become tighter it can pull on the muscles in the lower part of the spine and this is part of what creates the tilt in the pelvis. Weak glutes can lead to the pelvis being anteriorly tilted or tilted forward. This is known as anterior pelvic tilt.

The goal of this project would be to combat anterior pelvic tilt by designing a folding chair that puts the pelvis in a more posterior pelvic tilt position. By posteriorly tilting the pelvis, or tilting backwards, the spine is put in a more neutral position. This can align the spine and take the pressure off the lumbar section relieving lower back pain. This can be accomplished by altering the seat and back rest angle with the horizontal. Another goal was to produce a rough porotype model that could be further optimized for a relatively low cost through mass production.

## II. METHODOLOGY

According to a recent study [2], a seat angle of 5° helped relieve lumbar disc pressures. A back rest angle of 110° helped to reduce forward head posture as well. By having a posteriorly rotated seat angle, this rotates the hips backwards. When the hips are rotated backwards, the lumbar section of the spine flexes less and algins the spine. Taking these considerations into account, a rocking chair provides optimal comfort as well. When in the rocking position, a rocking chair provides a seat angle of 8° and a back rest angle of 116°, see Figure 1 below.

Figure 1: Optimal Seat Angle

The chair features a sliding bar mechanism on the bottom of the seat as shown in figure 2. This serves two purposes. The first being that is allows the chair to fold up and lay flat. This allows for ease of storage and transportation. The other purpose is that it will set the default angle for the chair.

The angle of the chair is the most important part of this whole project. This angle that the team will set will achieve the goal of fixing the anterior pelvic tilt. The sliding mechanism shown in the figure below will have a "hard stop" in order to stop the chair at the appropriate angle. The cross member that the leg bars will slide on will be made of aluminum along with the frame of the seat on the chair. It is welded to the bottom of the chair's seat frame. This is to allow for the chair to be as strong as possible, as to not change any angle. Wleding and common fasteners hold the project together. The chair is made out of low carbon steel and 3-D printed parts.

Figure 2: Sliding Bar Mechanism

## III. RESULTS

Performing Finite Elemental Analysis on the legs, bolts, and the chair as a whole, our team finds that most of the stress is concentrated on steel bolts that pass through the steel leg tubing. This is advantages to us because the bolts will be made of the strongest material on the entire chair. All other excess forces are placed the steel tubing for the legs which appears to hold up exceptionally well. The assembly was created using class 5 bolts and nylon locking nuts. In the FEA performed they exceeded expectations with no failures present. FEA models are illustrated in figures 3 and 4.

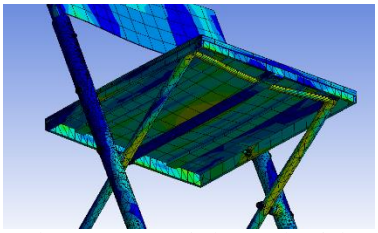

Figure 3: FEA Analysis on entire chair

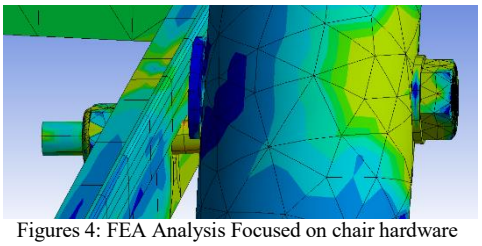

Figures 4: FEA Analysis Focused on chair hardware

Sitting in the chair feels good. The rocking chair position is nice an applies well to the folding chair. The chair can fold up and users can alter the back rest support position. Lower initial setting of the back rest will accommodate the average height for humans. From [1], the average height for adults greater than 20 years of age in the US is 69.1 inches (175.4 cm) in men and 63.6 inches (161.5 cm) for women. While the next adjustment up will be able to extend to help support for above average heights by adding a couple more inches of adjustment. The back rest adjustment is created by using telescoping tubing with holes for a detent pin to allow for sliding. The holes will be drilled to fit the size of the button pin. Then the detent pin will be slid in the tube. The tube on the back rest will have a slightly larger outer diameter to fit around the original tubing and allow for sliding.

## IV. CONCLUSION

Overall, the design was proven to be acceptable for the desired task or correcting spinal alignment and fixing anterior pelvic tilt. The chair's strength performs exceptionally well the design parameters set in place. The prototype was produced, and mass production of the model would reduce unit cost.

## V. ACKNOWLEDGMENT

We would like to thank Ghazi Malkawi (PhD), Sonali Rawat (Teaching Assistant) for their contributions and assisting with the critiquing of the design.

## VI. REFERENCES

[1] Herrington, Lee. "Assessment of the Degree of Pelvic Tilt within a Normal Asymptomatic Population." Manual Therapy, Churchill Livingstone, 11 June 2011, www.sciencedirect.com/science/article/abs/pii/S1356689X11000816

[2] Donald Harrison, Sanghak Harrison, Arthur Croft, Deed Harrison, Stephan Troyanovich, Journal of Manipulative and Physiological Therapeutics, Volume 22 Issue (9), 1999 November. DOI: https://doi.org/10.1016/S0161-4754(99)70020-5

# Autonomous Soil Analysis Unit

C. Keough, H. Tillhof, G. Schroeder, M. Kennett
Department of Mechanical Engineering, Department of Electrical Engineering
Northern Illinois University
DeKalb, Illinois 60115

***Abstract*—The Autonomous Soil Analysis Unit (ASAU) is designed for the use of the NIU Mars Rover Club; however, its applications span across many different fields. The purpose of the ASAU is to make the collection and analysis of soil samples autonomous and reliable. The ASAU employs multiple ideas and components to complete its goal and displays versatility in doing so. This prototype version of the ASAU is built so that sensors can be replaced to accommodate exactly what the user needs.***

## I. Introduction

Engineers are often diagnosed as introverts- focusing solely on their sphere of work. However, if the conversation between engineers and scientists became commonplace, technology could transcend past societal expectations. The birth of the first Mars Rover set the example for merging scientific research, mechanical design, and electrical innovation.

The Northern Illinois University Mars Rover Team is a robotics team that designs, manufactures, and analyzes an autonomous robot for the University Rover Challenge (URC). This international competition will test the capabilities, endurance, intelligence, and strength of the rover through several tasks. The Autonomous Soil Analysis Unit will focus on the science portion of the URC challenge- committed to finding traces of extinct or extant life.

The system must autonomously collect soil along a prescribed path, transfer the soil onboard, and study the sample using sensor instrumentation or chemical analysis. The capabilities of the rover extend past interplanetary examination and into agricultural development- exemplifying the value of engineering design through scientific background. ASAU merges the action of collection and investigation into a single mechanism.

The autonomous system can provide a solution to a lengthy and costly process that involves agricultural workers sending soil samples into labs for testing. The ASAU will grant farmers the ability to test soil samples themselves, search for suitable information pertaining to their needs, and eliminate the time-consuming process that is currently in place.

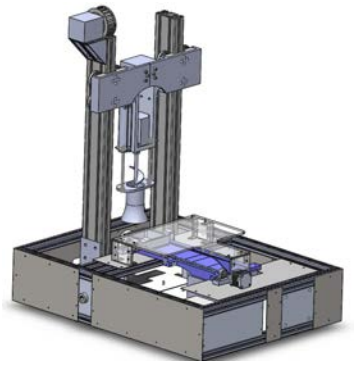

Figure 1: Full Model of ASAU

## II. Methods and Materials

The ASAU has three distinct subtasks integrated into one system to satisfy the main goal of collecting and analyzing soil samples. The three subtasks - soil collection, distribution and analysis- have been designed to work as one fluid, intelligent machine.

### *A. Soil Collection*

The actuation system is comprised of a heavy series timing belt pulley system mounted to two pillars of 15 series extruded aluminum. An H-series timing belt and mating heavy duty timing pulleys allows stability and control of the gantry plate through actuation. The trapezoidal teeth of the timing pulley and belt system provides high positional accuracy, power transmission, and durability.

The actuation system is attached to an assembly containing an auger and driving motor. The auger assembly is raised and lowered to collect and provide soil samples into the soil distribution subtask section. The auger assembly is comprised of mostly solid Acrylonitrile-Butadiene-Styrene (ABS) 3D manufactured parts with pieces of sheet metal to provide added reinforcement.

Figure 2: Auger Assembly

### B. Soil Distribution

Once soil is collected in the auger assembly, the auger is raised above a soil collection cup. The auger acts as a screw conveyor that will release ample soil that will be tested. The soil collection cup includes a track mechanism that allows the cup to move from the collection area, into the analysis area, and then finally deposits the tested sample into a waste bin. The track mechanism allows the cup to deposit the tested sample in a way that is efficient, without the use of extra motors. The collection cup, as well as the soil distribution track are 3D printed out of solid ABS material.

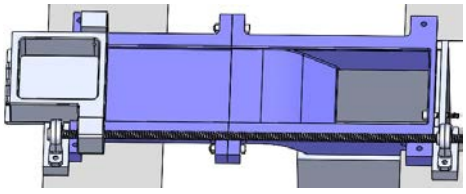

Figure 3: Track and Soil Collection Cup

### C. Soil Analysis

The analysis subtask section of the ASAU will contain two sensors: a soil moisture sensor and an environmental combo sensor. The environmental combo sensor will test for total volatile organic compounds, CO2 concentrations, temperature and humidity of the soil. These tests are only a small fraction of the possible data the design could collect- with the right adaptation of sensors and programing. The sensors incorporated to the analysis subtask will be mounted above the soil distribution track on an acrylic base. Soil Analysis is completed using an Arduino Uno, a Nema 17 motor, a DM542S motor driver, a solenoid linear actuator, a 24V power supply, and the soil moisture and environmental combo sensors.

## III. Applications

The ASAU is designed primarily for the NIU Mars Rover Club's use for the University Rover Challenge. However, the system can be implemented for an agricultural and scientific setting as well.

### A. Agriculture

Pesticides, unruly compounds, and loss of nutrition could ruin a field of crops if it is not ritually surveyed. ASAU, with the full capabilities of the Rover, can autonomously survey land with prescribed GPS coordinates, collect and reject soil samples, and provide meaningful data about the land. Data can then be streamlined and archived directly to a personal device for instant results and history accumulation. With a proper Graphical User Interface, a user would be able to see the biological parameters of the land change over time.

### B. Scientific Research

Just as NASA tests for specific compounds or signs of life on extraterrestrial planets, the ASAU can act as a primary tool in geological and biological research- with the relevant sensors attached. The ASAU can be adapted to test for minerals for mining purposes, detect specific organisms for biological research, evaluate environmental conditions within unhabitable spaces, or anywhere in between. The performance of soil collection and analysis does not require human intervention, leading to an easier investigation of unsympathetic territory.

## IV. Conclusion

The ASAU can be used in a wide range of applications- merging multiple fields of study and allowing greater harmony between scientific and mathematical researchers. This prototype design provides a basis for the NIU Mars Rover Team to build from, learn from, and encourage further creative advancements to the design. The Mars Rover Team has collected the fundamental research to extend the design past sensor basics and their future advancements leave great promise to the success of NIU student organizations. With recent developments and newfound excitement in space exploration, testing soil can lead to evidence of life on other planets- such as Mars. Perhaps, in some time, humans can even combine the task of agricultural and space exploration when the human species establishes civilization elsewhere.

## V. Acknowledgments

We would like to thank Northern Illinois University for allowing us the opportunity to be extremely creative and build something we are proud of. We would also like to specifically thank Dr. Peterson, Dr. Butail, Dr. Salehinia, Dr. Taesam Kim, Dr. Lee Sunderlin, Sonali Rawat, and the entirety of the NIU Mars Rover Team for their fantastic assistance and guidance.

# Remote Control of Laser Components

Peter Coffell[1], Erick Koenig[2] Teofanes P. Ruiz[3], Stanislav Baturin[4]
Department of Electrical Engineering [1, 3,4] Department of Mechanical Engineering [2]
Northern Illinois University
Dekalb, USA

***Abstract*—This project seeks to create a device by which drift due to temperature fluctuations can be corrected when using an optical table. Discussed herein are the development and testing relevant to the design of a mechanical device and the supporting code. For the purpose of this paper, the design is viewed in the context of a prototype developed at Northern Illinois University for an eventual implementation at Argonne National Laboratory.**

***Keywords-Optic table, Laser calibration, Automated Controller***

## I. INTRODUCTION

Thermal expansion is a phenomenon by which materials expand as their temperature is increased. These deformations are generally incredibly small. As an example, the coefficient for linear expansion in aluminum is $25X10^{-6}$ ($1/C^0$). While these dimensional variances might not have an appreciable effect in most cases, when working at high levels of precision, these variations must be considered.

Argonne National Laboratory is an industry leader in particle acceleration research. To these ends, they employ an optical table to create electron packets for use in their accelerator experimentation. When working at the atomic level, as is required in accelerator research, thermal distortions can provide an appreciable source of inaccuracy.

The device discussed was developed to provide a real-time correction for any thermal distortion encountered due to temperature fluctuations in an experimental setup. It employs two high-precision stepper motors to adjust the trajectory of the laser on both the horizontal and vertical axes. The magnitude and direction of these adjustments are determined by a Raspberry Pi running a code developed as part of this project that uses the input from a high-definition camera to assess what corrections are necessary.

## II. DESIGN METHODS

The solution proposed here utilizes a mechanical device that is driven autonomously by decisions made by a program developed during the execution of this project. This project contains both a mechanical component and a software element, which are discussed in this section.

### *A. Electrical Components*

This project is designed around the use of a Raspberry Pi 4b, a microcomputer with a Linux based operating system meant to be flexible for multiple uses. *Jupyter notebook* is an open-source software used to execute python scripts [1]. The Jupyter notebook interacts directly with the raspberry pi implementing the logic of the controller via a web service that allows users to write, edit and execute python scripts with the hardware. This service is essential, as it allows users to interact with the controller remotely, as the controller needs to be in proximity to be hardwired into the motors. For Argonne this is crucial as the enclosure housing the optical tables and controller can be hazardous at times.

Additional electrical components include the use of the Thor Labs KDC101 Stepper Motor and Controller. Two of these are necessary to fulfill the mechanical design of this project as two are needed to control the adjustments in the y and x axes. Thor Labs KDC 101 stepper motor can be adjusted for use in python by translating the hex-based codes sent to the motor into python, allowing for "Forced" commands [2].

### *B. Software*

The program receives the position of the laser as an input from a high-definition digital camera. Upon start-up, the position of the laser is noted by the program in terms of an X and Y component. These initial values are viewed, and the controller is designed to use this to make decisions to reach a desired target position. The software will continue to make all efforts to adjust the optical mount to correct the laser to the targeted position. The program continually assesses the value of both the X and Y values to make these corrections.

### *C. Mechanical*

The mechanical portion of the project incorporates two THOR labs stepper motors (P/N Z825B) to manipulate the horizontal and vertical trajectory of the beam. All components were machined from 6061 aluminum unless otherwise noted. This provides consistent thermal properties throughout the mechanism. The lens holder, seen in black, was provided by the Northern Illinois University physics department.

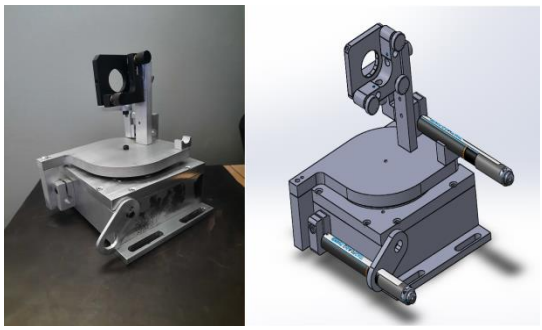

*Figure 1: Shown here is the actual device compared to the CAD model. Very few changes were made from the original design to the piece that was produced.*

As the horizontal motor extends, the rotational plate spins clockwise, moving the beam to the right. As the motor is retracted, the spring return located in the base keeps the push block tight against the end of the motor, moving the beam left. The rotational plate is located by a 360-alloy brass center pin. It rests on 8 5/16 steel ball bearings that are spaced by a 3D-printed retainer.

Vertical motion is accomplished by control of the stepper motor mounted to the mast. As the stepper motor is spun out, it acts against the vertical push block tilting the lens upward. As the motor is retracted, the spring keeps the push block tight against the motor thus lowering the beam.

## III. Results and Discussion

This design implemented currently works for any indoors environments and can be assumed to be functional in other indoor settings. The logic behind the corrections made in the software to adjust the Thorlabs motors is geared towards making micro adjustments relative to the change in temperature in an environment that might warp or otherwise change the optical setup in a way that is not intended by lab users. This software can run indefinitely and has the correct housing to ensure that it can run indefinitely save for loss of power. The housing acts as a heat sink and protects the pi from any external environmental factors.

The device employs two THOR Labs stepper motors (P/N Z825B). These units have a resolution of 29 nanometers[1] (3.94e-8 inches) per step. When combined with the lever arm used in the horizontal direction, each step of the motor results in a change of $3.5X10^{-7}$ degrees. For the vertical direction, the resolution is $4.1X10^{-7}$ degrees per step. At a distance of one meter, this translates to a deflection of 6.1 micrometers on the horizontal axis and 7.2 micrometers in the vertical direction.

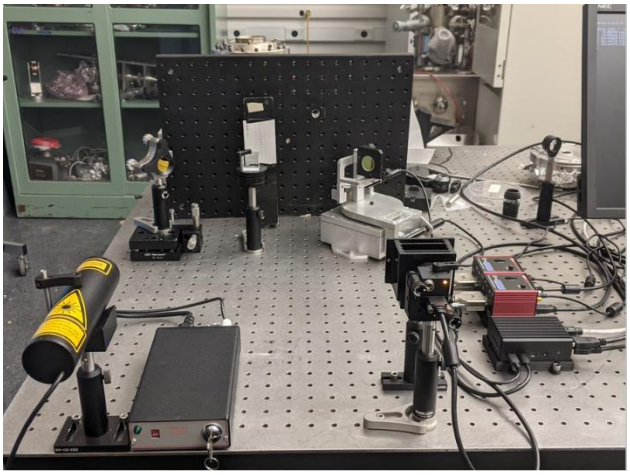

*Figure 2. Laser system set up.*

## IV. Conclusion

Through the course of this project, a program was developed allowing remote access to manipulate the trajectory of a laser system on an optical table. The supporting hardware was also created to allow for this process to occur. A Python script was loaded onto a Raspberry Pi that can manipulate two stepper motors to maintain a laser's trajectory based on input from a camera. The interface with the system happens through Jupyter allowing the device to be controlled from a remote location. Further development on this project could include a more refined mechanism that can accomplish the same high level of resolution with a smaller footprint on the optical table. The implementation of the laser positioning system will allow experiments to be run more efficiently and precisely. Various problems concerning the environmental effects on the position of the laser beam can now be mitigated. In the future the code can be refined to be able to handle more complex parameters.

## V. Acknowledgements

The authors would like to thank the NIU Machine shop for their assistance in production of portions of the device. Additional thanks to A.J. Dick for assistance with portions of the code. The authors would also like to thank Dr Stanislav Baturin for his guidance. Thank you to Dr. Piot and Argonne Labs.

## VI. References

[1] "Jupyter," [Online]. Available: https://jupyter.org/. [Accessed 08 04 2021].

[2] Thorlabs, "Thorlabs APT Controllers," Thorlabs, 2015.

[3] J. Beck, "Physical Computing with Python," *Projects Raspberry Pi,* p. 3, 2019.

[4] S. Hassan, "Controlling a DC motor with a Raspberry Pi 4," *Maker Pro,* 2020.

[5] R. Condit, "Brushed DC Motor Fundamentals.," *Microchip,* 2004.

[6] T. Magdy, "Controlling a DC Motor with Raspberry Pi and Python," *Electronics Hub,* 2017.

# Miniature, Lightweight, Unnoticeable, Hearing Aid

Senior Design Team 11

Pedro Hernandez, Rakshil Soni, Selina Cervantes

*Dr. Mohammad Moghimi*

College of Engineering and Engineering Technology Northern Illinois University, DeKalb, IL, USA

***Abstract* — Conductive hearing loss is a common defect in infants and younger children that can occur at birth or in later years. Conductive hearing loss involves physical deformation of the outer and middle portions of the ear [3]. If hearing loss is not resolved within a few days after being discovered, the infant may have trouble in developing language, speech, and communication skills throughout their life. The current solutions for conductive hearing loss include bone-anchored and cochlear implanted hearing aids [2, 3]. The problem with these devices is that they require invasive procedures such as surgery or implantable aid, which is not an ideal method to be carried out on newborn infants and younger children. The purpose of this device is to create a non-invasive solution for conductive hearing loss that is suitable for infants and young children.**

## I. Introduction

According to Boston's Children Hospital, "conductive hearing loss is the most common cause of hearing loss in infants and young children. It happens when something is blocking the outer or middle ear and preventing sound waves from reaching the inner ear."

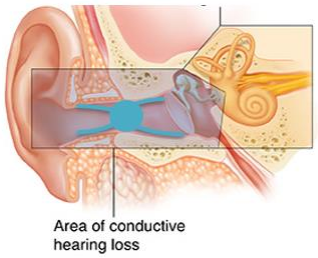


*Figure 1: Common area for conductive hearing loss.*

A blockage forms at the outer portion of the ear, this can be seen in blue in the above figure. The blockage prevents sound waves from reaching the middle and inner ear. Sound waves travel into the outer section of the ear and continue to flow into the middle and inner portion where the Tympanic membrane exists. The Tympanic membrane vibrates in response to these waves and allows us to hear [1]. Most children are either born with conductive hearing loss or others get an ear infection leading to this condition [2,3]. Existing devices and solutions are directed towards adults and are not proven to be suited for children under six years of age. These solutions require surgical procedures or implanted aid [4]. Waiting for a suitable age can be counterproductive: if hearing loss is not solved in the early stages of life, then a child can experience a struggle to develop language, speech, and communication skills, which will affect them in the long run.

## II. Project Design

The design for this project is a miniature device that has a strip like form factor that sits on the hairless portion of skin behind the user's ear. This emulates the functionality of typical bone-anchored and cochlear implanted hearing aids without the need for any invasive procedures. The uniqueness of this design is that using a contact actuator, the device will be able to vibrate against the skull and send signals to the inner ear [3,4]. These vibrations will be perceived as sound, making the device safe for children as it requires no invasive procedures. The focus of this project is to prove this concept by designing a prototype of the miniaturized hearing aid. The prototype has proven that the simplistic miniature design can be achieved through further research and development [3]. The main components for this device include a micro-electromechanical systems (MEMS) microphone, piezoelectric actuator, breadboard, and other necessary electronic components (resistors, capacitors, etc.) to fulfill the design needs for the project. Figure 2 shows an overview of the device's functionality in the form of a flowchart along with an image of the prototype.

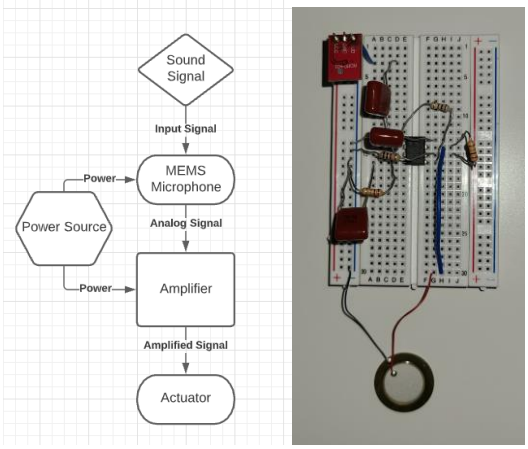


*Figure 2: Flowchart and prototype*

As shown in the flowchart the device can detect sound signals in the atmosphere using a MEMS microphone and convert that signal into an analog signal. The analog signal is filtered and amplified through the audio amplifier designed in the electronic circuit portion of the design. The electronic circuit and MEMS microphone are powered by an external power source. The amplified signal is finally sent to the actuator which will produce an analog vibration signal. To analyze the vibration signal being generated an accelerometer is used and placed on a flat surface along with the actuator.

## III. Results

The output of the device is tested by removing the MEMS microphone device and replacing it with a signal generator so that a constant signal is being sent through the device to get accurate results. Figure 3 represents the data collected from the experiment comparing the Input signal to the output voltage. From the graph it is made clear that there is almost no signal loss from the system

when tested from a frequency range of 20Hz-20kHz. The only major deficiencies occurred when the device was operating from 20-100Hz, this is because at lower frequencies the electronic components struggle to pick up such small signals.

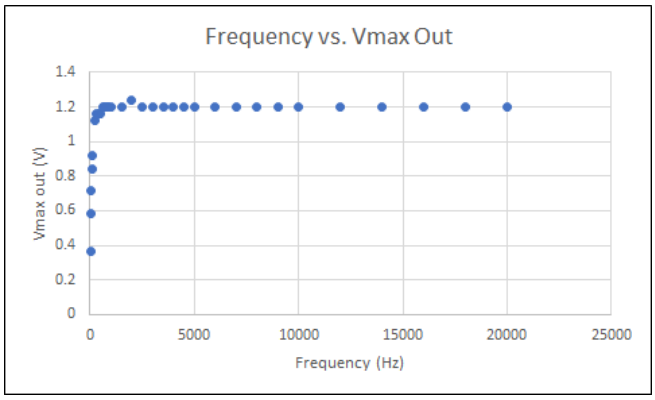


*Figure 3: Graph of Frequency vs. Vpp Out*

A test that was run involved testing the device with the MEMS microphone and the PE actuator connected. In this test it was observed that when speaking into the microphone the vibrations created by the PE actuator do in fact correspond to the audio signal being inputted [2,5]. The image in Figure 4 shows the input signal from the microphone in yellow and output audio signal going into the PE actuator in green.

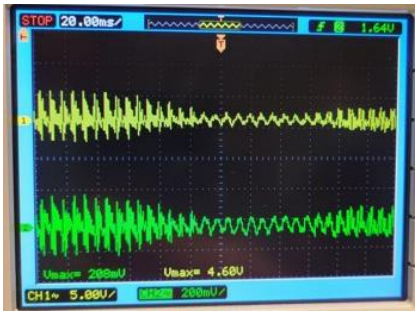


*Figure 4: Input/Output signal of the device via speech*

Additional testing was done to characterize the actuator [3]. The chosen actuator has a small radius and is thin (less than 1um). This actuator would have a resonance frequency below 1kHz in order to encompass the most common noises and was driven by the circuit used for the device [2,5]. Dampening of the actuator (by PDMS) was taken into account when deciding the final prototype actuator. In Figure 5 the input signal (green) versus the output signal of the chosen actuator (yellow) is shown.

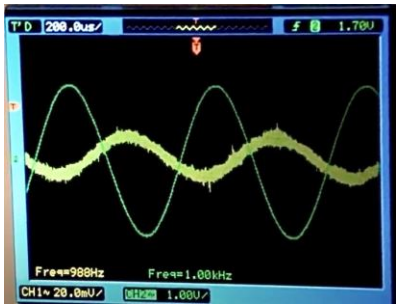


*Figure 5: PE actuator signal compared to input signal*

## IV. Conclusion

The next step to improve the device would be to fabricate the circuit and try to package the device in a smaller form factor which allows the device to be tested on individuals to see if the vibration signals are producing a strong enough signal for the individual to hear. This prototype has provided the proof of concept for future research and development. Along with that the device needs to be tested with a battery device such as a flexible battery as the external power source being used in this prototype is obviously not miniaturized for the final design.


## Acknowledgment

Members of this group would like to thank faculty mentor and client, Dr. Mohammad J. Moghimi and TA, Sandhya Chapagain for their support and guidance through this project. The group would also like to thank Mr. Edward Miguel for allowing the group to work in his lab and help us with our circuit design needs.


## References


[1] Alberti, P. W. (2006). The anatomy and physiology of the ear and hearing. Retrieved October 3, 2020, from https://www.who.int/occupational_health/publications/noise2.pdf

[2]Qin, X., & Usagawa, T. (2017). Frequency characteristics of bone conduction actuators – Measurements of loudness and acceleration. *Applied Acoustics, 126*, 19-25. doi:10.1016/j.apacoust.2017.05.007

[3] Shin, D., & Cho, J. (2018). Piezoelectric Actuator with Frequency Characteristics for a Middle-Ear Implant. Sensors, 18(6), 1694. doi:10.3390/s18061694

[4]Center for Devices and Radiological Health. (n.d.). Overview of Device Regulation. Retrieved from: https://www.fda.gov/medical-devices/device-advice-comprehensive-regulatory-assistance/overview-device-regulation

[5]M. (2018, February 5). Piezoelectric sound components. Retrieved from https://www.murata.com/~/media/webrenewal/support/library/catalog/products/sound/p37e.ashx?la=en-us

# Design of Automated Residential Window System

B. Howe, K. Kruse, E. Parker
Department of Electrical and Mechanical Engineering
Northern Illinois University
DeKalb, IL 60115

***Abstract*—The Automated Window System enables users to raise and lower residential single-hung windows from any web enabled device capable of browsing the web. It allows for opening and closing the windows to five different levels, as well as automatically locking the window in the desired position. Additionally, it is designed to be user-friendly, allowing users to operate the window at a simple click of a digital button from anywhere in their homes. The design includes precision magnetic limit switches for accurate and consistent opening and closing to desired levels. All devices required to operate the system can be powered from a single electrical connection.**

## I. Introduction

Homeowners often turn to electric cooling systems to regulate the temperature in their homes. Often this is done more so out of convenience than necessity. Navigating throughout a home to open windows to create airflow is a burden for some, and others may struggle to raise and lower windows. Utilizing electronic air conditioning to alleviate these issues increases power consumption considerably. Although this may seem minor, air conditioning systems alone account for 17% of the total residential electricity usage [1]. Utilizing this automated window system aims to not only add convenience to users, but also decrease overall residential power consumption by increasing the usage of home windows.

## II. Methods and Materials

The goal of this project was to create a system that is extremely easy to use, remains quiet during operation, and creates results that are accurate and repeatable. This was accomplished utilizing high quality materials and controls. The result of this project is a highly functioning proof of concept.

### A. Two 12VDC Worm Drive Gear Motors

The primary goal of the project was to raise and lower the window consistently with minor alterations to a standard residential single-hung window. Overcoming the natural friction of a window, as well as lifting the weight of the window, is a challenge for most small DC motors. This challenge was overcome by utilizing worm drive gearboxes in conjunction with the motors in order to reduce speed, but increase the torque tremendously. The result is smooth operation in a small package.

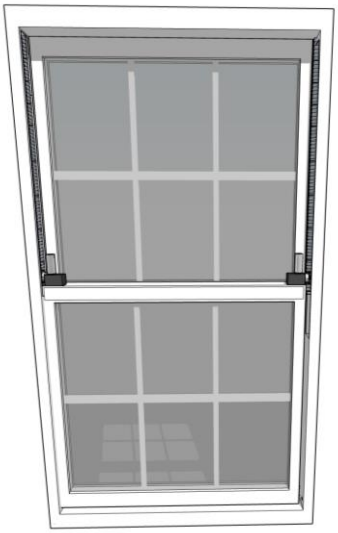

*Figure 1: DC Motors Mounted on Window Ledge*

### B. Rack and Pinion System

In order for the motors to lift the window, a mechanical connection point is necessary. A 1018 carbon steel rack is mounted inside the window channels and hidden from view of the user. These racks span the entire length of the upper portion of the window. High precision machined pinions are mounted on each motor to engage the rack. The motors and pinion travel with the window during operation.

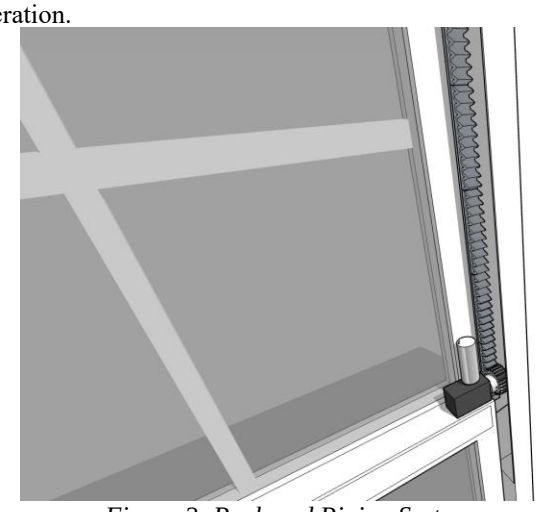

*Figure 2: Rack and Pinion System*

### C. Raspberry Pi Zero W

To control the system and generate a web server for user input, a Raspberry Pi Zero W is utilized. Using a single-board-computer allows for seamless integration with the users existing wireless network, as well as motor controls that are fast and precise. Dedicated pulse-width-modulation GPIO pins allow for motor speed control to be tailored to each individual application of the system. Utilizing a board with 40 GPIO pins allows for the system to be expanded to multiple windows without the need of an additional control board.

### D. 120VAC to 12VDC Transformer and 5VDC Converter

Another goal of this project was to produce a system that can be powered from a single electrical connection. This created a challenge due to the various voltages required for each design element. To accomplish this, a transformer is used to convert a standard residential power system to a 12VDC signal suitable for the motors used. Additionally, powering the Raspberry Pi through its GPIO pins requires a steady 5V, 1.2A signal. A transformer rated for 5A output current is used to provide sufficient current to both the computer, and the motors, even under load.

### E. Motor Driver

In order to utilize the 3.3v GPIO output voltage to adequately operate the 12v motors, a motor driver H-bridge is used. When connected to 12v power from the transformer, no additional power sources are required to use the system.

### F. Magnetic Limit Switch and Neodymium Disc Magnets

A limit switch is necessary within this design to safely turn off the motors when the window has raised or lowered to the user specified level. Due to space constraints within a standard window, a magnetic switch is used to eliminate the need for any physical contact. In conjunction with the magnetic switch, several neodymium disc magnets are mounted allowing the window to engage the switch at the various positions. This allows the window to raise and lower to exact positions consistently, with little to no maintenance required or excess friction created.

### G. Pulley and Counterweight

This design requires motors to travel approximately two feet while the window is in motion. This creates complications due to the distance in which the wiring to the motors must travel. To create a higher level of aesthetic, pulleys are mounted on the outer framing of the window, and use a counter-weight to smoothly retract extra wire when the window is raised. This allows for all slack to be retracted away from view of the user, and eliminates the risk of damage to the wiring.

## III. Results and Discussion

The prototype was designed to enable integration to existing windows in the user's home. To accomplish this, the design requires minimal alterations to the window itself, and all components are mounted on the exterior framing, with the exception of the lifting mechanisms. The prototype was fully developed and tested, and shown to create consistent and accurate results, well within design parameters. The user interface was developed to provide users exceptional ease of operation, as well as important information at their fingertips. This information includes current window position, as well as hourly and daily local weather.

## IV. Conclusions

The prototype developed as a result of this project was largely successful. Due to the space limitations and variety of residential windows on the market, more alterations to the window were necessary for successful operations than originally anticipated. However, this remained within acceptable levels as determined by the development group. Overall goals of the project include consistent raising and lowering, ease of use, a single power source, an aesthetically pleasing design, and quiet operation. The use of high torque motors, and high-quality rack and pinion system allow for complete functionality with repeatable results that meet all design goals.

## V. Acknowledgements

The success of this project was largely facilitated by the overall support and guidance of our faculty advisor Dr. Donald Zinger. Additional gratitude is extended to the team's graduate advisor German Ibarra. We would additionally like to thank Northern Illinois University College of Engineering for the organization and development of this program.

## References

[1] U.S. Energy Information Administration - EIA - Independent Statistics and Analysis. (2015). https://www.eia.gov/energyexplained/use-of-energy/electricity-use-in-homes.php)

# Senior Design Team 13: Two Degrees of Freedom Helicopter

Authors: Jonathan Cepeda, Vijaysinh Rana, Ryan Tuohy

Northern Illinois University Department of Electrical Engineering

Dekalb, Illinois

***Abstract*—The Two Degrees of Freedom Helicopter is a useful tool that will be used in a laboratory setting to study control systems and aerodynamics. This device simulates the movement of a fully-functioning helicopter by allowing both rotation and movement in a pitch and yaw motion. The data captured will show the angles and acceleration data of both directions in real time using MATLAB and Simulink software with a Raspberry Pi Microcontroller. This device was built to test control systems safely, to be economically affordable, and to be more accessible than similar systems currently on the market.**

## I. Introduction

This Two Degrees of Freedom Laboratory Helicopter system is designed to be used in a laboratory setting, specifically a control systems laboratory. This device allows users to study the control system of a fully functioning helicopter system on a small scale, which is both safer and economically affordable. The system can rotate in the clockwise direction and in the counter clockwise direction while being able to tilt in a pitch or yaw direction. The data for the system is then recorded through various sensors on the device and then the data is saved through a combination of MATLAB, Simulink, and the Raspberry Pi Microcontroller. The basics of this device can allow students studying control systems to view how control systems work and the concepts of aerodynamics.

## II. Design of Device

Figure 1: Current Mechanical Structure of the Laboratory Helicopter

This device is made to measure the rotation and motion in a pitch and yaw direction. On the opposite ends of the main control arm is a full rotor assembly with a rotor guard and propeller blades. One rotor assembly faces upward and the other faces sideways, which represent to motion for the pitch and yaw respectively. Both directions have encoders, which are small sensor boards for motion, that will capture data in real time. Once the data is captured form these encoders, it will be sent to the MATLAB and Simulink connection to store the data with help from the Raspberry Pi Microcontroller. The bottom aluminum box is designed to hold the electronic components on the inside.

### A. *Propeller/Propeller Guard System*

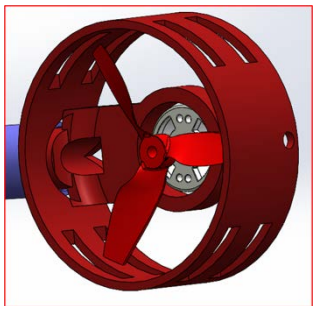

Figure 2: Propeller with Guard System

The mechanical structure of the propeller and guard system contains the inside shaft for the propeller to sit on and the guard piece itself is connected to a horizontal PVC pipe that connects across the upper bracket that acts as the main control arm for the pitch and yaw direction.

### B. *Upper Bracket Assembly*

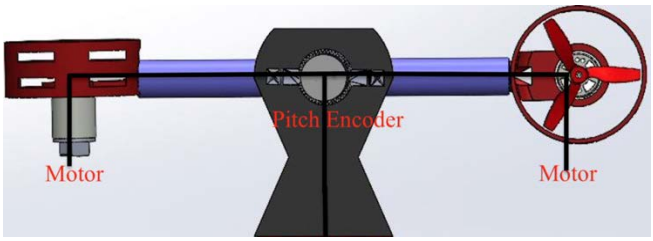


Figure 3: Upper Bracket Assembly

The upper bracket assembly of this device contains both rotor assembly pieces, the main PVC pipe arm, and the

upper bracket piece that is attached in the center. The main bracket piece contains the pitch encoder bracket attached to the side. The upper bracket contains a dowel rod that connects through the center of PVC pipe to the opposite end of the main bracket piece that will allow for the pipe to tilt.

### C. *Lower Bracket*

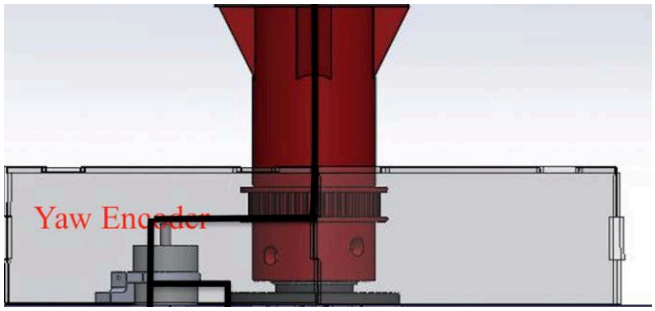


Figure 4: Lower Bracket/Rocket Piece

The lower bracket piece, also called the rocket piece, is attached to holes cut on top of the base box assembly. This piece is able to rotate in either the clockwise or counter clockwise direction. Through the rocket piece, wires are threaded up on the inside that connect from the electronics in the bottom of the box to the motors and encoders on the upper bracket.

### D. *Aluminum Box Base*


Figure 5: Side/Section view of Box Base

The last section of this device is the box base where the electrical components are stored. This is to keep the electronics in place for easy access and to keep the components safe from potential hazards. On the inside of the box is the Raspberry Pi 4 Microcontroller, Motor Driver, Power Adapter, Power Supply, and a connection that will connect from the device to a computer for data acquisition. The connections for these components are threaded up through the lower bracket piece, through a slip ring, and up to the electrical components that drive the device motion.

## III. Electrical Devices

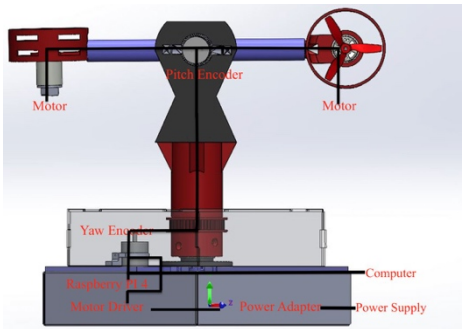


Figure 6: Full view of device with Electrical Components

As stated in the previous sections, there are several different electrical components that help power this device. The Power Supply runs at 24 Volts, which allows for the motors to run at full power. The Motor Driver will help power the motors and can be controlled by the MATLAB and Simulink interface to determine the power of the motors. The Raspberry Pi 4 Microcontroller contains the code that then is connected with MATLAB and Simulink software. This connection allows for user input to change the motion or direction of the device. The Power Adapter is 24 Volt AC to DC that can be plugged into any outlet for easy use. The computer port allows for this device to be controlled from a connection to the device to a computer by a USB plug in. The encoders for pitch and yaw directions will be giving back real time data from the code as the device runs. An IMU device will act as a gyroscope, which will allow the device to determine its orientation and speed. These motors can run from 15,000 to 20,000 RPM, which allows for sustainable rotation of the device.

### A. *Raspberry Pi/Simulink Connection*

To control this device, there is a connection from the Raspberry Pi 4 Microcontroller to the Simulink software through MATLAB. Inside of Simulink, there are Two PID controller block diagrams in which can be simulated to control the device through different variables or commands. To connect everything to the Raspberry Pi 4 Microcontroller, the microcontroller board comes with an SD card that needs to be loaded with data from the MATLAB program. After the connection is made from MATLAB/Simulink to the Raspberry Pi through using package add-ons that are supplied by MATLAB and Simulink, the SD card must be plugged back into the Raspberry Pi and the full connection will be made in order to use the PID controllers.

## IV. Final Remarks

The Two Degrees of Freedom Helicopter can be a beneficial device for students or professors to use to study how control systems work and the basics of aerodynamics. This iteration of the device is designed in mind so that it is widely available for universities or control laboratories to use since this model is made to be more cost efficient than similar devices that are on the market, like the Quanser AERO system. The replacement parts that are available for this device are made to easily available so that anyone that wants to use this device can fix or use it in an educational or laboratory test setting. We would like to thank our project client Dr. Hasan Ferdowsi, our teaching assistant German Ibarra, and Northern Illinois University for their help and support for this project.

# IoT-Based Patient Monitoring Device

Matthew Lowe, Matthew Baldwin, Tyler Dieter
Department of Mechanical Engineering
Northern Illinios University
Dekalb, IL United States

***Abstract*—the IoT is the Internet of Things which promotes increased informational utility by increasing the connectivity of devices either by Bluetooth or hardwired connection. These principals were applied to an integrated system which is capable of running three independent functions (data collection and processing, database updates, GUI and display) across two distinct processors (Raspberry Pi and Arduino Uno) with the ability to include additional hardware modules in the future.**

***Keywords- IoT; GUI; Health Metrics; Database; Sensor***

## I. INTRODUCTION

With the rise of computing technology becoming widely available, transparency and accessibility to information is expected to increase. The importance of accessibility in health information and services has inspired the design of a IoT-based health monitoring system. The conception was to allow an individual of any level of technological comfortability – hereafter referred to as the user – to interact with a high degree of transparency with their own biological measurements. Specifically, this would ensure either safety during recovery in situations like physical therapy or could also allow for maximizing the efficiency of a workout to allow for greater results or monitor with precision the degree to which a physical activity exerts the body. This data would be made transparent to the user via the graphical user interface (GUI) to display real-time data of a verity of different metrics. The initial conception includes an array of sensors which would measure the heart's beats per minute (BPM), the blood's oxygen percentage level (O2 level), the user's temperature, and the blood pressure. The GUI would display these three values as often as an update is received in three locations that can be viewed simultaneously as well as the duration of the session. Whenever the GUI is updated, the program would also log the values of the health metrics to a database for storage until a bulk transmission would be made. Once the session has been completed by the user, the data would have the option to be sent to a physician or logged likewise via the internet.

## II. DESIGN FEATURES

The device uses a pulse sensor that is connected an Arduino Uno that is then connected via a wire to a Raspberry Pi. An LCD screen is connected to the Raspberry Pi and it displays a GUI and a graph of the pulse sensor data. The system is powered by a Lipo rechargeable battery that is integrated through a battery board. The Raspberry Pi, LCD display, battery board, and battery are all enclosed within a 3D printed case.

### *A. Raspberry Pi*

The Raspberry Pi is the main hub of the device, it reads from the serial of the Arduino Uno to collect the pulse sensor data, and then displays the information in the GUI. The pi stores all of the necessary files and all the information either flows into or out of it.

### *B. Arduino Uno*

The Arduino Uno is a microcontroller board that is flexible and has numerous libraries and pins that are used to connect to the pulse sensor. It has a C based integrated development environment (IDE) that collects data from the sensor and pushes it to the serial plotter using the Pulse Sensor Playground library. See Figure 1 below.

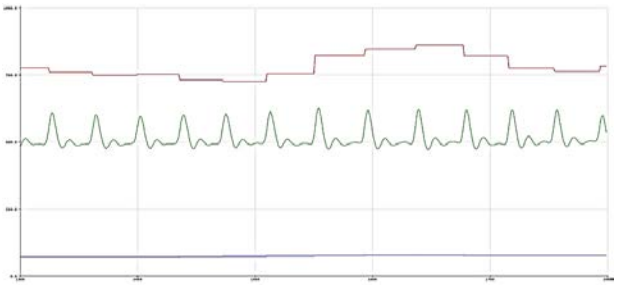

Figure 1: Serial Plotter of Pulse Sensor Data

### *C. Pulse Sensor*

The pulse sensor is used as the main health monitoring sensor for our project. This sensor is able to read beats per minute (BPM), amplitude wavelength, and the inter-beat interval (IBI). The sensor data is read by the Arduino Uno.

### *D. Power Supply*

The battery that powers the whole system is a lithium polymer ion 10,000 mAh rechargeable battery. The size of the battery needed was determined through empirical tests of how long a pair of 3600 mAh batteries lasted under multiple loading conditions. Then this data was linearly interpolated to allow for an expected 8 hours of battery life.

### *E. Housing*

The major mechanical process within the project was the case design. The case was designed with ease of maintenance. The case houses the Raspberry Pi, the LCD screen, and the battery/battery board. The switch on the outside of the case allows the user to turn the device on and off without opening up the case. The cord protruding from the side of the device allows for the battery to be charged easily as well. The ports are left accessible so that the

Arduino can be connected to the raspberry pi without any obstruction. This same slot is also used as a means for providing ventilation to the Rpi. The physical and virtual prototype design for the case can be seen in Figures 2 and 3 below.


Figures 2 and 3: Physical and Virtual Case Designs

### *F. GUI*

The GUI was built using a library that allowed for the insertion of buttons and display the data collection when the aforementioned buttons are pressed. Once the data collection is complete, the stop button is pressed which then sends the collected data to a file which is then handled by the database process. The GUI is displayed in Figure 4 below.


Figure 4: Graphic User Interface

### *G. Database*

Once the data is collected and sent to a file, it is then emailed. The email process utilizes a library to do so, and it is connected to a Gmail account specifically for the device. The email with the data file attached can be sent to any other email address required, including the user for their own records.

## III. Communication

Certain limitations reduced the efficacy of the wireless communication being the sole mediator between the main processor and the sensor array peripheral. The complexity of Bluetooth integration directly to the peripherals suggested more reliable results could be obtained by using wired connections from the peripherals to a external processor which would act as a hub for the data and a potential node for the Bluetooth connection specifically acting as the transmitter for the data. This unit was successfully integrated into the prototype and serves as a collection point and early data processing unit. The communication method has the remote processor – the Arduino Uno in the prototype – wired directly to the main processor – the Raspberry Pi – such that communication happens via this cable and the digital information is written to the remote processor's serial port and is read from there by the main processor. However, the digital infrastructure has been left in a modular setting such that future iteration can easily enhance the design by allowing for an upgrade to Bluetooth communication if found to be a viable procedure. However, the Bluetooth protocol structures had unexpected levels of complexity that were prohibitive to the progress of the project within the framework that would require such an inclusion be made.

## IV. Conclusion

The design connects the health metric sensors to the main processor which is able to log and display the data for the user and optionally submit the data to a medical professional for review. The user can view the data in real time and begin and end sessions at any time. Ending a session will trigger the submission of the data – if so desired – to an email address that they may designate. Iteration may be performed to increase the mobility of the unit by upgrading the physical connection to a Bluetooth version which would require notable computer science proficiency to accomplish. Like with many electrical components, reducing the excess volume is an area of great interest. To accomplish this would require reducing the size of the housing unit by increasing the packing efficiency in a way that still permits the circulation to properly cool the processor. Another way to improve the device would be allow the display of data over time, likely in the form a graph in the GUI; this can currently be done in the Arduino IDE, but isn't yet implemented into the GUI.

## Acknowledgment

The authors would like to acknowledge the College of Engineering and Engineering Technology for providing our group with the means and support to complete this project. We would also like to thank both Dr. Ji-Chul Ryu and Dr. Pradip Majumdar for their support, resources, and guidance during the entire duration.

## References

[1] Industries, A. (n.d.). Adafruit. Retrieved April 09, 2021, from https://www.adafruit.com/?gclid=CjwKCAjw9r-DBhBxEiwA9qYUpUvd2y4lgabJYX0VgJUA2VPbIL_VKN_42UWeDVGyAg7o7aok9cGfRxoCcy4QAvD_BwE

[2] Python Package Index. (n.d.). Find, install and publish python packages with the python package index. Retrieved April 09, 2021, from https://pypi.org/

[3] Raspberry Pi. (n.d.). Teach, learn, and make with Raspberry Pi. Retrieved April 09, 2021, from https://www.raspberrypi.org/

# Self-locomotive Spherical Rolling Robot for Social Interaction

Nicholas Feliciano, Daniel O'Dette, Mitchell Wehner
College of Engineering and Engineering Technology
Northern Illinois University
Dekalb, IL, USA

***Abstract*—With the rise of social isolation protocols put into place due to the Covid-19 pandemic, there has also been a rise in mental health issues. There is believed to be a direct correlation between these issues and social isolation. For that reason, the concept of a self-locomotive spherical rolling robot to counteract these negative effects of the pandemic was born. The spherical rolling robot propels itself through the rotation of its outer shell, and this rolling action is driven by the motion of internal omni-directional driving wheels. This layout allows the robot to have responsive movement and grant it the ability to make point-turns or turns where the robot can rotate while remaining in place. The robot's design is intended to also be semi-autonomous, allowing it to be capable of moving through a space on its own without the need for manual control by a human operator.**

## I. Introduction

The Senior Design Team has designed and built a moving mechanism housed in a spherical shape that enables the mechanism to move in a desired direction at a desired speed. The purpose of this design was to offer a form of interaction for individuals who are struggling adapting to the social isolation effects caused by the Covid-19 pandemic. The robot's design is intended to also be semi-autonomous, which means that it should be capable of moving through a space on its own without the need for manual control by a human operator. To facilitate this, the robot's outer shell is made of a clear plastic to allow internally mounted sensors to operate, granting the robot the ability to be aware of its own environment and perform simple obstacle avoidance. However, the robot remains capable of being guided manually by a human. By developing a mechanism capable of maneuvering independently or dependently, the negative health issues associated with long periods of isolation are hoped to be alleviated. The teams specific design is a self-locomotive design, meaning the external shape must be completely spherical. The design also requires a micro-controller or single-board computer to utilize sensors and actuators using a program created by the Senior Design Team. The program can collect data from the system, sending input signals to control the actuators, altering the signals using a feedback control system, and communicate wirelessly with the computer. By incorporating these specific components, the possibility of an independently moving mechanism relying on a feedback control system is possible.

## II. Materials

### A. Sensors

The specific IMU sensor that the team decided upon is the X-NUCLEO-IKS01A2 shown in figure 1. The X-NUCLEO-IKS01A2 is equipped with Arduino UNO R3 connector layout and is designed around the LSM6DSL 3D accelerometer and 3D gyroscope, the LSM303AGR 3D accelerometer and 3D magnetometer, the HTS221 humidity and temperature sensor and the LPS22HB pressure sensor. The IR sensor we decided to incorporate is the Adafruit GP2Y02YK. By incorporating the IR sensors into the team's design, the robot will in turn be able to detect its surrounding area by estimating distance between sensor and object.

**Figure1:** X-NUCLEO-IKS01A2

### B. Microcontrollers

The microcontrollers used within the design consists of motor controller the B-G431B-ESC1 Discovery kit motor controller and the STM32 Nucleo-144 development board with STM32F429ZI MCU. The motor controller is an electronic speed controller (ESC), designed to drive a single 3-phase brushless motor (BLDC/PMSM), performing both sensor less FOC algorithm and 6-step control with a speed regulation, and an active braking function algorithm [3]. The STM32 Nucleo-144 board has an on-board ST-LINK debugger/programmer with USB re-enumeration capability: mass storage, Virtual COM port, and debug port [4].

### C. Brushless DC Motor

Three Nanotec GF45M024053-A2 brushless DC motors were used within the design. This specific motor provided

the appropriate amount of torque and power to properly control the total mass of the system while also allowing for peak maneuverability.

### D. *Single Board Computer*

For this specific design, the team agreed upon incorporating the Raspberry Pi 4 Model B 8GB SD-RAM shown below in figure 2. The team felt the vast number of libraries and the ease of the Raspberry Pi's interface would be the most beneficial.

**Figure 2:** Raspberry Pi 4 Model B 8GB

## III. Integration of the System

### A. *Programming*

Programming was a very large part contributing to the success of this design. Many phases of programming were put into place to allow for successful communication amongst the microcontrollers, sensors, and single board computer. The process can be seen below in figure 3.

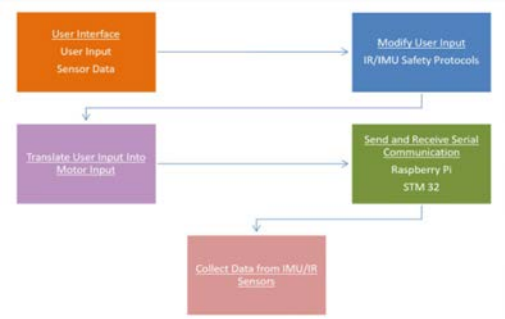


**Figure 3:** Programming Phases

### B. *Mounting Methods*

The internal mechanism of this design consists of three main components that securely mounts the various materials together. The three components consist of a lower chassis, upper chassis, and a top plate all shown below in figure 4. The lower chassis is used to secure the wheels, batteries, motors, and motor controllers. The upper chassis which directly sits on top of the lower chassis via M3 screws houses the microcontrollers and the top plate directly above the upper chassis houses the single board computer, camera, and IR sensors.

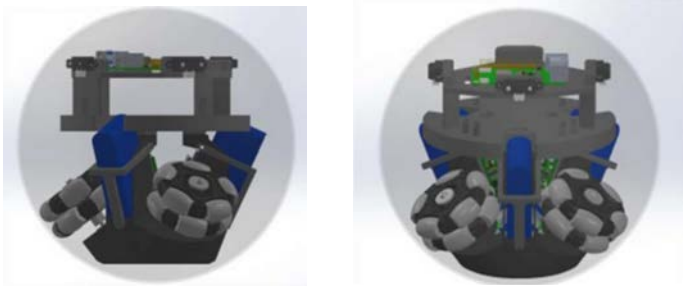

**Figure 4:** Fully Assembled Design

## IV. Conclusion

The spherical shaped rolling robot provides a form of interaction for individuals who are struggling adapting to the social isolation effects caused by the Covid-19 pandemic. Through the incorporation of various sensors and components, microcontrollers, and a single board computer, the ability to alleviate some mental health issues potentially caused from isolation by providing a form of interaction is now possible.

## V. Acknowledgment

This work was done with the support and guidance of the team's faculty advisor Dr Ryu and TA Aayush Patel with the Department of Mechanical Engineering at Northern Illinois University

## VI. References

[1] X-NUCLEO-IKS01A2. (n.d.). Retrieved December 04, 2020,https://www.st.com/en/ecosystems/x-nucleo iks01a2.html

[2] Burnett, R. (2020, October 28). Ultrasonic vs Infrared (IR) Sensors - Which is better? Retrieved December 03, 2020, https://www.maxbotix.com/articles/ultrasonic-or-infrared-sensors.htm

[3] (n.d.). Retrieved December 03, 2020, https://www.st.com/content/st_com/en/products/evaluation-tools/product-evaluation-tools/mcu-mpu-eval-tools/stm32-mcu-mpu-eval-tools/stm32-discovery-kits/b-g431b-esc1.html | APA | Citation Machine

[4] NUCLEO-F429ZI. (n.d.). Retrieved December 04, 2020,https://www.st.com/content/st_com/en/products/evaluation-tools/product-evaluation-tools/mcu-mpu-eval-tools/stm32-mcu-mpu-eval-tools/stm32-nucleo-boards/nucleo-f429zi.html

# Prototype Electric Vehicle Phase III

Angelica Rodriguez, Edgar Rodriguez, Leon Seun
Department of Electrical and Mechanical Engineering
Northern Illinois University, Dekalb IL 60115

***Abstract* - The primary purpose of our project was to continue development of the benchtop prototype electric vehicle through applications created by previous senior design teams. In previous years the teams designed a bi-directional converter which would drive an electric motor using a battery. There is a bi-directional converter which boosts and bucks voltage to transfer energy between the batteries, motor, and capacitors. Proportional-Integral control was chosen to control the bi-directional converter. Team 16 was tasked with implementing regenerative braking and a mechanical load through the processes of a torque transducer to control the load, while a direct torque control (DTC) would assist the system to install regenerative braking. Unforeseen issues came up which made the team change its focus onto building a torque transducer and organize the circuit with PCB boards.**

## I. INTRODUCTION

The main part of this project was to add a mechanical load to the system in order to give more power, torque, to the prototype when it travels on an incline. The mechanical load will be a DC motor which would be connected to the AC motor using two couplers and one sleeve that goes inside the two couplers uniting them by the motors' shafts' ends. Also, the implementation of regenerative braking is to store the energy release from braking when it accelerates and decelerates. Unforeseen issues came up with the power distribution forcing the team to change their focus onto time friendly challenges such as organizing the circuits with PCB boards to make it easier for the following team to understand and finding a torque transducer to potentially control torque and speed. Finding a torque transducer from a manufactured company was not budget friendly. Another idea to find motor torque is to measure the difference in weight from when the motor is on and off. Using a wheatstone bridge is how the team will scale the mass change. It is a simple math calculation once the mass change is found as shown in Figure 2.

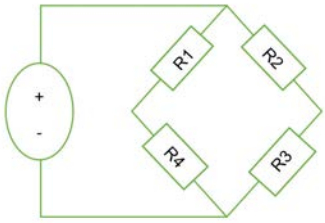


Figure 1: Wheatstone bridge circuit showing the 4 resistors that will read when a load is a strain or stress.

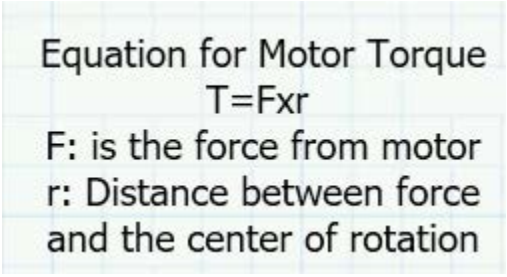


Figure 2: Math calculation to find motor torque

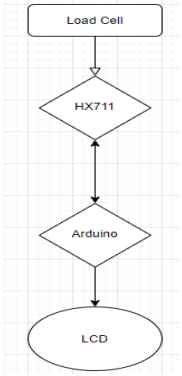


Figure 3: DIagram of scale sensor

## II. MATERIALS AND METHODS

The torque transducer consists of 4 pieces of 50kg half-bridge strain gauge load cell body scale weighing sensor amplifier to measure the mass. A strain gauge load cell is a transducer that changes in electrical resistance when under stress or strain. The electrical resistance is proportional to the stress or strain placed on the cell. The electrical resistance is linear therefore it can be converted into a force and then a weight. The team is using 4 pcs 50kg half-bridge strain load cells. Two load cells will be connected on the left of the motor and two on the right side as shown in Figure 5. This setup will be to calculate the weight on each side of the motor and is on and off. A HX711 amplifier is needed to convert the measured changes in resistance value changes through the conversion circuit into electrical output. The sensors have 3D printed frames to minimize error readings and to be easy to install under the board where the motor will be on. Arduino code is used to control the functions of the scale measuring sensor. Part of the code is shown in Figure 4. The end goal is to have a code to calculate torque. Printed circuit boards (PCB) were installed to the system to organize and better understand the circuitry of the system. The circuitry was difficult for the team to follow, but the installation of PCB made it much easier to troubleshoot and find nodes.

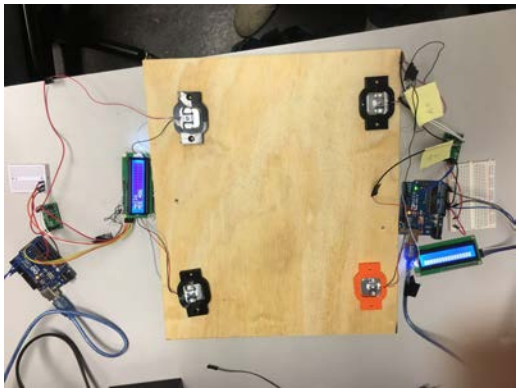

Figure 5: System set-up for scale sensor

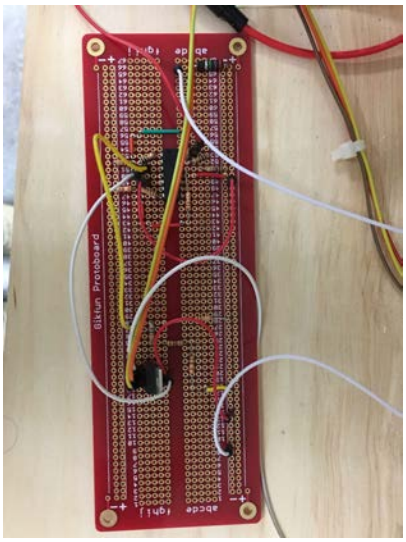

Figure 6: PCB boards

## III. RESULTS AND DISCUSSION

Team 16 faced issues with the power distribution in the system, not being able to turn the motor on which led the team to focus on different and time friendly issues such as the clean up of the circuit and creating a torque transducer with the end to eventually control torque and speed.

TorquesensorSRDesign §

```
#include <HX711_ADC.h>
#include <EEPROM.h>
#endif

//pins:
const int HX711_dout = 4; //mcu > HX711 dout pin
const int HX711_sck = 5; //mcu > HX711 sck pin

//HX711 constructor:
HX711_ADC LoadCell(HX711_dout,HX711_sck);

const int calVal_eepromAdress = 0;
unsigned long t = 0;

void setup() {
  Serial.begin(9600); delay(10);
  Serial.println();
  Serial.println("Starting...");
```

```
#include <LiquidCrystal.h>

const int rs = 4, en = 6, d4 = 11, d5 = 12, d6 = 13, d7 = 14;

LiquidCrystal lcd(rs, en, d4, d5, d6, d7);
#define DT 4
#define SCK 5
#define sw 3

long sample=0;
float val=0;
long count=0;

unsigned long readCount(void)
{
  unsigned long Count;
  unsigned char i;
  pinMode(DT, OUTPUT);
  digitalWrite(DT,HIGH);
```

Figure 4: Codes for scale sensor; the first code is for the HX711 to receive information from the load cells and send the information to the arduino. The 2nd code is for the LCD screen to receive the load cell output(weight).

## IV. CONCLUSIONS

The scale sensor will help calculate the torque and for with it eventually be able to control torque and speed. The team has worked on an Arduino code to be able to read torque instead of weight alone. The PCB boards will be installed to clean up and organize the circuitry of the system. Finally, the team's focus is to work on cleaning up the circuitry and make it easier for the following team to understand the system's power distribution along with controlling the torque and speed of the motor.


## ACKNOWLEDGMENTS

We would like to thank Dr Zinger for the different ideas to approach unforeseen issues for the past year and being flexible with his schedule to open the lab for us to work. Also, we would like to thank our TA, Sonali Rawat, for her advice and guidance and to NIU CEET for the opportunity to work on this project.

# Wearable Device for Detection of COVID-19 and Tracking Symptoms

Team 17

Noelle Maire , Courtney Bradley, Kyle White

College of Engineering and Engineering Technology

Northern Illinois Unversity, DeKalb, IL

*Abstract*—**The purpose of this project is to create a wearable device that provides the user with valuable health diagnostic information related to common COVID-19 symptoms. COVID-19 is a respiratory disease that is fast spreading and difficult to identify. The common symptoms currently include fever, dry cough, shortness of breath, low blood oxygen levels, and respiratory failure. In order to identify and monitor for these symptoms, the following project consists of an SPO2 sensor, temperature sensor, accelerometer, and a control unit. The data acquired from the device is sent to a mobile app which is able to indicate temperature, heart rate, SPO2 levels, and heart vibrations. This device provides a unique solution to allow for remote COVID-19 patient monitoring through the array of sensors included in the design.**

***Keywords-COVID-19, Wearable Device, Health Diagnositic Informaiton***

## I. INTRODUCTION

According to the CDC, there are over 30 million COVID-19 cases reported in the U.S., causing the world to be placed under a global pandemic. COVID-19 is a disease caused by a virus known as severe acute respiratory syndrome or SARS-CoV-2. The structure of these viruses has an organized “crown” like shape consisting of spike proteins. Spike proteins mediate coronavirus entry into host cells through a large ectodomain, a single-pass transmembrane anchor, and a short intercellular tail. Together these elements conduct receptor binding and membrane fusion, creating a never-ending vicious cycle. Stopping this cycle is very difficult due to the virus’s ability to adapt to new environments through mutation and recombination mechanisms. The human body serves as the primary means for indicating COVID-19 infection. The transmission of this virus is primarily through respiratory droplets that are released into the air. This project aims to provide indication of a potential COVID-19 infection by monitoring temperature, SPO2 levels, and respiratory data. The data collected through this device can assist with detecting the virus of asymptomatic individuals.

## II. DEVICE DESIGN

The wearable COVID-19 device design features an accelerometer, temperature sensor, SPO2 sensor, MCU, and a lithium-ion battery. Each component was selected based on size, accuracy, and low-cost. The accelerometer included in the design offers a low power solution with a 2V to 3.6V supply voltage. Its compact size (3mm x 5mm x 1mm) and user-defined bandwidth allowed for the most ideal sensor. A high accuracy (±0.1°C from -20°C to 50°C) temperature sensor was choosen for the design. The SPO2 sensor for the design features both a heart rate and pulse oximetry capabilities. A development board was selected in order to allow proper integration of all previously listed sensors. Lastly, an interchangeable rechargeable lithium-ion battery charger was implemented into the design to allow users to continusly wear the device. The block diagram of the device is indicated below:

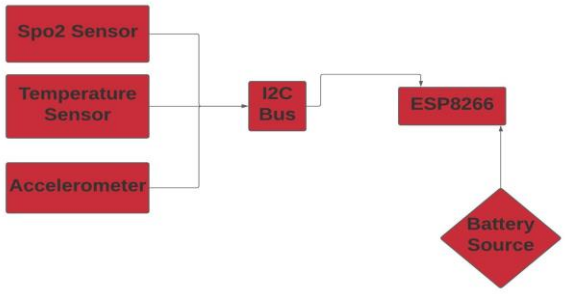


*Figure 1. Block Diagram of System*

## III. TESTING & DATA ACQUISTION

Each of the sensors included in the wearable design were individually tested using a data acquisition device followed by Arduino IDE software. In order to ensure that each sensor was working properly, a LabJack was used to generate data. Ultimately, a few sensors that were purchased were deemed unfit for the application and new sensors were purchased. An analog temperature sensor (LMT70) was generating inaccurate data and was eliminated from the project design. In addition, an analog accelerometer (ADXL335) was also removed from the final design based on the inaccurate data acquisition measurements. Both a new temperature (TMP117) and accelerometer (ADXL345)

sensor were then tested for accuracy using Arduino IDE. The new temperature sensor demonstrated accurate readings when compared with a digital thermometer. The ADXL345 accelerometer was tested by solely examining the Z-axis. Compared to the X and Y axes, the Z-axis picks up a heart signal significantly better since it is out of plane. The Z-axis is also able to indicate chest wall vibrations which includes cough vibrations. The ADXL345 was placed on the chest wall by medical tape in order to avoid unwanted body motion. Heart sounds and forced cough measurements were taken. To test the SPO2 sensor, the blood oxygen content along with heart rate generated from the sensor was compared with the data acquired from a phone app.

## IV. Results

The following graph in figure 2 represents the Z-axis of the ADXL345 accelerometer. This measurement was collected by placing the sensor on the chest wall and inducing a forced cough. The more drastic shaped peaks represent the forced cough action done by the user. The x-axis of the graph represents time in seconds and the y-axis is given in m/s^2.

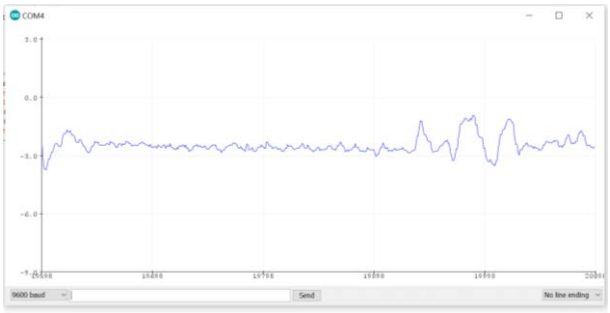

*Figure 2. Accelerometer Data*

To test the temperature sensor, Arduino IDE was utilized. The sensor was placed on the chest of the user as the data was being collected from the sensor. As shown in figure 3, the TMP117 exhibited accurate body temperature measurements. The measurements were then compared to those given by a digital thermometer which gave a reading of 97.2 degrees Fahrenheit.

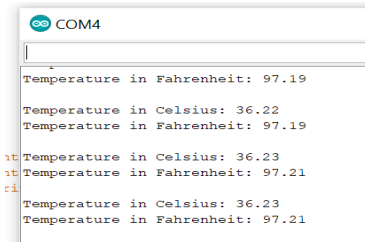


*Figure 3. Temperature Data*

A MAX30102 SPO2 sensor was tested for accuracy by comparing the data generated with a phone app. Figure 4 illustrates the data from the sensor which was outputting an oxygen saturation of 99%. This data was then compared to that of the phone app (figure 5) which gave a 98% oxygen saturation indicating accurate readings from the SPO2 sensor.

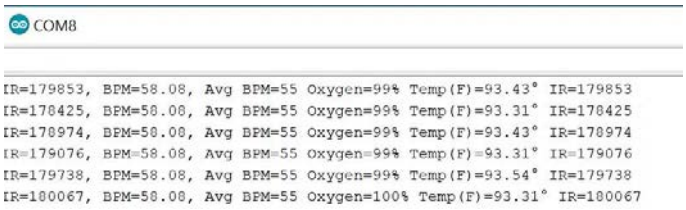


*Figure 4. SPO2 Sensor Data*

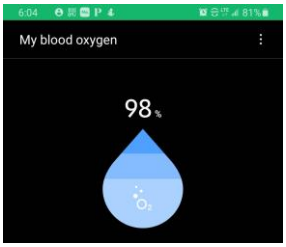


*Figure 5. SPO2 Phone Data*

After all three sensors were successfully tested for accuracy, the sensors were integrated into wearable encasements. The SPO2 sensor was placed into an ear mold and the accelerometer and temperature sensor were placed into a TPU chest encasement.

*Figure 6. Chest Encasement*

## V. Conclusion

The wearable device for detecting and tracking COVID-19 related symptoms seeks to relieve the dependance on the healthcare system for monitoring patient health. By providing temperature, SPO2 measurements, and heart sound data to the user via a mobile app, this device has the capability of reducing the spread of COVID-19.

## Acknowledgment

As a team we would like to thank our faculty advisor Dr. Moghimi for his guidance and assistant throughout this project. We would also like to thank our teaching assistant Aayush Patel for his continued support.

## References

[1] Fang L, “Structure, Function, and Evolution of Coronavirus Spike Proteins.” *Annual review of virology*, vol3(1): 237-261, Aug 2016, (https://www.ncbi.nlm.nih.gov/pmc/articles/PMC5457962/)

# Mobility Mat

Neal Tailor, Kris Kudla, Dom Johnson
Electrical Engineering, Mechanical Engineering
NIU Engineering Department
Dekalb, Illinois

***Abstract*— Within the Engineering department of Northern Illinois University students are put to the task of creating a Smart Mat for a client. Dr Emerson Sebastiao is our client for this project. He wanted our team to create a Smart Mat that would aide patients who need to go through various physical therapy sessions. Some of the main goals of this projects were to show and track users' steps through the various stepping patterns provided.**

***Keywords-component; Smart Mat, Pressure Sensor Matrix, LED matrix***

## I. INTRODUCTION

Physical Therapy is a key component in the rehabilitation process for people who have gone through a traumatic event/Ailments. Millions of people around the world struggle with basic movement functions and our goal was to create a tool that would assist this process. The Mobility mat is a mat that is designed to help people who struggle with movement limitations. What this mat will do is show a pattern that the user must recreate by stepping in the correct squares. This mat will also take in data and show it visually such as the amount of force by the foot, number of steps taken and if they have stepped correctly.

## II. MAT MATERIALS

As shown in Figure 1 the mat consists of 3 main layers and 5 components within those layers. LED's, clear car vinyl, velostat, rubber mat and copper strips.

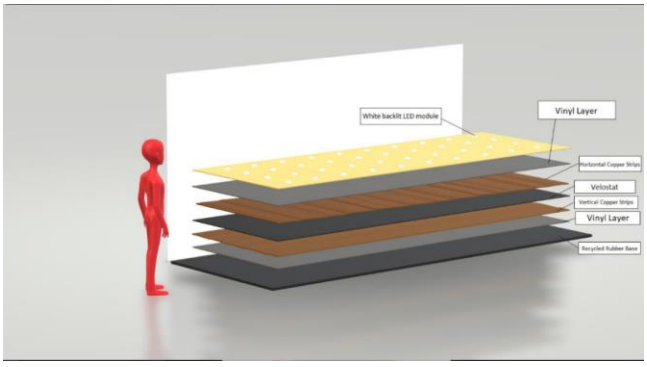


***Figure 1**: Layered Architecture*

### *A. Base Layer*

Starting from the bottom, the base will be a 100 % recycled rubber mat. It will be approximately 3 mm thick, and it will act as the non-slip material, so the mat does not slip or slide while in use.

### *B. Velostat Sandwich Layer*

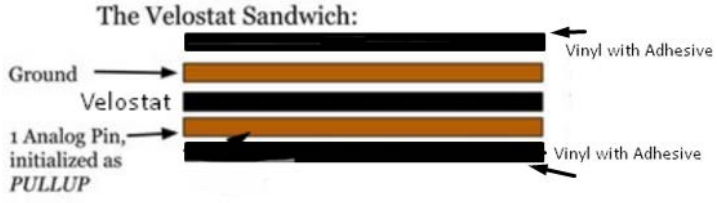


***Figure 2:** Velostat sandwich*

As shown in Figure 2 the Velostat Sandwich is comprised several different components. The main component is the Velostat which is a very thin polymeric foil that is electrically conductive. Adding copper strips to the bottom and top of the Velostat allows this layer to act as a big pressure sensor. It is then sandwiched again with car vinyl to seal the layers inside. By sealing it we can avoid electrical safety concerns and hardware safety.

### *C. Faux Lether Top Layer*

This is the top layer which the patients will be stepping on and it's comprised of the 100% Polyester Faux Leather with 40 cutouts for each of the LED modules.

***Figure 3:** Faux Leather Top with LEDs*

## III. LED MATRIX

For the LED matrix we used a decade counter (CD4017). This device allows us to manipulate certain LEDs at any given time. With this configuration we are able to display patterns throughout the mat using Binary Coded Decimal (BCD). We decided to use buttons to work as a switch in which we could cycle through various patterns. When the user wants to play a certain pattern, they simply press the button corresponding to that pattern. The mat then lights up according to the pattern that was selected and loops as many times as the user wants automatically. In order to stop the loop, the user in control of the mat can simply press the external reset button to stop it. From there the user can select a different button and the mat will display the pattern associated with that button.

## IV. PRESSURE SENSOR MATRIX

This Matrix is how we determine where the user is stepping and with how much force they are stepping with.
By using the Velostat sandwich accompanied by Shift register and Multiplexors were able to send and receive signals. With these signals we can use a Microcontroller to run the scripts. Then have a Python Script to visualize it. By using this Matrix configuration, we are able to manipulate the matrix data, and write conditions for it.

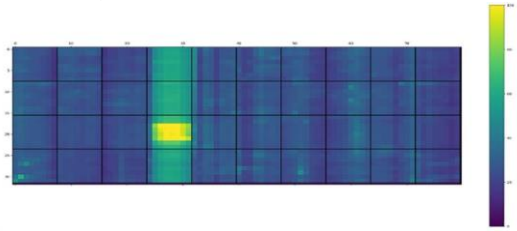

**Figure 4** Visual Software

### A. *Multiplexors*

Multiplexors are one major component used in this layer of the mat. What these Integrated Circuits (IC's) do are check voltage changes throughout the mat. By having these always checking certain areas of the mat were able to locate areas where pressure is being applied.

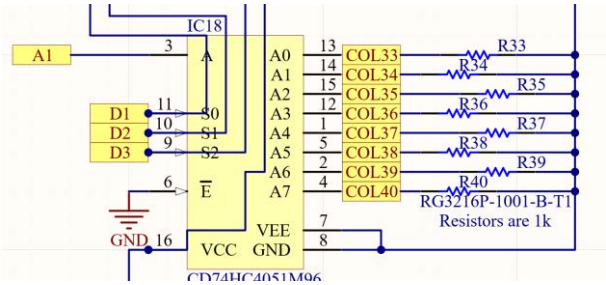


***Figure 5*** *Schematic of Multiplexor*

### B. *Shift Registers*

Shift registers are the 2nd main component of this layer, what these IC's do is send the initial signal that the Multiplexor will intake. These signals are what change when the velostat sandwich is pressed on.

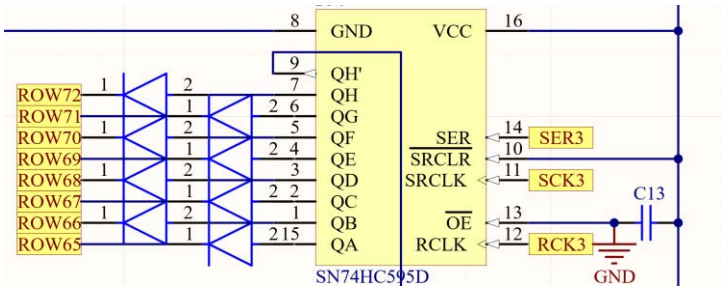


***Figure 6*** *Schematic of Shift Register*

## V. CONCLUSION

The end goal of this project is to successfully create an exercise mat capable of assisting trainers in their rehabilitation sessions and determining the progress of their patients. With the help of mobility mat, trainers will be able to more accurately pinpoint specific issues in posture, walking struggles that need improvement, and ultimately be more effective in their methods of getting people healthy and walking properly again. As engineers, we want to improve upon the ideas and scientific methods of those who have come before us and perhaps, if possible, create innovative technology altogether. Despite the similar ideas currently floating around the market, we are confident that our design is unique, and we feel that the ideas that we have developed for this project's implementation set us apart.


## ACKNOWLEDGMENT

We would like to express gratitude to Dr. Emerson, Dr. Alam, and Amin Roostaee. We also want to thank NIU for providing funds and resources for this project. Thank you for your support.


## REFERENCES


[1] A. M. Reps, "Pressure Sensor Matrix Mat Project," *repscc*, 01-Jan-2018. [Online]. Available: https://reps.cc/?p=50

[2] U. Syst3mX and Instructables, "Make a 8x10 L.E.D Matrix," *Instructables*,07-Nov-2017.[Online].Available: https://www.instructables.com/810-LED-Matrix-with-4017/.

[3] T. Okura, R. Shigematsu, and M. Nakagaichi, *Square-Stepping Exercise*, 2nd ed., vol. 2, 2 vols. Japan: Unkown, 2006.

# Design of a Noninvasive Ventilator Enabled by Non-thermal Plasma for Inactivation of Airborne Viruses

J. Baig[1], B. Nakum[2], W. Schoepke[1]

Department of Mechanical Engineering[1], Department of Electrical Engineering[2]

Northern Illinois University

Dekalb, Il 60115

***Abstract*— This paper describes the process used to create a portable system capable of generating Non-Thermal Plasma inside of a flowing tube path, while filtering out byproducts created by the discharge used to create the plasma. This system was created for the purpose of eventual connection to a portable ventilator, where it would be used to disinfect air being supplied by said ventilator to the patient.**

***Keywords Non-Thermal Plasma (NTP), Ozone***

## I. INTRODUCTION

The spread of SARS-CoV-2 during the COVID-19 Pandemic had been amplified by the nationwide shortage of hospital ventilators. Cross-patient infection occurred as a result of ventilators not being thoroughly disinfected in emergency rooms. The team designed a solution using a novel form of disinfection known as Non-Thermal Plasma (NTP). During operation, a high voltage AC discharge is applied through a gas such as air. Plasma is generated consisting of ions and free electrons – these short-lived reactive species are used as disinfection agents. Viral aerosol then passes through the discharge, interacting with the reactive species and safely inactivating. However, the air's interaction with the reactive species generates ozone, which is harmful to humans. There is a limited exposure amount set by Occupational Health and Safety Administration (OSHA): 0.05ppm over the course of 8 hours [1]. The team used the NTP concept to design and fabricate a disinfection system with ozone filtration that connects to a portable ventilator.

## II. REACTOR DESIGN

### *A. Chamber*

The NTP reactor's chamber design went through several iterations before its final configuration. Consistent among each iteration was the use of a 1-inch inner diameter (ID) and 1.25-inch outer diameter (OD) tube to ensure compatibility with the selected portable ventilator (NASA's VITAL). Two diametrically opposed rectangular openings are cut into the tube for the electrode plates. Different electrode configurations were considered as each geometry resulted in a different discharge. The electrode plates were initially both made of copper. 12 nails of ¼" lengths were used on the positive electrode plate. The pointed ends of nails were suited to the small area ideal for discharge to occur. On the grounding electrode plate were acrylic beads and $BaTiO_3$ powder (Barium Titanate) fastened with double-sided acrylic tape, each a dielectric material. The nails were eventually replaced with ½" length ones to shorten the distance for the discharge. The acrylic beads were found to be ignored by the discharge and therefore removed. The ½" nails were replaced by 18-gauge multithread wires. These wires were fed through a new 3D-printed plastic plate. By separating the wires using an insulated material the discharge became more distributed. This last configuration – 18-gauge multithread wires mounted on a 3D-printed plastic plate, diametrically opposed to the copper grounding electrode plate covered with double-sided acrylic tape and Barium Titanate – generated stable, repeatable discharge within the reactor chamber, as shown below in *Figure 1*.

## III. ELECTRICAL DESIGN

### *A. Power Supply*

To generate NTP, high voltage AC current from a neon sign transformer power supply took 120 volts from the wall and amplified it to the kilovolt (kV) range. The team had chosen to use a neon sign transformer as they are both cost effective and compact, which allowed the device to remain portable. Two neon sign transformers were considered: a 3kV 90-watt supply and a 6.5kV 195-watt supply.

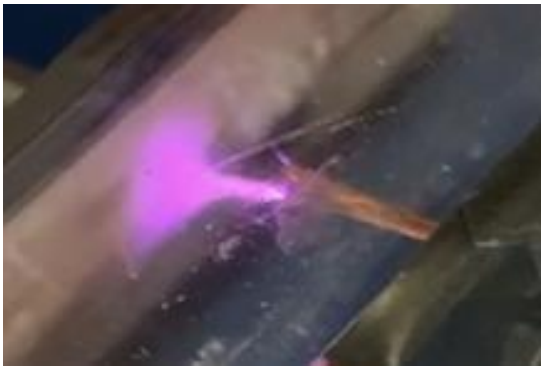

*Figure 1: Plasma Discharge*

### B. *Ozone Sensor Module*

To ensure ozone levels were below the 0.05ppm standard, a low concentration MQ-131 ozone sensor module was placed after the filtration system. The sensor increases its conductivity as more ozone is detected, which causes its voltage reading to increase. The sensor takes this voltage reading and converts it to an ozone level reading in ppb as it continuously samples the air. This was all coded and implemented through the Arduino environment.

## IV. Mechanical Design

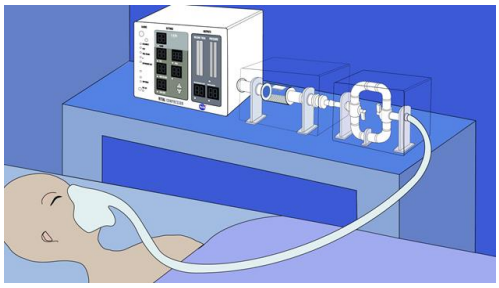

*Figure 2: System Concept Art by Angela Patricia Bello Rodriguez*

### A. *Materials*

The path for the airflow was made of different non-conductive materials. The 1"ID hard tubing which held the reactor was made of clear, polycarbonate plastic. The transparency was desired so the discharge inside the tube was visible. Two slots were cut opposite of each other on the surface of the tube to insert the electrode plates inside of. This was connected to a tube reducer, which connected to a ½"ID firm blue PVC tubing. The flow here was reduced to allow connection to the filtration system, which used ½" ID PVC ball valves to divert flow. The system is shown above in *Figure 2*.

### B. *Filtration System*

For the ozone at the outlet to remain under 0.05ppm, the system includes activated carbon filters which are effective at ozone adsorption. As the envisioned project was intended for use with a ventilator, a feature to allow in-service changing of filters was incorporated. This design uses two PVC ball valves to divert flow between one of two paths. While air flows through one path, the other path can be removed to exchange filters. These filters were prototyped as sections of a cut activated carbon pad hot glued onto a paper clip, as shown above in *Figure 3*. The ends are shaped to prevent the filters from sliding inside of the L-shaped connectors in the filtration design, as well as the filters themselves should they loosen.

*Figure 3: Carbon Filter Setup*

## V. Results & Conclusions

During the testing phase, the team found the ideal electrode configuration for a stable NTP discharge. The team also found that the 6.5kV power supply was too powerful as unstable white arcs would form, burning the polycarbonate tubing. As a result, the team used the 3kV supply connected to a voltage regulator. The voltage regulator allowed the team to control the voltage output from the wall via a rotational dial, giving us a range where stable NTP could form. The team measured the amount of ozone being produced at different voltages at a flowrate of 1 m/s to simulate the breathing rate of a patient on a ventilator. As seen in the plot, as voltage increased, the average amount of ozone present increased in an exponential manner. Although further testing must be done with viral aerosols to measure disinfection, the team can assume a better disinfection rate as higher levels of ozone mean more reactive species being generated.

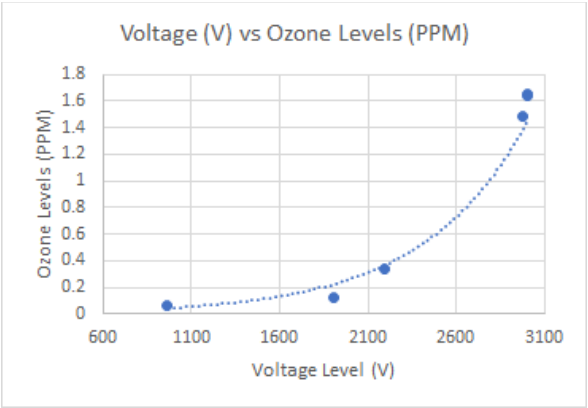


*Figure 4: Voltage vs Ozone Levels of the System*


## Acknowledgments

The team would like to thank Dr. Eric Lee for his sponsorship and assistance throughout the course of the project. The team would also like to thank Angela Patricia Bello Rodriguez for creating the illustrations and other visual aids.


## References


[1] *UNITED STATES DEPARTMENT OF LABOR*. OSHA Occupational Chemical Database | Occupational Safety and Health Administration. (2020, August 25). https://www.osha.gov/chemicaldata/chemResult.html?RecNo=9

# *Industrial Wash Process Six Sigma*

Staticstical Paint Pretreatment Verification

Elijah Wartgow
Mechanical Engineer
Northern Illinois University
Rockford, Illinois USA
e-mail: Z1877936@students.niu.edu

Sam Fisher
Mechanical Engineering
Northern Illinois University
Rockford, IL USA
e-mail: Z1840574@students.niu.edu

Gunnar Verace
Mechanical Engineering
Northern Illinois University
Rockford, IL USA
e-mail: Z1815742@students.niu.edu

***Abstract* — The team is working with Parker Hannifin Accumulator and Cooler Division to perform statistical analysis and experimentation on the client's parts wash system to identify variation and sources of defects. Parker Hannifin has a large, planned capital expenditure, an automated paint robot, being installed on the paint line in April 2021. To validate this expenditure, the client needs the parts wash station, which precedes the paint line, to contribute a minimal amount of variation and defects to the post-fabrication process, so that statistical analysis can be done on the paint line without other factors being variable. The parts wash process has not yet been subject to statistical process controls by the client and has instead been operating under specifications recommended by the parts wash manufacturer and the manufacturers of the different chemicals used. To ensure the best manufacturing practices are being met, it is important to the client to have this part of the manufacturing process statistically evaluated using design of experiments and continuous process improvement.**

***Keywords- SPC; Concentration; Exposure; Xbar-R; I-MR***

## I. INTRODUCTION

Paint pretreatment is essential in industrial applications. Painting the metal substrate without pretreating the surface would not enable the hydraulic accumulators to withstand the required environmental conditions experienced in the field. Hydraulic accumulators are highly pressurized vessels that are often essential safety features and must have a highly reliable surface integrity.

Paint pretreatment is the process by which a surface is prepared for paint by chemically cleaning and etching the surface using a system of sprayers. High production volumes dictate that the pretreatment process must remain efficient and should be highly reliable and repeatable. The pretreatment system under observation uses a four-stage method to treat the metal substrate. The first stage of the wash bath is an industrial detergent that strips the metal substrate of pollutants and oils that have been collected during production and assembly. The second stage of the wash bath rinses the metal substrate with DI water and removes any remaining detergent. The third stage of the wash bath bathes the metal substrate in iron phosphate, which is an acid. The acid etches the metal substrate by creating microscopic scratches on the surface. The etching process allows the paint to grab onto the metal substrate and increases paint adhesion. The fourth stage of the wash bath is a DI rinse stage to removes excess iron phosphate not used in the etching process. No scrubbing is performed during the pretreatment process, but instead relies totally on chemical reactions facilitated by spray jets.

## II. METHODS

All testing done in this project involved the use of test plates, otherwise known as coupons. These coupons are 4x8x0.032-inch sheets of cold-rolled steel. These test plates simulated the role of the normal Parker Hannifin accumulators, but without the risk of product failure. The sample size of plates used per experiment was determined through the use of Minitab and the team's knowledge of Six Sigma processes. To maximize efficiency and minimize the amount of line spacing needed, the team used the setup displayed in Figure 1 during experimentation.

***Figure 1:*** *Test plate setup used throughout the entirety of the project. This minimized line occupancy and maximized time and efficiency.*

Two experiments were conducted to analyze and confirm the effects of changing concentration and over-exposure to the wash bath and factory atmosphere. Experiment #1 focused on changing the concentrations of the 752 detergent and 758 phosphate [1]. Prior to the experiment, the 752 detergent was kept between 2% and 3% and the 758 phosphate was kept between 3% and 4%. To measure the effectiveness of concentration changes, four "quadrants" were developed that changed the concentration to above or below their current operating standards. After the plates were run through the wash bath and oven, adhesion testing, dry film thickness testing, salt pray testing, and phosphate weight coating testing was performed to test the usability of the plates. Experiment #2 focused on the over-exposure of the test plates to the wash bath and factory conditions. Currently, Parker experiences frequent line stoppages that leave accumulators sitting on the line for an extended period. This experiment verified the negative consequences these stoppages have to the quality of their product.

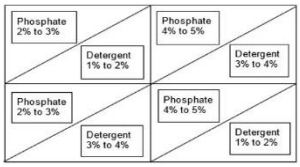


***Figure 2:*** *Chosen concentrations for each "quadrant." 2x2 experimentation allowed the team to explore all possible concentration combinations.*

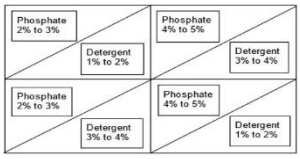


***Figure 3:*** *"Quadrants" for Experiment #2. Long Exposure means the line stopped for approximately one hour and short exposure means continuous line motion.*

## III. Results

### A. Results from 2 x 2 DOE #1

Results of the 2 x 2 DOE are displayed in 3 forms. Phosphate coating weight, paint adhesion, and salt spray resistance. Data for each of these categories can be seen below:

| EXPERIMENT #1 | | | | | | | |
|---|---|---|---|---|---|---|---|
| Quadrant 1 | | | | Quadrant 2 | | | |
| Plate ID | Weight (g/m2) | Plate ID (Replication) | Weight (g/m2) | Plate ID | Weight (mg/ft2) | Plate ID (Replication) | Weight (g/m2) |
| AVG | 0.78 | AVG | 0.76 | AVG | 0.69 | AVG | 0.61 |
| Quadrant 3 | | | | Quadrant 4 | | | |
| Plate ID | Weight (g/m2) | Plate ID (Replication) | Weight (g/m2) | Plate ID | Weight (g/m2) | Plate ID (Replication) | Weight (g/m2) |
| AVG | 1.35 | AVG | 1.27 | AVG | 0.58 | AVG | 1.61 |

***Figure 4:*** *Phosphate coating weights as determined by independent laboratory.*

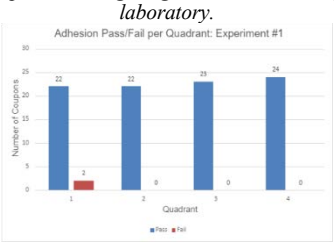


***Figure 5:*** *Paint adhesion passes are in blue and failures are in red.*

**RESULTS:**

| SAMPLE ID | 120 Hours | 240 Hours | D1654 Method 1 |
|---|---|---|---|
| C19 Q1 | Very Slight Red Corrosion & Some Blisters | Slight Red Corrosion & Some Blisters | 6 |
| C24R Q1 | Very Slight Red Corrosion & Some Blisters | Sight Red Corrosion & Some Blisters | 7 |
| C13 Q2 | Moderate Red Corrosion & Some Blisters | Moderate Red Corrosion & Some Blisters | 5 |
| C22R Q2 | Intermittent Red Corrosion & Some Blisters | Intermittent Red Corrosion & Some Blisters | 5 |
| C18 Q3 | Moderate Red Corrosion & Blisters | Moderate Red Corrosion & Some Blisters | 5 |
| C24R Q3 | Moderate Red Corrosion & Blisters | Moderate Red Corrosion & Some Blisters | 2 |
| C14R Q4 | Very Slight Red Corrosion & Some Blisters | Slight Red Corrosion & Some Blisters | 5 |
| C19 Q4 | Very Slight Red Corrosion & Some Blisters | Slight Red Corrosion & Some Blisters | 3 |

***Figure 6:*** *240-hour salt fog exposure results.*

### B. Results from 2 x 2 DOE #2

Results of the 2 x 2 DOE are displayed in 3 forms. Phosphate coating weight, paint adhesion, and salt spray resistance. Data for each of these categories can be seen below:

| Experiment #2 | | | | | | | |
|---|---|---|---|---|---|---|---|
| Quadrant 1 | | | | Quadrant 2 | | | |
| Plate ID | Weight (g/m2) | Plate ID (Replication) | Weight (g/m2) | Plate ID | Weight (mg/ft2) | Plate ID (Replication) | Weight (g/m2) |
| B1 AVG | 0.88 | B1 AVG | 0.69 | B1 AVG | 0.79 | B1 AVG | 0.61 |
| B2 AVG | 0.83 | B2 AVG | 0.67 | B2 AVG | 0.85 | B2 AVG | 0.61 |
| B3 AVG | 1.41 | B3 AVG | 1.34 | B3 AVG | 0.82 | B3 AVG | 0.64 |
| B4 AVG | 0.9 | B4 AVG | 0.89 | B4 AVG | 0.85 | B4 AVG | 0.65 |
| Quadrant 3 | | | | Quadrant 4 | | | |
| Plate ID | Weight (g/m2) | Plate ID (Replication) | Weight (g/m2) | Plate ID | Weight (mg/ft2) | Plate ID (Replication) | Weight (g/m2) |
| B1 AVG | 0.78 | B1 AVG | 0.6 | B1 AVG | 0.88 | B1 AVG | 0.73 |
| B2 AVG | 0.82 | B2 AVG | 0.66 | B2 AVG | 0.83 | B2 AVG | 0.77 |
| B3 AVG | 1.41 | B3 AVG | 1.39 | B3 AVG | 0.54 | B3 AVG | 0.59 |
| B4 AVG | 0.94 | B4 AVG | 0.8 | B4 AVG | 0.79 | B4 AVG | 0.52 |

***Figure 7:*** *Phosphate coating weights as determined by independent laboratory.*

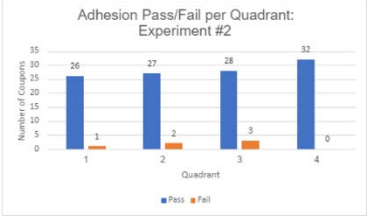


***Figure 8:*** *Paint adhesion passes are in blue and failures are in red.*

| SAMPLE ID | ASTM D1564 (Method 1) | | |
|---|---|---|---|
| C7 B1 Q1 | 0 | C8 B1 Q3 | 0 |
| C7 B2 Q1 | 0 | C9 B2 Q3 | 0 |
| C9 B3 Q1 | 0 | C7 B3 Q3 | 0 |
| C9 B4 Q1 | 2 | C5 B4 Q3 | 0 |
| C9R B1 Q1 | 0 | C6R B1 Q3 | 0 |
| C9R B2 Q1 | 1 | C7R B2 Q3 | 0 |
| C9R B3 Q1 | 0 | C9R B3 Q3 | 0 |
| C7R B4 Q1 | 4 | C9R B4 Q3 | 0 |
| C8 B1 Q2 | 0 | C8 B1 Q4 | 0 |
| C6 B2 Q2 | 0 | C5 B2 Q4 | 0 |
| C9 B3 Q2 | 0 | C9 B3 Q4 | 0 |
| C9 B4 Q2 | 0 | C5 B4 Q4 | 0 |
| C9R B1 Q2 | 0 | C6R B1 Q4 | 0 |
| C9R B2 Q2 | 0 | C5R B2 Q4 | 0 |
| C9R B3 Q2 | 0 | C8R B3 Q4 | 0 |
| C5R B4 Q2 | 0 | C7R B4 Q4 | 0 |

***Figure 9:*** *240-hour salt fog exposure results.*

## IV. Discussion

As seen from the results, the experimental data showed a wide range of phosphate data for both experiments, statistically demonstrating the effectiveness of adjusting the iron phosphate concentrations. Paint adhesion was consistent across all experimental procedure, indicating paint adhesion is less rigorous than a 240-hour salt spray test.

## V. Conclusion

The experiments conducted by the team yielded valuable data and root causes that the Parker team will continue to analyze in the near as they implement their new robotic paint system. From Experiment #1, the team was able to determine that the current operational concentrations are sufficient, but there may be underlying issues with the nozzles, pipes, detergent effectiveness, and frequent line stoppages. Experiment #2 further verified the detrimental effects line stoppages have on the parts. From the data collected, even line stoppages as short as ten minutes can have negative effects on the test plates/accumulators. Parker Hannifin will conduct experiments on the underlying conditions found by the senior design team in the near future.

## Acknowledgment

Team #20 thanks faculty advisor Dr. Ghazi Malawi, the Parker staff consisting of Melissa Childers, Brad Bomkamp, and Bill Mosher, and our teaching assistant, Sandhya Chapagain for their support and guidance throughout the project.

## References

[1] "GF PHOS 758 - Iron Phosphate - #1 Supplier Distributor Best Price." Chemicals Global Industrial Chemical Suppliers, 30 Aug. 2019, chemicalsglobal.com/shop/gf-phos-758-iron_phosphate/.

# *Improved Power Delivery and Portability for Sewage Sampling Equipment*

for Kishwaukee Water Reclamation District

Spencer Simpson, Omar Roman-Sanchez, Kevin Simms
Department of Mechanical Engineering
Northern Illinois University
DeKalb, IL 60115

***Abstract*— Sewage samping has become a vital component to monitoring public health, due to the COVID-19 pandemic. By testing samples of sewage for traces of COVID-19, health officials can predict a spike in cases weeks in advance. Kishwaukee Water Reclamation District requires the ability to quickly and efficiently deploy sampling equipment within the DeKalb community, as this can have a major impact on how local health authorities respond to health crises. This project aims to simplify the deployment process of existing sampling equipment through an improved mounting system and a more efficient power delivery system. Composite flow-paced sampling deployment is improved by a corrosion-resistant 316 stainless steel mounting system. This combines the flow meter, sampler, and power delivery system into a single unit. Efficiency is improved through a unified power delivery system created around a Milwaukee M18 Lithium-Ion battery pack. This has allowed the flow meter and sampler to run off a single M18 battery pack with more than double the original runtime and reduced weight.**

## I. Introduction

Recent studies have indicated that COVID-19 is detectable in human waste early in the virus's incubation period, regardless of whether the person is symptomatic. As a result of these studies, sanitary sewage has begun to be tested around the country as an indicator of the presence of COVID-19 in a community.

Kishwaukee Water Reclamation District (KWRD) is the sanitary sewer and wastewater treatment utility for the City of DeKalb and Northern Illinois University. KWRD requires the ability to quickly and efficiently deploy a portable area-velocity flow meter (2150 Area Velocity Flow Meter [1]) and composite sampler (GLS Composite Sampler [2]) while simultaneously improving the efficiency of the power source for both devices.

There are many different methods to implement composite sewage sampling using portable sampling equipment. Because of the large variance in flow volume within the sewage system, flow-paced composite sampling is necessary to provide the most representative sample for testing the presence of COVID-19 and other viruses.

Flow-paced composite sampling involves setting a specific sample volume to be collected and a specific volume of flow that must pass through the section of pipe before a sampling event is triggered. e.g. one 15mL sample triggered every 3,785 Liters (1,000 Gallons) of flow for 24 hours.

Flow-paced sampling consists of a flow meter device capable of measuring the volume of flow passing through a section of pipe in addition to the portable sampler device. The sampler would use flow volume data from the flow meter and a sampling event would be triggered once the volume of flow reaches the programmed value.

## II. Methods and Materials

### *A. Mounting System*

The mounting system is designed to keep all equipment secured in place, while remaining portable and allowing for easy access to the contained equipment.

The material used to construct the mounting system is 316 stainless steel. This material was chosen due to matching the material used on the portable sampler and due to the addition of molybdenum, which gives it excellent corrosion resistance.

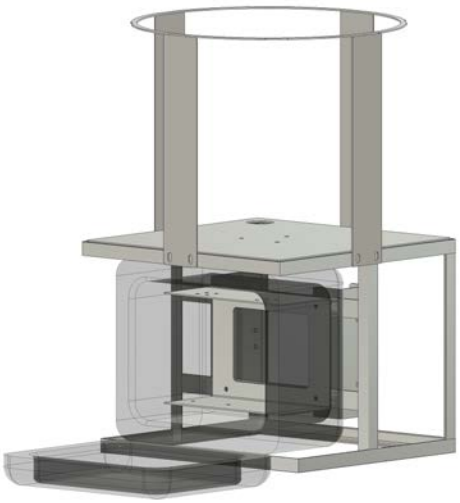

Figure 1. Autodesk Fusion 360 model of mounting system.

The main section of the mounting system is made out of $90^{\circ}$ angle stock. This allows the construction of a lightweight but extremely strong skeletonized frame. Having a mounting system that is skeletonized is extremely important

to allow for thorough cleaning of the surfaces. The remaining components of the mounting system are made out of 14 Gauge and 22 Gauge sheet steel.

The ring at the very top of the mounting system is designed to fit inside the lip on the bucket of the portable sampler. This allows for an extremely convenient, tool-less and non-destructive anchoring method to hold the portable sampler in the mounting system. The latches on the lid of the sampler swing into the lip on the bucket and in the process, sandwich the ring.

The Pelican iM2075 Storm Case contains a bracket designed to securely hold components of the power delivery system. It was bent into a "U" shape and allows for upper and lower mounting points. The middle has a 4 bolt pattern which is centered around a rectangular cutout.

Behind the case are two brackets designed to securely hold the portable flow meter. The two brackets were bent into a "U" shape, and the inside space is utilized for cable management and the two waterproof cable grommets exiting the case. On one side, the two brackets share the same 4 bolt pattern used to hold the case and internal bracket in place. On the other side are mounting blocks designed to hold the flow meter in place using the existing quick release mechanism. These mounting blocks allow for a convenient, tool-less and non-destructive method to secure the portable flow meter to the mounting system.

Figure 2. Flow Meter mounting brackets with blocks.

### B. *Power Delivery System*

The power delivery system is designed to act as a unified power source for the flow meter and sampler, replacing their original separate power sources. For power delivery, the system makes use of a detachable Milwaukee brand 'M18' Lithium-ion battery pack. This style of battery pack is designed to slide onto an internal dock and clip into place, requiring only a few seconds of the operator's time to be installed or removed.

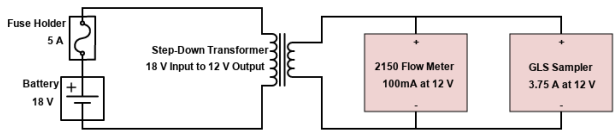


Figure 3. Wiring diagram of the power delivery system.

The battery has a rated output of 18VDC. This is incompatible with the 12VDC inputs of the flow meter and sampler, so the output is run through a step-down voltage converter and regulated power is passed to the equipment.

The battery pack is fused with a 5A blade fuse, which greatly reduces the risk of a short-circuit and of a thermal runaway incident. All power delivery system electronics are contained in the Pelican Storm Case, which is a fully waterproof case. As a result, the water-resistance rating of the equipment is not compromised.


Figure 4. Inside of the Pelican Storm Case showing the electronics.

## III. Conclusion

The mounting system dramatically improves the ease of deployment for flow-paced composite sampling by combining a flow meter and sampler into a single unit. Having a single unit allows the technician to make fewer trips into the manhole while setting up sampling. The power delivery system allows both the flow meter and sampler to run off a single M18 6Ah Lithium-Ion battery pack which reduces weight, saves space and provides more than double the runtime of the original batteries.

## Acknowledgment

We would like to thank our faculty advisor, Dr. John Shelton, our TA, Aayush Patel, and our industry client, Mike Holland from Kishwaukee Water Reclamation District.

## References

[1] Teledyne ISCO. (1999). *2150 Area Velocity Flow Module and Sensor: Installation and Operation Guide*. Retrieved from https://www.teledyneisco.com/en-us/waterandwastewater/Flow%20Meter%20Documents/Manuals/2150%20Flow%20Module%20User%20Manual.pdf.

[2] Teledyne ISCO. (1998). *GLS Compact Sampler: Installation and Operation Guide*. Retrieved from https://www.teledyneisco.com/en-us/waterandwastewater/Sampler%20Documents/Manuals/GLS%20Compact%20Sampler%20User%20Manual.pdf

# *Argonne Wakefield Accelerator Laser Phase Feedback Control System*

Saif Nasir, Ata Urrab, Peter Solomon, Hailah Aljarboua
Department of Electrical and Computer Engineering
Northern Illinois University
Dekalb, USA

Dr. Stanislav Baturin and Dr. Philippe Piot
Argonne Wakefield Accelerator
Argonne National Laboratory
Lemont, USA

**Abstract—Argonne Wakefield Accelerator (AWA) uses an intense laser system to produce electron bunches for use in accelerator experiments. The system is synchronized to a commercial laser oscillator device which operates at a 1.3 GHz Low Level Radio Frequency (LLRF). The 1.3 GHz LLRF signal is then frequency divided, and phase locked to an external 81.25 MHz reference signal using a mechanical phase shifter at Argonne National Laboratory (ANL). Because of certain limitations with the mechanical phase shifter, the phase relationship between the 81.25 MHz signal and the 1.3 GHz LLRF signal has the potential to drift. For this reason, a secondary system was designed to work with the current mechanical phase shifter that would ensure that the phase drift is reduced for the researchers during scientific experiments.**

## I. Introduction

The current phase shifter device used at ANL is a mechanical "trombone" like device. The mechanical structure involved takes up a lot of space, has a high latency of operation, and introduces unwanted noise and vibrations into the system. Most importantly however, changes in temperature adversely effects the phase control of this style of phase shifter resulting in the phase drifting over time. The mechanical phase shifter is guided by a Laser Phase Monitor (LPM) system developed by ANL to determine the level of phase adjustment to be made [2].

The LPM compares a photodiode associated 1.3 GHz signal against a 1.3 GHz LLRF signal. There are two techniques to obtain the 1.3GHz signal from the laser oscillator. A frequency multiplier can be used to multiply the 81.25 MHz signal by 16 to get a 1.3 GHz signal. Another option is to filter the laser oscillator photodiode signal by using a high quality factor 1.3 GHz cavity filter. Using an AD8302 phase detector board [1], a phase difference between the two signals can be converted into a proportional voltage. This proportional voltage is then used to adjust the coaxial line stretcher by the means of a stepper motor. However, using the LPM, a phase drift of roughly 1° degree per 1° C of temperature change was observed over a six-hour duration.

Realizing the limitations of this mechanical phase shifter design, the team developed a "second-stage" precision phase shifter system that works in conjunction with the existing mechanical phase shifter and satisfies the 0.00625° phase shift at the 81.25 MHz frequency outlined by the ANL researchers. The mechanical phase shifter would be responsible for the bulk of the phase shift while the auxiliary system would offer further precise control over the phase of the 81.25 MHz frequency signal.

## II. Methods

The team decided to use the theory behind Quadrature Vector Modulation (QVM) as the focal point for the device. By applying QVM, a signal can be split into its respective quadrature components and the gain and phase can be controlled by setting the values for the in-phase (I) and quadrature (Q) components [3]. If the I component (amplitude of the cosine wave) and the Q component (amplitude of the sine wave) is varied with respect to time, a full control of the amplitude and phase shift of the resulting summed waveform can be achieved. QVM is widely used in RF applications to control the amplitude and phase of high frequency signals.

## III. Control System

The laser phase feedback control system was designed with compatibility in mind for integration with either a Raspberry Pi 4 Model B or Arduino Nano. Mounting holes were drilled into the component mounting tray that would accommodate either device if needed. The control code was written in Python and C++ so depending on which configuration the researchers at ANL decide upon, they are able to quickly incorporate either device.

The electronics in the laser phase feedback control system are powered by a single 5V source supplied through a USB Type A pass-through mounted at the front of the enclosure. The control system (RPi 4 or Arduino Nano) operates by sending instructions to an AD5667 16-Bit 2-Channel DAC which outputs the correct voltage values to an ADL5390 RF/IF QVM using the Inter-Integrated Circuit ($I^2C$) communication protocol. The output voltage derived from the DAC determines the precise phase adjustments to be made from the ADL5390 QVM device to the 81.25 MHz frequency input signal.

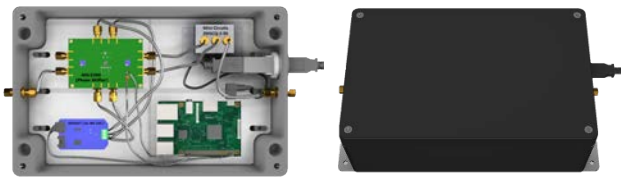

*Figure 1: AWA Laser Phase Shifter Assembly (CAD Model)*

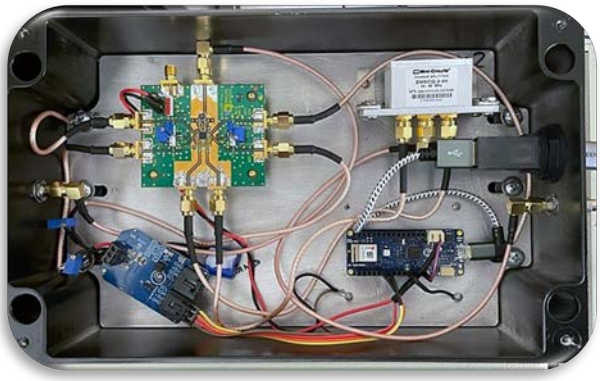

*Figure 1: AWA Phase Shifter Assembly (Realized)*

### A. *Summary of Operation*

1) Necessary phase shift is defined by a user and is received by the control system.
2) Control system's algorithm performs necessary calculations to determine the correct output voltages to be produced from the AD5667 DAC.
3) Calculated voltage values are converted to decimal values and then to hexadecimal values in order to be written to the AD5667 DAC registers.
4) Hexadecimal values are transferred to the AD5667 DAC through the I²C communication protocol and correct voltage is outputted to the intermediate (I) and quadrature (Q) inputs of the ADL5390.
5) ADL5390 QVM rectifies the 81.25 MHz signal by applying the user defined phase shift.

## IV. Enclosure

Electronic devices often need protection from external environmental factors. An exposed circuit board is more likely to be damaged than one that has been covered and also poses a potential safety risk when the device is being operated. A user could unintentionally come in contact with the unprotected traces leading to a possible electric shock. Because of these reasons, an enclosure was needed to protect the sensitive electronic devices.

The Polycase AN-23F enclosure is diecast from an A383 aluminum alloy and measures 260.10 x 160.02 x 90.42 millimeters (10.24 x 6.30 x 3.56 inches) with a total mass of approximately 3.8 kg (~ 8 pounds). The enclosure is IP68 rated, and electromagnetic and RF interference shielded to protect the electronics within. To achieve the IP68 certification, the enclosure has a durable impermeable cover that can be secured to the body of the enclosure using four stainless steel 8-32 machine screws.

A gasketed material made of nitrile buna rubber is employed between the lid and the body as an additional form of ingress protection. Two SMA pass-through connectors were embedded into the enclosure to allow the 81.25 MHz input signal and the phase adjusted 81.25 MHz output signal to be attached to the device. A USB Type A bulkhead adapter is also available externally to supply the 5V power and communication signals through universal serial bus. A mounting tray was machined out of a ¼" aluminum plate (3003 alloy) and fabricated so that the components could be attached securely inside the enclosure. The mounting tray was a necessary part for two main reasons. For one, the mounting tray ensures that the components are safely and securely fitted within the enclosure. Two, the mounting tray makes disassembly for maintenance or calibration much easier since all of the electronic devices come out of the enclosure together.

## V. Results

After testing the device, the results of the Laser Phase Feedback Control System were determined. At an operating Frequency of 81.25 MHz the theoretical resolution that can be achieved with this device is calculated to be 0.000437° degrees at 81.25 MHz (or 0.006992° degrees at the 1.3 GHz LLRF). The device has a phase control range of ±45 degrees at 81.25 MHz. Finally, the stability of the phase meets or exceeds the targeted $< 0.1°$ degree per 1° C temperature change due to the control system dynamically applying corrective measures to adjust the phase shift based on temperature fluctuations.

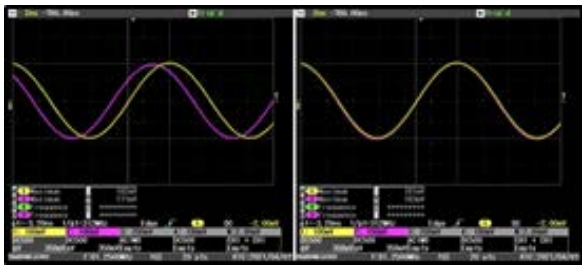

*Figure 3: 45º Phase Difference (Left), Phase Alignment (Right)*


## Acknowledgment

We would like to thank our faculty advisors, Dr. Stanislav Baturin and Dr. Philippe Piot for their extensive help and support throughout this project. We would also like to acknowledge Wanming Liu and John Power of Argonne National Laboratory for their contributions and assistance to the team as well.


## References


[1] "AD8302 2.7 GHz RF / IF Gain Phase Detector." DigiKey. Available from: www.digikey.com/en/product-highlight/a/analog-devices/ad8302-rf-if-gain-phase-detector.

[2] Power, John. Argonne National Laboratory. Argonne Wakefield Accelerator Facility [online].[Accessed 20 October 2020]. Available from: https://www.anl.gov/awa

[3] ROBERTSON, Neil. Phase or Frequency Shifter Using a Hilbert Transformer. [online]. 25 March 2018. [Accessed 7 November 2020]. Available from: https://www.dsprelated.com/showarticle/1147.php

# ZigBee Mesh and Graphical User Interface for a Wireless Tunable Laser Spectrometer Array Onboard the International Space Station

NASA Jet Propulsion Laboratory *(NASA/JPL-Caltech)*

J. Gehant, S. Eschbach, Z. Abbas
College of Engineering and Engineering Technology
Northern Illinois Univeristy
DeKalb, Illinois
Joseph.K.Gehant@Gmail.com, Susanna.Eschbach484@Gmail.com, Zahra.Abbas1551@Gmail.com

***Abstract:*** **Astronauts working onboard the International Space Station have reported recurring health issues that are potentially related to exposure of high levels of carbon dioxide. However, there currently is not a robust and reliable way to monitor the concentrations that astronauts are experiencing. Some studies suggest that long-term exposure to high levels of carbon dioxide can cause bone and kidney composition changes, chronic inflammation, and vision impairment, with short-term issues such as dizziness, lethargy, increased blood pressure, and headaches. Because exposure to high levels of carbon dioxide can result in these long and short-term health issues, it is important to measure carbon dioxide and other trace gases in real-time over a system-wide spatiotemporal range to provide an understanding of areas and times of high carbon dioxide accumulation.**

***Keywords:*** ***Wireless Sensor Networks; ZigBee; Carbon Dioxide Distributions; 2.4-2.5GHz Interference Avoidance***

## I. Introduction

A more extensive means of tracking carbon dioxide concentrations in real-time onboard the International Space Station (ISS) is required. Wirelessly transmitting tunable laser spectrometer sensor readings and network performance metrics in a ZigBee mesh network with six remote nodes to a base station graphical user interface (GUI) is the proposed solution.

The project features four primary objectives in the pursuit of fulfilling this task: First, interface microcontrollers attached to tunable laser spectrometers with ZigBee protocol communication modules to collect and wirelessly transmit low-layer network health metrics and spatiotemporal distributions of carbon dioxide and other trace gases to the network collector/coordinator. Second, optimize network transmissions by adjusting ZigBee networking parameters and designing a custom API in C. Third, design a graphical user interface for a base station laptop to receive, parse, visualize, and log network performance metrics and sensor readings for each remote node. Fourth, design an algorithm to actively sample the 2.4-2.5GHz spectrum to detect and actively minimize radiofrequency interference to coexist with other wireless communications operating on the same band.

## II. Materials

The two main components of this project are the ZigBee RF modules provided by Digi called XBees that are used to create the mesh network, and the custom JPL printed circuit boards (PCBs) with AVR and ARM-based microcontroller units (MCUs). The ZigBee protocol was determined to be appropriate for this wireless sensor network because of its versatile mesh-networking capabilities, high-configurability, low-power transmissions (<0 dBm), low RF overhead, minimum RF interference, low power consumption, and self-healing. For this project, seven XBee modules were used: Six XBees were configured as routers and interfaced with microcontrollers to collect and transmit data through the network, and one XBee was configured as a coordinator to receive, demodulate, and transmit payload data locally via UART serial communication to the base station for processing, logging, and then displaying on the GUI.

The XBee modules are connected to the JPL MCU PCBs via UART Rx and Tx pins. The MCUs are programmed to poll and collect data from tunable laser spectrometers via analog-to-digital conversion (ADC). *Figure 1* displays the XBee module attached to the PCB.

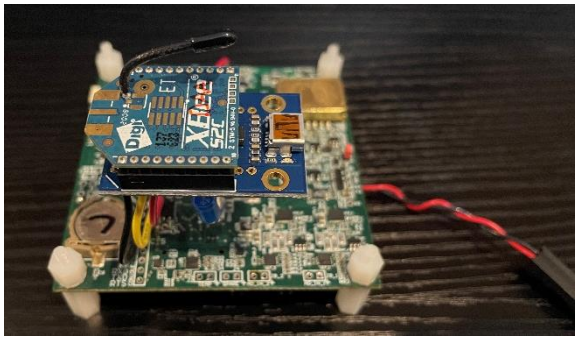

*Figure 1. JPL Microcontroller w/XBee Module*

## III. Methods

The microcontrollers are programmed in C and their task is to collect methane, ethane, water vapor, carbon dioxide, and pressure data from their attached sensors, and poll for neighbor tables, routing tables, link quality indicator, received signal strength indicator, APS acknowledgement successes, APS acknowledgement failures, MAC acknowledgement failures, clear channel assessment failures, APS RF retries, and 2.4-2.5GHz energy spectrum analysis values from their local XBee. To obtain the network health metrics from the local XBee, the microcontroller must send out several ZDO-layer request frames for each specific cluster identification number. When the XBee receives the

frame, it replies with the requested index and data in a response frame to the microcontroller's Rx pin. Once the microcontroller receives the data from the XBee and attached sensors, it parses out the relevant bytes, formats the data into transmit request frames with ZigBee packet payloads, and then sends the frames to the attached XBee via its UART Tx pin. The XBee then processes the frame and executes the commands and addressing bytes in the preamble to transmit the payload data via ZigBee protocol to its destination – the coordinator connected to the base station via FTDI to USB.

The base station is programmed in Java and it receives frames formatted by the coordinator containing payload data from each remote node through a serial data event listener with read blocking. Once a frame has been detected, the information contained in that frame is parsed out, stored in device objects, and then displayed on the GUI. The GUI displays the data in graphs through an open-source Java graph program called Telemetry Viewer (TV). Alongside TV are two additional custom graphs that have been created: An area chart to visualize carbon dioxide distributions more effectively over time, and a network topology graph of all remote nodes with active links. Windows are also being rendered to display network performance/health metrics that are better shown as numerical values in tabular form. *Figure 2* below shows the interconnectivity of transmissions through the network's primary system components.

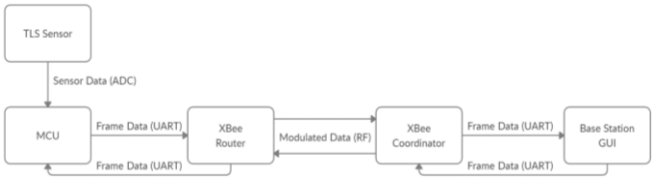


*Figure 2. Network Block Diagram*

## IV. Features

There are two main features that have been designed and implemented into this project. The first is a timeout buffer that has been added to the microcontroller code. The purpose of the buffer is to ensure 0% data loss in the event of an RF transmission timeout, failure, and/or network reset. The buffer operates as a circular/ring buffer and can store up to 8 minutes of timestamped sensor data before it is overwritten. Once the network can operate normally in real-time after the buffer is triggered, the XBee transmits the accumulated data in optimized payloads to the base station. This ensures that when the data is reviewed by the end-user at the GUI, they will always see a consistent logging of sensor data at the time the samples were collected at the microcontroller, and thus be able to reliably monitor spatiotemporal distributions of carbon dioxide throughout the ISS.

The second feature is an energy detection and channel changing algorithm called "ZigZag". The purpose of ZigZag is to ensure that the ZigBee network is operating on the channel with the least amount of RF interference and prevent the network from interfering with other coexisting networks operating on the same 2.4-2.5GHz band. ZigZag performs an energy scan on network startup to determine the best initial channel for the network to operate on. During network operation, ZigZag periodically scans all ZigBee channels at each remote node to determine if there is a channel with significantly less noise to operate on. If certain criteria are met, ZigZag will trigger a popup on the GUI and ask the user if they want to switch the network over to the new channel. If the user agrees, then the entire network will be switched over to the new operating channel.

## V. Results

The network has been tested in a controlled environment in both low and high-interference conditions. The tests have shown the network performs better in star-configuration (one-hop) than in multi-hop configuration. The network also performs optimally with <0.01% packet loss when it is not operating on the same frequency as the generated noise/interference, proving the need for ZigZag. However, by implementing the timeout buffer, data will only be delayed, not lost, in the event of a transmission failure. *Figure 3* provides results from tests in a controlled environment.

| Condition | Test Configuration | Packets | Retries | BufferCnt | Failures |
|---|---|---|---|---|---|
| Noise-Free | Star | 6933 | 172 | 29 | 0 |
| Noise-Free | Multihop | 6933 | 1240 | 50 | 26 |
| High-Noise | Star | 6933 | 1980 | 59 | 0 |
| High-Noise | Multihop | 6933 | 4660 | 259 | 34 |

*Figure 3. Network Test Results*

## VI. Conclusion

Several network health metrics have been implemented to monitor network performance. To reduce the probability of high levels of interference/noise compromising the network's integrity, a timeout buffer has been implemented ensure 0% data loss, as well as a channel energy spectrum analysis algorithm to determine the optimal operating channel and configure the network to operate on it. Under low-noise conditions, the network can gather and transmit data with <0.01% packet loss. When higher levels of noise are introduced on the same operating frequency, latency is increased, and the timeout buffer is utilized more frequently.

## Acknowledgments

As a team, we would like to thank the following individuals and institutions:

- Dr. Christensen for providing input to help improve the network, assisting with troubleshooting, and being involved with the project.
- Dr. Fonseca for all his help, guidance, and knowledge throughout this project.
- Northern Illinois University and NASA/JPL-Caltech for collaborating to make this project possible.

# Gantry Crane

Deep Babaria[1], Dhruv Thakkar[2], Manavkumar Patel[3]
Department of Mechanical Engineering
Northern Illinois University
DeKalb, IL, USA
Z1825374@students.niu.edu[1], Z1814324@students.niu.edu[2], Z1832687@students.niu.edu[3]

***Abstract*—Gantry cranes are used to lift heavy objects with ease and safety. This project has two main requirements: one is to have a maximum lifting capacity of 907kg (2000 lbs) and second is to have a foldable feature that allows the operator to store the crane in small space when it is not being used. The gantry crane built for this project will have similar and different features to other gantry cranes in the market. The crane built for this project will have an adjustable height feature to allow the operator to set the machine at a desired height. Using the same adjustable height feature, the operator can fully lower the height of the crane so that it does not consume more space and other work and experiments can be performed in the same room.**

## I. Introduction

An Electromagnetic Shaker which produces mechanical vibrations is used to conduct Hand-Arm Vibrations (HAV) tests in vibrations laboratory. These tests are done by orienting the machine in horizontal position and in overhead position. Moving the machine from horizontal position to overhead position, and vice versa, with less effort requires some sort of crane; in this case it will be a gantry crane. The main function of the gantry crane built for this project is to lift and move this machine which weighs around 227kg (500 lbs). The crane will be able to lift the machine off the concrete base, move it to a desired location and orient it in a desired position. The lifting of the weight will be done using a hoist which will be attached to an I-beam trolly which will allow the operator to move the machine along the length of the I-beam.

The other requirement of the project is to make the crane fit in small space when it is not being used. The crane will have an adjustable height feature which will allow the operator to make the crane shorter to store it in a small space. Additionally, the crane will be able to move with a manual push or pull which allows the operator to move the machine from one position to another. Overall, this crane will save the operator's time and make it less difficult to move the machine from horizontal to overhead position and vice versa.

## II. Methods and Materials

### A. Size and Material of the Gantry Crane

The size of the gantry crane is determined by measuring the area where the Electromagnetic Shaker is kept. The material for the crane is selected by considering the maximum lifting capacity, safety of the operator, and the budget of this project. The materials used for the crane are as follows:

Table 1. Material selected for the gantry crane.

| Parts | Material/Specification |
|---|---|
| Steel I-Beam | ASTM A992/A572-50 |
| Steel Rectangular tube | ASTM A500 |
| Steel flat bar | ASTM A569 |
| Hoist | 2000lb Capacity |
| Trolly | 2000lb Capacity |

### B. Adjustable Height Mechanism

As mentioned before, the adjustable height feature will allow the operator to make the gantry crane shorter or taller to either change the height at which the weight needs to be kept or to store the crane in a small space when it is not being used. This feature will work by having the vertical beam through a middle support beam whose cross section will be slightly bigger than the vertical beam's cross section. Fig. 1 below shows the mechanism of this feature. The highlighted piece in the figure is the middle support beam and the beam that goes through it is the vertical beam. This mechanism will allow the vertical beam to slide up and down which will change the height of the crane and the holes on the vertical beam will allow the operator to lock the height of the crane by inserting a pin through the lined-up holes of vertical beam and middle support beam.

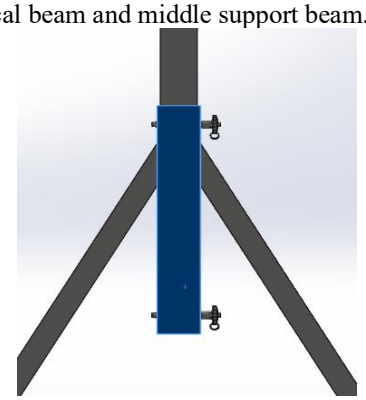

Figure 1. Adjustable height feature mechanism

### C. Construction of the Gantry Crane

To construct this gantry crane, several methods such as welding, cutting, drilling, and grinding will be used. First the 3in x 2in rectangular tube are cut into two 1.625m (5.33ft) pieces and four 1.219m (4ft) pieces. The 4in x 3in rectangular tube is cut into two 0.914m (3ft) pieces. The steel flat bar is cut into four 0.1143m x 0.127m (4.5in x 5in)

pieces and two 0.1016m x 0.127m (4in x 5in) pieces. Holes are drilled through each of the steel flat bar pieces, the two 1.625m (5.33ft) rectangular tubes, and the two 3ft rectangular tubes. The 60 degrees angled cut is made on one end of 1.219m (4ft) rectangular tubes, and 30 degrees cut on the other end. Then the end with 30 degrees cut is welded to the center of the 0.1143m x 0.127m (4.5in x 5in) steel flat bar pieces, and the end with 60 degrees cut is welded to the 0.914m (3ft) long rectangular tubes. One end of the 1.625m (5.33ft) tubes is welded to 0.1016m x 0.127m (4in x 5in) steel flat bar pieces. Then, the bolts and nuts are used to attach wheels to the 0.1143m x 0.127m (4.5in x 5in) steel flat bar pieces and I-beam to the 0.1016m x 0.127m (4in x 5in) steel flat bar pieces. Finally, the 3in x 2in rectangular tubes are passed through the 4in x 3in rectangular tubes and the metal pins are passed through the lined-up holes in 3in x 2in and 4in x 3in tubes to set the crane at a desired height. Once the gantry crane is constructed, it will look like the crane shown in the figure below.

Figure 2. Structure of the gantry crane

## III. Results and Discussion

The analysis of the gantry crane 3D model is done using ANSYS. For this analysis, the model was vertically cut in half and then imported to ANSYS because it was unable to calculate the results as the number of nodes and elements created were higher than the limit. This analysis includes the normal stress, shear stress, principal stress, and total deformation results of the crane when the 2224N (500 lbf) is applied to the crane.

| Results | Minimum | Maximum | Units |
|---|---|---|---|
| Equivalent Stress | 0. | 1.2767e+008 | Pa |
| Maximum Principal Stress | -1.1401e+007 | 1.3684e+008 | Pa |
| Shear Stress | -5.5741e+006 | 5.2496e+006 | Pa |
| Total Deformation | 0. | 3.7638e-004 | m |
| Normal Stress | -2.8398e+007 | 3.7157e+007 | Pa |

Figure 3. Result summary from ANSYS

Fig. 3 shows the result of the analysis performed on the gantry crane model. The factor of safety is calculated using the Maximum principal stress value and the yield strength of the overall crane. The factor of safety calculated using the results is 3.023 which is good enough for this gantry crane and confirms that the gantry crane will be able to safely lift the electromagnetic shaker, which weighs around 227kg (500 lbs), and will be safe for the person using it.

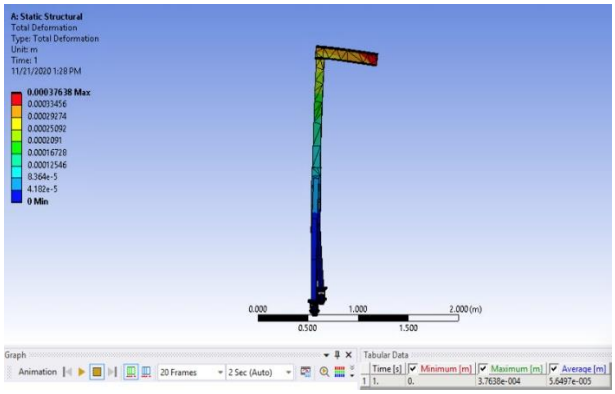


Figure 4. Total deformation

Fig. 4 shows how the crane will deform when the 2224N (500 lbf) is applied. The maximum deformation value is 0.00037638m. This shows that the maximum deformation value is significantly small with respect to the size of the crane and confirms that it will be able to lift the machine without failing the structure.

## IV. Conclusion

Gantry cranes are mainly built to lift and move heavy objects with ease and safety. Some are built just to focus on lifting and moving the objects. Whereas some of them are built to offer more functionality to the operator other than lifting and moving. The height changing factor is what makes the gantry crane, built for this project, unique. It allows the operator to not only use it for lifting and moving heavy objects, but also allows the operator to change the height of the crane and to store it in a small space when it is not being used.

Like mentioned before, the gantry crane will be able to lift anything up to 907kg (2000 lbs). It will be very easy and straightforward for the operator to use this crane as long as they follow the steps of using this crane properly and know all the safety issues related to this crane. Overall, this crane will make the task of moving the machine a lot easier and safer.

## V. Acknowledgement

We would like to thank Northern Illinois University and College of Engineering and Engineering Technology for providing us a $1000 fund for this project and an opportunity where students can do hands-on engineering work and gain knowledge about what a real engineering job will look like after getting the degree. We would also like to thank Dr. Xia for being a great mentor and providing us with a great Idea and opportunity to work on a real-life project which will be used in our Engineering building after we graduate. We also thank our TA, Ian Gilmour, for helping us out through many problems and for being available whenever we needed him.

# Smart End Effector for 6-DOF Robot

Adam Cotton, Victor Aguado, Jakob Furgat.
Department of Mechanical and Electrical Engineering, Northern Illinois University, DeKalb, IL 60115

***Abstract*—Collaborative robots, or Cobots for short, are a quickly emerging technology in Industry 4.0 [1]. These robots work alongside humans to perform repetitive tasks. The robot must change its tool or end effector in order to accomplish multiple tasks. Unused tools are securely stored in a tool rack, like in a CNC machine. The robot arm must interact with the rack to change tools. Improvements are needed to existing tool rack systems. We have worked to design a smart system by integrating microcontrollers into system components. A functional prototype was constructed to demonstrate the smart system.**

## I. Introduction

Although Industry 4.0 is the revolution of smart manufacturing, many existing tool rack solutions are lacking smart capabilities. Many systems are purely mechanical, and all of the tool change process data is programmed into only the robot arm. The robot arm stores the home position of all the tools. If tools are manually swapped or misplaced, the robot arm would return to the saved tool position and select the incorrect tool. Operations performed with and incorrect too could result in catastrophic damage to production parts or the tools themselves.

In this project, we wanted to design a smart end effector and rack with the help of microcontrollers. The microcontrollers store data regarding the tool positions and control most of the tool changing system. This takes some workload off the robot operating system. The robot operating system and the microcontrollers work as one to change and control various tools.

The robotic tool change system consists of three components: the end effector, tool rack, and tool. The end effector is mounted to the robot arm and selects tools from the rack. Figure 1 below shows how the components interact.

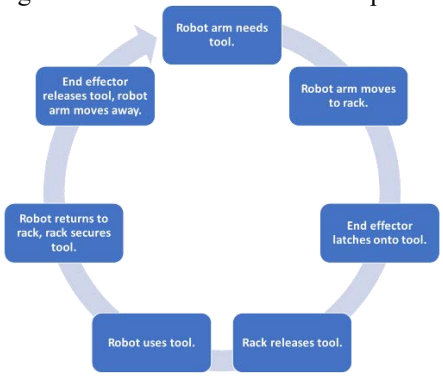


*Figure 1 Robotic Tool Change Process*

## II. Methods and Materials

### A. Electrical

Parallax FLiP microcontrollers are integrated into each component to control system functions. Each microcontroller holds code that operates each subsystem to run correctly. The microcontrollers communicate with other subsystems using infrared communication. The system's power is provided by NiMH AA batteries which total to 9 volts per subsystem. All electrical solder connections were made on through-hole protoboards as seen in figure 2. Sockets were soldered onto these boards to allow for swapping of microcontrollers and driver boards.

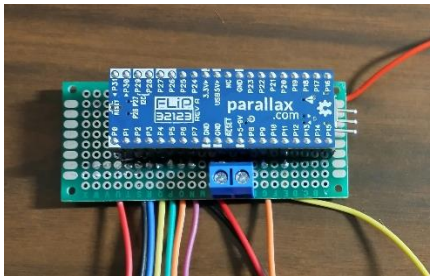


*Figure 2 Parallax FLiP mounted on THT proto board.*

### B. Demonstration Tool

As seen in figure 3, this prototype uses a gripper as a demonstration. Many different types of tools can be used with this system. The gripper currently in use on the prototype is actuated via a NEMA 17 stepper motor. The gripper demonstrates the precise control possible with a microcontroller and stepper motor. The demonstration tool also has infrared LEDs to communicate with the tool rack and end effector.

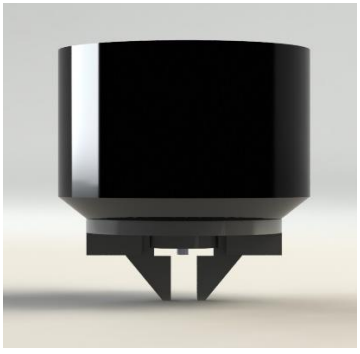

*Figure 3 Solidworks rendering of the demonstration gripper.*

### C. Tool Rack

The tool rack, shown in figure 4, holds the tools when they are not in use. It will be located near the collaborative robot so that the tool can be removed or changed easily. The tool rack has been outfitted with both an IR receiver and a limit switch to detect the position of the tool. Currently, on the prototype, there is only room for one tool on the rack. However, on the commercial version of product there would be multiple tool holders. The tool rack mechanism opens and closes to secure and release tools.

Another important feature of the tool rack is communication with the human operator via a display screen. A small OLED screen is mounted on the tool rack at a 45-degree angle for easy viewing. The OLED screen displays information about the tool in the rack. The screen also tells the operator whether the tool rack is open or closed.

*Figure 4 Solidworks Rendering of the Tool Rack*

### D. End Effector

The end effector (figure 5) is always attached to a robot arm. It has an internal servo mechanism to latch onto different tools. The end effector has copper contacts on the bottom that pair with contacts on the tool. These contacts provide power to the tool as well as signal connections between the microcontrollers in the end effector and tool.

The ring on the end effector may seem a bit bulky, but this was required to fit the six AA batteries needed to supply this component with 9V. This bulky ring can be eliminated in an industrial environment by feeding a DC power line to the end effector. A power connection to the robot arm will replace the bulky ring. For other components, the batteries were able to easily fit into the available space, resulting in slimmer overall parts.

*Figure 5 Solidworks Rendering of the Smart End Effector*

## III. Results and Discussion

We were able to fabricate a working prototype of the smart end effector and tool rack. The end effector, tool, and tool rack all work together as one system. Figure 6 displays the assembled prototype.

Looking into the future, the team has identified areas of the project that could be expanded upon. These areas include minimizing the size of the components, testing the system with multiple tools and rack positions, testing with a robot arm, and developing printed circuit boards to replace the through hole proto boards.

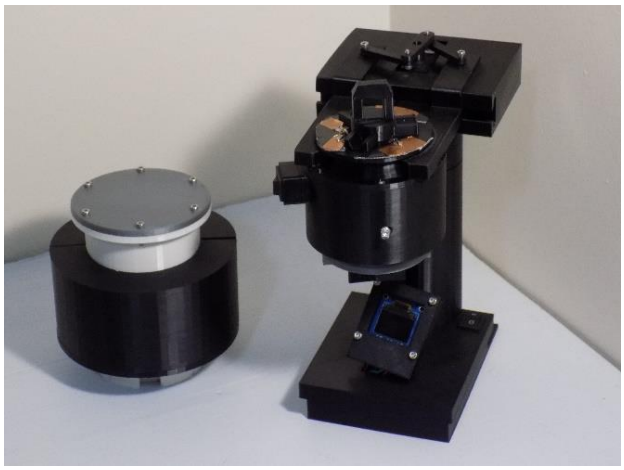

*Figure 6 Assembled system components.*

## IV. CONCLUSION

This smart end effector and tool rack system offers a mechatronics solution to the tool changing process for collaborative robots. This product more closely aligns the robotic tool change process with the smart manufacturing goals of Industry 4.0. This project is ready for further development, flowed by implementation into manufacturing processes.


## ACKNOWLEDGEMENT

The team would like to acknowledge our faculty advisor Dr. Frank Nickols as well as our TA Amin Roostaee for the help and guidance throughout the semester. Their efforts greatly helped the success of this project.


## References


[1] Why cobots?: All the benefits of COLLABORATIVE ROBOTS. (n.d.). Retrieved from https://www.universal-robots.com/products/collaborative-robots-cobots-benefits/

# Remote Piloted Drone for Cenote Water Collection

Noah Reid[1], Matthew Sebek[1], Jacob Sampson[2],
Nestor Alvarez-Popoca[3]
Department of Electrical Engineering[1]
Department of Mechanical Engineering[2]
College of Art and Design[3]
Northern Illinois University
Dekalb, United States

Dr. Sachit Butial
Department of Mechanical Engineering
Northern Illinois University
Dekalb, United States
sbutial@niu.edu

***Abstract*—Due to the difficulties and dangers associated with collecting water and data samples from areas of interest, unmanned aerial vehicles (UAV) have been used to reduce risk and increase efficiency of geological surveillance. This document provides both the design and development of a high durability, high payload capacity UAV. This drone will operate by combining power control systems, flight control systems, and data and sample collection systems in order to provide operators with a modular device that can operate in a variety of environments and assist in various forms of geological sampling.**

## I. Introduction

Over the past several decades, human development and its subsequent pollution levels have increased dramatically, and effect even the most remote areas. One indicator of the ecological health of a specific environment is the quality of water within. While water sampling is rather easy in urban areas with modern infrastructure, it can difficult and dangerous in environments with a large amount of vegetation, such as forests or jungles. The difficulties are amplified when cenotes, large chasms in the ground filled with water, are the intended areas of sample collection.

A sample collecting drone operating in an undeveloped area raises some immediate design concerns. It must have a high payload capacity, be susceptible to high-speed impacts and collisions, be able to implement a variety of information collecting technologies, and be modular in design to adapt to future missions. Essentially, this drone is a hybrid between long endurance agricultural drones or package delivery drones, and nimble hobbyist drones that focus on easily modifiable firmware and maneuverability. This paper will detail how the combination of these two drone families provides a functional design for a modular drone to assist in water sampling and data collection.

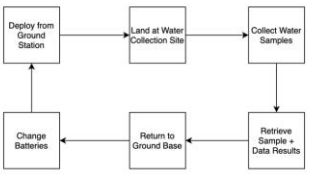


*Figure 1: Mission Deployment Summary*

## II. Prototype Design

There were two main pillars for design development. The first is a limited budget of $1000, with additional funds used to expand upon base features of the drone. Secondly, specific parameters were given for the design, including technical features and a minimum desired sample load. The prototype implements several systems that build on top of each other in order to achieve the desired performance. This design is such that many of the components can be purchased, replaced, or repaired from a local hardware store. Because of this, only a limited number of 3-D printed CAD designs were utilized.

*Figure 2: CAD Model of Drone*

### A. *Frame and Body*

The frame consists of aluminum arms notched to create an X formation. Centered on the cross-section of the arms is a water-resistant box housing the onboard electronics

### B. *Power and Flight Control*

Power is provided by two large, high voltage and high-capacity batteries to a step-down circuit ship which redistributes power to the flight control system, data collection system, and peripherals. Flight is governed by an IC connected wirelessly to an RC remote. This IC handles onboard flight adjustments and provides instructions for each of the four onboard motors. The combination of power, computational instruction form user input, and subsequent motor spinning allows for the drone to achieve flight.

### C. *Sample and Data Collection*

Water is collected by decoding a signal sent from the RC remote and using this to activate a servo motor which opens a PVC container. The data collection is managed by an onboard microcontroller connected to mission specific probes. This data is adjusted and stored to the microcontroller's onboard memory.

### D. *Optional Peripherals*

The addition of several peripherals is intended to provide more data on the areas of deployment and increase ease of use. An FPV (first person view) module is connected to the flight control system to provide a constant perspective from the drone's nose to the pilot. Additionally, a GPS chip has been installed to enable a real-time location of the drone.

## III. RESULTS

Based on preliminary simulations, it was determined that roughly 8 minutes of flight time could be achieved by using dual battery operation.


*Figure 3: Preliminary Flight Simulations*

Testing primarily involved verification of each of the subsystems. The frame and body coupled with the power and flight control systems acted as expected; fully functional flight from a distance of roughly. Similarly, collection of water data and operational function of the water collector were. Peripheral systems were successfully integrated before flight. While functional operation of peripheral systems was not achieved along with flight and sample collection, operation can be achieved through the implementation of another video transmitter IC.

```
ORP Average:           0349.6200
O2 Average:            0006.2200
PH Average:            0003.6789
Conductivity Average:  5801.8890
Temperature Average:   0052.2785
```

*Figure 4: Data Collected from Sensors*

## IV. DISCUSSION

While complete operation of all systems was not achieved simultaneously, this can be easily remedied. Instructions assistance to reach this completion will be provided. Therefore, the design has been validated and will be successfully used within the coming months.

Significant discussion has been given as to additional design ideas that could be implemented in a second phase of the project. One of the limiting factors in development was the budget constraint. This allows for the possibility of improved design elements. One addition would include the ability to adjust the depth of the water collector via the RC remote through implementation of a winch. Secondly, rotor guards would provide more protection to the carbon fiber rotors and increase overall design durability. Due to the modularity of this design, it possible to upgrade many of the current features to improve functionality wherever is necessary after field deployment.

## V. CONCLUSION

Based on testing, this drone does provide a reliable tool to assist in the gathering of water samples and data, although this prototype can be further improved upon with the help of an increased budget and better understanding of infield shortcomings.

## VI. ACKNWOLDEGEMENTS

The authors would like to thank Dr. Sachit Butail and German Ibarra for their continued oversight and advice for the design of this drone. Additionally, Dr. Donald Peterson and the College of Engineering at Northern Illinois University for providing the funds and facilities that allowed for the development. Lastly, Dr. Melissa Lenczewski and the Department of Geology and Environmental Geosciences for additional funding which allowed the success of this project.

# Wahl Clipper Assembly Optimization

Michael Pavlick, William Lee, Zackery Joy, Northern Illinois University, Department of Mechanical Engineering
Sponsor: Wahl Clipper Corporation, Sterling, IL.
z1857394@students.niu.edu; Z1854517@students.niu.edu; Z1854898@students.niu.edu

**Abstract- To streamline production for Wahl Clipper Corporation, a testing mechanism is to be developed that can encompass a wide variety of different quality assurance tests. These tests include internal testing on the charging station current, the motor current and the motor voltage. The tests also include external testing the battery indicator light brightness. The testing mechanism will need to be adaptable to fit a wide variety of products from Wahl. It will also need to have a built-in mechanism that can quickly change the parameter tolerances. For example, larger units will require a larger charging current, so an assembly line worker will need to be able to change the set tolerance for the current test in real time, to avoid downtime in the production process. This testing will be done by modifying the charging station provided by Wahl in conjunction with an Arduino Mega to run these tests concurrently or in quick succession. The user will be able to see whether the unit passes all the quality assurance tests or needs to be discarded.**

## I. Introduction

In order to keep all units produced by Wahl Clipper corporation to the level of quality that the company has cultivated over decades of production, a unit will need to be produced that can run a wide variety of tests concurrently, or in some cases in quick succession. To match production outputs of larger clipper producers, a method is to be developed that will allow for workers to assemble units as quickly as possible, all while adding more quality assurance. In order to ensure all units are working perfectly, tests that were previously only done in the testing lab will be added to test all units to have even more checks and balances for the unit.

The unit testing will be best understood as internal and external testing procedures. Internally, the motor current, the motor voltage and the current produced from the charging mechanism. This will all ensure that the unit is properly receiving power, charging appropriately, and then being able to store this power for an output voltage. All of these are tested internally and have output parameters that can be changed or narrowed down as shop floor usage gives the users a greater idea of the proper tolerances. The unit also has a variety of external testing procedures, and this system will incorporate one and have infrastructure for more. The unit will test the brightness of the battery indicator light. The battery indicator light test will confirm that when the eventual customer has the unit, they will be able to see how much battery is remaining, or when it is time to charge the unit. The unit will also need to be able to effectively adapt to fit different models on the assembly line. This means not only being able to adjust testing tolerances, but also having adaptable units that can fit different sized clippers.

## II. Mechanical Design

One of the main goals of the system is to remain modular while creating infrastructure that can house current tests, while making it possible to add tests for units created in the future. The best approach to that will be making every component of the system removable and adjustable to fit any size clipper.

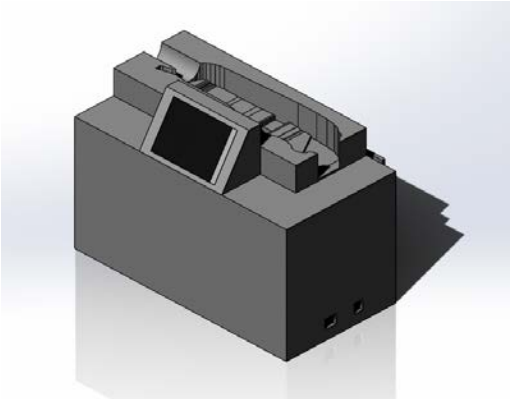

*Figure 1: Testing Station Model*

The mechanical design can be broken into two main components, the stationary part and the removable portion. The main box and the Arduino screen are stationary and can't be removed. These will be the same for each system, so it will save space and money for Wahl to be able to keep one main base unit and just adjust for different models. The other part of the system is the removable clipper holder. The clipper holder is built for form fit the clipper geometry, while leaving access to the charging port. The clipper holder has four vertical locaters that drop on to the stationary portion of the unit, that has extruded poles that will keep the clippers in place will in use. By making this component

of the testing mechanism modular, it allows for all different sized units to fit on the top of the testing dock, as well as allowing for future models developed by Wahl to work with the testing mechanism.

## III. Electrical Design

All components of the electrical portion of this design run through an Arduino Mega that is placed within the box portion of the unit. The Arduino Mega is connected to an LED shield monitor through a combination of jumper cables, that allow for the output screen to be easily viewed by the user. The Arduino allows for all of the tests to be run, collect the data and then produce a pass or fail output to the user.

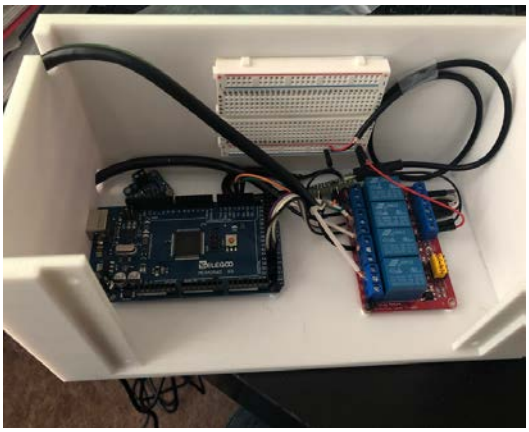

*Figure 2: Internal Arduino, Relays and Bread Board*

The system utilizes a modular relay to start the testing process. This is accessible by simply pressing a button on the box once the clipper is plugged in and sitting in the holder. The start button activates a code that is intentionally built to have the proper amount of time between tests, that allow for the tests to be cycled through as quickly as possible without causing an error for overlapping or conflicting tests.

Three tests are done through the internal computer in the clipper. The charge current, motor current, and motor voltage can all be found using the MCU and coding program TerraTerm. The code will pull information on all of those internal tests and confirm that they are within the predetermined tolerance range, and then giving an output to the user on if that particular test was passed.

The light sensor test is built into the top of the testing unit, but with all of the connections to the Arduino system within the box as well. The system will activate the unit to move the blades and to activate the blue indicator light located on the base of the unit. Both individual sensors will collect the information and confirm with the system that the values produced are within the spec.

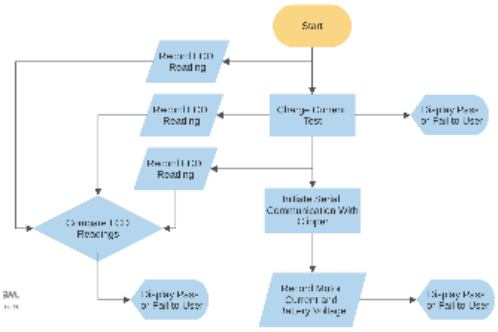


*Figure 3: Program Flowchart*

Above, in Figure 3, is a program flowchart that explains the logic of the system and all of the checks and balances in place to make sure all processes are done in the correct order and how the results compound on themselves.

Finally, one of the most important parts of the system is a failsafe for users who are prone to error. The testing mechanism is built to be able to have the unit prematurely removed without ruining the testing station. The unit will simply cycle through and be able to start up again with testing with the next unit. This is critical so offset the possibility of errors ruining the entire internal component of the design.

## IV. Conclusion

The optimization system will save a considerable amount of time for Wahl, all while increasing the quality control of each product. The worker will be given immediate feedback on the unit they just put together and can confidently set aside functioning units for shipping. The system will continue to be optimized as continued shop floor testing will help the users become more familiar with the process, and more data will allow for tolerance ranges to narrow down. The testing mechanism is also purpose built to allow for engineers to continue to add quality tests. New tests can be ran through the same Arduino board, taking advantage of the infrastructure in place and the modular nature of the testing unit.


## Acknowledgement

The Wahl Assembly Optimization team would like to thank Dr. Abul Azad, German Ibarra, Ed Miguel, David Todd and Matt Bowers for guidance and support on this project. The Wahl Assembly team would also like to thank Wahl production line workers for valuable information and insight on their working procedure.

# An Energy-Saving Smart Window System

Team 28

Lucas Enser *(Author)*
Mechanical Engineering
Northern Illinois University
Dekalb, Illinois, United States of America
Z1883021@students.niu.edu

Kevin Bottorff *(Author)*
Electrical Engineering
Northern Illinois University
Dekalb, Illinois, United States of America
Z1880288@students.niu.edu

Ivan Gomez *(Author)*
Mechanical Engineering
Northern Illinois University
Dekalb, Illinois, United States of America
Z1882940@students.niu.edu

***Abstract*—The energy-saving smart window is a system of window actuators that work together electronically through a wireless system to control the climate within a residential home or office. The components include an actuator that mounts onto a traditional sliding window to open and close in response to weather conditions. The actuation is controlled by a wireless system that is coded to appropriately react to weather conditions. The determining factors will be the temperature gradient, humidity, and wind speed. The aesthetics, safety, and ergonomics have been considered in the design.**

## I. Introduction

Temperature plays a large role in comfort and health. Controlling the indoor temperature and humidity to ease discomfort is balanced against the cost of the utilities that it takes to effectively heat and cool a home. An efficient solution is the use of windows. Windows allow for air exchange between the exterior environment and the interior of the home. This exchange can benefit the level of comfort a homeowner experiences and alleviate the burden of high utility costs. An automated system to do this would save the homeowner time and allow for an increased level of effectiveness in the process of maintaining interior air quality. Generally, cooling and heating are done by a heater or air conditioning unit. To have these units work efficiently, windows must be closed. The addition of windows to the living space opens the way to natural lighting, room ventilation, warmth, and improves the overall look of a home. Deciding on the type of window for a home determines the positive and negative effects such as airtightness and ventilation. The project being introduced incorporates natural elements into the home to improve efficiency, comfort, and improve healthy air and lighting in the home. The window prototype will open and close depending on certain conditions, and the user interface will be ergonomic for the user.

## II. Ease of Use

### A. *Realistic Constraints*

In compliance with the American Society of Mechanical Engineers (ASME), the hardware and measurements will have to be kept in the Imperial System of measurement. If the product were to expand into other countries, then the design would have to be worked into the metric system. Dimensioning and tolerance will need to be incorporated into the design although tolerance may not be needed for residential use. All ASME safety code regulations will need to be met. ANSI regulations will need to be met for the American Market.

### B. *Maintaining the Integrity of the Specifications*

The producer and the consumer will both face economic constraints with the product. The producer will have to price the finished product according to manufacturing production cost, distribution, and marketing. After the window design is complete, it will need to be incorporated into a bigger ecosystem of windows with the main controller so that they work in tandem. The ease and benefits of the design will need to be properly marketed to the consumer.

Certain economic constraints the user may encounter will be dependent on how many rooms will require the device. Ideally, as a producer, the product will go on every window to fully benefit from the design. However, the consumer will have to weigh the cost to benefit from outfitting the number of windows they need. The bigger the house, the more devices it will need, which can increase the cost of installing the devices on the windows throughout the house or office.

## III. Optimal Design

Temperature plays a large role in comfort and health. Controlling the indoor temperature and humidity to ease discomfort is balanced against the cost of the utilities that it

takes to effectively heat and cool a home. An efficient solution is the use of windows. Windows allow for air exchange between the exterior environment and the interior of the home. This exchange can benefit the level of comfort a homeowner experiences and alleviate the burden of high utility costs. An automated system to do this would save the homeowner time and allow for an increased level of effectiveness in the process of maintaining interior air quality. It would also save the homeowner time.

The system consists of four separate components, including two sensors that measure both temperature and humidity. These function to provide readings of temperature and humidity for both the interior and exterior of the home. This data is then passed to the next component, the controller. The controller interprets the data and produces a command for the mechanism that opens and closes the window to best reach the desired temperature. The final part is the mechanism that controls the window. This allows the flow of external air into the room affecting the interior air temperature. This feedback loop allows for a more comfortable interior air temperature.

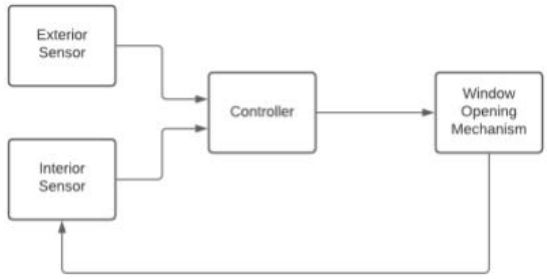


Figure 1: Component Diagram

### A. *Individual components*

The controller consists of a simple comparison algorithm that either opens or closes the window and is run through a small computer. The strength of this control system lies in its simplicity. It minimizes the opening and closing of the window over time by only operating the window mechanism when the direction of the temperature gradient demands it. It also makes the integration of additional window units easy by treating additional window units as binary units in a system and reduces the need for computing power. The control system will also account for the inclusion of humidity as a factor affecting indoor air quality. As temperatures rise the sensor will interpret higher temperatures in terms of the heat index to accurately gauge their effect on human comfort.

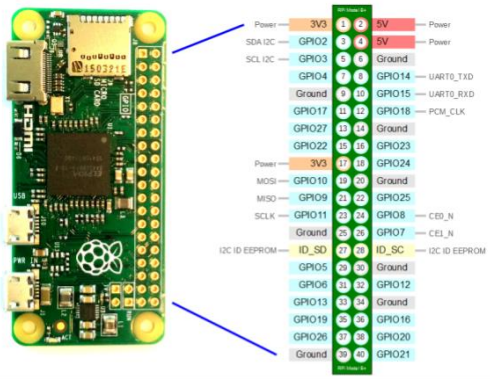


Figure 2: Pinout of Raspberry Pi Zero W

The window mechanism consists of a simple linear actuator mounted to the bottom of the frame of the window and the wall. The small forces demanded and the need for a compact design meant that a linear actuator was an economical and effective choice. Due to the dynamics of sliding windows, the bottom mount allows for a minimum amount of jamming by operating most directly against the force of friction caused by gravity. The mechanism will also include a safety latch for the release of the mechanism during emergency situations.

Figure 3: Actuator Mechanism with Bracket (Front View)

The final component chosen was the sensor. Sensors with a high tolerance of atmospheric temperature variations were chosen so that the external temperature sensor would operate in most environments. The chosen sensor also includes a humidistat so that changes in perceived temperature due to humidity could be accounted for.

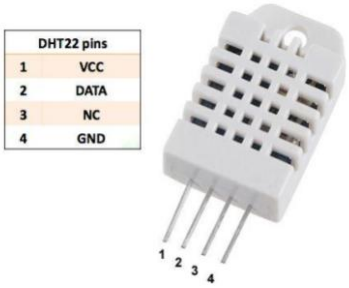


Figure 4: Pinout of DHT22 Sensor

### B. Equations

The first step is a comparison between the interior(Ti) and exterior temperatures (Te) and the desired temperature (Td) that is input by the user. The difference (ΔTa) between the exterior and interior temperature will be calculated as in Eq. (1) and the difference (ΔTd) between the interior and the desired temperature will also be calculated as in Eq. (2). These two values will then be compared in Eq. (3) to produce an operation parameter (OT).

$$\Delta T_a = T_e - T_i \quad (1)$$

$$\Delta T_d = T_i - T_d \quad (2)$$

$$O_T = \frac{\Delta T_d - \Delta T_a}{|\Delta T_d| + |\Delta T_a|} \quad (3)$$

OT will either have a value of either positive or negative one 1. If OT=1, it means the direction of the temperature gradient between the interior and exterior sensors was favorable to reaching the desired temperature and the window should open. If OT= -1 then the direction of the gradient was not favorable to achieving the desired temperature and the window should be closed.

After either temperature rises above 80For 40% relative humidity the system will automatically apply a heat index algorithm to the temperature to account for the increase in temperature and humidity on levels of comfort. A study in the John Hopkins School of Biostatistics underwent a comparative analysis of heat index equations and found several to agree with theoretical values in this range [8]. The heat index temperature is calculated in Eq. (4).

$$\begin{aligned} T_{HI} = {} & -42.379 + 2.04901523T + 10.14333127H - 0.22475541TH \\ & -(6.83783 * 10^{3})T^2 - (5.481717 * 10^{-2})H^2 + (1.22874 * 10^{-3})T^2H \\ & +(8.5282 * 10^{-4})TH^2 - (1.99 * 10^{-6})T^2H^2 \end{aligned} \quad (4)$$

This will allow for a more effective comparison of the exterior and interior temperature. The water content of the air may raise the perceived temperature of the air outside even if the actual temperature is lower. The system will be able to effectively account for the effect of humidity on the interior air quality.

The comparison by the controller will only take place every 2.5 minutes. The reason for this is that it limits the possible number of times the window can open and close. This limits the degree to which the noise of the mechanism can disturb the occupants of the home and limits the number of times it will open and close over the course of a day. .”

## IV. Conclusion

The introduction of technology into the home to allow for the better control of environmental variables is an integral part of the resource management process. Control over climate variables can be achieved using windows that allow for the perceived temperature to be optimized to preserve resources while heating or cooling the home. Though this could be done manually, the inclusion of a certain degree of automation will allow the user to reach desired outcome while saving a considerable amount of time. Due to the residential nature of the implementation of the design, safety must be considered in every aspect of the design to reduce the risk of harm.

The design has three primary components. First, a simple mechanism that utilizes an actuator could effectively open and close the window. A safety release and a minimization of force would be needed to ensure the safety of the users, especially considering the residential nature of its deployment. Second, Temperature and humidity would be read by an exterior and interior sensor that will transmit data to a control module. Finally, a control module would determine if the window should be in an opened or closed position to reach the desired interior temperature based on the temperature gradient between exterior and interior temperatures. This will create a feedback loop by altering the interior air temperature. The system will communicate via wireless internet connection and allow the components to communicate wirelessly.

Safety and simplicity are the guiding principles of the design. The design of devices, especially those that operate in residential environments requires a thorough consideration of the possible outcomes of the use of a product. Through the limitation of the force it can apply, the ability to remove it in an emergency, auditory and visual warnings, and the minimization of its movement the design should deliver the safest possible user experience while producing its desired behavioral outcomes..


## Acknowledgment

The faculty mentors, Dr. YJ Lin and Dr. Guangcheng Zhang, introduced the project and gave guidance for the project. The CAD design for the window was open sourced by Jose Damian Valdez on GrabCAD. The actuator and hardware CAD designs were acquired from the retailer McMaster-Carr.


## References


[1] Fenesta. (n.d.). Fenesta. Fenesta. https://www.fenesta.com/aboutus.php

[2] fenestra. (n.d.). fenestra. fenestra. http://www.smartfenestra.com/home

[3] Hogston, T. W. (n.d.). Programmable Automatic Window. Google Patents. https://patents.google.com/patent/US5605013A/en

[4] Home Controls. (n.d.). Automatic Window Opener Systems. https://www.homecontrols.com/home-automation/window-opener-systems

[5] LinkAYL. (n.d.). Linear Actuator for Window Automation. https://www.linkayl.com/linear-actuator-window-automation/

[6] Pella. (n.d.). Smart Home. https://www.pella.com/performance/smart-home/

[7] Rush, J. J. (n.d.). Automated Wireless Window Control. Google Patents. https://patents.google.com/patent/US20140167927A1/en

[8] Anderson, Brooke & Bell, Michelle & Peng, Roger. (2013). Methods to Calculate the Heat Index as an Exposure Metric in Environmental Health Research. Environmental health perspectives. 121. 10.1289/ehp.1206273.

[9] "Stopping the Spread of Fracking in Latin America." Interamerican Association for Environmental Defense (AIDA), 19 Aug. 2020, aida-americas.org/en/stopping-spread-fracking-latin-america?gclid=CjwKCAiA7939BRBMEiwA-hX5JwaRK3w-T9_yyjt7l32Ak_X7WQ6At9kiEMiDJgTTUddkFvKUl2hbeBoCXvcQAvD_BwE.

[10] United States. (2010). 2010 ADA standards for accessible design. Washington, D.C.: Dept. of Justice.

[11] Update or Replace Windows. (n.d.). energy.gov. Retrieved 5 3, 2020, from https://www.energy.gov/energysaver/design/windows-doors-and-skylights/update-or-replace-windows

[12]Valdez, Jose Damian. "Free CAD Designs, Files & 3D Models: The GrabCAD Community Library." Free CAD Designs, Files & 3D Models | The GrabCAD Community Library, GrabCAD, 3 Mar. 2017, grabcad.com/library/sliding-window-2

# *LEGO Power Brick Sorter*

William Dumoulin
Electrical Engineering
Northern Illinois University
Dekalb, IL

Rachel Dumoulin
Mechanical Engineering
Northern Illinois University
Dekalb, IL

Oscar Ramirez
Mechanical Engineering
Northern Illinois University
Dekalb, IL

Melissa Gates
Art and Design
Northern Illinois University
Dekalb, IL

***Abstract*— Our team was assigned to a project that was sponsored by a faculty advisor to demonstrate engineering tools, specifically the skills being taught in both the Mechanical and Electrical Engineering departments at NIU. Our faculty advisor, Dr. Demir, presented a project in the outcome was to design a product to sort LEGO bricks. The LEGOs will have their pictures taken by a light sensor and will be sorted into bins based on their color with an Arduino board. Through implementing recommended strategies, the student team hopes that the machine will sort the LEGOs in an efficient manner.**

***Keywords: Light sensor, Arduino board, automation***

## I. INTRODUCTION

The LEGO group was founded in 1932 by Ole Kirk Kristiansen and is a family business. The name LEGO is an abbreviation of two Danish words meaning "leg godt" which means play well. The LEGO business has come a long way in the production phase and is now one of the worlds largest manufactures of toys. LEGOs were created to simulate happiness and promote imagination, creativity, and development. The term "robot" comes from the Czech for "forced labor". Robots have been created to both look and act like humans [1].

Although various versions of this machine come before ours, there has been wonder if there was a more efficient way to sort LEGO bricks in a timely manner. Our team was responsible for designing a machine to sort LEGOs. In this paper, an Arduino board is used to read inputs-light on sensor and turn it into an output-activating a motor.

## II. PRODUCT DESCRIPTION AND STATEMENT

The desire for LEGOs started to slowly decline nearly 10 years ago back in 2010. Kids no longer wanted to play with them, but now, LEGOs are seeing a massive resurgence in popularity. With nearly seven sets sold a minute, the demand for LEGOs have skyrocketed. With the increased desire for LEGOs, there will be a direct correlation to the need and want for a device to sort an accumulation of LEGOs. This article clearly describes an efficient model that will sort the LEGOs in a timely manner, allowing the LEGO creator to spend more time building and less time sorting. This project will use Arduino board to help with prototype development.

### *A. Requirements*

The design constraint encountered was a financial budget of $1,000. Another requirement for this process was that it needed to be safe for all ages, in that it would not be a hazard for any age, adult or child. To ensure this product is safe, there are multiple switches to stop the machine if a part of the process failed. There was no requirement for the size or weight of the finished product.

### *B. Prototype Design*

Figure 1. correctly shows the fully assembled prototype of the LEGO Power Brick Sorter. It consists of a combination of several custom-made 3D components as well as ordered parts. The overall design was constructed around the idea of a light system and the program to sort the bricks. With both of those ideas working together, we were able to design a system to sort LEGOs to produce our final design.

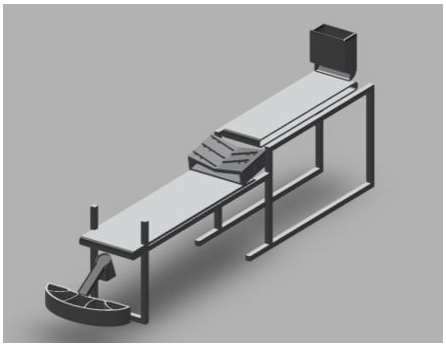

Figure 1. Fully assembled prototype

*1. Drive*

The drive consisted of DC motors that make two conveyor belts move and one for our light sensor. Motors were used to create movement in our vibration system so the LEGOs can be easily transitioned to each task throughout the process.

*2. Hardware*

The hardware used consists of conveyor belts, shaft, 3D components, and the quad track. All parts and components are mounted on the quad track and is interconnected.

*3. 3D Components*

Several parts were 3D printed: feeder, V-plate, shaft, chute system, and bins. These components were important in the overall design and each serve a big purpose. Figures 2a, 2b and 2c illustrates all components that were 3D printed by the NIU Machine Shop.

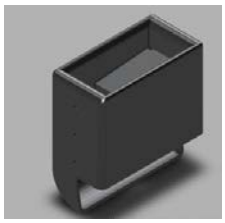

Figure 2a. Feeder

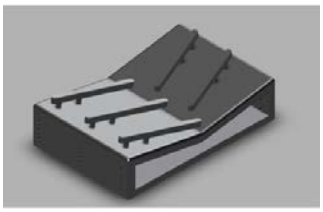

Figure 2b. V-plate

Figure 2c. Chute

*4. Sensors*

A light sensor will correctly identify the color of the LEGO brick so it can be sorted and placed into the proper bin.

## III. Results

Using the light sensor and the Arduino, we successfully sorted our LEGOs by color. The LEGOs were able to make its way from the feeder to the conveyor belt, down the chute system, and placed under the color sensor. The sensor was able to read the code and distinguish what bin the LEGOs should be placed in. The machine was coded to sort 2 x 2 bricks that are red, yellow, green, blue and brown in color. When the bricks fell into the chute system, they piled up in the funnel, but had the ability to sort their way through the system. After the LEGOs were processed, it was placed on the chute, and slid down into the proper bin.

## IV. Discussion

This project has given the researcher the ability to take our knowledge on coding and implementing it in an idea to help simplify a small task. Although there are other versions of a LEGO Brick Sorting machine, we invested many hours to create a new way to efficiently sort bricks. With the help of the Arduino board, we created code to read and sort LEGOs based on color. Due to awaiting parts and unplanned modifications, we were unable to fully execute the project by also sorting the bricks by weight. A more compact design for easy maneuvering is an improvement to be considered.

## V. Conclusion

With an increase in popularity of LEGOs, sorting many bricks can be a tedious and time-consuming task for LEGO creators. This project created an efficient solution while automating the process. While the overall design of our machine is simple and not difficult to build, we were faced with trial-and-error situations that ultimately altered our initial design. With conveyor belts, chutes, and our program, we were able to sort the LEGOs and while it correctly understood which bin to separate the bricks. The project requirements provided by our faculty mentor were satisfied while staying under budget and passing safety guidelines. In summary, we provided a way to take the labor out of sorting LEGO bricks, which lends more time to building LEGO creations.

## VI. Acknowledgements

This success of our project would not have been possible without the support of several people. Our teaching assistant, Amin Roostaee, who attended all our weekly meetings and helped us receive our parts. Our faculty sponsor, Dr. Veysel Demir, who not only provided us with the project but constantly challenged our thinking and provided feedback. And lastly, we would like to thank Michael Reynolds who helped us in the machine shop and gave us an understanding of how to manufacture parts.

## VII. References

[1] "LEGO." *Companies History - The Biggest Companies in the World*, 20 Nov. 2020, www.companieshistory.com/lego/.

# Ball Nut Ball Bearing Injection System

S. Dodd, S. Duffy, A. Ward
Department of Mechanical Engineering
Northern Illinois University, Dekalb, IL 60115
Rockford Ball Screw, Rockford, IL 61101

***Abstract*—This multiphase project for the senior design capstone program at the College of Engineering and Engineering Technology at Northern Illinois University was proposed by Rockford Ball Screw (RBS), an industry leader of ball screws and linear guide rails. The goal of this project was to design and fabricate an electromechanical workstation system which can be utilized by their team to aid in and increase the efficiency of the final assembly steps of their ball screw products. The aim of this design was to assist in the loading of ball bearings into ball screws while maintaining flexibility of usage for a range of their full line of products. To meet specifications the system features interchangeable components as well as ball bearing count control with programmable logic and implements safety and user-friendly features as daily use is expected. The system was designed in Solidworks®, validated with analysis software and hand calculations, and fabricated with machined and 3D printed parts.**

## I. Introduction

The ball screw is a mechanical actuator that translates rotational motion to linear motion using ball bearings. Ball bearings are driven helically in either an internal, external, or other circuit type between the threads of the screw and nut, permitting for translation with little friction and the ability to withstand high thrust loads. They have many applications where precise linear motion of high loads is desired. Currently, assemblers at Rockford Ball Screw load ball bearings into their ball nut products by hand. This process is done by loading ball bearings into unique steel tubes which hold a specific size and amount of ball bearings depending on the nut. The nut is then fed the ball bearings via a circuit channel entrance while the screw is turned through the nut, drawing in the appropriate amount of ball bearings. The main problem with this process is that it is timely which increases labor costs and slows down production. Also, it induces repetitive motions in the loading of the tubes and turning of the screw which could lead to strain or joint injury over a long period of time.

The solution is the Ball Nut Ball Bearing Injection System which administers a specific amount of ball bearings with accuracy and does so while maintaining flexibility of usage for a range of ball diameters. As the design is to be used as a workstation tool, features of safety, ease of use, and handleability were implemented. This includes a ladder logic control system that uses a panel interface for accessible usage by the RBS team after minimal training. One of the primary goals of the project was to design something to be time efficient, specifically, faster than the current assembly process. Therefore, the system was designed to translate ball bearings in a rapid manner, is capable of many ball nut loadings before a refill is required, and has purge capabilities for when product demand changes throughout a workday.

## II. Design Overview

The system consists of a hopper, handheld administration portion, and a control interface, shown in Fig. 1. It is mainly built from various 3D printed sections for containing and conveying ball bearings along with steel and plastic tubing. Electrical devices controlled with a PLC are also utilized in the design and are responsible for actuating components for ball bearing conveyance, output control, and safety. Although the system is made to be suitable for a range of ball bearing sizes by utilizing interchangeable components, for the sake of this prototype two ball sizes were selected to build around.

Figure 1: From front to back; handheld piece, hopper, and control system portions

### A. Mechanical

The hopper is made of multiple components that make up the whole hopper portion. The hopper motor housing is the main containment unit for the ball bearings and houses a motor which actuates a rotary feeder. Attached to the motor shaft is a feeder shaft connector, the hopper motor housing and feeder shaft connector are noninterchangeable

components of the hopper. The feeder shaft connector is designed for quick change out of the remaining interchangeable ball bearing translation components of the hopper. The rotary feeder takes in the feeder shaft connecter for rotational actuation from which ball bearings are drawn with gravity through the part by way of a through channel. The rotary feeder output shaft connects to a bearing which sits within a section that connects to the feeder unit base, said part connects to the hopper motor housing unit with fast access locks as this is the point of manual changeout. All the hopper components were 3D printed; the rotary feeders used stereolithography and the remaining components were fabricated with fused deposition modeling printers to save on cost.

The hopper nozzle tip connects to a length of interchangeable plastic tubing which translates the ball bearings single file to the handheld nozzle portion. Like the hopper the handheld portion of the system is made of multiple 3D printed parts with some machined and electrical components. The plastic tubing from the hopper connects to an interchangeable piece of steel tubing which mimics the steel tube assemblers at RBS currently use. This tube sits within the rest of the handheld portion and features machining which accounts for the position of the tube, allows for the actuating escapement pin element to interrupt the flow of balls, and the pass-through sensor to detect and count ball bearings as they pass through. The case for the handheld portion is made up of halves that interlock and is where the output control elements are housed, the bottom portion is where the user grips the machine.

The control interface enclosure houses the power supply, central processing unit, and the human machine interface Fig. 2. It was machined to fit these components and presents the control interface off axis from tabletop to the user for ease of use.

Figure 2: Control interface and enclosure

### *B. Electrical*

The electrical components of the system are a motor, actuating element, sensor, safety sleeve, and the control system. The system operates under 24 volts direct current, the electrical components work in tandem via the user operated control system.

## III. Results

The system was determined to achieve the focal requirements as requested by the client. The final prototype showed reliability and ease-of-use for daily implementation with minimal operator strain. Several areas of improvement have been specified to the client regarding the physical design. The handheld portion will require a modified interlocking mechanism due to clearance issues in the initial prototype. Additionally, manufacturability options will require consideration with respect to weight and component adjustability.

In testing it was determined some modifications were required of the control program to maintain accuracy, once these changes were made the system dispensed ball bearings to the setpoint more frequently. It was also determined that when testing with a larger diameter ball bearing the choice of element for flow interference was underspecified, a new part was selected to replace the original. Once these changes were implemented the system showed reliability for the task it was designed for.

## IV. Conclusion

Overall, to enhance production in the assembly steps of Rockford Ball Screw's ball screw products a novel system has been conceptualized, designed, and prototyped to meet the demands described. The optimal design chosen is a gravity fed ball bearing dispensing system that consists of hopper, nozzle, and control system subunits. The system is operator controlled and works to feed ball screws with ball bearings in an accurate and controlled manner. The team succeeded in producing a functional prototype of this system. Further iterations of the design are recommended before full scale application of the product.

## Acknoledgments

The authors would like to thank Rockford Ball Screw for sponsoring and providing the opportunity to work on this project. They welcomed us openly to their area of expertise and were very informative, helpful, and understanding throughout the course of this project. Appreciation goes out to our faculty advisor Dr. Yueh-Jaw Lin and our teaching assistant Sandhya Chapagain for their continued insight and NIU's machine shop staff whose physical contributions brought our designs to reality. Lastly, the team thanks its educational institution, Northern Illinois University, and its staff for providing a thorough education and capstone design project that has the depth to prepare us for industry.

# Design of a Human Assisted Robotic Platform for Monitoring Round Goby in Lake Michigan

Robert Heck, Max Kubale, Hayley Mellin
Northern Illinois University
College of Engineering and Engineering Technology
590 Garden Road
Dekalb, IL 60115

***Abstract*—The Great Lakes region of the United States has an invasive species problem. The Round Goby has proliferated out of control becoming one of the largest species groups in the region even though their native habitat is half way across the globe. In order to understand the species better, the design and construction of an underwater camera housing is needed. As the Round Goby is known to live near the bottom of the lake, the device needs to withstand very high pressures as well as have the ability of multiple uses. Many different methods were designed and considered but ultimately the choice of using a cost-effective PVC material was used. The mechanism chosen eliminates the need for human presence to control it in the entirety of the recording process. Our design brings the ability to drop the project to the bottom of the lake for a period of time to be retrieved later for analyzation.**

## I. Introduction

Lake Michigan and the Great Lakes are a very important part of the Midwest. They help the region economically through shipping route and tourism. But there is a problem below the surface that is strangling the ecosystem of the area. Since the early 1990s, the species, Neogobius melanostomus, or better known as the Round Goby has had a population boom. They have invaded the area after being brought here through the ballast water from European ships. Currently, the Round Goby can be found in every great lake and have devastated the local specie's habitat. They spend most of their time on the lakebed, at about 100 meters below the surface. At such depths, pressure and adequate lighting are major design constraints that were considering.

## II. Methods and Materials

### A. PLA Proof of Concept Design

The designs that are being put forward are modular and can be used with most commercial cameras and underwater lights. The most thought-out design involved Figure 1 seen below. It was to be printed using polycarbonate or machined using aluminum. This would ensure that it can survive the depth requirements needed for data collection.

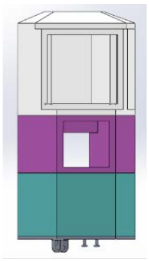

*Figure 1 Proof of Concept Full Assembly*

The device is shaped hexagonally as it allows for flat areas that can be used to attach the latches needed to connect each section. The top section comes to a slight peak as it was derived from an earlier version that was conical. This was changed as a clear cone would add distortion to the recordings for the data collection. This section would then be watertight with a clear polycarbonate window which would lessen or even eliminate any distortion in the recordings. Polycarbonate was chosen for its mechanical properties and can be cut to size. Pressure analysis was done at the required depth of use which is 150 psi. Figure 2 shows how well this design would hold up under those conditions.

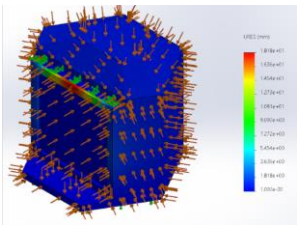

*Figure 2 Pressure Analysis Camera Mount*

The middle section would be open to the environment and contain the diving light. Figure 3 shows the pressure analysis of this section similar to the previous one.

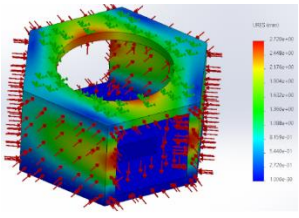

*Figure 3 Pressure Analysis of Lighting*

Leaving this section open to the environment takes away the effect of glare that would be created if the light were inside

similar to the top section. Having this section open also takes away from the buoyancy factor of the device, but that is handled with the bottom section as it is mostly open space.

The bottom section is just to house the Arduino for the release mechanism. It is watertight and contains the Arduino and its battery pack. Connected to the Arduino will be a nichrome wire that is holding the weight used to submerge the device. The weight will be hung over a metal bar and that bar will be in contact with the wire. After the allotted time, the change from the battery pack will be sent through the wire and because of it high burn resistance, it will heat up and snap releasing the weight thus resurfacing the device. Each section will also have a rubber seal between them to ensure that it is a watertight device. Below is the pressure analysis done at the same pressure as the two previous sections.

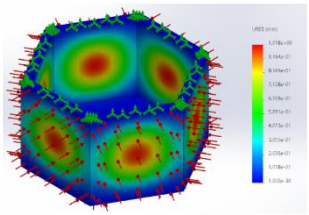

*Figure 4 Pressure Analysis of Electronics Compartment*

### B. PVC Design

The PVC design follows the exact same path as the PLA proof of concept except that is uses a different material. Figure 3 shows the full assembly of the device. It is made from a 6-inch diameter PVC tube that has been cut into two separate sections and a 6-in corner piece for the camera housing. The window will be attached to the outside of the camera housing via bolts. These bolts will go through a clear half inch thick plexiglass into a PVC ring that is attached to the outside of the corner piece. This will make all the pressure on the device push the glass onto and not into the camera compartment. As the corner piece is made specifically to fit with the straight pipe sections, latches will only be needed to connect the lighting section to the bottom electronic section. A circular cutout will sit need to be placed in the corner piece to make sure water does not enter that portion. A similar cutout will be placed at the bottom of the lighting section to ensure that water does not affect the electronics. Finally, a cap will be added to the bottom to close off the compartment. Similar to the proof-of-concept design, rubber seal will be used between sections though they are in different places One seal will be between the lighting and electronics section while the other seal will be on the window as a seal will not be needed between the lighting and camera sections as that will be adhered together using PVC cement.

### C. Electronics

The electronics compartment houses an Arduino Uno and a 9V battery pack. This compartment controls the release mechanism. The bottom of the electronics compartment has two bolts and T bar that can pivot. The two screws are connected to with 36-gauge nichrome wire. At a user set time, a current is sent through the nichrome wire which can heat up to 1500 °C and burns the wire releasing the natural weight (ideally a rock). The rest of the monitoring device is naturally buoyant and returns to the surface.

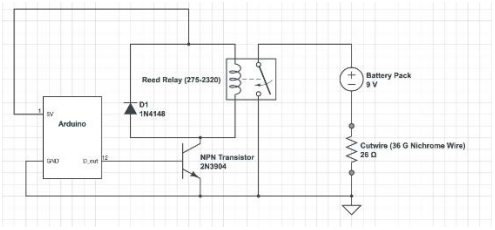


*Figure 5 Schematic of Release Circuit*

## III. Discussion

As of now, no data was collected on the Round Goby, but all of the research into the material properties used and the construction of the two devices points in the direction that data can be collected by them. The main advantage this device has is that it is cost effective and easy to make. This leads to the point that multiple devices can be produced expanding the range of data collection. The PVC device is an especially affordable device seeing that $35 of PVC is enough to make almost eight devices.

The proof-of-concept design is more costly, but offers a more robust and efficient design. The final product of this design would be made of a strong polycarbonate or aluminum both of which are strong yet lightweight. This would add more security to the design opposed to the simple PVC design. Also, as the proof-of-concept design is shown, the flat sides would make adding either addition lights or even addition compartments simple.

## IV. Conclusion

For all our research, the designing of a device that is waterproof is waterproof is just the tip of the iceberg when it comes to submersible items. The main problem is created a device that can stand up to the pressurized environment that is the bottom of a lake. Many materials can go down 5 or 10 meters. It's when devices need to go to 50 to 100 meters that the problem starts to be seen. The PVC design offers a cheap and usable design at this moment while the PLA proof-of-concept design offers a more thought out deign that can be improved upon in the future.


## Acknowledgment

We would like to thank NIU for how they worked with us through these last two pandemic semesters. A thanks is also needed for our faulty advisor and client Dr. Sachit Butail and Michael Reynolds for their feedback and direction when it came to design and material decisions. Finally, a thanks is needed for our teaching assistant Alex Wills for his help.

# Integration of a NAO robot with an autonomous mobile platform, phase II

Adam Spear, Bryce Papke, Dylan Russom
College of Engineering
Northern Illinois University
590 Garden Rd, DeKalb, IL 60115

***Abstract*—The autonomous mobile platform needs to have capability to navigate the Engineering building on its own with the ability to detect obstacles in its path. It will also be able to detect where it is in the building so that NAO can give the tour from on top of it. In case of emergency, or malfunction with the autonomous driving, it will also have the capability to be driven manually.**

## I. Introduction

Northern Illinois University's engineering department is planning on revamping their tours of its building. The main reason for this is to attract new potential students by showing the work that can be done by their student body. This tour revamp will include a NAO6 robot giving tours of the engineering building. However, there is one problem with doing that. The robot itself is not able to move at a fast enough pace, as well as being unable to protect itself if someone bumps into it. Therefore, an autonomous mobile platform needs to be constructed for the NAO6 robot to give the tours of the engineering building.

## II. MECHANICAL

The frame of the autonomous mobile platform is constructed using 6063-T5 aluminum alloy 2020 T-slot bars. These bars were assembled as a 2' x 1' x 6" box, with additional bars at the middle of the length. The bars are attached together via t-slot connectors. On the back of the platform there are 3" caster wheels, which are also supported by another bar on the bottom. On the front of the platform there are motorized hoverboard wheels. They are attached to the frame with angle brackets.

Figure 1: Frame of the platform

## III. ELECTRICAL

### *A. Power*

The autonomous mobile platform is powered by a rechargeable 20V battery, similar to the ones used for power tools. This will allow for the system to be powered with no issues.

### *B. Motor system*

The driving force behind the movement of the platform are two motorized hoverboard wheels on the front. They have been set to about 15% power for safety reasons.

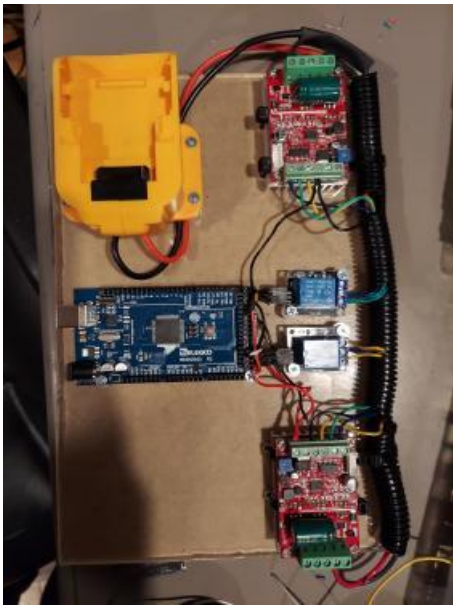

Figure 2: Electrical Components

## IV. PROGRAMMING

The code for this project was all done in C. The platform was programmed for two different tasks, following a line on the floor and receiving inputs from a controller and moving accordingly.

### *A. Line Tracking System*

The platform has been developed to follow a line in order to give autonomous tours. This system is also equipped with sensors that will cause the platform to stop if it will collide with anything. This system is still a work in progress.

### *B. Manual Control System*

This platform has the ability to be driven remotely using a playstation controller. This is in the case that a tour guide would need to take control of the platform for safety reasons.

## V. CONCLUSION

With the construction of the autonomous mobile platform finished, work can be done on integrating it with the NAO6 robot. However, there was a problem with that. When brought out to test, a servo on the left arm was no longer working. The time it would take to be repaired was going to be longer than the spring semester, so there will have to be a third phase to this project. However since the platform itself is finished, this third phase should be the last one.


## ACKNOWLEDGMENT

The authors would like to thank Donald Peterson and Ian Gilmour for helping guide us towards the right directions during this project. Justyna Kielar and Trevor Rogneby for helping the group receive all of the materials needed. And finally the authors would like to thank Brad Spear for consulting during the electrical portion of this project. This project would not be in its current state without him.

# *Integrated Wearable Feedback Device for Human Walking*

*Haley Hoppe, Nathan Moser, Nathan Tom*
College of Engineering and Engineering Technology
Northern Illinois University
Dekalb, IL
Z1827745@students.niu.edu, z1843982@students.niu.edu, z1823247@students.niu.edu

## I. INTRODUCTION

The purpose of the integrated wearable feedback device for human walking is to assist people who have experienced stroke or other neurological pathologies, which have caused them to lose the ability to walk due to damage in their brain or neuromuscular system, with a feedback system based on their performance. People who have lost their ability to walk must go through the rehabilitation process to regain their ability to walk, but rehabilitation is expensive, time consuming, and does not transfer effectively to environments outside of the rehabilitation facility. To solve this issue, the device will be mobile, wearable, and low profile so the user could wear this inside the laboratory environment.

The integrated wearable feedback device for human walking is a sensor, processor, and feedback system which allows for reinforcement learning of walking gait rehabilitation patients to occur in many different environments, which will lead to better patient outcomes, as well as a more complete understanding of the learning process. The system consists of two sensors to measure the relative angle between the thigh and the shank. An Arduino microcontroller is used to record and transmit the data to a computer, and a MATLAB program computes the measured values with desired values set by the client or therapist. The system provides real-time feedback to help the user correct their gait, and to help them regain proper walking form during everyday use. The final component of the system allows the stimulus applied to be corelated to an electroencephalograph (EEG) device to read brain activity. This allows the client to study the effectiveness of different types of reinforcement learning.

To measure relative knee joint angle of the user, inertial measurement units (IMU) will be placed on the user's lower thigh and upper shank. IMUs are used because of their high accuracy output, and their low profile. The data gathered from the IMUs are sent to an Arduino Uno to process the data. At the same time, the EEG device is sent a time pulse via MATLAB program so that brain activity can be analyzed at the significant instances of when a reinforcement feedback is displayed. The Arduino Uno computes the angle between the thigh and the shank by using fused IMU data produced from the gyroscope, accelerometer, and magnetometer.

The Arduino Uno will transfer the measured and calibrated angle to a computer which creates the feedback system. The types of feedback system vary to observe the effects of different feedback strategies. The feedback system displays the set goal and current angle, or in indicator if the goal has been met, while another feedback system will reward, punish, or do both by giving the user a score based on their performance. The data from the EEG helps to conclude which feedback system is most effective for locomotor rehabilitation. The system is shown below in figure 1 as a block diagram.

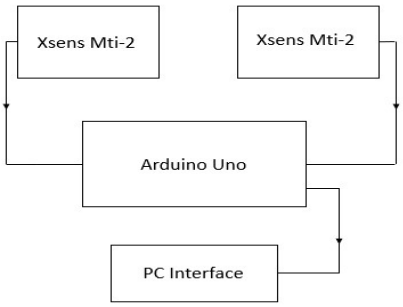


*Figure 1: Block Diagram of the system*

## II. SENSORS AND ONBOARD PROCESSING

This assembly will consist of several components integrated into a system that will provide measurements of knee movements while walking by using sensors which will be placed on the thigh and shank of the user.

The sensors chosen to measure the flex angle between the thigh and shank of the user's leg are two Xsens Mti-2 inertial measurement units. Both sensors were placed in such a manner to rotate around the X-axis. Circuits were constructed to provide power and data transmission in accordance with manufacture recommendations, and 3D printed cases enclosed the completed boards and sensors. The cases were mounted to the leg with Velcro strappings. A 5-pin wiring harness connects the two sensors and the Arduino for processing and communication. This arrangement is shown in figure 2 below.

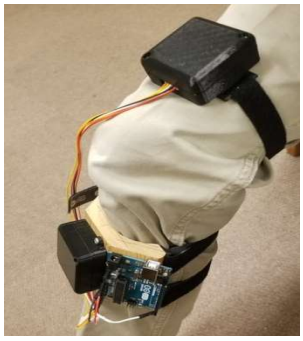

*Figure 2: Location of IMU sensors and packaging.*

This initial prototype connects the Arduino to a desktop PC via a wired USB connection, to allow for signal processing and feedback as well as powering the microcontroller. In later iterations of the device, an onboard battery will also be fitted to power the Arduino and sensors. This subunit comprises both sensors and a processer, and it outputs a digital signal with angular position to other components of the system.

## III. FEEDBACK RESULTS

The sensor angle output is read into a MATLAB script to analyze the recorded gait and provide the user with feedback on their performance. The client, Dr. Hill provided several different types of feedback that were desirable for his research. This feedback is crucial to fulfilling part of the purpose of the device; to test the theory that encouraging patients to find solutions through their own self-guided inspection leads to subjects retaining the learning effect longer. By analyzing the results of the users' learning retention of the walking gait pattern with the variable being the forms of feedback provided, Dr. Hill will be able to determine the most effective form of reinforcement. Figure 3 shows the concept presented at the beginning of the semester course showing a conceptualization of what the scoring system could be represented as.

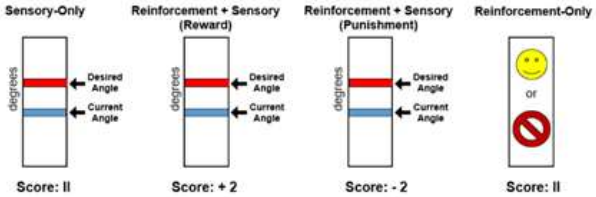


*Figure 3 (Hill, 2020). Feedback Options. [1]*

Several types of feedback are offered; these include both positive and negative feedback, strictly positive or negative feedback, pictorial feedback, and no score-driven feedback. Feedback would be in the form of points given or taken away, with the user's score displayed throughout the exercise. It could also take the form of positive and negative images such as a smiley face or prohibition sign. By attaching point values to actions, several methods of reinforcement learning could be studied to find the most effective method for maximum skill retainment.

After assembling the sensor system and completing the MATLAB programing, testing was undertaken to validate the methods of feedback. Sample data taken from the system is shown in figure 4 for a portion of a walking exercise.

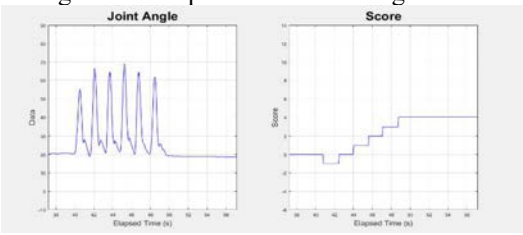


*Figure 4: Example data collected displayed near delivered feedback reinforcement.*

Negative scores were attributed to the user for steps that fell out of the bounds set by the exercise, and positive scores were given for joint angles in the proper range.

## IV. EXTERNAL INTEGRATION

Finally, the device must mark the time that feedback was given to the user onto the recorded data of the EEG. By studying learning outcomes and corelating feedback delivery and EEG brain activity data, conclusions can be drawn on the rate and retention of learning for the participants. these three possibilities that exist to offer a real-time evaluation of the user's performance.

The time of score application to the user is sent to the EEG using MATLAB. The program sends a TTL pulse to a parallel port which is connected to the amplifier of the EEG. This feature will be utilized in the lab along with a 32 channel Neruoscan EEG operated in the Joan Popp Motor Behavior Laboratory. The marker signal will cause the EEG recorder to place a timestamp in the brain activity recordings, which will then be able to be examined for the effects of the applied stimulus to brain activity. The EEG analysis allows for conclusions to be made regarding how different exchanges of reinforcement feedback can improve the user's retention of the correct walking gait they are aiming to successfully attain.


## ACKNOWLEDGEMENTS

Dr. Moghimi for his mentorship.
Dr. Hill for his input and positive feedback.
NIU College of Engineering for funding.


## REFERENCES


[1] Hill, C. *Senior Design Presentation* September 2020

# CNC Hand-Held Operator Station

Tserendemberel Gantulga
Electrical Engineering
Northern Illinois University
Dekalb, IL
Z1841422@students.niu.edu

Ken Braswell Gantulga
Electrical Engineering
Northern Illinois University
Dekalb, IL
Z1857423@students.niu.edu

Eucario Matos Mechanical
Gantulga Engineering
Northern Illinois University
Dekalb, IL
Z1728057@students.niu.edu

*Abstract* – Most machine tools today require some form of handheld operator pendant to perform certain tasks. Part setups, tooling changeovers and general operation of the machine are made much easier with the use of a handheld controller. The current market has several offerings to meet this need. Some offer minimal function with consideration being function over design.

These lack any ability to interface further with the machine and instead concentrate on basic manual operation. Others offer more function with computers and software, but they lack any operator friendly controls for manually operating machines.

There is a lack of designs, that combine these two ideas of basic operator friendly function and the ability to fully interface with the machine. The F1 controller offers basic function in an imaginative design while allowing operators to fully create and edit part setups as well as operate the machine in all CNC modes.

## INTRODUCTION

The desired result of this project is to design a handheld control unit for operating and programming machine tools, not limited to but including hobbers, grinders, lathes, and mills. The control shall have all needed functions for operating the machine in manual modes and automatic functions.

Preferred features include a touchscreen integrated for customer HMI and programming of the machine tool. Needed design work would be the 3D design of a case to contain all components, and internal circuit design to meet all requirements of the controller for control of multi-axis machine tools.

The design should be done so as manufacturing can be completed in house at Bourn & Koch, and all parts are readily available. The controller`s primary purpose is to make sure the operator can set up and operate the machine comfortably with limited constraints. Also, the handheld controller to be designed shall be visually like a Formula 1 steering wheel. The reason behind the idea is to make the controller more comfortable and exciting to a younger generation of machine operators.

## BACKGROUND

Bourn & Koch currently offer a standard stationary controller on their CNC machine. However, a stationary controller isn't ergonomic enough for the end users to perform part setups and tooling change overs. Therefore, the company wants a handheld controller that is an ergonomic, safe, and visually appealing controller for their CNC machines.

## METHODS AND MATERIALS

Time frame – Time for each operation, collection and work done with different time. To develop the whole controller had several scheduled works for this project. Therefore, the team can make the controller and changes to it in timely manner.

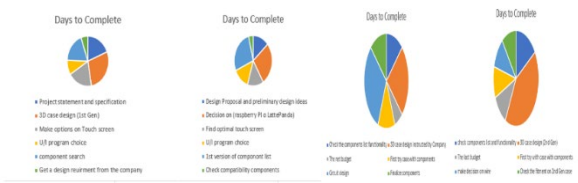


## THE HAND-HELD CONTROLLER MOTIVATION

This product will be a functional prototype for the company. Bourn & Koch`s new CNC machine is under construction. The design of this new CNC machine is visually quite attractive: color, angles and other new cool integrated technologies will be part of this machine. Therefore, they need a new design for the controller for the machine. There are other handheld controllers. However, currently there is no such controller that exceeds their expectation in the market. The current controllers on the market are complex and overwhelmed with different types of buttons, switches, and thumb sticks. Bourn & Koch is looking to simplify the handheld controller, reducing the number of buttons needed to operate the machine and locating them in strategic locations for intuitive use.

The current controllers on the market have most of the desired functionality but lack any aesthetic appeal. Bourn & Koch is making a push to give a facelift to the appearance of their machine tools and would like to see this same facelift on the handheld operator interfaces used on the machines. A younger generation of machine operators are coming into the industry, and the hope is to put in their hand something that can feel more familiar.

The design should be done so as manufacturing can be completed in house at Bourn & Koch, and all parts are readily available. The controller`s primary purpose is to make sure the operator can set up and operate the machine comfortably with limited constraints. Also, the handheld controller to be designed shall be visually like a Formula 1 steering wheel. The reason behind the idea

is to make the controller more comfortable and exciting to a younger generation of machine operators.

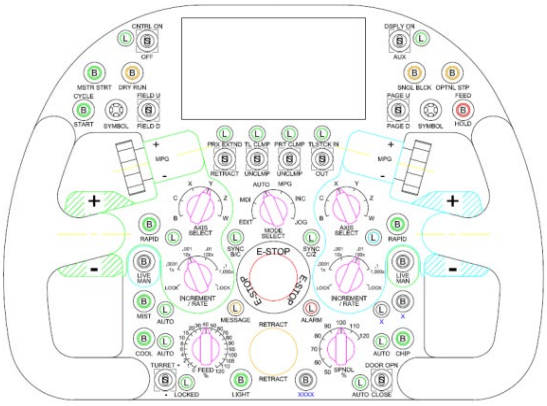


## CIRCUIT DESIGN

Most physical operators will communicate back to the machines PLC via an I/O module connected to the CNC via ethernet. A standard industrial protocol will be used for this communication called EtherNet IP. It is a protocol widely used in the automation and machine tool industries, which will allow for a smoother integration with the machine tool.

Some components will still need to be hardwired back into the machines safety circuit as well as into specific CNC connectors. Shown below is the integration of the F1 controller's E-stop into the machines safety circuit as well as the controller's MPG's into the CNC's specific connector.

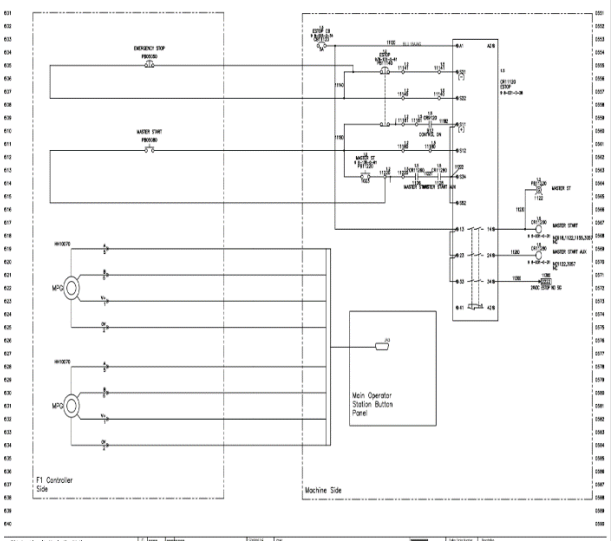


## CONCLUSION

This expansion on what a handheld controller can be will offer users a very in depth experience with the machine as well as a unique experience. The borrowed design elements give a newer generation of machine operators an experience that will more liken to modern video game controllers. This would allow a more familiar feel and potentially a greater expansion of capabilities within the machine tool industry to catch up with the design and capabilities of the future controllers.


### ACKNOWLEDGEMENTS

Thank you to the NIU department of Electrical Engineering and Mechanical Engineering, as well as Dr. Niechen Chen for guiding and supporting us throughout the project. Thank you to Mr. Peter Mischler for making this project possible.

# Acoustics and Musical Instrument Design to Create a Robust, Stable, Flexible Berimbau Instrument

**Team 35**

Clayton Smith, Matthew Hasto, Michael Abukhader

Mechanical Engineering Department, Dr. Hasan Ferdowsi

Northern Illinois University

DeKalb, IL

***Abstract*— The Afro- Brazilian berimbau is an instrument with a rich history and unfortunately a limited potential. The single string instrument requires multiple players to create complex compositions. Dr. Gregory Beyer, along with his non-profit organization called Arcomusical, dedicated to the spread of knowledge and enjoyment of the instrument, have commissioned through the School of Engineering at Northern Illinois University to create a stable multistring instrument that solves some of the most common issues with the berimbau, while expanding the potential for a single instrumentalist. The final design that has been completed contains a modified berimbau staff that contains a second string and tuning mechanism as well as a bridge clamp mechanism meant to be able to slide along the staff of the instrument, as well as acting as the bridge for the strings and the gourd connection. This design utilizes hooks to bridge the strings and allows the use of multiple clamp mechanisms to bridge the strings at different locations along the staff.**

## I. Introduction

### *A. History of the Berimbau*

The berimbau is an African-Brazilian instrument strongly linked to the dance fighting technique of Capoeira. Capoeira is a martial art that focuses on fluidity and elegance and it is extremely common for those who practice it to own and play the berimbau, as is traditional to the art. In its root this instrument was used to muffle the sounds of slaves learning martial arts so the owners would not be able to hear and find out that the slaves were learning combat. The berimbau is traditionally formed with a staff of hardwood, with a string being brought from one side of the staff to the other where typically there is a tuning mechanism to adjust the tightness of the string. It bows not unlike a hunting bow. Then a dry hollow gourd, acting as a resonance chamber, is attached to the staff using cord. The cord is also tied around the string to bridge the instrument into two separate lengths. It is played by pressing a key usually made of stone or brass into the string right above the location the string is bridged, and the string is struck with a wooden stick to create the sound. Because of how it is played it is considered a percussion instrument.

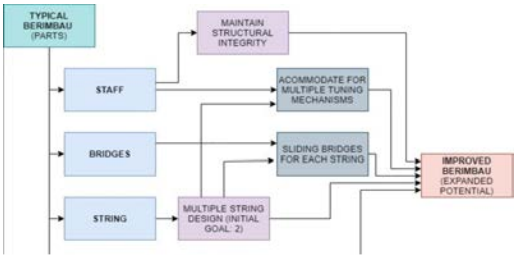


**Figure 1:** Block Diagram

### *B. Project Goal*

The berimbau's one stringed design causes limited ability for a single instrumentalist. The goal is to expand the melodic potential of a single player by creating a stable multi-stringed berimbau instrument, as well as to address common issues with the berimbau to improve it overall. The addition of a second string as one can assume will at the very least double the ability of a single instrumentalist allowing for much fewer musicians to play much more difficult and complex pieces. Other issues that must be addressed are that of the uncomfortable hold of the instrument, as well as the tendency of the bridge to slip while playing.

**Figure 2:** Dr. Beyer's 2-String Prototype

## II. Optimal Design

### *A. Improved Staff*

The solution includes a new berimbau staff with a larger bulb to account for a second tuning mechanism as well as modified bridges on each end to set the lengths of the playable string for each string.

### *B. Clamp Mechanism*

Also, the addition of a new mechanism has been added to the instrument to replace the cord originally used. This is called the bridge clamp mechanism and it contains many vital improvements to the original instrument. There are two functional clamp mechanisms, one more suited to holding the gourd utilizing an improved cord configuration in which a housing allows for the cord to be easily tightened by a wing screw mechanism.

The alternate design is better suited as a secondary clamp for if an instrumentalist would prefer to bridge the strings at different locations along the berimbau. This clamp is more robust and most resistant to movement along the staff, which was one of the desired improvements of the instrument.

### C. *Bridge and Hooks*

Both clamp mechanisms contain a bridge slot for the string hooks to enter and a set screw that is meant to pin the hooks in place. The hooks themselves are an improvement to the original design as they are made from steel making them much more robust than the cord originally used. The hooks have also been coated in a flexible plastic providing more friction and reducing the ability of the bridge to slip, as the former bridge is prone to in the original instrument. These hooks have two different forms, a single hook form for use with two clamp mechanisms allowing the strings to be bridged at two different locations, as well as a double hook permutation in which only one bridge clamp mechanism is required. This version allows the strings to be bridged at the same location on both strings.

**Figure 3:** New Prototype-Clamp Mechanism and Hook insert

### D. *Handhold*

Both bridge clamp designs also have been modified in that they both contain an ergonomic hand hold which the original instrument lacked. This is built directly around the slot for the hook and is made for the comfort of the players finger, as the instrument is typically held up by a single finger. This part is made of hardwood similar to what is used to make the staff to ensure that it is robust enough to handle the weight of the instrument being carried by it as well as the tension of pulling the strings back.

## III. Sustainability and Maintainance

The berimbau itself requires slight maintenance to increase its longevity as any instrument does. As the instrument is prone to bowing farther and farther as time goes on, it is important to relieve tension as much as possible when not playing the instrument. This includes removing the bridge mechanism and relieving the tension on the string by loosening the tuning mechanism.

It is important not to overtighten or strip any of the twisting components including the set screw or the gourd tightening housing.

## IV. Results and Discussion

Due to the original limitations of the berimbau a second string drastically increases the functionality for a single player. The ability to bridge the string in multiple locations along with the use of an additional string means that much more complex compositions may be played by fewer musicians. This includes different positioning on either string completely changing the functionality of the original instrument. The original instrument could change the tension point on a singular string allowing for two different notes to be available to a player separate from using the coin. Additionally, with the double hook in place, the instrument now has two strings being tensioned at one point allowing for four notes. The incorporation of the mount makes moving the double hook up and down the staff extremely efficient and easy to do in the middle of a composition. Now, the two mounts using two separate hooks expands the potential even more allowing off set notes on either string. If the musician wishes to keep one string in tension, they can move the other tension without interrupting the initial string. This adds an infinite number of notes that can be played with easy movements. With the robustness of the hook mechanism the slipping of the during use of the instrument has been addressed, as well as the uncomfortable handhold of the instrument being significantly improved according to client feedback.

## V. Conclusion

The addition and design of a clamp capable of holding two strings rather than one is increasing the melodic potential of the instrument by more than double. Also, the option of having two clamps applying tension at different areas on either string allows musicians to change playing styles fluidly in the middle of a composition and have access to a plethora of different playable notes.


## Acknowledgments

***Dr. Gregory Beyer*** – Founder, President, and Artistic Director of Arcomusical

***Dave "Snappy" White*** – Arcomusical's personal woodworker handcrafting musical bows.

***Dr. Hasan Ferdowsi*** – Faculty Advisor Team 35

***German Ibarra*** - Teaching Assistant Team 35


## References


*[1] Beyer, Gregory, 2020, Arcomusical. [online]. 2020. [Accessed 4 November 2020]. Available from: https://www.arcomusical.com/about-arcomusical/#*

[2] *Lyra, Claudia, 2020, Center for World of Music. [online]. 2020. [Accessed 20 October 2020]. Available from: https://centerforworldmusic.org/2015/06/world-music-instruments-the- berimbau*

*[3] Beyer, Gregory, 2020, Northern Illinois University College of Visual and Performing Arts. [In Person].*

[4] *Watson, Nathan W., 2017, Miami University [online]. 2017. [Accessed 20 November 2020]. Key Factors In The Evolution and Globalization of The Berimbau. Available from: https://scholarship.miami.edu/discovery/fulldisplay/alma991031447354202976/01UOML_INST:ResearchRepository/*

# Design of a Human Assisted Robotic Platform for Automated Sampling Water flea Populations in Nearshore Regions

Leonardo Lopez, Dakota Rivard
Northern Illinois University
DeKalb, IL USA
Z1738299@students.niu.edu

***Abstract*— The Great Lakes have nearly two hundred invasive species that severely impact the drinking water, shipping, and recreational industries for the surrounding areas. This has also led to a noticeable shift in the ecological balance of the land. Water fleas are one of these species. spiny water fleas can have a huge impact on aquatic life in lakes and ponds due to their rapid reproduction rates. The impact of this directly affects the young fish and species survivability. A critical step in controlling the spread is to monitor them frequently across large areas. Automation of any steps in the collection process will help with such a labor inducive task and a large area to cover. The project will focus on automating the collection process while preserving the samples from contamination.**

## I. INTRODUCTION

The Spiny Water Flea is an invasive aquatic species that tend to pray on other microscopic organisms essential to the life of the native fish. As they are not found to be prey for any of the native species, they propagate fast leading to endangering the life. As mentioned above; this senior design project will focus on the design and modeling of an automated test sample retrieving module. This will later be concatenated with a design for a robotic platform for monitoring water flea populations. This research will focus mainly on the spiny water fleas (Bythotrephes longimanus) and the fishhook water fleas (Cercopagis pengoi) found in Lake Michigan. Currently the process to collect samples and study the data of the spiny water fleas come from marine biologists going into the field and casting out plankton nets, with a cod-end attached to a sampling bucket, into the lake. They let the net reach a desired depth before then pulling it back up and retrieving the sample.in order to speed this process an initial design was created by Rafal Krzysiak in which six cylindrical sample containers are rotated in a cycle during the collection process. This allows for up to six different samples to be taken at any one time compared to other products that only allow one sample per submersion. We will be expanding on this design focusing on the electronics that will be doing the automation. As well the waterproofing and water sealing of the device to ensure proper operation and no contamination of the samples.

## II. PROBLEM DESCRIPTION

The automated device should be able to sample water fleas in nearshore waters, up to depths of 50 m. using electronics underwater means that proper attention must be placed on an electronics compartment for a microprocessor that is water proof but still allows information to be obtained by sensors in contact with the outside environment. Moving parts cause even more reason for this attention as they are prone to leaking by nature.

To help speed up the sampling process the device would be able to open a sample bucket when the desired depth has been reached and close the sample bucket when the sample is done being taken.

Once that sample has been collected is will be sealed off from outside contamination. The device can then be moved to a new location or a new depth and collect a new sample without the labor-intensive process of switching out sample buckets. Again, it is clear the importance for proper sealing when operating underwater.

## III. OBJECTIVE

The desired result of the project would be to have made significant improvement to the design provided to us. The more autonomous we can make this process the closer we can get to this goal. The Water Flea Sampling Device will allow for up to six samples to be collected before needing to go back to land. The initial design lacked any electronic elements and will be a prime focus of the design additions. The additions will allow the detection of the devices depth and communicating that to a servo motor and the user. The initial device also did not contain much for the water sealing of the device and as such is another prime objective of this work.

## IV. ELECTRONIC DESIGN

the electronic design consists of; a micro controller (Arduino nano every), a barometric pressure sensor (MS5803-14BA), servo motor (30KG, continuous), an OLED screen (0.96 inch oled i2c display), A lipo battery (7.4 V, 1000 mAh), and a 5 volt regulator. figure below shows a simple wiring schematic of all these devices. The pressure sensor needed to be prepped for I2C connection using a SOIC8 breakout board, a 10K resistor, and 100 nF capacitor. These components are shown in figure 2 below.

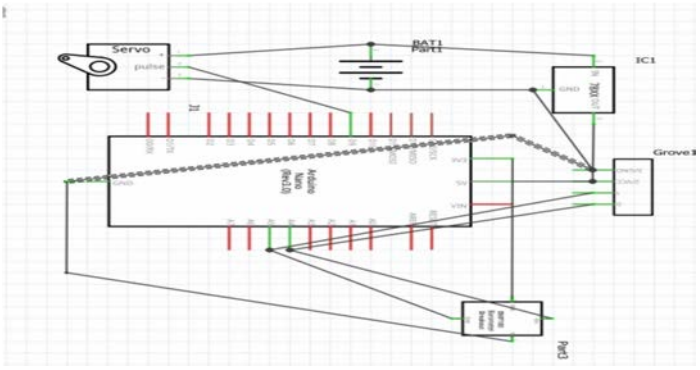


*FIGURE 1 – wiring schematic*

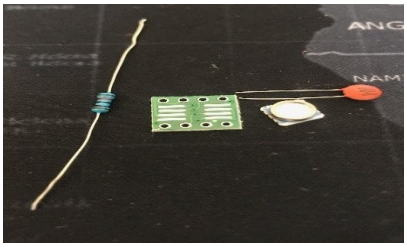

*Figure 2 - sensor components*

The battery will power the servo motor with its full voltage while the voltage regulator will decrease the output voltage to 5V for the Arduino. The 5V can also be used to supply power to the OLED screen. The pressure sensor will have to powered from a standard 3.3V Arduino pin. The sensor and the screen will be communicating with the Arduino via an $I^2C$ connection. The servo will be controlled by the Arduino using pulse width modulation.

## V. MATERIALS AND METHODS

The process goes as follows; using the pressure sensor detect the initial pressure in the air for a base. Then continue to read the pressure. These readings along with other important values will be displayed on the OLED screen. Using the pressure readings, we are able to calculate the depth by applying the equation below.

$$(P_{real} - P_{base})/98 = depth(m)$$

Equation 1

For initial testing we will be using a predetermined depth for our servo to operate. For example, 10 meters could be a possible depth and once that depth is calculated the servo motor will be signaled to operate and open a sample bucket. A count down will then initiate for how long until the servo again turns and closes the sample bucket.

## VI. ELECTRONICS COMPARTMENT.

When designing the electronics compartment the restraints were for it to fit within the initial dimensions of the design given to build off of and to be waterproofed to be safe for electronics. The main material is PVC. Two PVC caps are connected with 3 bolts and compressed with a gasket in-between.

Figure 2 image of PVC cap

the sensor and OLED screen are connected through PVC threaded plugs. The plugs are mounted to the caps with PVC cement. Once secure a hole can be drilled to allow wiring to be passed through to allow connection. These holes will be covered on the inside of the cap using an epoxy stick. The inside of the plugs will be filled with nonconductive epoxy as to allow the proper function of the sensors circuit board, and to prevent water from entering the compartment.

## VII. MECHANICAL DESIGN

The main mechanical components added to the pervious design are a Geneva drive for the servo motor to interact with and sealable caps for the sample buckets.

A. The Geneva drive

The Geneva drive will act as an error buffer for the servo motor. When rotating it is possible that the servo goes slightly further and slightly shorter than its intended distance. When ensuring no contamination this could cause issues.

B. Sample bucket caps

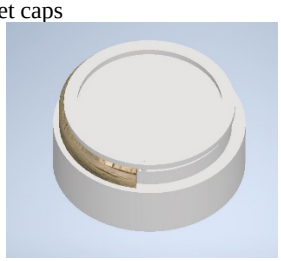

*FIGURE 3 – Sample Bucket Cap*

These lids will seal shut when not in position for sampling using a spring-loaded cap compressed against the metal chassis of the device.

C. Full Assembly

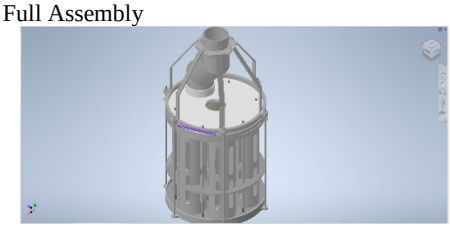

*FIGURE 4 – Full Assembly*

This is the full assembly in which will allow the cod ends to rotate. The sampling containers will rotate underneath the top plate aligning them with the piping that will be connected to the net. This will allow for the six containers to be filled individually without ever needing to bring it back up between samples.

## VII. TESTS.

Tests have been conducted to ensure proper operation of the proper operation of the circuit and that the compartment is waterproof.

A. circuit tests.

The pressure sensor had to be installed to a breakout board and properly connected using a capacitor and a resistor to prepare it for I2C connection. Once connected the circuit could be tested using a “Scanner” code that detects weather an I2C device is connected and displays its address.

to test the connection of the servo with the pressure sensor, I needed to simulate high pressure on the sensor using a syringe. When the pressure needed to simulate a certain depth was reached the servo rotated.

B. Waterproofing

The sensor chamber was filled with epoxy and connected to the Arduino again to ensure the epoxy had not damaged the sensor. Then the sensor chamber was submerged underwater. After it was tested again with the Arduino and was operational

## VIII. CONCLUSION

There is still a lot more to design for the full automation of multiple samples of spiney water fleas but a contribution has been made here. The electronic circuit needed will bring clarity on specific parts needed and the dimensions needed to fit for further progress.
The waterproofing of the electronics will bring peace of mind when considering building a larger structure around this.


### AKNOWLEGMENTS

I would like to thank NIU for providing the budget for this project. Also to Sachit Butail and Rafal Krzysiak for providing an initial design for us to build off of.

# *A Wearable Wireless Video/Audio Recording System for Live Streaming Undergraduate Engineering Labs*

Jacob Witecha
CEET, Northern Illinois University
DeKalb IL, USA
Z1864809@students.niu.edu

Alec Krabbe
CEET, Northern Illinois University
DeKalb IL, USA
Z1818596@students.niu.edu

Harsh Gandhi
CEET, Northern Illinois University
DeKalb IL, USA
Z1850943@students.niu.edu

***Abstract*—The current challenges our institutions are facing during the COVID-19 pandemic have required instructors and students alike to approach learning in ways we never have had too before. Some courses are built from the ground up with an online learning environment as the goal, but for the majority of courses that is not the case. They have had to adapt in major ways, and this has severely impacted instruction. That is where this affordable, wearable, wireless audio-visual streaming device comes in. The target application for this device is the laboratory, but any sort of remote learning can really benefit for it. It will be built to incorporate all the capabilities of its competitors on the market currently but manufactured for a fraction of the cost.**

## I. INTRODUCTION

This project is about developing a wearable technology with its central purpose aiming to make teaching labs to students easy and efficient in a remote setting (device seen in Figure 1). This device will help record different kinds of presentations regardless of their time duration. This device will be worn by the TA or the lab instructor. It will include a lightweight camera which will make it easier for the user to carry it around. The camera will have tactile zoom functionality. Also, it is easy to integrate the camera to the microcontroller. The camera will be attached to a comfortable strap that will be worn on the user's forehead. The device will be specially built to be able to focus on the experimental apparatus. It will record the experiment with a sufficient video/audio output quality which will also help the students virtually present in labs. A wireless lapel microphone will be utilized in conjunction with the other components to offer increased audio quality and flexibility for the user. The students will be clearly able to see the experiment while it is in progress due to its sharp video quality feature. Furthermore, the audio capturing device will feature efficient noise cancellation technology that will help minimize any unwanted background noises. The device will be built so that it consumes minimal energy so that typical two-hour labs can be performed without any obstacles. This will make the device even more effective by not having to recharge it in the middle of a presentation. This device will also be able to zoom in/out and focus where the user wants it to. Using this feature, lab instructors will be able to aim attention on what they want to show the students. Also, this device is not going to be limited to lab purposes. Our budget goal was under $200 and it will cost just over $120.

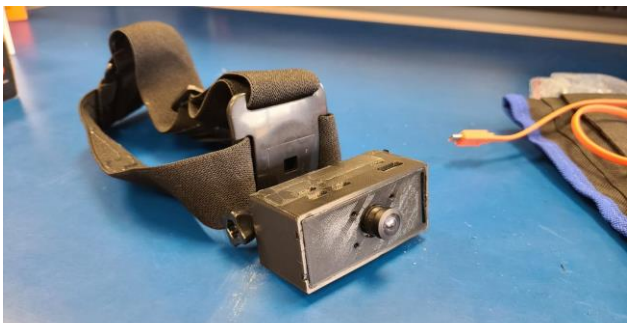

*Figure 1: Completed Prototype*

## II. BACKGROUND

The current global pandemic has led to many challenges for today's society. People have been forced to isolate, unable to go to work and even being laid off. Schools have been forced to close leaving students unable to learn in a traditional fashion. Many schools have resorted to online learning to try and keep students engaged. This has led to the rise of live-streaming platforms such as Microsoft Teams, Zoom, and many others. With these platforms, teachers can engage with students and teach them to live. While this can be good for traditional lectures, problems arise with classes that rely on a more hands-on approach. With live-streaming platforms, students may not have the means to perform a project or lab at home, so they are forced to observe a professor. However, some classroom or lab settings lack the equipment to properly Livestream projects to students. That is, cameras are positioned so that students will be able to see exactly what the professor is doing.

## III. PURPOSE

The purpose of this project is to provide professors an easier way to livestream their labs. This project will provide an inexpensive camera setup that can be worn or mounted by a professor to provide optimal viewing angles for students. With a worn camera, students will be able to see exactly what the professor sees, eliminating confusion about what is being

worked on. Block diagram of interconnected components can be viewed in Figure 2.

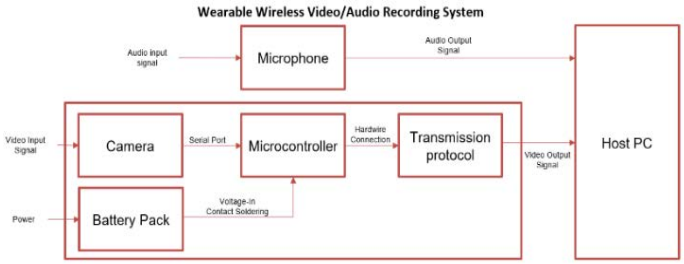


*Figure 2: Level 1 Block Diagram*

## IV. DESIGN

*A.* MICROCONTROLLER: RASPBERRY PI ZERO W [1]
This MC (microcontroller) fits all the requirements of the device. It can interface with a camera through a dedicated serial port. The selected battery along with the integrated Wi-Fi and Bluetooth capability allows the device to operate completely wirelessly between charging sessions.

*B.* CAMERA: RASPBERRY PI CAMERA MODULE (G) W/ FISHEYE LENS [2]
This camera provides the desired quality for viewing streamed video through the internet, as well as a tactile zoom capability to allow the operator to manually change the zoom to improve the lab experience.

*C.* BATTERY: PI SUGAR [3]
The PiSugar was designed as a 3rd party accessory to the Pi Zero W to give the MC wireless operation capability through seamless integration. The matched form factor also allows for improved case design.

*D.* MICROPHONE: WIRELESS LAPEL MIC [4]
A simple wireless lapel mic offers flexibility and ease of use to the operator. The device has plug and play capability with any device that uses an audio microphone jack, but specifically for this design it will be connected to the same host PC as the camera.

## V. CAPABILITIES

A. VIDEO
Device is able to comfortably achieve 720p at 30 frames per second. This video has been tested in the NIU lab setting and is clear enough to make out details in circuits as well as introductions by the lab professor.

B. AUDIO
Microphone provides 360° coverage within 160ft of open space. Operates in the 2.4 GHz band providing high stability, low interference, fast transmission, and short delay (20ms). Easy to use plug in play with any host PC equipped with an audio jack and USB port to supply power to the transmitter.

C. BATTERY
Rated at 1200mAH / 4.4Whr. Measured power draw of the device was 2.2W with WiFi connected and camera stream running. This equates to a 2hr operation time of the device due to battery capacity.

D. CONNECTIVITY
The device can either operate in a fully wireless state utilizing the integrated WiFi and battery pack, or in USB mode which offers higher quality audio in areas where network quality is not as reliable. These modes can easily switch by utilizing the interchangeable SD cards labeled for each build.

## Conclusion

In the current pandemic, in person lectures and labs needed to be moved to fully remote just as most of the industry experienced. This project will provide a device that will solve this problem, designed by students within the department. This device is designed with the internet of live streaming labs so students can still receive a lab experience while attending virtually.

## ACKNOWLEDGMENT

We would like to thank Dr. Korampally for sponsoring this project and providing advice, as well as Amin Roostaee Hossein Abadi for guiding us through each process. We would also like to thank Michael Reynolds and Greg Kleinprinz with the Makerspace for assisting us with 3D printing.

## REFERENCES

[1] Introducing the Raspberry Pi Zero W. (2018, September 19). Retrieved November 06, 2020, from https://www.raspberrypi-spy.co.uk/2017/02/introducing-the-raspberry-pi-zero-w/

[2] robotshop.com.(2015, November 10) Rasberry pi camera manual, https://www.robotshop.com/media/files/pdf/raspberry-pi-camera-module-g-fisheye-lens-User-Manual.pdf

[3] PiSugar, "PiSugar/PiSugar," GitHub. [Online]. Available: https://github.com/PiSugar/PiSugar. [Accessed: 13-Nov-2020].

[4] Wireless Lavalier Lapel Microphone. Retrieved April 12, 2021, From https://www.amazon.com/Microphone-Professional-Omnidirectional-Transmitter-Performance/dp/B08HWMDQVG/ref=sr_1_5?dchild=1&keywords=GINKHY&qid=1618251536&sr=8-5

# Noninvasive Wireless Chargers for Implantable Devices and Epidermal Electronics

J. Jersey, N. Dmitruk, K. Perez
College of Engineering and Engineering Technology
Northern Illinois University
Dekalb, Illinois

***Abstract*—Conventional powering of implanted medical devices like pacemakers requires periodic invasive surgery for battery replacement. These surgeries can be a physical, psychological, and financial burden on patients. In the case of epidermal health monitoring electronics, power is supplied through large invasive wires which can damage the fragile skin of neonatal babies. This wiring also reduces human interaction for these infants, a vital component in development after birth. Wireless charging presents a solution to these problems by providing a convenient, noninvasive, and elegant alternative power source. Wireless charging promises to eliminate the need for battery replacement surgeries and the network of messy wires involved in epidermal electronics. This wireless charging solution will work overnight, not requiring for the user to spend any additional time to charge their device. The goal of this project is the development of biocompatible charging configurations which show sufficient wireless power transfer through bone and tissue analogues. A key result is that a five-centimeter outer diameter coil receives sufficient power at a realistic distance for a pacemaker application.**

***Keywords-wireless charging; pacemaker; magnetic induction***

## I. INTRODUCTION

Wireless charging works on the principle of magnetic induction. If a conductive receiver coil is exposed to a time-varying magnetic field produced by a larger transmitter coil, then the receiver coil will have an alternating current induced within it. Thus, power transfer is possible between two electrically isolated coils through the medium of air. Although this method of power transfer is less efficient than common wired power transfer, it presents distinct advantages in certain situations.

For example, implanted medical devices like pacemakers and bone-anchored hearing aids require regular invasive surgery for battery replacement. This surgery is an additional cost for patients and occurs every 5 to 7 years. Wireless charging has the potential to greatly reduce or eliminate the need for these periodic invasive surgeries. This would increase the quality of life of about 7 million Americans[2]. Another technology which wireless charging can revolutionize is epidermal health monitoring electronics. These epidermal devices are typically powered by large and messy wires which can cause physical damage to the fragile skin of neonatal babies. Eliminating these wires allows for these babies to have the essential skin on skin contact they need for their development and health. Approximately 10-15% of babies in the U.S. are born into the NICU (neotnatal intensive care unit) and require some type of epidermal health monitoring[1].

The project features two main objectives in pursuit of solving these problems. First, to design a wireless charging configuration which uses coils appropriately sized for the relevant biomedical applications. Second, to demonstrate sufficient power transfer within such a configuration through human bone and tissue. An essential component of both goals is safety. The materials selected must be biocompatible and not present any hinderance or danger to the patient.

## II. MATERIALS

The quality of materials and components are important for minimizing losses and attaining maximum efficiency in a wireless charging configuration. It is also important that the materials be safe for users. Frequency is a key consideration in the design. The transmitter coil is selected to operate around 180 kHz (kilo Hertz). Avoiding the GHz (giga Hertz) range is a goal of the project in light of concerns raised over the safety of GHz frequencies when in close proximity to users. Radiation exposure must be kept to a minimum when working with wireless charger technology. The transmitter coil selected is manufactured by Taidacent and has an outer diameter of twenty centimeters. A coil of this size can be placed underneath a bed, assuming a typical measurement of resting 53 cm to 83 cm above the ground, and a user with an implanted receiver coil can then charge to a full 100% of power for seven to eight hours every night while sleeping or resting.

*Figure 1. Taidacent Transmitter Coil*

Two different types of copper receiver coils are tested with the transmitter coil. A 5-centimeter outer diameter coil made

by Taidacent is tested for a pacemaker application, and a 1.27-centimeter outer diameter coil manufactured by Wurth Electronics is tested for an implanted hearing aid application. Both coils are encapsulated in biocompatible PDMS (dimethylpolysiloxane/dimethicone) flexible substrate. This material is safe to be in contact with the human body, as it is biocompatible, and it creates a waterproof barrier between the metal coil and the body. This encapsulation of the coils protects them from corrosion, and also helps protect the coils from any mechanical shock or deformation. The conductive leads of the coils are the only parts which are not covered by PDMS in experimentation.

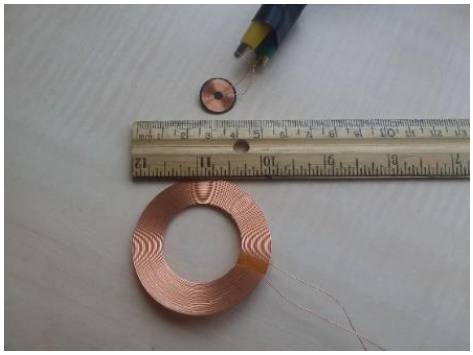

*Figure 2. Receiver Coils*

## III. Methods

Multiple charging configurations are designed, and the received voltage is measured with an oscilloscope. Preliminary testing is done with only air between the coils. The receiver coils are kept flat and parallel with the plane of the transmitter coil as the distance is varied. The receiver coils are moved vertically upward until power transfer is no longer detectable with the oscilloscope. Each coil must be tuned in order to achieve resonance. This is done by placing an appropriate capacitance in parallel with the receiver coil. This forms an LC tank circuit where the resonant frequency, $f_r$, is given by the following equation.

$$f_r = \frac{1}{2\pi\sqrt{LC}}$$

In order to charge a battery, the received voltage must be converted to direct current. This is done by using a diode bridge rectifier. Schottky diodes are selected for their lower forward voltage compared to ordinary silicon diodes.

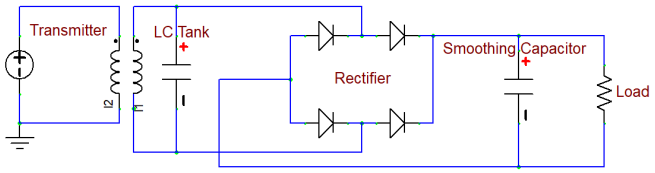


*Figure 3. Wireless Charging Circuit*

Both coils are tested through the medium of synthetic human tissue, real human parietal bone, and real baboon skull.

## IV. Results

Through the variety of experiments performed, testing shows that the 5-centimeter diameter coil is able to receive sufficient power at realistic distances for a pacemaker application to be charged through a bed overnight. The 5-centimeter diameter coil picks up around 0.7 volts RMS even at 46 centimeters above the transmitter coil. This distance is more than enough for a successful charging configuration with the transmitter coil attached under the bed of a user. The smaller 1.27-centimeter diameter coil loses voltage too rapidly with distance to work for an implanted hearing aid application. The smaller coil can only receive sufficient voltage at very close distances which are unrealistic for a user to achieve for significant amounts of time. However, future modifications could overcome this. A larger and more powerful transmitter could potentially solve this problem. Another modification to be considered is increasing the number of turns in the coil or modifying the shape of the coil into a square. Research has shown that these changes may be successful in increasing power.

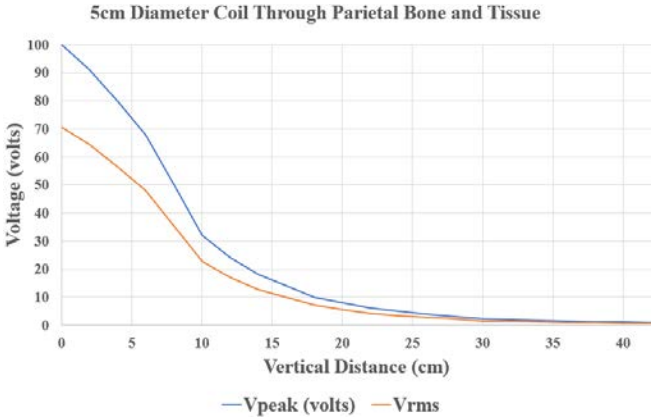


## Acknowledgment

The team is grateful to Dr. Mohammad Moghimi for his guidance and expertise throughout the project, as well as helpful notes from Aayush Patel.

## References

[1] Which Babies Need Care in the NICU? (n.d.). from https://www.oakbendmedcenter.org/which-babies-need-care-in-the-nicu/

[2] Silvestrini, E. (2017, October 17). Medical devices & Procedures, surgical tools & FDA recalls - DRUGWATCH (1298790930 956175376 K. Connolly & 1298790931 956175376 D. A. Daller, Eds.). from https://www.drugwatch.com/devices/

# Team 39: FFT-Based Vibration Signature Analysis

Sponsored by Omron Automation

Ryan Shaw
Mechanical Engineering
Northern Illinois University
DeKalb, IL
z1860945@students.niu.edu

Dexter Kling
Mechanical Engineering
Northern Illinois University
DeKalb, IL
Z1815231@students.niu.edu

Riley Plock
Mechanical Engineering
Northern Illinois University
DeKalb, IL
Z1843487@students.niu.edu

***Abstract*—For this project, a student team elected to assist Omron Automation to design a program in a programmable logic controller that would classify vibrating parts into categories based on their fast Fourier transform signatures. The program designed detects changes in amplitude at frequencies characteristic of worn gears in motors. The experimental results indicate this program could reliably be used to autonomously and precisely measure changes in amplitudes of vibrating parts.**

## I. Introduction

Omron Automation is investigating the feasibility of including vibrational diagnostics in their products. Analysis of the vibrational patterns of worn and unworn motorized parts has shown significant changes in their amplitudes in frequencies between 1 and 10 kHz. Vibration analyzers for diagnosing when motorized parts need maintenance are already on the market and have shown commercial success. Therefore, the team opted to design a system that could detect changes in signals of frequencies between 1 and 10 kHz.

## II. Problem Description And Statement

The manufacturing process has many points at which quality of manufactured parts can decrease. Vibrations can be used to test for these defects, using a sensor and an OMRON Programmable Logic Controller (PLC) to compare vibrational patterns to a baseline using analysis software. Using this comparison, workers can use this system to gain accuracy in quality control.

## III. Methods And Materials

### A. Overview

A signal is created digitally using a function generator and an exciter transforms the signal into measurable vibrations. An accelerometer attached to the exciter converts the measured vibrations into an electrical signal interpretable by an analog input/output bus attached to a PLC. Using a Fast Fourier Transform (FFT) program, the PLC transforms the signals to the frequency / amplitude domain. The vibration signal from the exciter is run with various amplitudes and the PLC program used to measure the variety. Based on comparisons between the desired amplitude and the recorded amplitude, the PLC will set flags for downstream effectors.

### B. Materials

Hardware

- TIRA Vibration Test System TV 51120 (exciter)
- TIRA BAA 120 Power Amplifier (power to exciter)
- PCB Piezotronics 621C40 (accelerometer)
- PCB Piezotronics 480E9 (signal conditioner)
- OMRON NJ-501 1320 Version 1.3.20 (PLC)
- Digilent Analog Discovery 2 (function generator)

Software

- Sysmac Studios (PLC program)
- Digilent WaveForms (function generator program)

### C. Methods

Creating The Comparison Signal

*Setup:* A test was conducted using a constant sine wave signal created in the Digilent Function Generator with an amplitude of 1 (unitless) and a frequency of 3000 Hz. The signal was amplified by a TIRA Power Amplifier to match the input specifications of the TIRA Vibration Test System. The PCB Piezotronics 621C40 attached to the TIRA Vibration Test System converted the measured vibrations into a +/- 1V signal. That signal was fed into the PCB Piezotronics 480E9. The gain of the PCB Piezotronics 480E9 was set to 10, so that a signal of +/- 10V was fed into the NX-HAD402 connected to the NJ-501 1320. The NJ-501 1320 was programmed to read 2000 samples from the exciter 10 times every millisecond for 200 milliseconds (2000 samples total) during steady-state and take the FFT of the collected samples, storing them in an "FFT" array. The FFT array was scanned for amplitudes both significantly higher than others and consistent over several cycles. These amplitudes and frequencies were recorded in a "key" array.

Using The Comparison Signal

The procedure for creating a comparison signal is repeated using an amplitude lower than 1. The resulting values are

stored in a "sample" array. The ratio of the input amplitudes to the function generator are compared with the ratio of the amplitudes of the key and sample arrays.

## IV. Results

### A. *Amplitude Comparisons, Individual Signals.*

| Trial | Input Amp. | Input Freq. | Sample Array Freqs. | Sample Array Amp |
|---|---|---|---|---|
| 1 | 1 | 100 | 50 | 0.5290 (split) |
| 2 | 1 | 1333 | 650 | 0.7220 (split) |
| 3 | 1 | 2546 | 1240 | 0.5170 (split) |
| 4 | 1 | 3000 | 1465 | 0.6667 |
| 5 | 0.5 | 3000 | 1465 | 0.8181 |
| 6 | 1 | 3871 | 1890 | 0.5815 |
| 7 | 1 | 5000 | 2440 | 0.8416 |

The table in A. shows the values recorded by the PLC when the function generator was used to create single sin wave inputs. (split) indicates the signal was split into 2 or more signals over 5-25 Hz.

### B. *Amplitude Comparisons, Combined Signals*

| Trial | Input Amp. | Sample Array Freqs. | Sample Array Amp |
|---|---|---|---|
| 1 | 1 | 100 | 0.2710 |
| 2 | 1 | 1333 | 0.2490 |
| 3 | 1 | 2546 | 0.1155 (split) |
| 4 | 0.5 | 3000 | 0.5474 (split) |
| 5 | 1 | 3871 | 0.4729 |
| 6 | 1 | 5000 | 0.1406 |

The table in B. shows the values recorded by the PLC when the function generator was used to create a signal of the sum of the sin waves in part A (excepting trial 4). (split) indicates the signal was split into 2 or more signals over 5-25 Hz

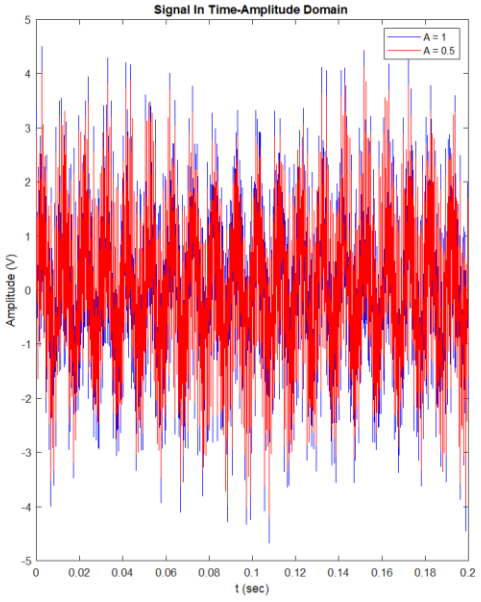


The figure above titled "Signal In Time-Amplitude Domain" graphically displays what direct readings from the accelerometer would look like for the combined signal if the 3000 Hz signal has an amplitude of 1 (blue) or 0.5 (red).

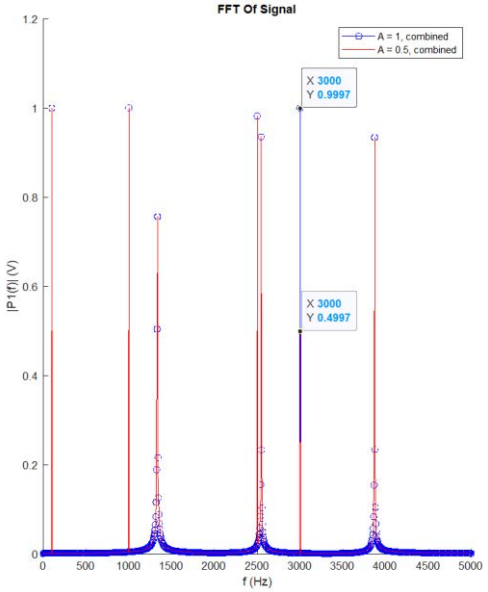


The figure above titled "FFT Of Signal" graphically displays the theoretical results the PLC calculates from the FFT function performed on the signal from part B. if the 3000 Hz signal has an amplitude of 1 (blue) or 0.5 (red).

## V. Discussion Of Results

Comparing the results in A to the results in B. shows that with a variety of signals of comparable amplitudes, our program cannot yet consistently distinguish small changes in amplitudes from signals. The frequencies displayed in the PLC sample array are not always consistent with the input frequencies, but they are consistent with how they are measured (i.e. during the test the sample array frequency of 650 was always associated with the actual input frequency of 1333). It is suggested for future research to create a running average of the sample array amplitudes as they could vary by 1 or more order of magnitude per reading.

## VI. Conclusions

The program's ability to separate frequencies in signals in the frequency spectrum where the wearing of motorized parts can be detected make it suitable for pursuing further research in developing a program capable of automating this process, but first a consistent way of measuring the amplitude in the sample array must be developed.


## VII. Acknowledgments

The team would like to thank the OMRON team of Matthew Labadie, Douglas Browne, and Peter McEneaney, the NIU Baxter Lab Team: Simon Kudernatsch, Dr. Donald Peterson, & Dr. Ting Xia, and our team TA: Ian Gilmour

# Automated Edge Rounding of Steel Sheets

Senior Design Project for CST Industries

Noah Adams, Blake Buccola, and Zach McNamara
Northern Illinois University
College of Engineering, Mechanical Engineering
Dekalb, Illinois

***Abstract* — The purpose of this project is to propose a device for CST Industries that can round the edges of their steel sheets of various gauges and dimensions. Ultimately, the team's research and proposed designs have allowed CST to move this project forward more quickly. The team has proposed a CNC milling device that will consist of four major systems: The Milling system, Adjustment System, Tolerancing System, and the Support/Guide System. These systems will work together to allow the device to round the edges of all of CST's sheets in a more efficient and cost-effective manner. Based on the team's recommendations, CST contracted a custom machine designer to get the bulk of their CNC device fabricated. Using a contractor will allow CST to use the team's effort and research to guide a company whose main service is building these types of systems. CST plans to have the team's system fabricated and installed over the summer.**

## I. Introduction

CST Industries is a worldwide company that produces industrial storage silos for bulk materials. CST uses a proprietary enamel to act as paint and defend the sheets from harsh weather conditions. However, the enamel cannot be effectively applied to surfaces with sharp geometry. In order to ensure that the steel plates that make up the silos will be capable of receiving the enamel, all the edges of the sheets must be rounded. CST currently does this rounding using a combination of sanding, rolling, and hand beveling depending on the gauge of the sheets. However, this is very costly due to the time and manpower required to use the rolling and beveling systems. Alternatively, CST's sanding operation is completely automated and far more efficient. The problem with the sanding system is that it is only able to round the edges of CST's thinnest gauge sheets. The end goal of this project is to incorporate a bulk material removal process into the sanding line in order to round the edges of all gauges of material.

## II. Material Specifications

Table 1. shows the required radius for each sheet gauge manufactured by CST [1]. These are the radius requirements that CST has determined will allow the enamel to effectively adhere to the sheets. The final system must create these radii on the sheet corners in order to be acceptable to CST.

| Gauge size (in) | .228 | .262 | .293 | .322 | .354 | .375 | .438 | .500 |
|---|---|---|---|---|---|---|---|---|
| Req. Radii (in) | .125 | .125 | .1875 | .1875 | .1875 | .1875 | .1875 | .250 |

TABLE 1: GAUGE SIZE VERSUS. REQUIRED RADIUS (IN)

## III. Sanding Line

CST Industries currently uses a conveyor belt system utilizing sanding machines to remove the sharp edges on the thinnest gauge steel panels. These belt sanders are mounted at a 45-degree angle with the backing plate removed so that the belt conforms to the edge of the sheet, creating the desired rounded profiles. There are two sanding machines on each side of the conveyor system to round the top and bottom of the sheets at the same time.

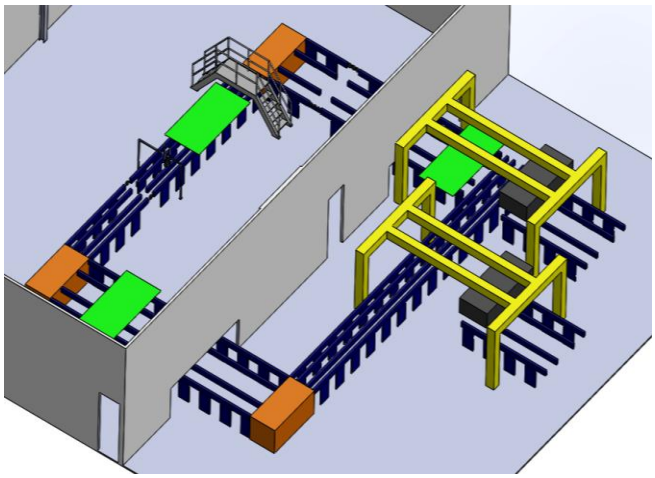

FIGURE 1 - SANDING LINE LAYOUT

The system does not rotate the sheets throughout the rounding process, instead it uses a combination of conveyors and moving wheels to translate the device around the system. The system can complete the sanding process within the first half of the conveyor line. The second half of the line is where the team's optimal design will be implemented to accommodate for the larger gauge sizes.

## IV. Proposed Solution

### A. *Milling System*

This system will include a high-powered spindle on both sides of the sanding line to round the edges of the sheets. As per our calculations, it was found that three horsepower is the power requirement to achieve the desired material removal rate [2]. These spindles are implemented to accommodate for the larger gauge sizes that cannot be handled by the sanding belts alone. Four spindles are necessary to achieve the desired profile on each side of the rectangular sheets. These spindles will be fitted with internal radius cutters to remove material from the panels. This will create a profile that will be desirable for the enameling process.

### B. *Cutting Tool*

Each different panel gauge requires a different sized milling bit in order to accurately remove the corners. After numerous meetings with professional machinists and representatives from tooling companies, the conclusion that was drawn was that an indexable carbide milling bit would be best for this application. This is because the milling head and cutting indexes are separate. When the indexes wear down, they can be easily replaced. This is much more cost effective than replacing the entire cutting head, which is the case with solid carbide bits.

### C. *Actuation System*

To allow for treatment of the full variety of different panel sizes and gauges, the milling spindles must be adjustable to align with each corner. To accomplish this, the milling spindles are mounted onto linear actuators, similar to a CNC system. This system will need to move the milling system, tolerancing system, driven wheel, and guide rollers to accommodate for the full range of sheet sizes.

### D. *Tolerancing System*

The raw steel sheets that CST receives are not perfectly sized or squared due to manufacturing tolerances. In order to accurately remove the sheets' corners, the actual profile of the sheets must be known. A spring-loaded roller follows the profile of the sheets as they pass by on the conveyor. The distance that the roller deflects is recorded and passed on to the actuation system. This allows for the surface profile to be perfect regardless of the original geometry of the sheets.

### E. *Support/Guide System*

After the main systems of this device, there are still two major hurdles that need to be addressed. The first is reducing chatter within the system. Milling bits used for bulk material processing need to be incredibly rigid. Chatter within the system will cause the bit to collide with the sheet in undesirable ways, drastically reducing tool life. To combat this, rigid support rollers will be aligned with the spindle in order to hold the sheet in place as it moves through the mill. A second structure will also be built to add rigidity. This will be a large motor-driven guiding wheel that serves two purposes. The first being support and the second is to help pull the steel sheet through the system against the added friction of the milling and guide systems.

## V. THE FUTURE

There is still work to be done on this device going forward. The construction of this device is being outsourced to a custom automation/robotics company called Vention. They are using their expertise in the creation of custom CNC equipment to fabricate the proposed structure and actuation system. Although the optimal tooling for this project has been established, finding the right tooling distributor is key due to the need for custom bits with complex geometry. The effects of this tooling dilemma ripple into the rest of the device. The major effect of this problem is that tooling will define the final milling spindle used in the device. This leads to a problem where it is unknown how the milling spindle will be mounted. Therefore, the design of the adjustment system is difficult. However, work has been done with Vention to allow for custom fixtures to be mounted to the device after tooling has been finalized. This will allow Vention to continue the production of the device while CST determines a tooling contractor without either party being hindered by the other.

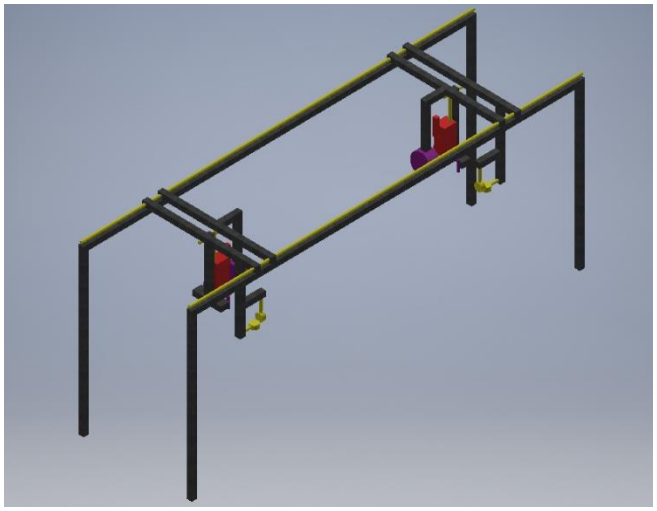

FIGURE 2 - PROPOSED DESIGN FOR FINAL DEVICE ASSEMBLY

## VI. CONCLUSION

Ultimately, once constructed, the proposed device should be able to accomplish the task set out by CST industries. The proposal submitted by the team has moved CST forward in their ability to streamline their edge rounding process. CST is in a position where they will be able to have the CNC device itself constructed by an experienced company who is more than capable of satisfying their needs. The only work left in the hands of CST is to find the proper tooling contractor to produce the optimal cutting tools.

## VII. ACKNOWLEDGMENTS

The CST team helped in any way they could when the team was discussing the current system. The team would like to thank the CST team for making it to our weekly progress meetings promptly and with an eagerness to achieve success.

Team #40 would like to also thank Dr. Gau and our teaching assistant, Ian Gilmore, for guiding the team throughout the project. They helped point the team in the right direction when things were difficult. Dr. Gau was able to connect the team with a contact at the machine shop who gave the team very useful information. They were both very knowledgeable and supportive throughout the year.

## VIII. REFERENCES

[1] "Sheet Steel Edge Coat Radii Requirements", CST, Columbian Steel Tank Industries, 2020.

[2] Kalpakjian, Serope, and Steven R. Schmid. *Manufacturing Engineering and Technology*. 6th ed., Pearson, 2009.

# Fluid Power Vehicle Challenge - Frame Design

Thomas Stewart, Pawel Jakubczyk, Joshua Rogers
Department of Mechanical Engineering
Northern Illinois University
Dekalb, Illinois, United States of America
gmalkawi@niu.edu

***Abstract*—Fluid power is an integral subject of society, seen in numerous facets all around the world. Fluid power systems are used in everything from energy production to manufacturing, and can be seen embedded into many systems in various forms. Fluids provide an excellent method of generation, storage, and use of energy that have revolutionized the way the human race operates. The goal of this competition is to get more young people involved in the fluid power industry and provide a better understanding of where it has been, where it is, and where it is going. The project involves designing and building a frame for a vehicle that incorporates both human power and fluid power. Teams from many universities come together for a competition to evaluate which has developed an all-around dominant design.**

***Keywords-Unidirectional; Omnidirectional; 3k 2x2 Twill Weave***

## I. Introduction

The Fluid Power Vehicle Challenge (FPVC) is arranged by the National Fluid Power Association (NFPA). The NFPA appoints judges for the annual competition. Each team is judged based on several criteria including sprint race performance, efficiency, endurance, best use of pneumatics, innovative use of electronics, design, reliability & safety, workmanship, teamwork and presentation. The vehicle must be produced to meet each of these measures adequately for a successful entry into the competition. A main objective in the competition is to achieve power transmission without the use of direct electrical or mechanical power conversion through the use of chains, linkages, or electric motors. The system involves a fluid link between a hydraulic pump and hydraulic motor that must serve to create motion. The use of pneumatics in any form other than power generation is required, but not specified as to how this must be achieved. It is recommended that each team integrates an electronic control system to regulate the components and assist in the monitoring of the system. Similar to pneumatics, electronics cannot contribute to the power generation of the vehicle. Another requirement involves the implementation of regenerative braking within the hydraulic circuit. With all of these considerations, it is imperative that the frame design allows for a strong, lightweight, ergonomic, and modular design capable of integrating the various systems effectively.

## II. Methods and Materials

In order for entry into the competition, the overall weight of the vehicle produced must be less than 210 lbs. Due to the number of components required, and the size of these components, a lightweight material must be considered for the framework of the vehicle. Comparing material properties for various metals and composites shown in Figure 1, it can be determined that reinforced Carbon fiber provides a higher stress resistance at a fraction of the weight as opposed to some commonly used metals.

**Table 20.1 Density ($\rho$), Strength ($\tau_f$), the Performance Index ($P$) for Five Engineering Materials**

| *Material* | $\rho$ ($Mg/m^3$) | $\tau_f$ ($MPa$) | $\tau_f^{2/3}/\rho = P$ $[(MPa)^{2/3}m^3/Mg]$ |
|---|---|---|---|
| Carbon fiber-reinforced composite (0.65 fiber fraction)* | 1.5 | 1140 | 72.8 |
| Glass fiber-reinforced composite (0.65 fiber fraction)* | 2.0 | 1060 | 52.0 |
| Aluminum alloy (2024-T6) | 2.8 | 300 | 16.0 |
| Titanium alloy (Ti-6Al-4V) | 4.4 | 525 | 14.8 |
| 4340 Steel (oil-quenched and tempered) | 7.8 | 780 | 10.9 |

* The fibers in these composites are continuous, aligned, and wound in a helical fashion at a 45° angle relative to the shaft axis.

Figure 1: Comparison of common engineering materials [1]

With a performance index of 72.8, Carbon fiber provides a more-than-adequate strength to density ratio, allowing for sufficient reliability and safety, while maintaining a vehicle under the required weight restriction.

Since Carbon fiber is composed of woven composite strands, this makes fabrication and fastening a challenge as the fibers have a tendency to break apart and tear when they are disrupted e.g. drilling, cutting, bending. Because of this, it was crucial to find a solution that was less intensive on the material in order to maintain the integrity of the composite. The solution came from Rockwest Composites, which offers numerous types of carbon fiber tubing in different shapes and weaving to accommodate nearly any project. Along with unidirectional and omnidirectional patterns, a non-intrusive method of connecting the tubing was available with the CARBONNect ® connectors. The connectors are composed of 6061-T6 aluminum, and serve as the joints for the frame. The adapters are lightweight, and boast tremendous capabilities. CARBONNect ® connectors offer modular configurability and a mounting solution for metal plates to attach necessary components. These connectors were selected, as well as the INFINITubeV Standard Modulus round Carbon fiber tubing. The Carbon fiber

tubing has a diameter of 1.5 inches, and consists of a 3k 2x2 Twill Weave for a balance of strength and formability.

## III. FEA Analysis

With the fluid powered vehicle frame being a custom design, the frame design needed to be subject to analysis that would determine unknown characteristics. The CAD model of half the frame was imported from Solidworks into Ansys in order to perform a deformation and maximum stresses analysis. It was determined that half the frame provided accurate results due to the frame design being symmetrical, as well as simplifying the time of solving for the solutions. Once the loading conditions were determined and the boundary conditions, the total deformation of the frame was solved for. With a loading force of about 275 lbs on half of the frame, the total deformation was 0.053439in.

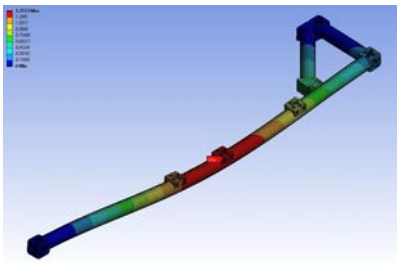

Figure 2. Ansys total deformation contour plot

Then the maximum stresses were found. Using the same loading conditions, the maximum stress was 21,450 psi.

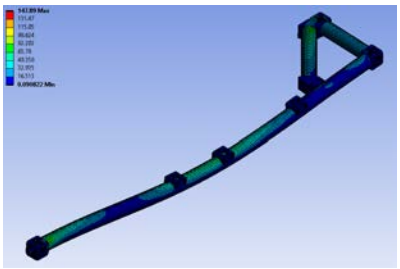

Figure 3. Ansys total deformation contour plot

To verify whether the solutions of the analysis were producing accurate results, a convergence study of both the deformation and maximum stresses was performed, and concluded that the solutions were accurate. As a result, this is a viable frame design to use for the vehicle due to little deformation, and its strength

## IV. Results and Discussions

The frame prototype of the fluid-powered recumbent tricycle is designed to be lightweight and structurally sound holding the rider and all the hydraulic, pneumatic, and electrical components. The research into carbon fiber tubing is a beneficial part to the design of the frame to keep the frame lightweight. The main frame was made with carbon fiber tubing and CARBONNect ® connectors and the main mounting pieces were made with aluminum. Thick ¼" 6061 Aluminum plating is the plating used in the mountings for all the components. A majority of the mounting pieces were manufactured using DXF files and the OMAX ® waterjet in the NIU machine shop. This is another approach to reduce the overall weight of the vehicle. The frame is rigid and is capable of holding up a significant load. Although, due to an unforeseen reduction in the production timeline, the prototype was not able to be tested thoroughly. However, due to drawings in CAD, an FEA Analysis, and a circuit simulation using Simulink® it is shown that the frame prototype of the fluid-powered recumbent tricycle will be a success in the FPVC.

## V. Conclusions

The frame prototype for the fluid-powered recumbent tricycle is an original design. The originality of the frame and the mounting components gives this tricycle an edge in the FPVC competition where a majority of the FPVC teams use pre-manufactured frames and parts. Although the manufacturing process of all these frame parts is time consuming, the end goal is reached. The end goal is to produce a strong lightweight frame capable of carrying a great deal of weight.

## VI. Acknowledgments

**NFPA** - Event organization
**Danfoss Power Solutions** - Host, Industry Supplier
**Norgren** - Host, Industry Supplier
**Eaton, Lubrizol, Parker Hannifin, Source Fluid Power, Sunsource, Iowa Fluid Power** - Industry Suppliers
**Bruno Risatti** - Mentor - Caterpillar
**Michael Reynolds** - NIU Machine Shop
**Doug** - NIU Machine Shop
**Jeremy** - NIU Machine Shop
**Dr. Ghazi Malkawi**- Faculty Advisor

## VII. References

[1] Callister Jr. William D. (2001) Fundamentals of Materials Engineering (5th ed.)

# CandyWorx Revolv Belt Coater Belt Cleaner

Chris Schmidt
Mechanical Engineering
Northern Illinois University
Dekalb, IL
Z1567642@students.niu.edu

Robert Ciavarella
Mechanical Engineering
Northern Illinois University
Dekalb, IL
Z1852936@students.niu.edu

Tim Cullinan
Mechanical Engineering
Northern Illinois University
Dekalb, IL
Z1858993@students.niu.edu

***Abstract*—For this project, the group assigned was partnered with CandyWorx to find a solution for the accumulation of product buildup on the Belt of the CandyWorx Revolve Belt Coater. This project is to display the mechanical knowledge of the team through various forms of problem solving. The team used CAD, mechanical calculations, finite element analysis, and assembly to test the skills provided through Northern Illinois University. Through this project the team used various methods and calculations to produce a one-of-a-kind prototype for CandyWorx to improve upon to incorporate into their line of products. CandyWorx is an engineering company that provides solutions for the confectionery industry in the form of equipment, engineering services, and custom designs. The impact on the industry has reached all over the world and they are on the front line of innovation. The Revolv Belt cleaner is an add-on to one of their existing products, that highlights the attention to detail the company maintains throughout all their products. The team was tasked with developing a product that could be self-contained within the Revolv Belt Coater, that in eventuality would use steam as the main vessel of sanitation, along with a form of mechanical agitation to remove any larger accumulations of product layered on the surface of the belt.**

***Keywords-Prototype, Belt Cleaner, Mechanical agitation, Steam, CAD, Calculations, Finite Element Analysis, Assembly.***

## I. Introduction

Modular plastic belts are a typical component for conveyors throughout the food processing supply chain. One drawback to modular plastic conveyor belts is that they can be challenging to clean in between their various joints and hinges. With an ever-increasing focus on food safety in the industry, the ability to thoroughly clean modular plastic conveyor belts with repeatable accuracy is of great interest to Candy Worx as a food equipment manufacturer. Thus, Candy Worx would like to design a Revolv Belt Cleaner.

## II. Problem Description and Statement

The Revolv Belt Cleaner prototype shall be a device that contains a mechanical cleaning device to agitate loose debris from the surface of the belt. The device shall also simulate the application of low-pressure steam and a sanitizing solution to the surface of the belt to help release affix debris, penetrate between the hinges and gaps in the modular plastic pieces, and prevent the future growth of bacteria. Finally, the Revolv Belt Cleaner must also traverse the width of the belt to clean the entire belt surface while the belt slowly travels past the Revolv Belt Cleaner's pathway. By the end of this project, it is expected that the Revolve Belt Cleaner prototype will be complete for demonstration and testing.

The objectives for the project include:

- Design Of Prototype
- Heat Transfer Analysis

## III. Design

### A. Design

The team produced a novel design through various forms of research, calculations, out of the box thinking, and CAD. This was achieved by combining all the knowledge provided throughout their education, guidance of the faculty advisor and Industry client. Through multiple iterations and evaluation an optimal design was decided upon and fabricated. Using Computer-Aided-Design the production of the optimal design was done in a cost-effective manner. Computer-Aided-Design eliminated the necessity of various physical changes to be made and allowedFigure 1 is a visual depiction of the end design produced in Solidworks, that was then fabricated to the exact specifications of the model.

for a product that fit the customer's needs.

*(Figure 1 - The Master Assembly)*

*(Figure 2 - Internals of Belt Cleaner)*

### B. *Method of travel*

A major constraint within the project was the decision on how to modulate the belt cleaner to across the span of the Belt Coater belt. The decision to use a rod less air slide was a major success, due to its compact design, simplistic operation, and compatibility within the existing system. This allowed for the optimal design to fit within physical constraints of the Revolv Belt Coater's enclosure. The rod less air slide required for the prototype capitalizes on the use of compressed air, which is in common supply with CandyWorx field of work.

### C. *Sanitation*

The reduction of cross contamination within the Revolv Belt Coater was a major factor within the design of the belt cleaner. CandyWorx required a design that could simulate the reduction of bacteria traveling from one product batch to another. By utilizing steam and cleaning solution as a basis for calculations and consideration, the prototype employs a three-nozzle system, each equipped with a fan style head, that allows for adequate coverage of the belts surface as it travels across its length, as well as triples the amount of effectiveness due to the nozzles. To ensure the nozzles compatibility for the prototype the team calculated the pressure required to remove product from the belts surface.

### D. *Mechanical Agitation*

Due to the amount of large accumulations of product that occur on the belt during operation it was required that a form of mechanical agitation or scraper be attached to the belt cleaner. To achieve this, Viton rubber was utilized due to its food safe composition and attached to two linear actuators that allow for the scraper to be extended during operation or retracted during production. The scraper also doubles as a method of reducing fugitive steam and encapsulating it within the ring focusing the steam in the directed area.

### E. *Stabilization of Head Assembly*

To take into consideration the slope at which the belt coater belt is angled the team implemented a rotational axis through the method of mounting the assembly to a bracket with bronze bushings for free form motion. As the linear actuators are extended and the scraper comes into contact with the belt the entirety of the head assembly will begin to self level against the surface of the belt allowing for the head to accurately attack the product on the belt. Once the cleaning process is complete two torsion springs were employed to allow for self correction of the head assembly, bringing it back to plumb.

## IV. Results

During the process of designing the mounting bracket concern was raised based upon the amount of force being applied to the mounting bracket for the head assembly due to the force applied by the belt during its rotation, as well as the sheer mass of the body. Through Ansys analysis, a justification was made to upscale the mounting bracket from a ¼ in. x 1 in. mounting bracket to a ⅜ in. x 2 in. mounting bracket to reduce stress and deformation placed upon the bracket and overall increase longevity.

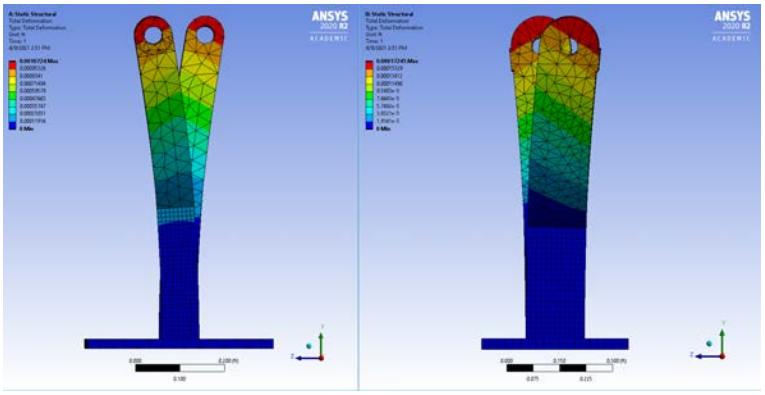


*(Figure 3 - ¼ in. x 1 in. vs ⅜ in. x 2 in. Mounting Bracket)*

## V. Conclusion

Overall, the team was able to produce a fully functional prototype device, that highlights all of the key points required to fabricate a large scale model required for the CandyWorx Revolv Belt Coater.


## Acknowledgements

The team would like to thank Bobby Sinko (PHD), Kevin Laud (VP of CandyWorx), Dan Statkus ( Project Manager of CandyWorx), Chris Moore (Engineering Manager of Spec Engineering), Brian Bernard (President of Spec Engineering), and Meredith Perry (VP of Spec Engineering) for the opportunity to develop this product, as well as the neverending support and guidance throughout the project.

# SpellVision 2.0

N. Emerson, E. Taylor, C. Maldonado

College of Engineering & Engineering Technology

Northern Illinois University

Dekalb, IL

***Abstract*—This project was created intending to use computer vision to be able to recognize the American Sign Language (ASL) alphabet in real time with high accuracy. The reason for such a project is to help diminish the gap between those who can hear well and those hard of hearing or even deaf. This can be overcome by creating a large dataset of images that correspond to the letters of the ASL alphabet applied to deep neural networks. These images are labeled according to the letter being signed. They are processed through a neural network using transfer learning to help the machine "learn" what is being signed after already having been taught on larger datasets of many more images and classifications.**

***Keywords-American Sign language, neural network, transfer learning***

## I. INTRODUCTION

There is a growing need for a reliable way to communicate with others that have hearing disabilities. There are approximately eleven million people, about 3.6% of the United States' population, that consider themselves to be deaf or have significant hearing issues [1]. There is an organization called the Registry of Interpreters for the Deaf (RID) that can be helpful to those who are in the non-hearing community. Although, there are only about 15,000 recorded members in this organization [2]. Having a means to communicate more effectively where the non-hearing and hearing communities interface could be life changing for those who cannot experience seamless communication with most of the world right now. It is quite the hefty task to create a real-time communication scheme between the hearing and non-hearing communities and this design hopes to be one large step toward that end goal.

## II. METHODS AND MATERIALS

Other designs have been attempted to solve the issue of two-way communication between the hearing and non-hearing. Most designs include hardware that can be difficult to carry around or more than one camera. These designs can be useful but are not ideal for those who are hard of hearing to use in many public spaces. Also, these designs limit accessibility by requiring unnecessary hardware. This project creates a simpler implementation that can be used in almost any situation. The hardware that is needed for this design is a camera and a simple cotton glove. The glove is something very simple that can be carried around and not make the individuals using this design standout. Many pictures need to be taken to train a neural network. The pictures that are taken need to represent each of the ASL letters. The letters "J" and "Z" are not trained in the network due to the letters themselves requiring dynamic movements. Transfer learning is used, and the network being used only accepts static pictures. Once the images are taken, a file needs to be created that can describe to the network the letter being signed - as well as where in the image the glove is. These images and extra files are separated into training and testing folders. The testing partition gives a good representation of how the network will identify new images that the network has never seen. So, the training and testing datasets are passed through a previously created neural network using transfer learning. Training of the network can take a full day without a dedicated graphics processing unit (GPU). Once the network is trained, detections can be made in real time.

### A. Overall Design

SpellVision 2 takes the live video input from a webcam and scans the frames to detect the hand of a person wearing a color-coded glove. The video frames are processed through a mobilenet single-shot-detector (SSD), and when the desired confidence of a hand sign is met the computer places a box around the hand and states the letter being signed. Along with the SSD box and labeling of the letter being signed, it will also display the confidence it has in its choice. SpellVision 2 achieves this architecture using machine learning and transfer learning.

### B. Programs/Software

- Anaconda
- Python 3
- Jupyter notebook
- TensorFlow

### C. Components/Devices

- HD Webcam
- Computer
- Latex/cotton glove
- Paint

### D. Dataset /Labeling

A large dataset is created that represents the 24 static letters in the ASL alphabet. Each of the letters represents a class to the network. The only letters that aren't represented by this dataset are "J" and "Z" since they include dynamic motion. The networks that are created take about 1,440

images. That means that there are 60 images of each letter created. All the images must be labeled according to the letter being signed. The location of the colored glove and the label of the letter are created and exported to a file with these details being specified in a way the network can read. Each image and label go through a random image augmentation to expand the dataset and create images that seem new to the network being trained.

### *E. Training*

Training is done in python using the Machine Learning platform called TensorFlow. The datasets and label files need to be converted into a format that TensorFlow can process to use transfer learning. The folders representing the training and testing data are transferred to tfrecord files. The models that have been created for object detection need to be downloaded to start training a network using transfer learning. The configuration files need to be adjusted slightly to represent the number of classes in the dataset. The classes are each of the letters in the ASL alphabet. So, the configuration file number of classes is 24. The number of training steps used is 20,000 to create high accuracy, but it comes at a cost to training time. The training of a network with 20,000 steps can take around 24 hours without a GPU.

## III. Discussion and Results

SpellVision 2, was able to detect someone performing American sign language, with a color-coded glove in real time. To check the performance of the program the performance metrics were obtained, also known as the mAP (mean average precision). Through the performance evaluation it was shown that the ASL translator had a precision of 88.4%.

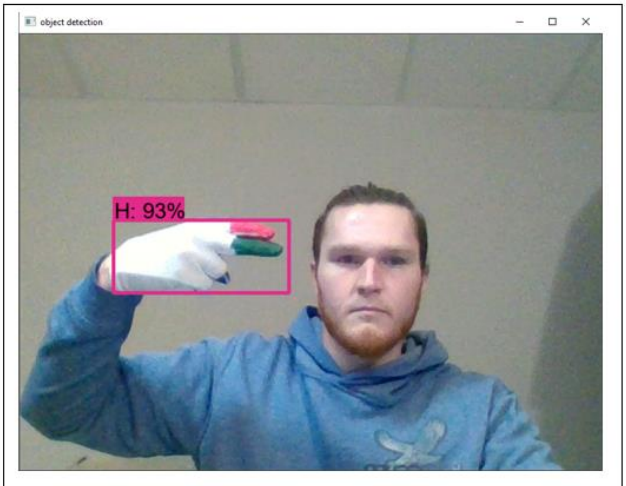


Figure 4. Showcase of live detection with confidence level shown

```
['N']
['N', 'B']
['N', 'B', 'H']
['N', 'B', 'H', 'E']
['N', 'B', 'H', 'E', 'L']
['N', 'B', 'H', 'E', 'L', 'L']
['N', 'B', 'H', 'E', 'L', 'L', 'O']
['N', 'B', 'H', 'E', 'L', 'L', 'O', 'W']
['N', 'B', 'H', 'E', 'L', 'L', 'O', 'W', 'O']
['N', 'B', 'H', 'E', 'L', 'L', 'O', 'W', 'O', 'R']
['N', 'B', 'H', 'E', 'L', 'L', 'O', 'W', 'O', 'R', 'L']
['N', 'B', 'H', 'E', 'L', 'L', 'O', 'W', 'O', 'R', 'L', 'D']
```

Figure 5. Demonstration of letters being saved, to spell out word.

In Figure 3, the chart and corresponding data is given for the mAP score. The ASL translator obtained a score of 88.4% with 20,000 steps. The highest possible score for this test would be 100%, meaning that the translator is correct every single time. Most of the time the network can detect what letter is being signed. There are a few minor examples in which rotating the hand by about 20 degrees will show detections of the wrong letter, but these can be learned easily with more data in the future. Increasing the dataset with well labeled images will increase the accuracy of the system. Many people sign letters a little differently, and thus creating this larger dataset with more people will allow for a little variety - an even better network for the masses.

## IV. Conclusion

SpellVision 2's goal was to improve upon the initial SpellVision 1 team's design. This task was accomplished as SpellVision 2 is able to perform live video detection and translation of people using ASL with high accuracy.

A future group for SpellVision will hopefully take it one step further and create a mobile application made available for download on Android and Apple platforms that can classify entire word symbols by integrating facial expressions and relative motion of the hand from the face.

## Acknowledgment

The authors would like to thank Dr. Ting Xia with the Department of Mechanical Engineering at Northern Illinois University. We would also like to thank Ian Gilmour for being our teaching assistant throughout the entire process.

## References

[1] [1] RIT Libraries. (2011). Deaf Demographics and Employment: Demographics Statistics. Retrieved from https://infoguides.rit.edu/c.php?g=380750&p=2706325

[2] Mitchell, R. E. (2006). How many deaf people are there in the United States? Estimates from the Survey of Income and Program Participation. PubMed, 11(1):112-9. doi: 10.1093/deafed/ENJ004

[3] Renotte , Nicholas, director. *Real Time Face Mask Detection with Tensorflow and Python | Custom Object Detection w/ MobileNet SSD*. *YouTube*, YouTube, 1 Nov. 2020, www.youtube.com/watch?v=IOI0o3Cxv9Q.

# Photography System for People in Wheelchairs

Team 44- Daisy Hernandez, Daniel Avila, Malak Zayed
College of Engineering and Engineering Technology
Northern Illinois University

***Abstract* — Basic photography poses difficulty to people with physical differences. A lack of commercially available solutions was identified, and the subsequent solution was designed. The object of this report is to describe and evaluate the possible design solution created. Evaluation of the designed solutions identified a monopod as the optimal solution. The monopod consists of an attachment point for a wheelchair, onto which a retractable shaft is attached, which supports the digital single-lens reflex (DSLR) camera electronically controlled positioning mount. The device helps the physically limited to set up and operate camera functionality with little to no assistance. Evaluation of current market offerings suggests not only will the modified tripod be a viable solution to the issue, but also a probable solution for the lacking market. The device is to be implemented in a high school classroom setting to enable those with physical differences to participate in still imagery.**

## I. Introduction

Currently available tripods do not offer enough flexibility, portability, and mobility for persons with physical disadvantages. Some of the challenges they face can include, but are not limited to, the inability to change the camera position at certain heights, manipulate the tripod effectively due to lack of strength, and access the camera due to the tripod's structure being unaccommodating. Oftentimes, people with disabilities cannot view through the camera lens or change the settings of the camera comfortably. While there is a wheelchair camera mount on the market currently to help persons with physical differences, it is restricted in the help it provides. This tool limits the range of height and angle the photographer can use, which is a big issue when wanting to take pictures from different views. The purpose was to create an alternative system with the same range of height as a standard tripod (about 40 cm -130 cm). This gives the user the ability to control the angle and position of the camera through a remote control or mobile application.

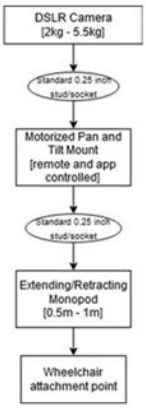


Figure 1: Flow Chart of Design Methodology

The photographer is able to simultaneously change the angle and position of the camera with the remote, observe the camera's viewfinder, and take the picture with the included remote or their smartphone. This system is portable, lightweight, and easily adjustable so that people with disabilities may use it without difficulty. This includes having a wide space under where the camera is attached, so that those in wheelchairs or with walkers can easily have access to the camera. Unlike commercial tripods, this system allows people with disadvantages to comfortably position the structure and change the height of the camera.

## II. Design Description

### *A. Motorized Pan and Tilt Camera Mount*

The objective of the pan and tilt mount is to allow the user to adjust the camera's positioning from a seated position. The camera attaches to the mount via a standard 0.25-inch (6.35 mm) socket that comes on all cameras, tripods, and tripod accessories. This attachment makes securing the device into place simple and adaptable to most existing photography accessories. Once secured, the camera will not require any handling. The camera will be able to swivel left and right 180° and rotate up and down 180°. This was accomplished by using two standard servo motors. One to control pan and one to control tilt. These motors can meet the desired positioning adjustments. The mounts positioning adjustments can be made using a remote controller or a mobile application installed on the user's cellphone. This allows the user to position the camera in the intended position without having to extend and retract their arms to physically make the changes. The mount is joined to the extendable and retractable monopod. The motorized mount is built using ABS plastic and aluminum to ensure the device remains sturdy and lightweight. People with physical differences often have difficulty maneuvering heavy objects Hence, the design placed significant importance to being as light as possible while meeting the necessary photography criteria. The target was to keep the overall mount to a weight under 1.5 kg to minimize the overall weight of the device and make it accommodating to a large variety of physically limited individuals.

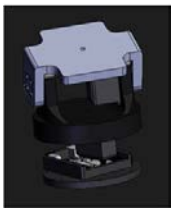

Figure 2: Camera Mount

### B. *Motorized Center Column*

The camera mount sits on top of the structure's center column. In order to be able to change the height of the camera, a linear actuator is used for the center column. This is constructed with a motor, long threaded screw, a nut, and two aluminum sliding tubes. The rotary motion from the motor is converted to linear motion, causing the inner tube to move up and down. With this linear actuator, the camera will be able to have a displacement of about 12 inches (30.48 cm).

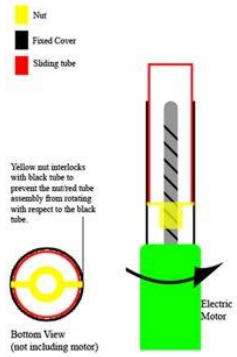


Figure 3: Linear Actuator

### C. *Wheelchair Mount System*

Most tripods have three legs for stability, but this monopod includes a rectangular aluminum tube with a length of 381mm, that reaches across the user's lap. This tube is the base that carries the load of the motorized pan tilt camera mount and center column. L-shaped connectors were designed to extend the aluminum tube horizontally to accommodate varying wheelchair arm distance. The horizontal extension is done through slots which are implemented through base and connectors. The slots are locked in place through a quick-release locking mechanism which includes a clamping-handle with a T-shaped thread. Attached to the connectors are angled mounting brackets to increase the height of the monopod and provide clamp support. Two toggle clamps go directly through the mounting brackets and clamp to the wheelchair arms.

Figure 4: Wheelchair Mount System

## III. RESULTS

### A. *Testing*

Once constructed, device functionality testing was conducted. The motorized monopod was tested to ensure it met the previously discussed requirements. The base structure was loaded with weight surpassing that of the device assembly to ensure rigidity, longevity, and stability of the structure. Once structure requirements were verified, the extending and retracting center column component was tested. The client required the device to extend to a height maximum of 1 meter. The column was tested to ensure it could reach the required heights under load. Like the structure, the component was loaded in excess to conduct rigidity and function testing. Once the column functionality was verified, the three structure components were assembled to test the electric mount function. The mount can pan and tilt in a 180° field, meeting the range requirements. The mount remote communication was tested by simulating a photography environment to ensure desired function. As a complete device, the motorized monopod met the requirements of the client to be released for use.

### B. *Implementation*

The device is to be implemented and used with high school students with physical differences.

## IV. CONCLUSION

The design of a photography system for persons with physical differences is valuable device as there are currently no available devices that provide the needs for photographers with physical disabilities. Professional photography operates using both gross motor and fine motor skills. Though this may seem simple to those without disadvantages, it becomes complex on those with them. The modified motorized tripod discussed accommodates persons with physical disadvantages and allows them to freely participate in photography.


## ACKNOWLEDGMENT

We would like to extend our sincere gratitude to the client, Dr. Kelly Gross, without whom this project would not have been possible. We would also like to thank our faculty advisor, Dr. Ting, for his guidance and constructive feedback throughout this project. Additionally, we would like to recognize our teaching assistant, German Ibarra, for his hard work and help during the completion of this project.


## REFERENCES


[1] "Aluminium Production & Environmental Impact", *Green Spec*, (https://www.greenspec.co.uk/building-design/aluminium-production-environmental-impact/)

[2] Chandrasekaran S, "Make a Simple RC (Remote Controlled) Robot Car", *Embed Journal,* May 2013, (https://embedjournal.com/make-a-rc-robot-car/)

[3] Dexcraft, et al. "Carbon Fiber vs Aluminium - Comparison." *Carbon Fiber Blog*, 18 Aug. 2020, (www.dexcraft.com/articles/carbon-fiber-composites/aluminium-vs-carbon-fiber-comparison-of-materials/)

# *Drone Enabled Sensing and Monitoring of Tree Canopies*

J. Holder, E. Kues, C. Peterson
Northern Illinois University
College of Engineering & Engineering Technology
Dekalb, IL, USA

***Abstract*—This project was proposed to Northern Illinois University, College of Engineering and Engineering Technology by The Morton Arboretum. The objective was to design and create a device to mount and retrieve a sensor arrays in tree canopies. These sensor arrays will be used to give the arboretum a better understanding of the environment of the canopies. The device that was created is to be attached to and manipulated by the DJI Matrice 600 Pro drone. The device utilizes multiple systems that are interchangeable onto the drone to deploy and retrieve the sensor arrays from tree canopies.**

## I. INTRODUCTION

The conditions of the tree canopy can provide information on tree health, outbreaks of pests and disease, and a better understanding of tree failure. The objective of this project was to find a more efficient way to study tree canopies due to their large size.

The team worked on two specific subcomponents, which is part of a larger scale project with various other systems. Morton Arboretum would like to have a sensor array, or other devices, that can be placed in and removed from a tree canopy. The current prototype allows for the devices to be fixed to a universal sensor mount (USM) shown in figure 1(B). The USM will be deployed into the tree canopy by a deployment system (DS), shown in figure 1(A), that is fixed to a pole attached to a drone.

When the device is to be removed from the canopy, the DS will be replaced with the female end (funnel) of the retrieval system (RS), figure 1(C). This configuration will enable the drone to make a connection with the USM and remove it from the canopy. After the USM has been retrieved, the arboretum can access the data collected by the sensor array or other devices.

The information that is attained by the devices deployed into the canopies is detrimental for a greater understanding of the environment of the canopies. The purpose of this project was to make it safer and more efficient for devices to be deployed and retrieved from areas that are difficult to reach by a person.

## II. METHODOLOGY

Universal Sensor Platform:

Since the universal sensor platform is being lifted by the drone and left in a tree for extended periods, the weight must be kept low. Polylactic acid (PLA) plastic was chosen because it is used in 3D printing as well as its cost effectiveness and relatively low density. Aluminum was used for parts that experience loads. A requirement of the USM is that it must be able to host an array of sensors and devices, so many attachment points were necessary. The USM remains attached to the tree using aluminum claws. There are two rigid claws that can be moved to allow different sizes of branches. The other two claws provide the clamping force using torsion springs. Part of the retrieval system is also attached to the USM. There is now a bracket which allows for the retrieval spike to be mounted away from the tree branch to ensure clearance for the retrieval funnel. The spike is attached to the end of the bracket and provides a connection point for the funnel during the retrieval process.

Delivery System:

The delivery system houses the USM during transport and engages the claw mechanism on the USM. It connects to the drone through a 12-foot telescopic pole. The DS has a servo motor powering a clamp that holds the USM in place. This clamp also pushes the USM out of the DS when a positive connection between the USM and tree branch is made. Another, more powerful, servo motor was added that turns a cam that overcomes the springs on the USM and opens the claws, allowing the claws to reach around the branch. The clamp then releases and the USM is left on the branch. Since weight is a significant design factor, components that were not load bearing were made from PLA. The system was also skeletonized to remove any unnecessary weight. Any load bearing components were machined from 6061 aluminum. The DS was also redesigned to accommodate the new USM design.

Electrical System:

The electrical system for the DS was completely redesigned from the original concept. With the replacement of the main drive servo for a larger model came a larger demand for current. This forced the team to use a battery pack external to the drone power supply. The team decided to use two lithium-nickel-manganese-cobalt oxide ($LiNiMnCoO_2$) batteries that were able to supply the required current and voltage. Additionally, an Arduino Uno microcontroller is utilized to generate the pulse-width modulation signals that are utilized to create the position data for the drive and clamp servo motors. Furthermore, the microcontroller takes the data input from the drone and measures the input signal pulse width to determine the switch positions on the drone remote controller. Using the switches on the drone remote allows the drone operator to control the position of the servo motors while the deployment system is in flight and during sensor platform deployment operations.

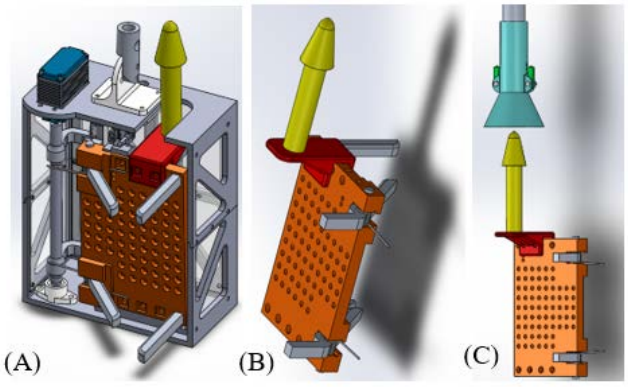

Figure 1: DS and USM (A), USM (B), RS and USM (C)

Retrieval System:

The retrieval system retrieves the USM after the data collection is over. It also connects to the drone using the same 12-foot telescopic pole. The RS is made from PLA, like the other systems for weight reasons. The RS connects to the spike on the USM, and the drone removes the USM from the tree. It was designed to give the drone operator a large margin of error when retrieving.

## III. RESULTS

### A. Retrieval System

The testing of the retrieval system was conducted on free standing branches of various sizes. The extension pole was attached to the drone with the retrieval funnel attached at the end. The drone pilot maneuvered the drone above the USM, and carefully lowered onto the spike of the USM. The latch of the cone engages the spike, and then the drone removed the platform from the branch.

### B. Deployment System

Currently, the DS has been tested on a bench but has not been flight tested. Simulations of various pieces of the DS have been successful, including software testing. Drone data output has been verified.

### C. Universal Sensor Mount

The testing the USM underwent showed that it was successfully able to clamp onto branches of various thicknesses. It was discovered that when the branches are very thin, the USM has difficulties attaching.

## IV. DISCUSSION

### A. Future Direction

One future consideration for our team was to remanufacture the sensor platform components from a more durable material than PLA plastic. Aluminum, or other lightweight metals, would hold withstand elemental forces and heat far better than that of plastic. Deformation of the PLA will be a consideration of long-term use of the sensor platform.

### B. Issues

The main issue we encountered with our design was the proper sizing and operation of the drive servo motor. The first servo motor that we were using was incorrectly rated for the required amount of torque that was required. When the team performed a torque analysis of the original servo, it was discovered that the manufacturer of the servo misrepresented the amount of torque that was supplied by the servo.

### C. Successes

The modification of the deployment system to accommodate the larger servo motor went especially smooth. Despite nearly the entire case for the deployment system needing to be re-printed to make the accommodation, the redesign did not create any timeline setbacks. Additionally, the entire retrieval system was redesigned. This allowed easier removal of the USM from the tree canopy as well as simplifying the attachment of the drone to the sensor platform during the removal process.

### D. Some Common Mistakes

One of the minor mistakes that the team encountered during the build of the design was the choice of wire connectors during the build of the electrical components. During original assembly, wire splices were used in place of a complete build of a wire harness. This caused several issues with open connections and system functionality.

## V. CONCLUSION

The prototype that was developed for Morton Arboretum to help study tree canopies. The environment of tree canopies can help the arboretum understand disease, insect life, wildlife, and overall tree health. The previous are important to know because it will allow for a deeper understanding of the problems in tree canopies. This information will give Morton Arboretum, as well as other groups, a better understanding of how to handle canopy issues. This information can also help understand tree failure. Tree failure can be very dangerous to the health of people as well as preventing property damage.

The team refined and redesigned an existing prototype to address functionality issues and new restraints. The primary alterations where completely redesigning the RS and near completely redesigning the electrical system.

Throughout this project the team was faced with numerous problems and limitations. Relying on the knowledge gained from their studies and past experiences, the team was able to effectively and efficiently use their engineering skills to overcome these obstacles.

## ACKNOWLEDGEMENTS

Our team would like to thank The Morton Arboretum, specifically Colby Borchetta and Chuck Cannon, for the opportunity to work with them on this project. We would also like to thank our faculty advisor, Dr. Sachit Butail, and our teaching assistant, German Ibarra. They have been a crucial part of our learning and have helped us in countless ways. Finally, we would like to thank our learning institution, Northern Illinois University.

# Phase-Change Induced Passive Cooling in Electric Vehicle Battery Systems

Abbas Alaidroos[1], Daniel Skurski[2], Scott Chavez[3]
Department of Mechanical Engineering
Northern Illinois University
DeKalb, IL USA
z1795175@students.niu.edu[1], z1768583@students.niu.edu[2], z1860589@students.niu.edu[3]

***Abstract*— Electric vehicle battery systems are being used to replace internal combustion engines that run on fuel to create a friendly "green" environment. Uncontrollable excessive heating of batteries is a common problem in electric vehicles, posing hazards such as fires and impairment in systems themselves. There are various cooling methods for electric battery systems already on the market but essentially lack a reliable cooling method without leakages. Phase-Change Induced Passive Cooling (PCIPC) is a method that involves the cooling of battery systems that will increase the cooling efficiency, reducing uncontrolled excessive heat generated from the batteries. The PCIPC method uses the principles of evaporation and condensation to heat and cool the working fluid which increases the heat transfer rate from the batteries by 10 times. In the proposed project, various designs employing increased heat pipe surface areas will be analyzed through computational-fluid dynamics (CFD) and then through experimental validation to define the best PCIPC structure. In the CFD simulation, effects of working fluid materials and solid case materials, heating and cooling temperature, heat generation from batteries and the heat removal capacity will be analyzed. Selected materials and structure will be used to develop a battery test setup to validate the best design and structure.**

## I. Introduction

The concept of PCIPC involves evaporation and condensation of a working fluid to effectively release heat in an economical and efficient way. This method enables using refrigerant which is found in all vehicles. Typical battery systems such that you find in Tesla and Boeing are compact and connected in a series, which increase the likelihood of excessive heat generation and fires. The Tesla Model S being an example of a popular vehicle although having a simple cooling system, has the flattened cooling tube not directly in contact with all cells in the module making it difficult to protect battery life longevity. The Chevy Volt is another example using plate-like batteries with cooling passages in between them. The structure is complicated and there is a leakage problem. This is an indicator of a major electric vehicle industry problem, one of which that requires careful experimentation and troubleshooting to the rapidly evolving technological concept of battery powered vehicles. PCIPC is a simple yet effective method that involves the cooling of battery systems that will increase the cooling efficiency, hence reducing uncontrolled excessive heat generated from the batteries.

## II. Project Objective

The purpose of this project is to design a novel cooling system that is capable of cooling battery systems by means of PCIPC and to provide first-hand research that favors the method of PCIPC.

## III. Material and Methods

The main materials needed for the design of a passive cooling system are heat pipes. Copper is used because it has a high melting point and a high thermal conductivity. The high melting point will allow it to stay intact when the batteries begin to overheat. A block of aluminum 6061 is used as a base for the lithium-ion battery pack as it has approximately the same heat capacity as a lithium-ion battery. Cartridge heaters will be inserted into the aluminum block(battery) to generate the temperatures typical of electric vehicle batteries under operating conditions. The water coolant used will act as the vehicle refrigerant for testing under room temperature and ice-cold water to observe the differences.

### *A. Battery cell simulation*

The PCIPC method was inspired by lithium-ion battery modules that were not ideally safe. Batteries are a main component in the cooling system which provide the power to begin heating the passive system, which then enables cooling. Although heat generation is essential, it becomes the very issue in overheating and shortages in the battery which could lead to an undesirable event of thermal runaway. An ANSYS Fluent li-ion battery model (**Figure 1**) designed to simulate multiple discharge rates over time steps will give an idea of how much heat generation is in a lithium-ion battery and what proper methods can be used to cool effectively. This includes cooling structure, surface contact, heat pipes, working fluid and suitable materials to observe the typical battery conditions.

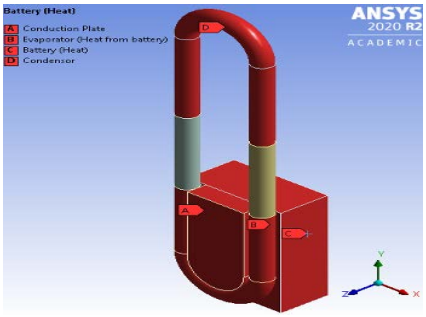


**Figure 1:** ANSYS Fluent cell simulator

### B. Heat Pipes

In terms of heat pipes, the structural factor in the design of effective heat transfer would be that of how the heat pipe is designed by wicks or gravity. Wicks are a porous material found in heat pipes that do the job of carrying the condensed liquid (cooled) to the hot region from the cold region (**Figure 2**). Wicks are substantially better in terms of allowing the structural freedom of heat pipes and provide flexibility. The downside is the expensive cost of using wicks, but after all materials considered, it was an economical decision.

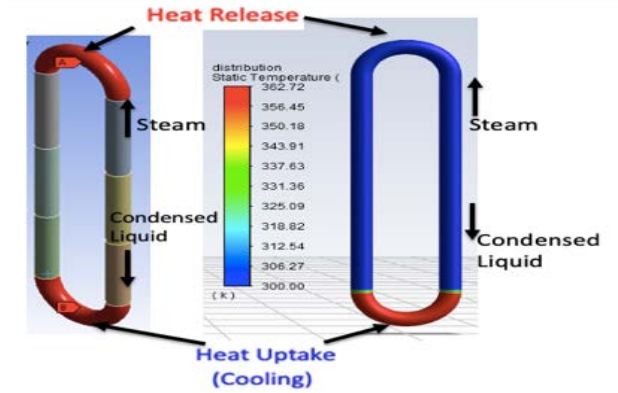


**Figure 2:** ANSYS Fluent heat pipe simulation

### C. Structure

The final PCIPC structure developed considers the principles of increased surface area contact, simple design and a manifold above the battery module acting as a coolant chamber (**Figure 3**). The cooling phenomenon enables phase change induced passive cooling to work exclusively with two heat pipes between each battery, maximizing cooling effects. The condenser section ensures the coolant delivers a fixed temperature stream and flow of coolant, so the heat pipe is always condensing the heated fluid.

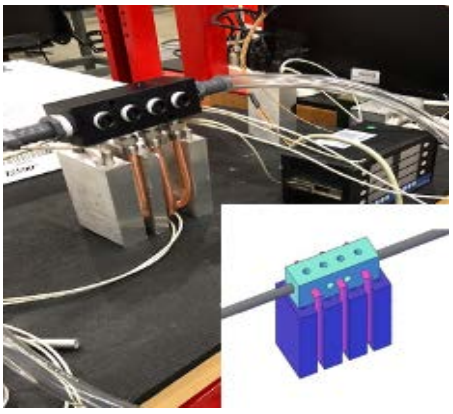

**Figure 3:** PCIPC design apparatus

## IV. Data and Results

The goal for our PCIPC structure is to control battery temperature to avoid overheating, or worse, thermal runaway. The optimum operating temperature is between 20°C- 45°C and the temperature difference between batteries shouldn't be more than 5°C. The heat transfer equation by conduction is:

$$\dot{q} = \frac{kA\Delta T}{L}$$

where $k$ is the thermal conductivity, $A$ is the exposure area, and $L$ is the depth of the solid, $\Delta T$ is the temperature difference between hot and cold.

Below is the data obtained from our experimentation:

TABLE I. Inner Battery Cell Data

| Inner battery: Cell1 | | | | | |
|---|---|---|---|---|---|
| Discharge Rate: | | 1C | 2C | 3C | 4C |
| | | Temperatures(°C): | | | |
| Time(min): | 0 | 27.3 | 30.1 | 39.6 | 52.8 |
| | 5 | 27.8 | 29.5 | 39.0 | 52.8 |
| | 10 | 27.3 | 28.5 | 36.6 | 54.5 |
| | 15 | 27.0 | 27.6 | 35.7 | 55.3 |
| | 20 | 26.0 | 27.1 | 34.1 | 58.4 |
| | 25 | 25.5 | 26.7 | 34.0 | 58.9 |
| | 30 | 25.7 | 26.9 | 33.6 | 58.7 |
| Heat transfer rate(BTU/hr): | | 10465.96 | 20931.93 | 39023.89 | -37969.7 |

TABLE II. Outer Battery Cell Data

| Outer battery: Cell2 | | | | | |
|---|---|---|---|---|---|
| Discharge Rate: | | 1C | 2C | 3C | 4C |
| | | Temperatures(°C): | | | |
| Time(min): | 0 | 26.3 | 27.1 | 38.3 | 52.2 |
| | 5 | 27.0 | 27.7 | 38.7 | 53.2 |
| | 10 | 26.4 | 27.3 | 36.4 | 54.1 |
| | 15 | 25.8 | 27.0 | 35.9 | 54.5 |
| | 20 | 25.1 | 26.5 | 35.4 | 55.0 |
| | 25 | 24.7 | 26.1 | 34.9 | 56.7 |
| | 30 | 24.3 | 25.0 | 34.7 | 58.0 |
| Heat transfer rate(BTU/hr): | | 13082.45 | 13736.576 | 23414.33 | -37326.2 |

## V. Conclusion

Managing the excess heat generation of batteries in electric vehicles is the number one challenge in being able to have an efficient, reliable, and safe product. Being able to manage this issue can completely change the way consumers and engineers view "green" transportation overall. Flat heat pipes increase the thermal contact area which allows maximum cooling effectiveness, increasing the heat removal rate. By using principals of pulsating phase-change heat pipes, no additional power is drawn from the battery system as the PHP is already expelling excess energy from the system. The evaporated working fluid in addition to the existing refrigerant in vehicles is what starts this passive and efficient process of reducing excess heat. Because of this phenomenon, PCIPC is quite efficient and simple when the right materials are selected.

## Acknowledgment

We would like to thank Dr. Kyu Taek Cho and Alexander Wills for their support and guidance for this project during these past two semesters.

# Hydraulic & Pneumatics of a Fluid Power Vehicle

## Fluid Power Vehicle Challenge

Jason Fidder, Trey Fry, Grant Heckel

Department of Mechanical Engineering

Northern Illinois University

Dekalb, IL, 60115

***Abstract*—The Fluid Power Vehicle Challenge (FPVC) is a yearly competition organized by the National Fluid Power Association (NFPA) in which teams from different universities compete to build a vehicle based on fluid power. The vehicle requires a use of hydraulics and pneumatics where the designed vehicle will be judged based on the vehicle's efficiency, speed, and endurance. The team will be given a budget from sponsors in the industry including Iowa Fluid Power, SunSource, Norgren, and an additional budget from Northern Illinois University (NIU). The project includes a collaboration with two teams where one will focus on the hydraulic and pneumatics of the vehicle while another team focuses on the frame of the vehicle.**

***Keywords-component; hydraulics; pneumatics; circuit;***

### I. INTRODUCTION

The FPVC focuses on vehicle design, electro-hydraulic/pneumatic system design, and controls programming. It requires the designing of an electro-hydraulic system, storing energy during vehicle operation, then utilizing that stored energy to drive the vehicle. Propulsion is accomplished through hydraulics with human power serving as the prime mover in the system. To incorporate pneumatics, a parking brake is applied to the system. The frame team has selected a three-wheel carbon-fiber frame, with pedals to generate mechanical energy. The goal is to create a safe, lightweight vehicle that will compete with other universities in the competition.

### II. MATERIALS & METHODS

The hydraulic circuit consists of four major components. These components include a reservoir, accumulator, motor, and pump. The reservoir is a storage tank for the hydraulic fluid to be stored and continually reused in the overall circuit. The fluid is drawn from the reservoir by the pump and is deposited back into the reservoir through the motor. The hydraulic motor is the actuator in the system that converts the energy from the hydraulic fluid to mechanical energy that drives the system. The motor takes the flow and pressure of the hydraulic fluid to convert the energy into torque and angular rotation to drive the vehicle. The hydraulic pump generates flow for the hydraulic fluid in the system. The accumulator is the energy storage system that provides supporting fluid flow to the circuit that provides supporting fluid flow to the circuit. The components are connected by a series of fittings, valves, and line bodies.

The pneumatic circuit is composed of two pneumatic cylinders connected in series. The actuation of one causes the other to extend in the opposite direction. Through this reaction the vehicle's parking brake is engaged. This circuit also features a flow control valve to improve rider safety.

The electrical components are powered through a 12V circuit design. A 12V battery is in series with a power terminal block which leads to a power disconnect switch, which is in series with the rest of the electrical circuit. A momentary push button switch is in series with a 3-way 2-position valve. A three way ON/OFF/ON switch in series with the 4-way 3-position valve. The Arduino is connected to the terminal block for power. The method of connection of these components included soldering, fastening down wires with set screws and using battery terminal connectors.

### III. OPERATIONS

The hydraulic circuit converts human power into mechanical energy within the system with a linkage between the pedals and the pump. While the human operator is

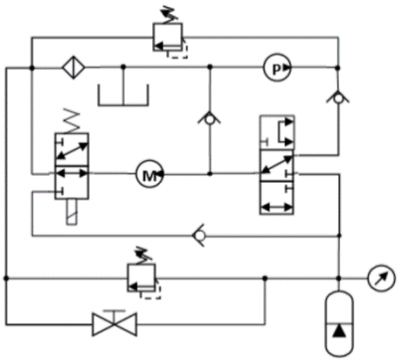

*Figure 1: Hydraulic Circuit*

pedaling, the pump is generating fluid flow from the reservoir which activates the circuit. While the rider is pedaling and the pump is generating fluid flow, the fluid flow is directed to the motor. This motor-pump linkage drives the vehicle. Figure 1 shows the connections between the main components in hydraulic circuit diagram. As the operator ceases pedaling, the pump stops drawing liquid from the reservoir; however, fluid flow is still generated through the motor. This fluid can be sent to the accumulator where it is stored as potential energy. The stored energy can be discharged back into the circuit when desired and drive the vehicle through the accumulator discharge.

The pneumatic circuit is tasked with engaging the vehicle's parking brake. It is engaged when the human operator pulls a lever that actuates a double acting pneumatic cylinder. Pressure is built up in this cylinder and forces the second cylinder, a reverse single acting cylinder, to change state. The end of the second cylinder is connected to a standard bicycle rim brake. To prevent potential harm from befalling the rider, a flow control valve is positioned in series with the cylinders. This allows for the lever to slowly return to its original position.

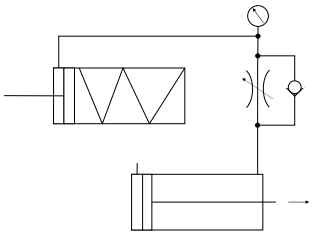

*Figure 2: Pneumatic Circuit*

The electrical components allow for key valves to actuate and to power a digital controller that will notify the operator of pressure charge within the circuit. The 12V battery sends charge to the power disconnect switch. The power disconnect switch allows for safely connecting components and connecting wires while in the off position. The power disconnect switch also allows for safely powering on the circuit rather than getting a power surge if the circuit was directly connected to the battery at once. The power disconnects switch supplies power to the terminal block. The terminal block acts as hub to distribute power to the electrical components. A momentary push button switch allows for actuation of the 3-way 2-position valve when engaged. While not engaged the button does not send power to the valve. The 3-way ON/OFF/ON 3-way toggle switch will allow for actuation of the 4-way 3-position valve. The middle position of the switch sends no charge, while to top position charges a coil to pull the valve, and bottom position pushes the valve. The Arduino controller allows for digital readouts from a pressure transducer in the circuit and will allow for the operator to monitor charge in the system. All components are grounded to common metal piece on the frame.

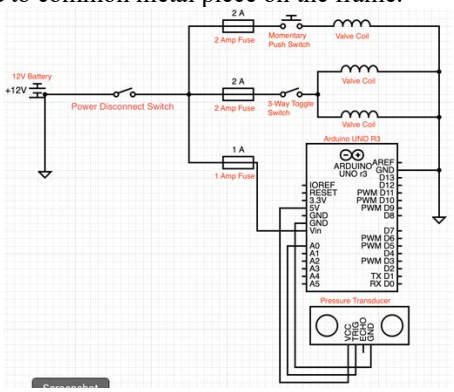


*Figure 3: Electrical Circuit*

## IV. Conclusion

As the first team from NIU to participate in the FPVC, the team believes they have created a solid vehicle for the competition. The vehicle functions as expected, and although the vehicle may not take first place in the competition, the team has created a solid vehicle that will be the stepping stones to better vehicles in the future of this competition for this university.


## Acknowledgment

We would like to thank Northern Illinois University for their full support over the challenging and unprecedented semester. We would like to thank our industry mentor Bruno Risatti for the guidance on this project. Also, thanks to Dr. Peterson, Dr. Malkawi, Sandhya Chapagain, and Stephanie Scaccionoce of the NFPA for working closely with us in the course.


## References


[1] National Fluid Power Society, "Fluid Power Reference Handbook," Innovated Designs and Publishing, Inc, First Edition, April 2019. *(references)*

# *Battery Storage Stack Design with an Intelligent IoT-based Active Cooling System*

Optimized Battery Storage for Ease of Manufacturing and Use

Eric Holmes[1], Iris Johnson[1], Nolan Magsamen[2]
Advised by: Pradip Majumdar[2] (pmajumdar1@niu.edu)
[1]Department of Electrical Engineering, [2]Department of Mechanical Engineering
Northern Illinois University, DeKalb, IL 60115

***Abstract*—Large scale battery solutions for energy storage are becoming more prevalent. The increased and faster charge cycling increases the thermal load on charging circuitry and the batteries used. This project proposes an IoT system to control the active cooling in order to prevent thermal runaway while controlling noise levels. A 1:10th capacity scale model using four Lithium Iron Phosphate (LFP) batteries was designed and fabricated using less than one third the volume of the previous design with greater performance. The goal was to maintain a temperature of less than 60ºC, to support less stable chemistries that are currently used more.**

***Keywords - Lithium ion; cooling; Energy Storage***

## I. INTRODUCTION

This project's scale model solution has a few key features. Monitoring the batteries for any problems. Forced air cooling for a cost-effective temperature management, extending lifetime, increasing system efficiency, and preventing hazardous situations. Modularity to allow for more flexible deployments.

Current market solutions for a single-family home have a capacity around 10kWh, advertised as enough for a single day. The developed scale model contains only 0.7 kWh. The scale model uses four Lithium Iron Phosphate (LFP) batteries. A full system would likely have 52 of these cells. The scale prototype enclosure will use LFP batteries, a type of Lithium ion, and should be easily adaptable to other battery types.

### *A. Battery Heat Generation*

Batteries through discharging and charging increase in internal temperature as a result of internal resistances and entropy form the reversible chemical reactions. Internal temperature will modify the internal resistance, and effect efficiency. The prototype solution looks to dissipate the heat generated and lower the temperature of the batteries to reduce overall power loss (from the internal resistance), for more efficiency and a longer life cycle.

### *B. Purpose of the Project*

The purpose of this project is to design an enclosure using cost effective manufacturing methods and to evaluate the performance. The scaled down standalone enclosure will be allow measuring the cooling capacity, providing a reference for the amount required in a full-scale system. A previous team's prototype, with the same capacity, also used forced air cooling; however, it was larger than practical for a full-scale.

## II. HARDWARE DESIGN

The scale model will operate at 12.8V and should deliver an average of 10 amps, with peaks of up to 20 Amps, similar currents to the full-scale but at reduced voltages. The designed enclosure uses two "air spaces". The first and largest will house the batteries and the fans; The second will house the controlling hardware and sensors. A Raspberry Pi was used selected for the controller on the prototype. It should be noted that the control hardware in the lower "air space" takes up a larger percentage of space on the scale model than on a full-scale system.

### *A. Enclosure*

The enclosure in Fig 1 is designed to house the batteries in a secure and robust manner for indoor location, while being lightweight and compact. This current design houses four batteries. In order to be competitive in the market, the volume to be met is $0.01m^3$ to give a power density of 76.8 $kWh/m^3$, and a weight in the range of 10kg.

The construction is made from formed aluminum. Fig 1 shows the extent of the design and battery layout. Wall thickness of 1.0mm proved rigid enough for structure while allowing tight bends. Fig 1 also shows the additional hardware space for the controller and circuitry, along with the safety circuit break on the side. Fig 1 right shows tie downs and busbars. In the event of a drop or impact the batteries are held secure and ample space is provided all deformation and to prevent shorting. The pair of 92mm fans are mounted on the rear panel, opposite the openings.

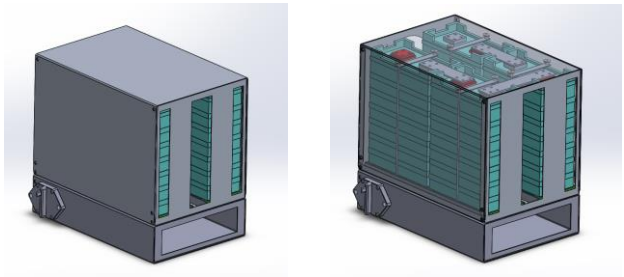

Figure 1: Proposed enclosure design

### B. *Batteries*

LFP was chosen for several reasons including: significant charge cycle lifespan, safety, direct comparison to the previous team's prototype and, new LFP cells would-be a near identical drop-in replacement. Newer LFP offerings are rated for more cycles and is overall a promising chemistry. LFP cells are also some of the safest due to their high thermal runaway temperature (270°C) [1] and relatively low reactivity to puncture. They also don't depend on cobalt, which is facing ethical mining concerns.

## III. TESTING

Simulations using CFD and FEA in SolidWorks were carried out with a simplified enclosure model and a 44 $m^3/h$ air flow rate. The 92mm fans used in the final design would operate at 1500rpm with 70$m^3/h$ air flow rate and are capable of 80$m^3/hr$. Battery heat was modeled using volumetric heat generation in a solid and the thermal conductivity was set to k = 0.4 W/mK, typical of a lithium cell [2]. Heat generation was set for 63 W, close to the rated a 3C discharge rate, per cell with air at STP.

### A. *Simulation Results*

Results of the simulation proved very promising; temperatures were kept well below 100° C at 52° C average between the four batteries. The results and temperature spread can be seen in Fig 2(b). Fig 2(a) shows the simulation model.

To show the benefits of forced air cooling, the same setup and parameters were used with fans off, Fig 2(c) shows the simulation model for this state. In this quiescent state, the temperatures were in excess of 150° C.

Forced air flow cooling performance decreases as the air temperature in the enclosure increases. The test results from the simulation were validated using a one-dimensional wall assumption using the air velocity and properties to calculate convection. Results were 1% lower in temperature than the results of the simulation, likely due to simplifying the battery construction for calculation and averaging the convection values.

### B. *Physical/Software Testing*

The constructed prototype can be tested at up to 30 amps discharge and 24 amps charge currents, independently. Generating less than 2.0 Watts max, per cell, the prototype is subjected to more stress than the previous design and far less stress than the simulations.

## IV. CONCLUSION

While the overall concept proposed of regulating battery temperature is not novel; the design still contains several components such as overall enclosure design, thermal regulation method and control system design that need to be evaluated. Previous preliminary work suggests that focusing on a forced-air convection system and strategically placed sensors will allow the system to proactively react without waiting for battery temperature itself to rise. Overall, this approach will allow for optimizations in both performance and cost relative to the previous design.


## ACKNOWLEDGMENT

Mike Reynolds for assistance with fabrication, Ian Gilmore, Trevor Rogneby, Amin RoostaeeHosseinAbadi-Teaching assistant


## REFERENCES


[1]. *BU-205: types of lithium-ion.* Types of Lithium-Ion Batteries – Battery University, updated: 2020 -07-10, retrieved: 7 Nov 2020, https://batteryuniversity.com/learn/article/types_of_lithium_ion

[2]. Mathewson, S. (2014). *Experimental measurements of LiFePO4 battery thermal characteristics* (Doctoral dissertation, University of Waterloo, 2014). Waterloo, ON: University of Waterloo


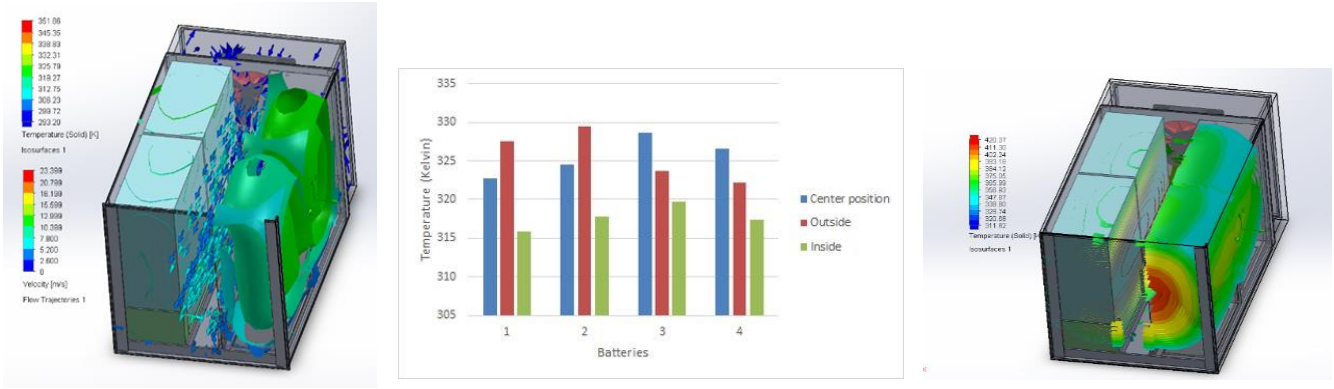


Figure 2. (a- left) Simulation with air velocity and battery temperatures. (b - center) Battery Temperatures. Measured on centerline ⊥ to main air flow direction. (c- right) Fans of

# *PIP-II Warm Unit*

Kyle Kendziora, Melinda Gunderson

Client: Fermi National Accelerator Labortory

Batavia, IL

***Abstract*—**The Warm Units are a vacuum manifold that joins the superconducting cryomodules of the PIP-II linear accelerator (linac). The primary function of the Warm Unit is to provide vacuum pumping for the cryomodules. There are no vacuum pumps in the linac other than the ones provided by the Warm Units. They also provide the opportunity for beam characterization instrumentation to be installed periodically along the linac. The key design tasks were defining the geometry for the instrumentation that will be included in the Warm Unit and the interface to the cryomodules. Coordinating with the groups responsible for these systems was the key to the successful designing of the support structure and bellow restraints for the Warm Units.

## I. Introduction

PIP-II is a $900 million project to upgrade the Fermilab accelerator complex to provide a higher intensity beam to run multiple experiments at Fermilab. This upgrade will include a super-conducting linear accelerator (linac) that is consists of several super-conducting cryomodules. Between each pair of cryomodules is a warm unit that will contain the vacuum pumping for the cryomodule as well as beam characterization instrumentation. The warm units will have to interface with the cryomodules in 2 ways. The Warm Units will have to attach to the cryomodule structurally so that the warm unit and the cryomodule can be aligned to each other and the warm unit will have to attach to the cryomodule at the beamline with a hydroformed bellows. The structural interface is a reinforced bracket and the hydroformed bellows requires tooling to be designed to safely compress it and protect it from damage during installation. This bellows restraint must be able to compress the bellows far enough to gain clearance for installation, but it must not compress the bellows to the point the bellows becomes damaged. The bellows restraint will also act as a bellows protector by not allowing the bellows to be over extended and to limit access to the convolutions.

## II. Design and Validation of Support Bracket

The load bearing capability, stiffness, location, and clearance from other features are all factors that went into the design of Warm Unit Support Bracket. The Warm Unit bracket needs to be able to support the load of the Warm Unit which will be a maximum of 100kg. The warm unit will also be sensitive to frequencies below 10Hz and at 30 Hz, so a modal analysis needed to be performed to make sure it does not resonate at any of those frequencies. The location and size had to be chosen such that it does not interfere with other features on the cryomodule and gives enough clearance to allow for the installation of the bolts for the end plates. The location relative to other features was also chosen so that the brackets could be manufactured accurately, and their position would be repeatable since several cryomodules would have to be joined by the warm units.

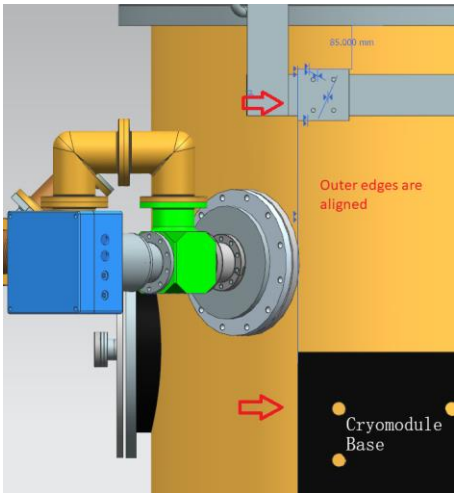


Figure 1 Bracket Positioning

The outside edge of the bracket is aligned with the outside edge of the base of the cryomodule. This alignment will help ensure the brackets are located perpendicular to the horizontal surface of the cryomodule stands. The edge of the bracket facing the end of the cryomodule is spaced out 85mm to give room for the end plate bolts to be installed and for wrenches to get in and tighten the bolts.

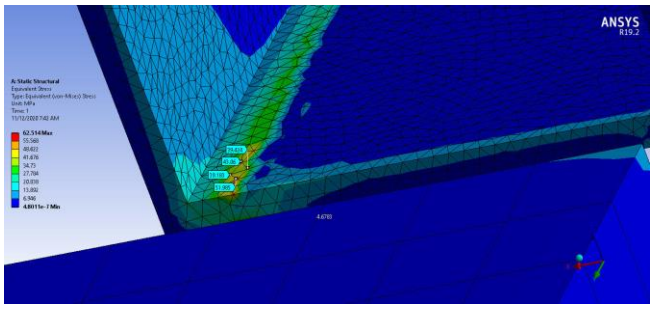


Figure 2 Stress Probes

A structural Finite Element Analysis (FEA) was performed to validate the structural capacity of the bracket. The highest stress shown in the FEA was 52Mpa. The material used for the brackets has a yield stress of 250Mpa.

The brackets were able to safely support the required load with the exposed stress over material yield stress being 5.

To address the vibration constraints a modal analysis was conducted. The analysis was setup using the brackets and the entire warm unit support structure with "dummy load" to simulate the instrumentation and its center of gravity. The only mode were the brackets played a large role is the one shown above at 22.85Hz. This is not a frequency that is an issue but there was a mode at 30Hz as well. To help stiffen the structure to move the mode out of the 30Hz frequency a gusset used, along with other stiffening methods all the modes were able to be shifted above 30Hz.

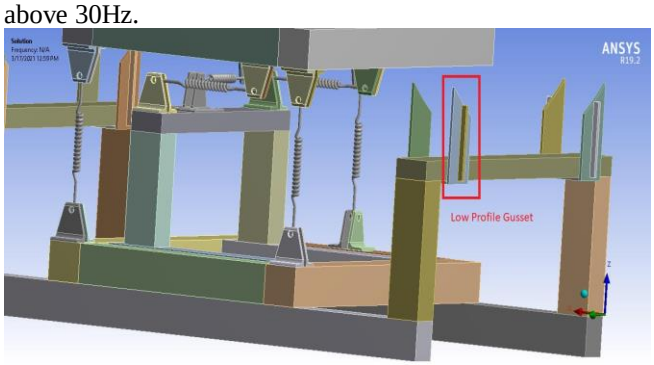


Figure 3 Stiffening Gussets

## III. Design and Validation of Bellows Restraint

To safely install and handle the warm unit beamline hydroformed bellows a restraint and protection fixture was required. This fixture needed to be made from vacuum safe materials that would not rust over time and create iron oxide. The fixture needed to be able to be easily disassembled so it could be cleaned regularly to maintain the cleanliness of the cleanroom and vacuum space environments. When these cleaned materials rub against another component of the same material they will gall and fuse together. The fixture design had to take this into account as well and all the components that contact each other must be of dissimilar materials.

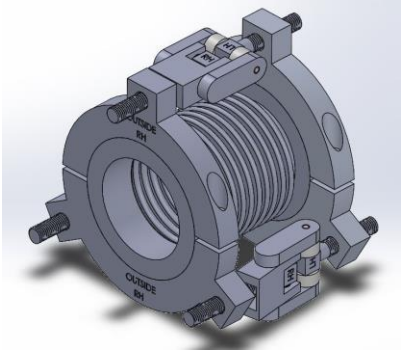

Figure 4 Bellows Restraint Fixture Attached to a Bellows

To provide a locking force the pin holes in the locking handle were off set. The off-set holes will force the handle down once the handle is closed.

The threaded rods have a left-handed thread end and a right-hand thread end this allows for fixture length adjustment while it is attached to a bellows. Based on the length of the bellows used, the restraint fixture can compress the bellows up to 9.25mm maximum.

The fixture must be able to compress and resist the pressure applied by the compressed bellows. To verify the strength of the fixture's design a structural FEA was performed. A 35N force was used. A max stress of 5.2Mpa was found.

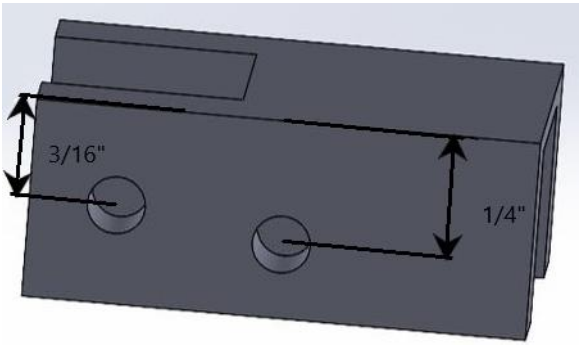


Figure 5 Locking Handle with Off-Set Pin Holes

This maximum is located on a Titanium rod which has a yield stress of 827 MPa which is well above the maximum exposed stress.

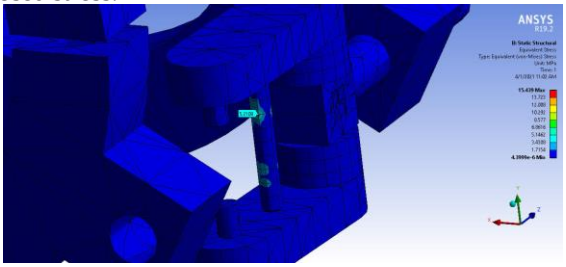


Figure 6 Location of Max Stress

## IV. Conclusion

These components had very specific requirements that were dictated by their location and application. The support bracket had loading and location constraints that drove its design. The bellows fixture had to be able to resist the force of a compressed bellows, it also had to be able to be cleaned for use in a cleanroom. For the bellows restraint to be properly cleaned it must be able to be easily disassembled and the components had to withstand the cleaning process without rusting. All these parameters had to be carefully considered and designed for to make a viable product for the PIP-II project.

## References

[1] Ball, M., Burov, A., Chase, B., Chakravarty, A., Chen, A., Dixon, S., Edelen, J., Grassellino, A., Johnson, D., Holmes, S., Kazakov, S., Klebaner, A., Kourbanis, I., Leveling, A., Melnychuk, O., Neuffer, D., Nicol, T., Ostiguy, J. -F., Pasquinelli, R., Passarelli, D., Ristori, L., Pellico, W., Patrick, J., Prost, L., Rakhno, I., Saini, A., Schappert, W., Shemyakin, A., Steimel, J., Scarpine, V., Vivoli, A., Warner, A., Yakovlev, V., Ostroumov, P., and Conway, Z. *The PIP-II Conceptual Design Report*. United States: N. p., 2017. Web. doi:10.2172/1346823.

# Query-by-Humming System to Illustrate Signal Processing Field for Prospective Students

Benjamin Peter Leonard
Department of Electrical Engineering
Northern Illinois University
Dekalb, USA
Z1865180@students.niu.edu

David Goldberg
Department of Electrical Engineering
Northern Illinois University
Dekalb, USA
Z1634095@students.niu.edu

Nathan McDonald
Department of Electrical Engineering
Northern Illinois University
Dekalb, USA
Z1788059@students.niu.edu

***Abstract*—Query-by-humming is a content-based music information retrieval system where a user hums part of a tune into a microphone, the audio is sampled and processed by a computer and compared against a database of stored songs. The tune hummed by the user is identified, a matching score is provided, and the actual song is replayed back to the user. This system has software framework that allows for real time use, and a graphical user interface which displays the hummed signal, matching information, and has buttons to control the application.**

***Keywords-Query-by-Humming, Graphical User Interface, Software Framework***

## I. INTRODUCTION

High school students often have a limited view of all the fields of electrical engineering. This limited view may cause students to overlook electrical engineering as a career. This project highlights the field of signal processing by developing a real time Query-by-Humming system paired with an informative interactive GUI (graphical user interface). This system is divided into 4 sub-components: Audio processing framework and real time usage, feature extraction, matching & decision making, and the GUI. Python was used to code the feature extraction, matching & decision making, and the GUI. While C++ was utilized as a framework allowing real time audio analysis.

## II. METHOD AND CODING

### A. *Audio processing Framework*

The audio processing framework is built using C++ for the main portion of the code. The Application programming interface, and the graphical user interface control the main program and are implemented in python. The main program has three persistent sub processes that handles the extracting, matching, and decision steps. Each of these processes pulls code from the user creating an instance of this program. It can take code in the form of either a C++ executable or a Python script. This framework model allows for iterative design, as well as being a basis for a real time application. The API/GUI communicate with the main program using named pipes, a method for inter process communication. The Main program communicates with the subprocesses using a similar method. In the case of a real time application, Audio data comes into the API/GUI, and is piped directly to the extraction process. The features are extracted using the user supplied code. The resulting extracted features are piped directly to the matching process, where they are compared against the existing database. The output of this comparison is piped to the Decision process, where the correct match will be decided. This result is then communicated to the main program, and then subsequently communicated to the API/GUI, which will then display the graphics informing the user of the match.

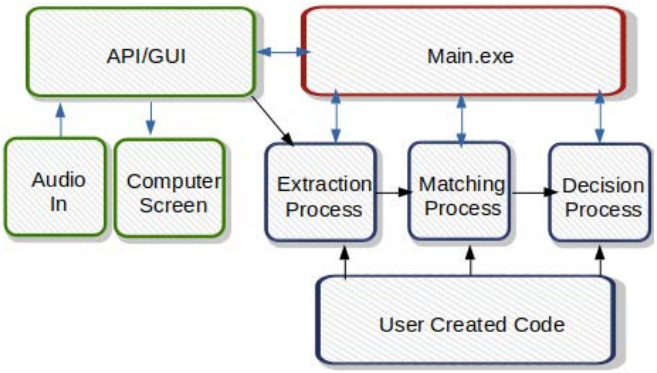


Figure 1: Block Diagram of Audio Processing Framework

### B. *Feature Extraction Algorithm*

The feature extraction process begins by analyzing the energy of each frame from the time series audio data. If the energy is greater than a minimum value (chosen from experimentation), the frame of data has its pitch extracted and the value is stored into a list. If the value of energy is below the min energy, the frame is discarded. An average over the extracted pitches is computed and the average value is stored into a list. A frame with energy less than the min value corresponds to when the user ends humming a particular tone. Taking the average allows us to account for fluctuations in raw pitch values and obtain an approximate value for the intended tone.

Pitch extraction is done by using the python library 'Librosa' [1]. The function used is an implementation of the

YIN autocorrelation method which estimates the fundamental frequency of a signal, which corresponds to pitch [2].

Once there are two values in the average pitch list, the last entry is compared with the second to last entry each time the list is updated to generate another list referred to as the up-Down List. If the average pitch value increase, a "1" is placed into the list. If the value decreases a "-1" is placed, and if the values are within a certain threshold, they are considered the same value and a "0" is placed.

In summary the feature extraction algorithm converts raw time series audio data into a series of '1s', '-1s', and '0s'. These values directly represent the relative pitch of the hummed input query.

### C. *Matching & Decision Making*

As the up-Down list is being generated from the feature extraction algorithm it immediately begins the matching process by being compared to a database of preprocessed songs with a function called fast dynamic time warping [3].

Fast dynamic time warping (DTW). This technique makes an informed low-resolution estimate of the DTW path, then increases the resolution over the initial path and calculates the Euclidian distance between two time series data sets by generating a lowest cost matrix. This method is much faster than a true full DTW cost matrix and allows us to calculate the distance between the hummed input and each of the stored songs in the database in real time.

The name of each song and the corresponding distance is stored inside a tuple. The tuple is sorted in descending order and saved. The shortest distance calculated directly corresponds to the most likely match of the input hum and is stored in the first entry of the tuple. Simple string-matching logic is performed that checks the first entry of the tuple for the name of the song and it prints the name of the song and a matching score as output to the user.

### D. *Graphical User Interface*

The GUI (graphical user interface) is how the user will interact and learn about signal processing. Only relevant information regarding the entire process is shown. Real time audio input (Figure 2), graph of the extracted pitch & the averages pitches (Figure 3), graph of the relative pitch of the hummed input (Figure 4), graph of the relative pitch of the corresponding song in the database (Figure 5), and a text box which displays the name of the matched song.

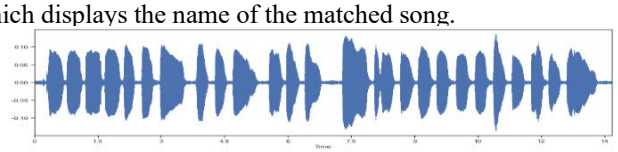

Fig 2:Real time Audio Input

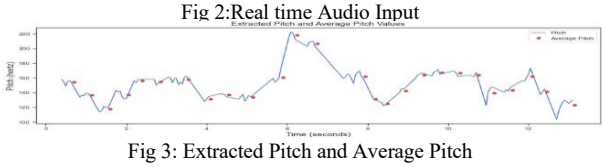

Fig 3: Extracted Pitch and Average Pitch

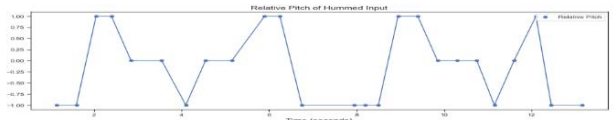

Fig 4: Relative Pitch of Hummed Input

Fig 5: Relative Pitch of corresponding Song

## III. RESULTS

The goal for the performance of the query-by-humming system was to have an overall probability of error less than 10%, and to be able to function for male, female, and children users. All performance goals were met, however due to covid-19 we were not able to obtain a proper diverse sample size. The testing was conducted with n=45 samples from 3 adult males, 1 adult female, and 1 female child.

Table 1: Results Breakdown

| **Song Name** | | **Prob. Of Error** |
|---|---|---|
| Happy Birthday | | 9.09% |
| Jingle Bells | | 9.99% |
| Itsy Bitsy Spider | | 12.5% |
| Twinkle Twinkle Little Star | | 0.0% |
| Mary Had a Little Lamb | | 9.09% |
| *Total Prob of Error* | | *8.88%* |

The 5 songs were selected with the intent of picking songs with the most likelihood to be known by the most amount of people. Virtually everyone born and raised in the United States hears each of these songs as a child and knows them by heart.

## IV. CONCLUSION

In this paper we present a real time Query-by-Humming system to illustrate signal processing for prospective students.


## ACKNOWLEDGMENT

The authors would like to thank Dr. Benedito Fonseca and Dr. Mansoor Alam, from the Department of Electrical Engineering at Northern Illinois University, and Sandhya Chapagain for their constant and continuous technical support throughout the development of the Query-by-Humming system.


## REFERENCES


[1] Brian McFee, Vincent Lostanlen, Alexandros Metsai, Matt McVicar, Stefan Balke, Carl Thomé, … Taewoon Kim. (2020, July 22). librosa/librosa: 0.8.0 (Version 0.8.0). Zenodo. http://doi.org/10.5281/zenodo.395522

[2] De Cheveigné, Alain, and Hideki Kawahara. "YIN, a fundamental frequency estimator for speech and music." The Journal of the Acoustical Society of America 111.4 (2002): 1917-1930.J. Clerk Maxwell, A Treatise on Electricity and Magnetism, 3rd ed., vol. 2. Oxford: Clarendon, 1892, pp.68–73.

[3] Stan Salvador, and Philip Chan. "FastDTW: Toward accurate dynamic time warping in linear time and space." Intelligent Data Analysis 11.5 (2007): 561-580.

# Mechanical Forging for the Construction of a Standardized Steelpan Instrument

Josefina Buan
Department of Electrical Engineering
Dekalb, IL, US
z1827198@students.niu.edu

Gabriel Gandara
Department of Mechanical Engineering
Dekalb, IL, US
z1819436@students.niu.edu

Nicholas Grimes
Department of Mechanical Engineering
Dekalb, IL, US
Z1829691@students.niu.edu

**Abstract— The steelpan drum is an instrument native to Trinidad and Tobago, with a history dating back to the early 19th century. The process to create the instrument is long and difficult, taking upwards of two weeks for a trained professional to complete. During this time, the manufacturer is subjected to repeated vibrations along their arm and high noise levels, both of which are dangerous to the manufacturer. The purpose of this project is to discover a method of automation that could reduce the time needed to create a steelpan instrument, along with reducing the potential harm towards the manufacturer of said instrument. The proposed method incorporates incremental sheet forming (ISF) technology to reduce the time required to hammer the initial concave shape of the instrument. This process involves a significant portion of the time required to fashion a steelpan instrument, and as such would be beneficial to the creator.**

## I. Introduction

The steelpan drum is an instrument originating from Trinidad and Tobago in the Caribbean. The creation of a steelpan drum has largely remained unchanged since its invention, involving the deformation of used oil drums to create a concave surface with note indentations. This process is performed with handheld hammers and can cause a great deal of harm to manufacturers over time. The noise level of hammering steel can damage the ears, and the repetition of hammering steel can damage the arms, muscle, and skeletal structure. These harms have forced manufacturers into early retirement, despite the need for trained professionals.

The most prominent improvement to the process is the application of pneumatic hammers, but this does not address the physical harm potential of the process. The existence of a faster, safer process would mean that creating steelpan instruments would no longer be dangerous to the manufacturer. Additionally, this would result in an increased rate of production and a decrease in production cost for the instrument.

## II. Desired Results

The goal of this senior design project was to develop a method of reducing the time required to form a steelpan drum. This would increase the production rate of manufacturers and reduce the danger to the manufacturer. With this in mind, the chosen path was to have a system of incremental sheet forming automate the deforming of a scaled down drum in the form of a steel bucket to fit the design of a steelpan instrument. This would involve the designing of a model to base the deformation path on, the conversion of this model and actions to G-Code, and the use of a CNC machine that could interpret the code into action.

## III. Methodology and Materials

### A. Deformation Programming

Incremental sheet forming is based on the application of G-Code with CNC machine technology to automate manufacturing. Because of this, the creation of G-Code was the most important aspect of this project.

To complete this, the basis of the G-Code was created in SolidWorks 2020 to match a scale model of a typical steelpan instrument. This model was imported to Autodesk FeatureCAM, where a milling operation was created to simulate the results of the model. This operation produced G-Code from which the results could be tested.

### B. CNC Machine

The type of machinery used to conduct the forming of the steelpan was a CNC machine. This machine can read the incremental forming G-code and form the steelpan according to the code using a custom round-tip forming tool.

Since great forces are required to form steel, it is important to secure and support the steelpan firmly to prevent any unintended damage to the pan or machine. The use of a thick lubricant is also critical for the process to reduce the development of heat from the substantial frictional forces between the forming tool and steelpan. By doing this, the life of the tool can be extended and steel hardening on the surface of the drum can be prevented.

### C. Deformation Mold

The use of a mold was considered to help maintain the bucket's position during the deformation process. The mold would be placed beneath the bucket and be fastened to both the bucket and the machine, securing both the mold and bucket in place. While a hard plastic or metal material would have been the ideal material for its resistance to deformation, the hardwood mahogany was chosen due to its relative strength and greater availability.

## IV. RESULTS

### A. G-Code Testing

The production of the G-Code underwent numerous stages, with challenges met at each iteration of the tested code. Starting with a 4”-diameter scale deformation to be tested on sheet metal, the working code successfully shaped the sheet metal exactly as desired. This test and all subsequent tests for the G-Code were performed in the NIU Machine Shop, using the HAAS CNC machine.

The final test using the HAAS machine included the full scale of the steel bucket (9.5” diameter), more accurate note indentations to better reflect real steelpan designs, and a decreased step increment to result in a smoother surface finish. This last step was hindered by the lack of memory in the HAAS machine, requiring the reduction in smoothness for the finishing pass. Despite this, the test worked as predicted, resulting in a half-scale steelpan drum. This was done within three hours of testing.

**Figure 1: 9.5" scale deformation test results**

### B. CNC Machine Production

The designing of the CNC machine was performed in SolidWorks. It was required to have a spindle tool that could be moved in three separate axes and follow commands provided to it through an Arduino uno. Along with this, it needed to support the drum as it was being deformed.

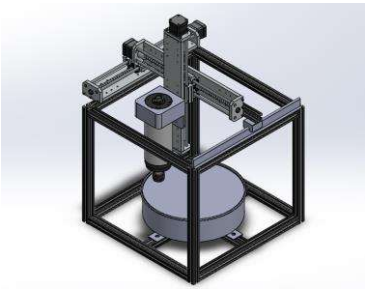

**Figure 2: Designed CNC Structure**

The construction of the CNC machine was a difficult process, ensuring that the materials needed were correct for the design. The frame was constructed, and the linear actuators were successfully attached. Unfortunately, due to time restraints the project could not be completed, and the results of the HAAS machine could not be replicated with the CNC machine.

**Figure 3: Created CNC Machine Structure**

### C. Wood Mold Production

With the design’s approval by Mike Reynolds, once the material arrived it was given to the machine shop to be formed. Because of the testing with the G-Code in the HAAS machine, it was demonstrated that the mold was not necessary to form the drum to the specified design given a strong enough supporting bracket.

**Figure 4: Completed Wood Mold Product**

## V. CONCLUSIONS

The purpose of the project was to have developed a method of shortening the time to construct a steelpan drum from beginning to end. Based on the conclusions of the G-Code experimentation using the HAAS machine, this appears to have succeeded. The process of creating the initial curve and notes for a half-scale model was done in a matter of hours. The half-scale model proves that the concepts of CNC machining and incremental sheet forming can be used to aid in the process of steelpan manufacturing, reducing the amount of time to create an individual drum. This process is also able to greatly reduce the amount of harm manufacturers risk in the process by removing the hammering of steel from the creation of the instrument. To further the tests of this project, the use of a larger CNC machine capable of containing a real oil drum and testing on a fully-sized scale would be the next step.


## ACKNOWLEDGMENT

The team of Mechanical Forging for the Construction of a Standardized Steelpan Instrument would like to thank Dr. Jenng-Tern Gau for advising the project, along with Aayush Patel in assisting the team. Mike Reynolds and Jeremy Peters in the NIU Engineering Building’s Machine Shop also provided immense support and guidance throughout the construction and testing phases of this project.

# *Robotic Human Nose Simulator*

Team 52

J. Panzica, J. Martinez, J. Vonderhaar
College of Engineering and Engineering Technology
Northern Illinois University
DeKalb, IL, USA

***Abstract*— The robotic human nose simulator is a novel device that accurately simulates human breathing patterns. The motivation for the project is to aid researchers by giving accurate models of the dispersal of particles, harmful or harmless, in a detailed human nasal cavity by way of a piston driven breathing system. The piston drives air through a 3D printed cast of the upper respiratory system, taken from a CT scan of a cadaver and split into slides.**

## I. INTRODUCTION

The purpose of creating a robotic nose simulator is to accurately model and simulate airflow through the upper respiratory system, with the ability of detecting and collecting nanoparticles for the purpose of researching their effects on said system. A 3D-printed, accurate-to-human cast of the nasal cavity with accurately simulated airflow could be used in a biohybrid model for assessing air quality, drug delivery research, healthcare/therapy in the otorhinolaryngological field, and a multitude of other practices involving the upper respiratory and nasal region. In harmful environments, such as warzones, factories, mines, and sewers, not much information is known on the health effects the air quality has on persons in the area, so a device that closely mimics a human's respiratory system could help reduce these negative effects.

## II. DESIGN

### *A. Design Overview*

The device uses a model of the human nose, derived from a CT scan, cut into multiple sections, and 3D printed in a clear resin cast. These materials make it possible to emulate an anatomical human nasal system, along with using an air pump to simulate human breathing and air flow. The device also has removeable slides and access points that come out of the model for different uses, such as an insertable flow velocity measurement device, or insertable probes with cultured nasal epithelial cells for accurate portrayals of biological interactions. The device also contains a connection port between the pseudo-pharynx and bottom of the device.

### *B. Components*

The Simulators Design can be broken into 4 main components: the piston, the nasal cast, the nasal probes, and the microcontroller.

The piston is the largest and most important design piece, it consists of a 6-inch inner diameter PVC tube that acts as the pistons body. Within the tube there is a plunger created from a rubber sheet and a plastic backing piece for support. The plunger is connected to a linear actuator which pushes the plunger through the tube to force airflow into the nasal cast.

The nasal cast itself is 8 3D-printed resin slides created from a CT scan that was exported into a set of STL files. The slides are then connected using M5 threaded rods and nuts to create a tight seal.

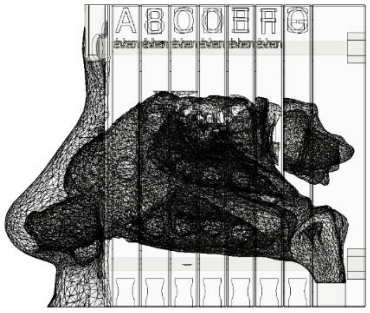


Figure 1. All 8 slides of the cast put together in Solidworks.

The nasal probes are small 3D-printed resin inserts that fit into small holes on the sides of the nasal cast slides. The probes can either be fillers pieces to seal the airflow or they allow for an anemometer to be inserted to measure the airflow, the design allows for multiple uses to cater to a number of situations.

Finally, the microcontroller is an Arduino Uno and a motor controller wired to a breadboard. The Arduino is connected to a laptop for power while allowing for user commands to be input. The component also houses a 12V battery pack to power the linear actuator.

### C. *Operation*

The device is operated by inputting the desired breath speed and length into the laptop and then sending that code to the Arduino. Once activated after that the linear actuator will follow the commands and data can be gathered from any attached probes. To activate the device all that the user needs to do is activate any probes they may be using and to turn on the 12V battery pack and the Arduino will run the actuator as desired.

## III. RESULTS

The device has been tested to ensure that all components were functional, and the device was able to operate reliably. To accomplish this test, the actuator was operated with our control system.

## IV. CONCLUSION

Airborne nanoparticles are present in the daily lives of many persons. Military-relevant scenarios drive the need to analyze and research how possibly harmful these situations are. Nanoparticles released during manufacturing or from explosions pose a great risk to those restricted to those environments [1,2]. Inhaled nanoparticles from these events can congregate in the nasal passageways and potentially cause health issues such as neurotoxicity [3] and pulmonary inflammation [4].

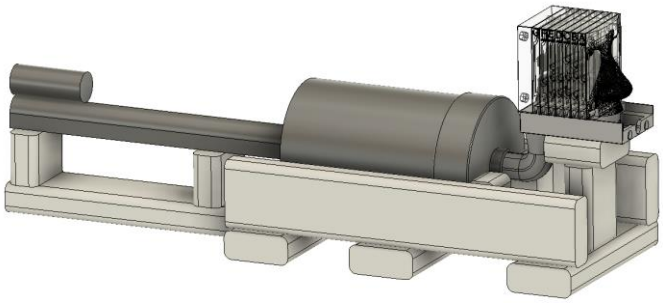

Figure 2. Assembly of the full system.

This device would allow for a simple and cost-effective way to figure out what might be affecting an area and to allow for proper treatment and prevention to take place.


## ACKNOWLEDGMENT

Special thanks to Dr Angela Dixon for her guidance and the initiation of the project, the staff of the NIU Maker Space for their help with initial printing, and Ian Gilmour for printing the nasal cast parts in high quality with his own 3D printer.


## REFERENCES


[1] Brouwer, D. (2010). Exposure to manufactured nanoparticles in different workplaces. Toxicology, 269(2-3), 120-127

[2] Machado, B. I., Suro, R. M., Garza, K. M., & Murr, L. E. (2011). Comparative microstructures and cytotoxicity assays for ballistic aerosols composed of micro-metals and nanometals: respiratory health implications. International journal of nanomedicine, 6, 167.

[3] Win-Shwe, T. T., & Fujimaki, H. (2011). Nanoparticles and neurotoxicity. International journal of molecular sciences, 12(9), 6267-6280.

[4] Roedel, E. Q., Cafasso, D. E., Lee, K. W., & Pierce, L. M. (2012). Pulmonary toxicity after exposure to military-relevant heavy metal tungsten alloy particles. Toxicology and applied pharmacology, 259(1), 74-86.

# Active Noise Control for Automobiles

R. Guzman, E. Mims, M. Mir, and F. Olmedo
Dr. Lichuan Liu
College of Engineering and Engineering Technology
Northern Illinois University
590 Garden Road
DeKalb, IL, USA

***Abstract*—Active noise control (ANC) is used to reduce unwanted sound by producing an "anti-noise" signal that cancels undesired sound, this is based on the principle of destructive interference. This project focuses on creating a cost-effective solution to reduce ambient noise inside a vehicle. The design consists of 4 microphones, an audio interface, mini-pc, amplifier, and the vehicle's existing sound system. The ANC algorithm is run on the mini-pc and designed to cancel low frequencies in the range of 46 Hertz to 1500 Hertz by 5dB to 10dB.**

***Keywords-Active; noise; canceling; audio***

## I. Introduction

There are more drivers today than ever before. More safety measures must be in place to keep everyone safe. Constant ambient noise can cause driver fatigue. About 2.5% of fatal car crashes are a result of a fatigued driver. [2] In addition to reducing fatigue, the system is designed to make the driver more comfortable so that the driver can focus more on driving and less on the unimportant noise around him or her.

## II. Noise Cancelation

Sound travels in waves. During their interactions they can either increase or decrease the volume of the sound, see Figure 1. ANC systems use this property of sound to reduce the level of ambient noise. The algorithm takes the input sound filters it, and then inverts the amplitude. Systems like this are most effective in enclosed spaces where the "anti-noise" sound wave can stay near to the ambient noise source. This technology is used in phones, headphones, and automobiles.

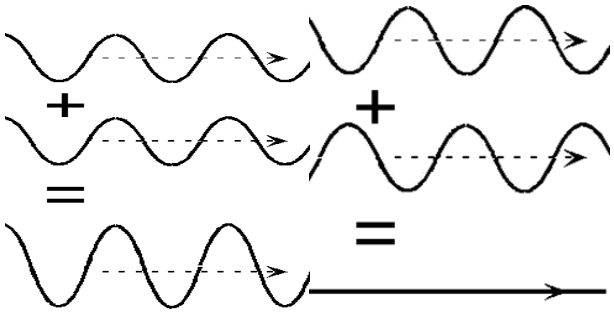

*Figure 1: Constructive (L) and destructive (R) interference [1]*

## III. Component Setup

### A. *Microphone Placement*

The microphones have been placed at the optimum locations to ensure the best sound detection. There are four microphones, two reference and two error mics. The reference mics are placed in the vehicle's footwell under the dash to detect engine and tire noise. The error mics are placed near the driver's and passenger's heads to measure how much of the initial sound is still being heard by the occupants.

### B. *Necessary Connections*

The microphones are connected to a USB audio interface via XLR cables. The audio interface provides phantom power to the condenser mics, and acts as a pre-amplifier for the mic signals. The audio interface is connected to the mini pc via a USB cable. This provides power to the interface and allows for data transfer. The mini pc is connected to a standard vehicle amplifier with a 3.5mm TRS jack and converts the signal to dual RCA ports. The speaker wires coming out the amplifier are wired in parallel with the vehicle's stereo system so that the ANC system can run, or the stereo can play.

### C. *Speaker Placement*

The speaker placement was also considered as to obtain the maximum noise cancellation through uniform sound distribution throughout the vehicle. The team chose to utilize the existing speakers in the vehicle since the automotive manufacturer has placed them fully intending the best sound of encapsulating the occupants.

A diagram of the system can be seen in Figure 2 below.

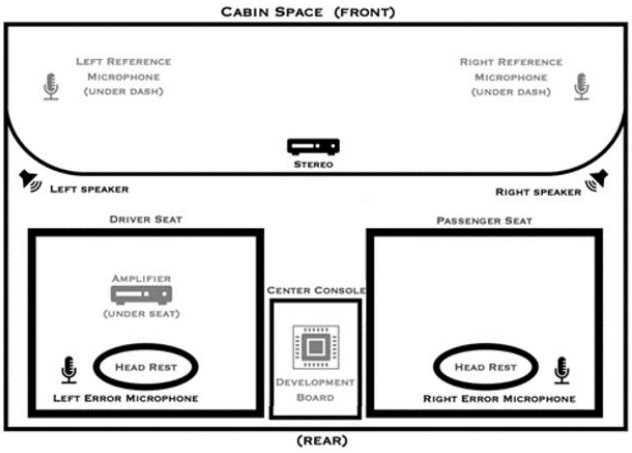


*Figure 2: Diagram of ANC System*

## IV. ANC ALGORITHM

The ANC system operates in two domains, an acoustic domain, and an electrical domain. The acoustic domain represents the cabin space in which the noise propagates through. While the electrical domain represents the electrical path, or the path the signal undergoes in the filtering process. An ANC algorithm can represent both domains in a simple block diagram, as shown in Figure 3 below.

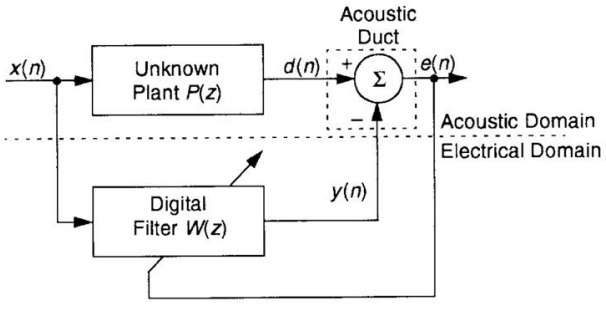


*Figure 3: Block Diagram of ANC System [3]*

Accounting for both domains is essential for functionality of the system and represented in the complete FxLMS algorithm,

## V. CONCLUSION

In conclusion the designed ANC system aims to reduce physical noise with a frequency of 46 Hz to 15000 Hz by 5 dB to 10 dB inside the vehicle cabin. The ANC system is based on a FxLMS algorithm to filter the signal shifted by 180º, the signal is received by two microphones, and send it to the DSP that contains the designed algorithm and is produced by the car's audio system to finally be updated by the microphones near the passengers.

## ACKNOWLEGEMENTS

This work was accomplished with the support and guidance of Dr. Lichuan Liu, Dr. Donald Peterson, and TA German Ibarra. The team would also like to thank NIU's College of Engineering and Engineering Technology for providing funding for the project.

## REFERENCES

[1] *Constructive and Destructive Interference*, www.phys.uconn.edu/~gibson/Notes/Section5_2/Sec5_2.htm.

[2] National Center for Statistics and Analysis. (2017, October). Drowsy Driving 2015 (Crash•Stats Brief Statistical Summary. Report No. DOT HS 812446). Washington, DC: National Highway Traffic Safety Administration.

[3] Kuo S.M., Morgan D. R, (1999, June). Active noise control: a tutorial review, in *Proceedings of the IEEE*, vol. 87, no. 6, pp. 943-973, doi:10.1109/5.763310.

# *Cost Effective Bead Resin Unloding System*

A. Rowe, I. Lopez, M. Rizzo
Department of Mechanical Engineering
Northern Illinois University
Dekalb, IL 6011

***Abstract*— The focus of the resin unloading device was to create a mobile, low maintenance, cost effective and functional system that decreased the risk of accidents. The device decreased the waste experienced during unloading. Considering this, various aspects of the system were designed with the intention to reduce waste and increase the safety of unloading. These features not only helped create a safe work environment, but they added to the ability for the device to be used on various smaller particle flows. These features made the system more versatile for multiple industry applications.**

## INTRODUCTION

The purpose of the bead resin unloading, and transportation device is to cut costs while also improving the safety and efficiency of work. The proposed device would allow for an opportunity to eliminate the need for manual transportation while also increasing the safety of unloading and transportation. The goal of the project is to find a safe, cost effective way to unload resin beads while also meeting industry standards for flow rate.

The project idea stems from an experience a group member encountered while visiting a factory. Here the manager explained the current system. The current system takes full shipping containers, lifts them via forklift where they are then dumped into a reactor. The containers dumping hole size is not much larger than that of the reactor entrance, however without the use of a contained funneling system contamination and waste are encountered. Contamination is defined by any contact with a foreign surface. Here a foreign surface is any surface that is not enclosed or sanitized. Contaminated particles are then considered waste and have to be scrapped.

Current products on the market only address the transportation of particles without addressing the need for a safer more efficient unloading. Typical belt conveying systems are used in many particle transportation systems. However, many of the current systems are built for large scale operations where the cost of these products run high. This is due to the higher cost in tension rollers and conveyer belt costs. Creating a system for a smaller scale operation allows for a more cost-effective solution to be utilized in smaller manufacturing settings. A smaller more efficient unloader would make smaller businesses able to afford a new, more effective unloading system.

This new resin unloading system also reduces the amount of floor space used. The unloader is mounted onto 5 casters. Each caster provides reinforcement to the system while also providing mobility. The system takes up roughly four square feet of floor space. This allows smaller companies to roll the system out onto the floor, use the device, then roll it back and away in storage.

## MECHANCICAL DESIGN

### *Material*

The primary goals of the newer resin unloading system was to provide a more efficient, mobile device capable of moving resin up a 5-foot incline. To fulfill the goal of a more efficient device the resin needed to be constricted down to a smaller transportation method. To accomplish this 3-inch schedule 40 PVC was used. The PVC reduces the area for the resin particles to escape when they enter the reactor.

To create a mobile and structurally sound device, casters were mounted to the steel base frame. The steel allows the device to support upwards of 550 pounds while also providing a strong anchor point for the casters to be attached. The casters provide points of contact at each corner, while also providing a point of contact in the center of the design.

### *Blower*

The system runs and relies on the AC Infinity inline blower to transport the resin from the hopper to the reactor.

*Figure 1: AC Infinity Inline Blower [1]*

The blower is attached to the edge of the base frame and is then reduced to meet the PVC where resin is dropped into the flow stream. The blower is capable of producing up to 800 cubic feet per minute of air through the system. However, the blower can reduce the amount of air pushed through the system by adjusting the speed on the handheld controller. Reducing the amount of air through the system creates a better, less turbulent flow stream. However the amount of resin reaching the reactor per unit time is reduced dramatically.

*Frame/Hopper*

The frame is comprised of 1 inch by 1 inch 1/8th inch thick steel tubing. The steel provides a sturdy foundation that is capable of supporting a fully loaded system. Steel also provides a robust and durable design. A lighter option such as aluminum would be more susceptible to impact damage that could be encountered in a manufacturing environment.

The frame design was created with strength at the forefront. The frame was constructed by welding the steel tubing into a square section then welding in a center cross member that spans the length to the square frame. Then, angled supports were welded as seen in Fig. 2.

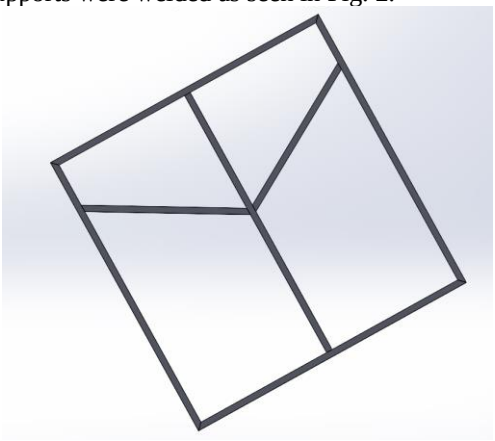

*Figure 2: Steel Base Frame with Angled Supports*

The angled supports not only provide a relief for the stress developed, but they also allow for the barrel stand to be attached. The barrel stand has 3 supporting legs that are spread equidistant around the hopper. These legs are then centered and welded on each support member as seen in Fig. 3.

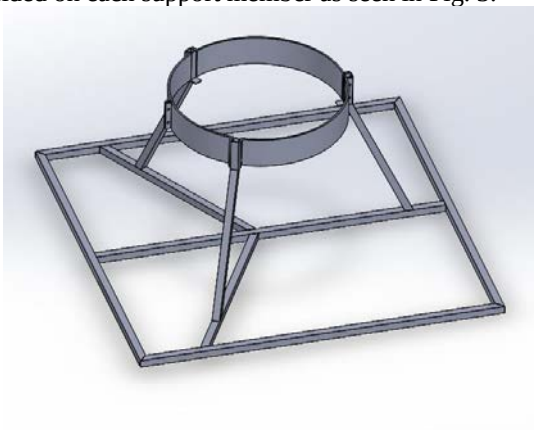

*Figure 3: Barrel Stand Mounted on Frame*

The hopper then rests on the barrel stand where it is secured by tightening the band around the barrel.

## FLOW ANALYSIS

*Blowback*

The design constructed initially had a few drawbacks, specifically blowback into the hopper. When the resin levels in the hopper were low, approximately the last 5%, the resin was being pushed back up into the hopper. This prevented the resin from flowing down into the flow stream and up to the reactor.

Preventing blowback was tested in many different ways. One way was to reduce the volume flow rate as the resin got to lower levels. This reduced the blowback but prevented all the resin from climbing up to the exit. Another method was to add a longer radius WYE fitting. This would provide a near parallel entrance of the resin into the flow stream. However, under certain applications the resin would create a clog since it is meeting the flow with nearly no velocity.

*Pressure*

After flow analysis was conducted, it was concluded that not only turbulent flow was causing blowback but also pressure. It was concluded that the higher-pressure inlet at the blower created an issue with the flow. The resin is added midway through the horizontal run. Here the higher-pressure flow seeks out a lower pressure exit. Since the resin entrance is encountered first and the pressure at the entrance is at atmospheric pressure, the flow attempts to push back into the hopper thus creating blowback.

Addressing this issue was quite simple. The hopper being used is a 55-gallon drum. A lid was attached to the top of the drum. When the system is starting up, blowback is still being created. However, after running for a short period a small pressure is built up in the hopper. This dramatically, reduces the blowback and the system runs more efficiently.

## CONCLUSION

The resin unloading system decreases the amount of waste produced, provides a more mobile option, and increases the safety provided the device is used correctly. This compact design will allow resin to be transported from shipping containers into the reactor more efficiently and at a lower cost than comparable designs currently used in the industry. The mobile design will allow smaller facilities to utilize the device. The design also provided the option for the system to be moved out of the way by simply unlocking the casters and pushing the system by the supports. Overall, the device has decreased the waste produced thus increasing profit margins for the user.

## ACKNOWLEDGMENT

The authors would like to give a special acknowledgement to Dr. Bobby Sinko and Sonali Rawat for their support and guidance throughout this project. The authors would also like to acknowledge the Northern Illinois University College of Engineering program for providing funding for the project.

## REFERENCES

[1] HVAC Ventilation, CLOUDLINE T8, Quiet Inline Duct Fan System with Control, Accessed April 8th , 2021. https://www.acinfinity.com/hvac-home-ventilation/inline-duct-fan-systems/cloudline-t8-quiet-inline-duct-fan-system-with-temperature-and-humidity-controller-8-inch/?gclid=CjwKCAjw07qDBhBxEiwA6pPbHoNSgHp_BVytWLoZf1aDl8kPO4Ox1oSzSZDrwZZOFyD4ImQaKwmqUxoCJWsQAvD_BwE

# Micro-Impacts Deriving from Improper Walking

## *Brain Impact Sensor*

## NIU Engineering Design: Sponsored by Pizur Financials

*James Carratt*
Major: Biomedical Engineering
Minor: Applied Mathematical Sciences
Northern Illinois University
Dekalb Illinois, United States
z1859424@students.niu.edu

*Mackenzie Little*
Major: Mechanical Engineering
Northern Illinois University
Dekalb Illinois, United States
z1810510@students.niu.edu

***Abstract* — The *Brain Impact Sensor* is to be advertised as a medical accessory device that individuals can purchase and use anywhere. The device is to track the impacts every instant the user's heel strikes the ground. By installing the appropriate components into a 'baseball style hat', the device will now be located in the most fit location to track micro-concussions that are detrimental to brain cells and causing long term health effects such as Alzheimer's and Insomnia. The *Brain Impact Sensor* applicational purpose is to aware the user's improper walking patterns in order to prevent future health complications by displaying their data via graphs and numerical data.**

### I. Introduction *(Purpose)*

The project was purposed by an individual named Thomas Pizur who had spent several time studying specific fighting stances and techniques. He came became aware that certain stances transfer energy currents directly through the body depending on how much force the target matter is contacted with, and also the angle at which the force was dealt at. These two factors could knock an individual onto the ground at the moment the move is executed.

Researchers have been noticing an increase in Alzheimer (along similar diagnosis related to these symptoms) cases over the past several years and been relating the causation from micro-concussion. Originally, sports were the main focus due to the amount of hits being taken in per game, but the amount of force that can be constantly impacting the brain even more has been improper walking patterns. With the past recent studies being discovered regarding spinal alignment issues or other lower back incidents, brain damage cases are increasing and micro sized impact forces are becoming a contributing factor.

### II. Objective

The objective of the designed prototype is to create a device that can record every instant the user takes a step and represent their data visually to inform to them if they are currently obtaining micro sized force impacts. The data being obtained will be visually accessible through smart phone applications that show the user's real time impacts in a graphical form or quantifiably. Through their results, the individual will know to alter their walking patterns in order to reduce the amount of force being traveling up to the brain.

In order to best derive data by the user while he/she is walking to determine if their walking patterns are detrimental, the equipment needed would be best to fit inside something an individual can place on their head, such as hat, headband, i.e.. The best solution determined was to utilized the shape of the baseball cap for two specific reasons.

To graphically obtain the most accurate data, fundamentally their should be a sensor located at the highest point, this being the crown of the skull. Another feature that lead the baseball cap selection was its opening on the rear side for adjustable purposes. This space will not only be wide enough to fit the necessary components required to measure the data, but also allows the required pieces to be concealed enough so it isn't recognizable by simple bystanders walking past.

With the baseball hat being the best option to install the equipment finally concluded, further research needed to be conducted in order to first obtain this degree of data (i.e. which kind of sensors are capability of measuring micro-concussions). The sensors also needed to be small enough to fit in the amount of space that is now established.

### III. Experiments (Installation)

#### *A. Electrical Components (Materials)*

The amount of components that actually need to be purchased to first start calculating micro sized force impacts are a total of five items:

- Adafruit LIS3DH Triple-Axis Accelerometer
- Arduino mini-PRO Atmega 328P Microcontroller
- Arduino HC-05 Bluetooth Module
- 3.7 V Lithium Ion Battery
- Lithium Ion Battery Charger

These parts are located in two different locations inside the hat which are necessary in order to receive the most accurate data. All of the main component housing is located in Fig. 1, while the accelerometer will get its own housing as

seen in Fig. 2. Fig. 3 shows the lid that can be detached to access the electrical components. The accelerometer is housed at the crown of the skull so the axis are in the up right position and at the highest point of the individual. The four remaining parts are looped all inside the main housing above the adjustable size strap in all universal hats.

The housing has all been printed using a 3-D printer which was accessible any moment necessary. Throughout the process of re-ordering correct parts, the printing solution has lead to many benefits. If the dimensions were even off by a centimeter, the according changes could be made within a several hours, decreasing the third party use of Northern Illinois University's 3-D printer.

### B. *Equipment Testing (Program{s})*

The program running the experiments in order to send the proper instructions to the certain pins for signal receiving/dispatching was Arduino. Their free online downloadable program allowed for the code to be inputed so that when the circuit is functioning, the signals are being appropriately dispatched to the following pins and thus, receiving a visual output in the form of graphs or numerical charts that are derived from the accelerometer.

The experiments that were required were different walking patterns in order to determine if the data were to be accurate and the graphs were adjusting according to the force of the different impacts. The following tests were normal walking and hard impact walking.

## IV. Results (Functioning Prototype)

Through installing the necessary sensors into the hat, the device was now able to track daily impacts arising onto the user from daily walking. The micro concussions are representing energy transferring to the brain which have been linked to chronic illnesses which is why this product is to be marketed as a medical device to prevent similar diagnosis. Fig.4 visually represents the prototype functioning as an accessible feature and medical tracking device.

### A. *Figures*

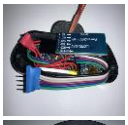

Figure 1: Main Housing (open)

Figure 2: Accelerometer Housing

Figure 3: Main Housing (closed)

Figure 4: Brain Impact Sensor (Prototype)

### B. *Troubleshooting (Future Development)*

The brain impact sensor is functioning fully within the housing that was 3-D printed into an accessible hat, finishing the fundamental features for the project were not able to reach its fullest potential. At the moment, in order to visualize the incoming impact forces either graph or numerical forms of data, the user must connect to a third party application. The realistic goal is to have its own app on the application store for all platforms (IOS, Android, i.e.) which displays all of their records visually appealing to the eye. Unfortunately, none of the following developers are focusing on computer engineering.

Acknowledgment

The following project is something that we see helping a lot of individuals with specific health conditions related to micro-concussions. The project was first sponsored and brought to us and without ever have meeting this individual, our knowledge about this sort of thing was very limited. Everyone from Team 55 are extending are deepest gratitude for Tom Pizur (sponsor) through discovering and teaching us the idea of energy movement from simply walking everyday, into concussions based from our every step. The team would also like to thank Northern Illinois University and Dr. Donald Peterson for without the two, projects elaborated such as this would not have been possible to design. The last two individuals we would like to thank would be German Ibarra and Dr. Venumadhav Korampally for not only their wisdom and knowledge about out entire process, but because they wanted us to succeed more then anything. They even implemented daily updates on the project's status via emails because they were beginning to see our potential being wasted. Through the optimist gestures and tips throughout the entirety of designing, we would like to give them a special thank you.

## References

[1] He, D., Winokur, E., & Sodini, C. (2012). An ear-worn continuous ballistocardiogram (BCG) sensor for cardiovascular monitoring. Retrieved October 24, 2020, from https://www.ncbi.nlm.nih.gov/pmc/articles/PMC4384813/

[2] Wiens, A., Johnson, A., & Inan, O. (2017, March 1). Wearable Sensing of Cardiac Timing Intervals from Cardiogenic Limb Vibration Signals. Retrieved November 05, 2020,from https://www.ncbi.nlm.nih.gov/pmc/articles/PMC5667313/Source: https://www.circuitstoday.com/arduino-nano-tutorialpinout-schematics

# Precise Temperature Control of a Laser Room at the Argonne Wakefield Accelerator

M. McNames, K. Parrish, C. Ibarra
College of Engineering and Engineering Technology
Northern Illinois University, Dekalb, IL, USA

***Abstract*—At the Argonne Wakefield Accelerator (AWA) at Argonne National Laboratory, the main laser that is used in the laser room is delicate when it comes to the operating temperature inside the laser room. The current heating, ventilation, and air conditioning (HVAC) unit that is installed is not efficient enough to have the room temperature controlled in the desired operating temperature. This project aims to create a system that will observe and record the temperature changes in the room at all times, with or without operation of the laser. The system will have 5 wireless thermocouple configurations consisting of: an Arduino MKR WIFI 1010, a SHT-25 temperature and humidity sensor, and a 3.7V, 2.2 Ah Li-Po battery. These will be placed in various locations around the laser room while communicating to a Raspberry Pi 4 that will be logging the data within an online database to be analyzed later. Along with the actual design of the thermocouples, an airflow simulation will be made within ANSYS Fluent to show the current airflow efficiency that is being produced by the current heating and cooling system. From the result of the system and the simulations, a solution to the current HVAC system will be recommended to the researchers at Argonne.**

## I. Introduction

The researchers from the AWA at Argonne National Laboratory[1] are in pursuit of a precise temperature control system that should be able to stabilize the temperature within the laser room at the facility. The temperature of the laser room needs to be controlled at a temperature of 70 (°F) with a stability of +/- 0.5 (°F). This is the optimal temperature to be able to use the laser without interference or failure of usage. The laser room at Argonne was recorded with the following dimensions in SI: 7.3m x 4.2m x 2.5m (L x W x H). The current HVAC unit that is operating in the laser room, a Carrier 38TRA036330, is not efficient enough to supply the necessary airflow to the different parts of the room. This HVAC unit has a fixed speed compressor which is set at a desired temperature and once that temperature is achieved, the HVAC unit shuts off until the temperature drops. This results in a temperature change gradient that is too large for the laser to run accurately. The laser room is in need of a new compressor to be installed into the current HVAC unit or to replace the existing HVAC unit altogether.

## II. Objective

The goal of this project is to be able to create a series of thermocouples to analyze the areas of the laser room that are contributing to the temperature change. The setup needs to consist of the thermocouples to be wireless so there won't be any restrictions when it comes to placing the thermocouples around the room. To be able to achieve this controlled temperature, the researchers need to know all of the factors that contribute to the change in temperature which includes: thermal noise from different pieces of equipment in the room, poor airflow and efficiency from the current HVAC unit, and poor insulation of the room. Figure 1 shows the laser phase monitor (LPM) temperature and the laser phase that was recorded previously by the researchers at Argonne. This shows the effect the different factors are having on the function of the laser.

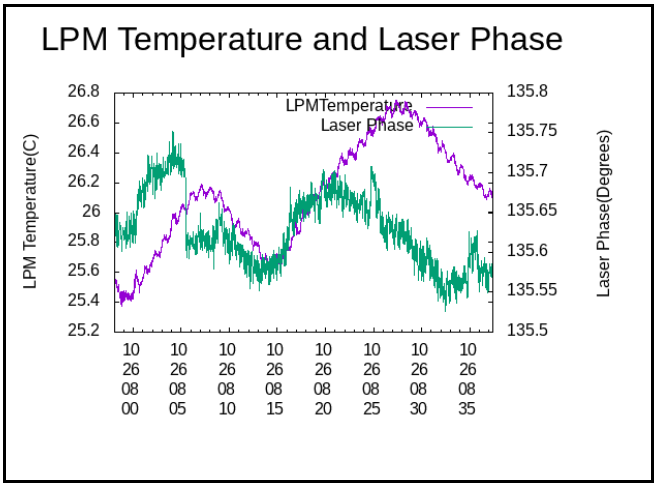


Fig. 1. LPM Temperature and Laser Phase of AWA Laser

The thermocouples will be able to collect the temperature data of the laser room and store it into a database to be referenced later to analyze these factors and where in the room these temperature changes occur. Along with creating a series of wireless thermocouples, the researchers at Argonne are also in need to analyze the airflow of the current HVAC unit through thermal simulation with the use of the program, ANSYS Fluent[2]. With the help of this simulation, the researchers will be able to see where exactly the airflow of the HVAC reaches. Along with these simulations, the researchers at Argonne are in need of a recommendation for a new compressor for the HVAC unit or a completely new HVAC system.

## III. System Setup

### A. Thermocouple Configuration

For the temperature data collection, the temperature that is being measured must be an accurate measurement. The

sensor that is being used to collect this data is a SHT-25 Humidity and Temperature Sensor. This sensor is able to sense the temperature of the laser room with an accuracy of +/- .36 (°F). The SHT-25 is also able to sense the humidity of the room as well that may be analyzed to see if the humidity affects the functionality of the laser. Once this data is collected, the data is transported physically through an I2C connection to an Arduino MKR WIFI 1010. This board is appropriate to be used from its low cost, Wi-Fi compatibility, and battery charging capabilities. This board is able to be hooked up to a 5V USB source and while this is connected, can charge a 3.7V battery while the device is operating. Once disconnected from the USB source, the board will continuously be importing and exporting the data from the SHT-25. The code that will be flashed onto the Arduino MKR will command the board to communicate to the SHT-25 to receive the temperature and humidity and prepare to send it wirelessly to a message queuing telemetry transport (MQTT) broker. The code will also command the board to send the voltage of the battery so the operator of the device may see the battery percentage. This will indicate when the device needs to be connected to the USB and charge the battery. There will be a total of 5 of these sensor configurations setup around the laser room and will be contained in specialized 3D printed housing units. A basic setup of the configuration can be seen in Figure 2 below and the final configuration next to it.

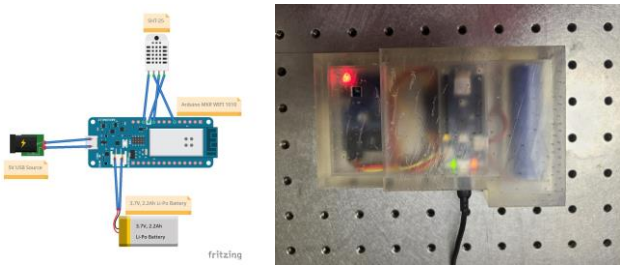


*Fig. 2. Wireless Thermocouple Schematic, Final Wireless Thermocouple Configuration*

### *B. MQTT Broker*

The microcomputer that will be used as the MQTT broker will be the Raspberry Pi 4. This is a necessary option due to its low cost and ability to have the multiple Arduino MKRs connect wirelessly to it. The Raspberry Pi 4 can be connected anywhere at the Argonne facility and will be connected to the Argonne network. Once connected, the Raspberry Pi will run Node-RED[3], a program that is able to connect wirelessly to the Arduino MKR and will display the data in graphs and gauges. Along with Node-RED, the data will be sent to InfluxDB[4] and Grafana where the data can be stored for long term use and have a more compact way of viewing the incoming data. While the Raspberry Pi is connected to the Argonne network, faculty members are able to access the data from anywhere through the Argonne virtual private network (VPN).

## IV. SIMULATION

The airflow simulation of the laser room was done through the program use of ANSYS Fluent. This simulation shows the quality and effectiveness of the airflow that is emerging from the current HVAC system. The results of this gives more insight on how efficiently the current HVAC system is decreasing the gradient in temperature change in the room. After there is additional analysis of the temperature data, the results may be incorporated into the simulations for further understanding of the airflow in the laser room. In Figure 3 below, an airflow simulation may be observed.

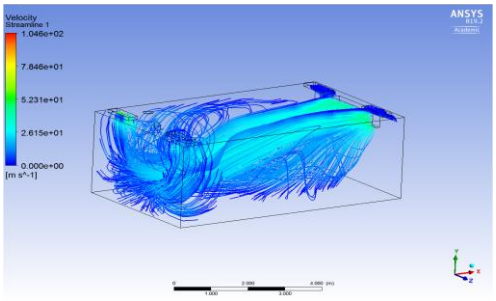


Fig. 3. ANSYS Airflow Simulation

## V. CONCLUSION

This wireless thermocouple setup will be able to monitor the temperature changes in the Argonne laser room that will be analyzed in future use. This design is to help the researchers at Argonne understand the current factors that are interfering with the accurate data collection of the laser as well as defining where these factors are occurring the most in the laser room. After an elongated period of time for the temperature data to be collected, the researchers at Argonne may interpret the extent of the simulation and data collection into a decision of either replacing the HVAC system as a whole for a new and more efficient system or implementing a variable drive into the current unit to control the compressor operation.

## ACKNOWLEDGMENT

The authors would like to acknowledge the support and guidance from Dr. Stanislav Baturin and Amin Roostaee-Northern Illinois University, Dr. Philippe Piot and Wanming Liu-Argonne National Laboratory.

## REFERENCES

[1] Argonne Wakefield Accelerator Facility, Argonne National Laboratory, https://www.anl.gov/awa

[2] ANSYS Fluent Simulation Software, ANSYS, https://www.ansys.com/products/fluids/ansys-fluent

[3] Node-RED, JS Foundation, https://nodered.org/

[4] InfluxDB, InfluxData, https://www.influxdata.com/

[4] Grafana, Grafana Labs, https://grafana.com/

# SecuriBot: Autonomous Security Robot

*Jerrel Grays*
Dept. Of Electrical Engineering
Northern Illinois University
DeKalb, Illinois
z1772036@students.niu.edu

*Daniel Ingalsbe*
Department of Electrical Engineering
Northern Illinois University
DeKalb, Illinois
z1852172@students.niu.edu

***Abstract: This is the second iteration of the SecuriBot project at Northern Illinois University's College of Engineering and Engineering Technology. The goal of the SecuriBot project is to develop a reasonably priced autonomous system for monitoring a number of safety, security, and environmental related conditions in an indoor setting. This design for SecuriBot has focused on using well documented components together with software in order to ensure that troubleshooting and future development can both go smoothly.***

## I. INTRODUCTION

Many of the active security systems available on the market today are designed for commercial or government use. The existing solutions for home security are static and primarily focus on passive monitoring.

The SecuriBot robot is designed to be able to monitor an indoor space for changes in temperature, humidity, and barometric pressure. SecuriBot is also capable of detecting motion within the area that it patrols. Any detection of irregular environmental conditions or motion while on patrol can then be sent via email to a specified individual so that the situation can be rectified immediately.

## II. MECHANICAL DESIGN

The primary component responsible for SecuriBot's mobility is the Create 2 robotics platform manufactured by iRobot based on their popular Roomba robotic vacuum. The Create 2 includes a large number of sensors onboard which can be used to provide a large amount of information to the rest of the system. The Create 2 also comes with a charging dock which includes IR signaling to enable automated docking of the robot for autonomous charging.

*Figure 1: The Create 2 by iRobot*

The electrical components of SecuriBot are housed on a 3-D printed platform which provides a place to mount the motion sensors as well as the camera. The platform is attached to the top plate of the Create 2 using #6-32 machine screws and locking nuts to ensure that they do not back off during the small vibrations caused by movement.

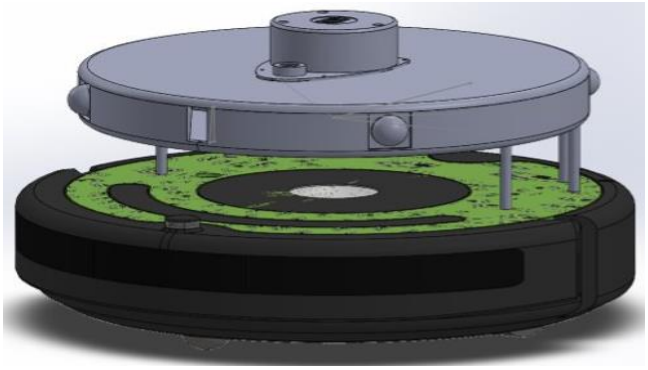

*Figure 2: SecuriBot designed in Solidwork*

## III. ELECTRICAL DESIGN

### *A. Power Delivery*

The power supply for SecuriBot is drawn from the onboard battery of the Create 2. The Mini-DIN connector on the top of the Create 2 is capable of supplying 200 milliAmperes of 12 Volt power, this power is routed through a 5V regulator to power an Arduino Mega.

The Raspberry Pi and USB hub have their power provided by the main brush drive circuitry on the Create 2. This power system is designed to power an inductive load like a motor directly, so it was necessary to add a fixed inductor into the circuit to ensure smooth and reliable power delivery. The main brush drive power is supplied to a Buck converter capable of supplying up to 20 watts.

### B. *Communication*

The Arduino Mega acts as a communication handler between the Raspberry Pi and the Create 2, as well as controlling the docking and undocking procedures which are conducted with the Raspberry Pi powered off. The processing components communicate via the UART (Universal Asynchronous Reciever-Transmitter) protocol at high speed to minimize any potential bottlenecks caused by communication between the modules.

User input is only required to setup the system and is conducted primarily through a controller connected to the Raspberry Pi through the USB hub.

### C. *Sensors*

The motion detection system relies on four motion sensors connected to the Arduino to provide 360° coverage of the area around the robot. The overlapping fields of view help to increase the directional accuracy of detected events in order to correctly orient the system so that an image can be captured of the object in motion.

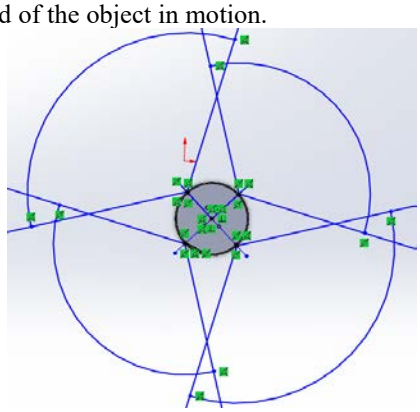

Figure 3: The overlapping sectors covered by the motion detectors at a distance of one mete

Using signals and the atmospheric pressure we can properly and accurately detect the change of atmospheric pressure thanks to the pressure sensor, and it gives us the current pressure at its given time.

The temperature Sensor gives out the current temperature at that time, but it also gives alerts when the temperature has changed. It measures the temperature of its environment and converts the input data into electronic data to record, monitor, or signal temperature changes.

The hazardous gas sensor is one of the most important sensors allows for the detection of dangerous gases with the same concept as the other sensors which are signals. The sensor identifies gases by measuring the current discharge in the device.

## IV. Software Design

### A. *Arduino*

The software flashed onto the Arduino Mega has been designed to loop rapidly through a single function to ensure fast response to any input from the Raspberry Pi. Multiple signal wires, in addition to the serial lines, are connected from the general purpose Input/Output lines of the Raspberry Pi to the digital pins of the Mega to enable the logic running on the Arduino to quickly differentiate between different control conditions.

Using the documentation supplied by iRobot, a number of functions are implemented in C to handle the communication with the Create 2 to control the motion of the platform and query the numerous onboard sensors to ensure safe operating conditions and prevent the battery from running to low and causing damage.

### B. *Raspberry Pi*

The Raspberry Pi Zero W was selected for this project to control the main logic because of its low power requirements, as well as its fast processing, and built in support for the PYTHON programming language.

The Pi handles the higher level functions and data processing that would be difficult and time consuming to implement on an Arduino.

The libraries available in PYTHON are used to simplify many aspects of the programming. The GPIOzero library was used to control the GPIO pins of the Pi for signaling the Arduino. The PiCamera library enables direct interaction with the camera attached to the Pi through the onboard camera connector.

## V. Conclusion

The current version of SecuriBot is able to monitor the environment, and send e-mails with alert messages. It can also patrol a course, that is setup with user input, and scan for motion at designated points along that path. If motion is detected, SecuriBot can capture an image in the direction of the motion and then e-mail it to the designated individual.

SecuriBot can also dock and undock with the charging station to ensure battery safety and continued operation without user input.

The original design of SecuriBot included a 360° LIDAR rangefinder, which would have allowed for better localization along the path as well as obstacle detection. Due to logistical issues and the global health crisis, there was less time for troubleshooting than would have been ideal.

## Acknowledgment

The SecuriBot Team would like to thank Dr. Peterson and Ian Gilmour for their help and understanding during the process of design and prototyping.

# *Split-Hopkinson Pressure Bar Apparatus*
Team 58

*Joie M. Vittetow, Joshua Clark, Lee Bowen, Jenn-Terng Gau Ph. D.*
College of Engineering and Engineering Technology
Northern Illinois University
Dekalb, USA

***Abstract*—The goal of this project is to solve the Split-Hopkinson Apparatus Device issue of the incident bar projecting multiple hits in a system where it is to receive only one hit. There are multiple factors that contribute to causing this issue, which lead to many designs for different parts of the device implicated into the project. For the project, there were five different designs made for multiple parts of the Split-Hopkinson Apparatus Device. The designs include redesigning a high pressure air tank and it's operational features, a gun barrel along with its mount, and an enclosure for safety and sample catching.**

## I. Introduction

A Split-Hopkinson Pressure Bar apparatus is a device used to dynamically test material properties for constructing constitutive models and can be used for high strain rate deformation research and experiments. It can be used to help determine material constants such as Young's modulus and mechanical stress in dynamic conditions. The main components include a high pressure air supply (compressor), a pressure chamber/air tank, a bun barrel, a striker bar (projectile), and input/incident bar, the specimen sample, an output/transmission bar, and a stopper. The only parts that should be moving during operation are the striker, which travels down the gun barrel, creating an impact on the specimen. After a sufficient amount of air is collected, the backside portion of the pressure chamber releases some pressure causing a pressure drop which pulls the plug from between the pressure chamber and the gun barrel causing pressurized nitrogen through the gun barrel, forcing the striker into the incident bar creating an elastic wave pulse which goes through the specimen and out the output bar. In order to calculate the forces that will be exerted on the material there are strain gauges installed in precise locations to determine the strain caused by the elastic wave pulse.

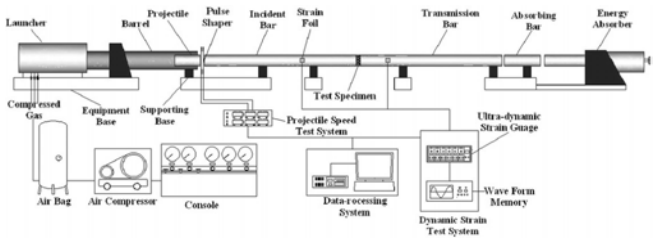


Figure 1. Split-Hopkinson Apparatus Device Schematic. Reprinted from "Assessment of impact mechanical behaviors of rock-like materials heated at 1,000°C," by S Liu, J Xu, X Fang, 2020, High Temperature Materials and Processes, Volume 39 Issue 1. Retrieved from https://www.degruyter.com/view/journals/htmp/39/1/article-p489.xml. Copyright 2020 Walter de Gruyter GmbH.

The Split-Hopkinson apparatus has been continuously worked on for improvements since its original design from 2015. The focus of this project will be on the striker launching module. Once the pressure from the tank is released for the striker's first impact, the pressurized air continues to come out of the tank causing a repeated impacting motion that causes false data points to be collected. The approach is to make the air tank smaller to prevent excessive air within the tank itself. The current gun barrel used in the SHPB apparatus is made with a 4340 high strength seamless tube that has an inner diameter tolerance of ± 0.008 inches. The current air tank was made with a 1022 hot-rolled seamless steel pipe. Figure 2 shows the specific dimensions of the current pressure tank set-up at Northern Illinois University.

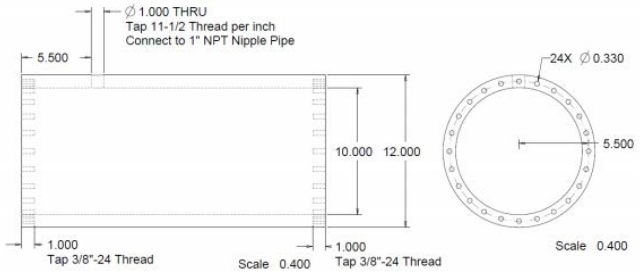


Figure 2. Dimensions of Air Tank. Reprinted from "Stress Analyses on the Gas Pressure Tank for NIU Split Hopkinson" by J. Gau, 2017, p.1.

## II. Materials and Methods

Solenoid valves are a binary valve that can either be open or closed. With a solenoid valve system, the current piston tank can be removed and replaced with a simplified pressure tank that has a solenoid valve controlling the airflow to the gun barrel. The current tank with ports on the exterior which can be used to hold attachments. Such as pressure sensors or a pressure release valve and a port on the back which will be used to fill the tank and finally the port on the fron which is where the solenoid valve will be attached, connecting the tank with the gun barrel, and control the release of pressure during operations. Figure 3 is a generic solenoid valve used in the system. Minimum assembly will be required and since the main requirement

for the air tank will be a 300 max operating pressure, most safety testing on the tank will be done by the manufacturers.

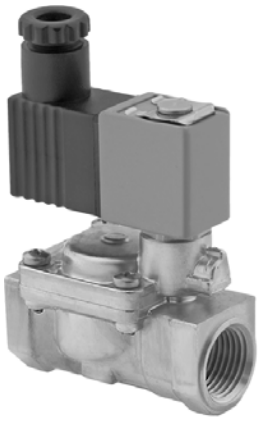

Figure 3. Solenoid Valve. Reprinted from "Brass Body Solenoid On/Off Valve" by McMaster-Carr. Retrieved from https://www.mcmaster.com/4738K158/. Copyright 2017 McMaster-Carr Supply Company.

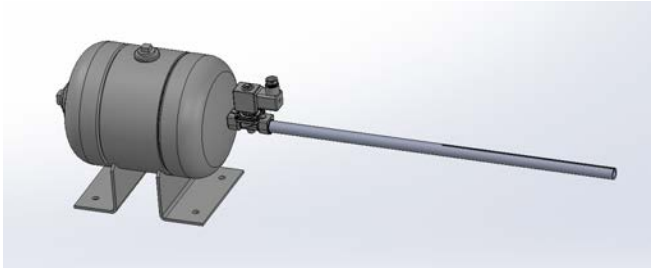

Figure 4. CAD Model of Device. Obtained from "Horizontal ASME-Code Compressed Air Storage Tank" by McMaster-Carr. Retrieved from https://www.mcmaster.com/1481K12/. Copyright 2015 McMaster-Carr Supply Company and "Brass Body Solenoid On/Off Valve" by McMaster-Carr. Retrieved from https://www.mcmaster.com/4738K158/. Copyright 2017 McMaster-Carr Supply Company

## III. Results and Discussions

The updates to the Split-Hopkinson apparatus the device will see the data collected in the experiments to have a higher accuracy in the measurements. This is a direct result of fixing the prior problems in the device that were coming from outdated parts that have been updated on the device. Also will have an easier use of the system with the enclosure as the specimen that is being tested will be collected inside of the enclosure which will also reduce any data collection error. With these improvements NIU Engineering students now have the ability to test and acquire the dynamic response of materials at high strain rates.

## IV. Conclusion

The Split-Hopkinson Pressure Bar apparatus is a highly sophisticated and advanced material sampling equipment for compressive and tensile testing. The launching module is divided into three main portions; the pressure tank, the pressure release, and the gun barrel. Each portion requires a redesign and replacement. The focus for the pressure tank is to properly mount into position and condense the size as only 300 max psi is required. The pressure release is to control the release of pressure from a safe distance at a high flow rate to reach the 100 m/s required velocity, and the focus for the gun barrel is to prevent corrosion in the bore and to have the correct so that the striker properly fits the inside diameter. The launching module in the Split-Hopkinson apparatus is the most dangerous aspect of the apparatus and is the portion that needs improvements. Currently, false data is taken from secondary strikes on the incident bar directly caused by the launching apparatus. The pressure tank plays a very big role in the system and also could take a big chunk of the budget to replace. Figuring out what is going to be done to the pressure tank needs to be thought out rigorously.


## Acknowledgment

Acknowledgement to the client and faulty advisor, Dr. Jenn-Terrg Gau, for all the help and information he has given and the extra funding he had provided for the project. Dr. Jenn-Terrg Gau has been very helpful in regards to any questions that have been asked during the process. Acknowledgement to Northern Illinois University for providing funding on the project as well.The team would like to say thanks to the TA, Aayush Patel, for guiding and answering any questions in a timely manner.


## References


[1] Gau, J. (2017, October 31). Stress Analyses on the Gas Pressure Tank for NIU Split Hopkinson Bars. (pp. 1-14, Rep.).

[2] HBM. (2020, January 03). Split-Hopkinson Bar Material Tests. Retrieved October 02, 2020, from https://www.hbm.com/en/2996/split-hopkinson-bar-material-tests/

[3] Liu, S., Xu, J., & Fang, X. (2020). Assessment of Impact Mechanical Behaviors of Rock-Like Materials Heated at 1000°C. High Temperature Materials and Process 2020, 489-500.

[4] McMaster Carr (2020). Retrieved from http://www.mcmaster.com.

[5] REL, Inc. (2019). Split Hopkinson Pressure Bar / Kolsky Bar. Retrieved October 13, 2020, from https://www.relinc.com/split-hopkinson-bar-kolsky-bars/split-hopkinson-bar/

# Autonomous vehicle with automatic lane following

Northern Illinois University

Antaruo Mama, Liam Soroghan

***Abstract*—The objective of this project is to design and produce a scaled vehicle that can automatically detect lanes, follow the lanes that are detected, and avoid obstacles impeding the vehicles path. The components of this vehicle included on the platforms allow the vehicle to perform as described above. These main components include an RPlidar, along with multiple cameras (Intel Realsense D435 and Intel Realsense T265) and finally the Nvidia Jetson Xavier. The RPlidar will be used to measure range by sending light in form of a laser while the two cameras are for vision. The D435 is used for RGB and depth sensing while the T265 is used for tracking. The Jetson Xavier is used as a mini-Linux computer that connects the programming to the connected sensors.**

## I. INTRODUCTION

This project will focus on building an autonomous vehicle with automatic lane following, lane changing, and obstacle avoidance. The objective of the project is to make a small scale self-driving vehicle that uses several sensors to drive itself by avoiding any obstacles that can be encountered on the road. The motivation behind this project is to expand on previous research and studies of autonomous vehicles on a smaller scale with lower budget. With most existing autonomous vehicle being valued at high prices, Team 59's project will help future RC autonomous vehicles to be more cost efficient. The work done on a small-scale vehicle will create an opportunity to further the university's research on autonomous vehicles as well as transfer knowledge and technology to the automotive industry.

## II. METHODOLOGY

Team 59 decided to split the project into two parts. These parts are the hardware section of the project and the electronic components, including the programming of the vehicle. The first half of the school year was dedicating to studying the problem, developing solutions and researching components of build. The second half of the school year was dedicated to completing the electronic components such as the programming and integrating all the component into the chassis build.

### *A. Hardware.*

The hardware part of project includes machined acrylic platforms, computer automated design (CAD) cases to hold the sensors, which were formed in Solidworks, and the assembly all the components. The autonomous vehicle is one-sixteenth scaled, therefore it cannot support the loads of all the components tight packed on top of the chassis. Due to this, two acrylic platforms were designed to evenly distribute the weight and raise the center of gravity of the vehicle allowing it to function properly.

The vehicle includes three different levels. The first level consists of the base of the chassis, steering components and the motor. The second level consists of a high voltage battery to power the Jetson Xavier and the attached sensors, as well as the RPliadar and the T265. The lidar is located in the front of the vehicle due to the position allowing maximum view of the surrounding area. The high voltage battery is located on the second level due to its size and weight. Finally, the T265 is located between the first and second level. This position allows a clear view of the track and allows the tracking feature of the T435 to be fully

optimized due to the full vision of the sensor. On the third and final level, we have the D435 , the Jetson Xavier and the USB hub. The position of the Jetson Xavier and the USB hub allow easy accesses to the computing components of the project. At the top of the vehicle, adjustments to the program or anywiring issues can be easily located and fixed. The Intel Realsense D435 is located at in the front of the third level and just above the RPlidar. This positions allows for easy angle adjustment if needed and allows the sensor to see a board display of the surrounding area with no impleaded view.

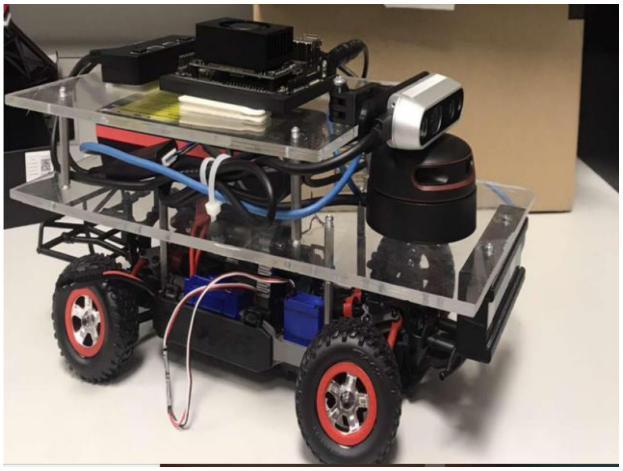

### B. *Programming*

For the programming aspect of this project, Dr Hassan Ferdowsi referred us to multiple sources including F1tenth.org and JetsonHacks.com. In these websites, the steps to achieving an autonomous vehicle are laid out in step by step instruction. In this code, the D435 will send snapshot of its vision and will be analyzed to find the lanes that the vehicle will need to stay within, as the images change and the lanes begin to move, the vehicle will adjust and stay within the visible lanes. Along with this, the D435 will work with the RPlidar to detect oncoming obstacles impeding the vehicles path. The use of the depth sense function on the D435 and the RPlidar will display a depth field view of the upcoming surroundings. As objects begin to approach the vehicle, the sensors will detect this and allow the vehicle to switch lanes. Finally, the T265 will allow the path of the vehicle to be tracked, keeping the information of the obstacles that are in the way.

## III Results

After the loss of a group member due to him dropping out of the university, Dr. Hassan Ferdowsi allowed us to use only the D435 and the T265 sensors due the increase in workload on the remaining members. With this change in in the project, Team 59 successfully used the Jetson Xavier to program both Intel Realsense cameras and write a feedback loop program that allowed these sensors to receive the intended data and give that data to the Jetson Xavier. With the known data constantly changing, the vehicle was able to move lanes and avoid obstacles.

## IV . CONCLUSION

While researching and developing new information on this project, Team 59 was able to expand on the project statement, background ideas, and purpose of the project, which is to create an autonomous vehicle that can change, follow the lane, detect obstacles in front of the car and on the side the car, and automatically change lanes.

The Team was a little behind because of a teammate that dropped out mid semester, but the team is going to complete the project as intended by the client, Dr. Hassan Ferdowsi. The final specification from the client that will allow us to complete the project are completing the hardware parts and implementing a code that will manually move the car.

**Acknowledgement:**

Team 59 would like to Acknowledge Ian Gilmour, Dr Hassan Ferdowsi with all their support and time they dedicated to team 59. Team 59 will also want to thank Dr Peterson, Justina and all the senior design faculty members for their guidance throughout the semesters.

# Low Friction Feeder of Enhanced Specular Reflector Material for CMS Detector

*Anthony Antoine, Brandyn Jay, Joshua Song*
Mechanical Engineering Department
NIU College of Engineering and Engineering Technology
DeKalb, IL, USA

***Abstract* — With significant advancements in the field of particle physics, continuous upgrades to the sensors and machines used are necessary. One of those upgrades is the manufacturing of scintillator tiles for the CMS detector, which requires the punching and folding of 3M enhanced specular reflector (ESR) material. Feeding the material into the die punch manually for thousands of tiles can prove to be a daunting, time consuming task. Significant automation of the task can realize cost savings in both time value and reduction of waste material. A machine was designed to transport strips of the ESR material into the die punch, all the while taking into consideration issues with strips sticking together, strips being scratched during transportation, and strips being damaged by folding/bending/creasing.**

***Keywords – Scintillator, pick and place, suction, conveyor***

## I. INTRODUCTION *(HEADING 1)*

Scintillator tiles are small plastic tiles that, when particles are passed through, produce light. The light produced can then be measured to investigate properties of the particle which passed through. These tiles are wrapped in a reflective material (ESR) that helps to contain all the produced light so that measurement of the light is both easier and more accurate [2].

These scintillator tiles are used in the Compact Muon Solenoid (CMS) calorimeter at CERN to measure the trajectory of high energy particles immediately following an extremely high velocity collision between two particles in the large hadron collider (LHC) [1].

The ESR material, produced by 3M, has a nominal reflectance of greater than 98.5 percent. To maintain this level of reflectance, great care needs to be taken in handling the ESR material, including the avoidance of abrasion, creasing, and dirt or oil getting onto the material.

The vendor of this ESR material, 3M, changed from manufacturing rolls of the material to manufacturing only sheets of the material. This meant that to feed the die punch, a mechanism for selecting single, thin layers of material and feeding those thin sheets into the die punch needed to be designed.

## II. MATERIALS AND METHODS

### A. *Design Requirements*

A comprehensive list of requirements for the design was crafted early in the process. First, the product must be able to feed ESR strips into the die punch without damage to the strips. This is a basic requirement that shaped much of the final mechanism design. Second, the product must be able to feed the product with little to no input by an operator, who would remain nearby for observation and reloading of the machine but would not be continually feeding the machine. This also shaped much of the mechanism design. Third, the machine must be able to feed at a sufficiently fast rate such that the die punch and folding portions would not be waiting on the feeder, which quantitatively means approximately 1 die punch per every 5 seconds. The last primary requirement for the machine was full integration into the existing die punch and folder both mechanically and electronically.

### B. *Mechanism Design*

A review of existing products used for feeding materials into another machine, especially materials that are thin or delicate, was done. A patent was found for a suction-based pick-and-place machine used for processing and transferring a thin film material [3]. Other mechanisms that used the idea of a firearm magazine-like holding devices for feeding were considered, but ultimately inspiration was taken from the suction-based design due to the performance gains in reduction of damage, reduction of operator input requirements, and the ability to still feed at a sufficiently fast rate. In addition to the suction-based design, a conveyor was needed for fully feeding the material into the die punch. After cost considerations, a belt conveyor was chosen over a roller-based conveyor. A pinch roll mechanism was added at the end of the conveyor for tight control of the linear feeding of the ESR strips.

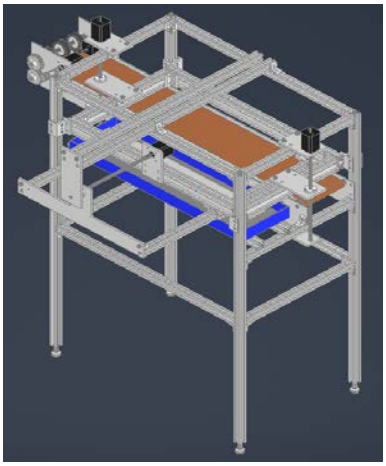

**Figure 1: Suction-Based Feeder with Belt Conveyor**

### C. Controls and Electrical Design

Failure points and safety need to be taken into consideration for all designed mechanisms. The suction mechanism is prone to failing if a sheet fails to be picked up by the vacuum cups for a variety of reasons, such as significant dust being introduced, failure of vacuum system, etc. For this reason, an infrared proximity sensor is used for detecting if a strip has been picked up from the strip holder, so that the system may return to the sheet stack and attempt to pick up a sheet once more. The conveyance system is also prone to potential failure if a sheet is somehow jammed and is not being fed into the die punch. To avoid this problem, another infrared sensor is included to detect the feeding of the sheets into the die punch.

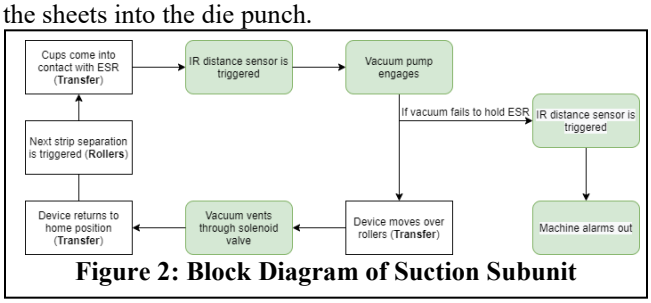


**Figure 2: Block Diagram of Suction Subunit**

During controls design, both a CNC and an Arduino-controlled system were considered. The Arduino was chosen for a few reasons. First, it is cheap, simple, and has existing libraries for driving steppers, reading sensors, and other various functions. Second, Arduino has been proven to be robust in not only fabrication of prototypes, but also basic, fully functional machines. Lastly, it was chosen due to its compact size and easy of mounting.

### D. Materials

To accomplish a sufficiently high rate of feed speed while simultaneously focusing on reduction of cost, aluminum was used in much of the machine. This choice was combined with NEMA 17 stepper motors with a holding torque of 65 N.cm. It was used for the entirety of the lifting and translation systems, as well as all portions of the suction system where possible. The frame and support structures for all systems were built out of 1" square extruded aluminum profiles. This material was chosen primarily for its ease of use and significant strength. Aluminum plates were used for the lead screw translation system, along with steel lead screws and bronze bushings for all rotating components.

The suction system requires a delicate touch. To achieve this, silicone vacuum cups with bellows that allow easier compression of the cup were chosen. These vacuum cups are often used in the food industry for picking up items with variable height. This is beneficial for this machine, considering the strip holding device will be slowly depleted of strips, meaning there will be variable height product to be moved.

For the conveyance system, a neoprene belt was chosen to avoid scratching, and soft neoprene-coated rollers were chosen for the pinch rolls, to reduce scratching and increase grip on the strips. To avoid significant wear on the rotating shafts, bronze oilite bushings were chosen due to the low rotational velocity and low load required. The pinch roll drive was managed using a set of steel gears, chosen primarily for longevity with low wear.

### E. Manufacturing Methods

Fabrication processes for this machine were straightforward. The production of the entire frame was done with the use of a simple bandsaw, due to the choice of extruded aluminum bars as the frame. Production for all aluminum plates was done using a waterjet cutter as well as drills and reams for any holes with tighter tolerances, such as those that held bronze bushings for rotating shafts. The production of all other parts that required any significant amount of machining were done using CNC mills as well as CNC lathes. Lathes were used to manufacture the rolls for the conveyor, for example, and mills were used for production of take-up bushings for the conveyor. Some fused deposition modeling additive manufacturing was used to fabricate small mounts for sensors, controllers, and other electronic equipment as well.

## III. Conclusion

In summary, creating a machine which aids in the automatic die punching of thin, delicate sheets requires careful systems design and proper integration of a variety of devices from multiple manufacturers into a cohesive machine. The full system consisted of devices such as stepper motors, infrared sensors, vacuum solenoids, vacuum cups, conveyor belts, and multiple other mechanical as well as electrical components requiring careful selection and integration into the machine.

With this design in use, all design requirements can be met, including a sufficiently fast feed rate that will not allow backing up of the machines downstream of the feeder, minimal input by an operator, and delicate handling of the strips to avoid damage to them.

## Acknowledgment

We would like to acknowledge the help of and express our gratitude toward Dr. Nicholas Pohlman, Dr. Iman Salehinia, Gerald Smith, Mike Reynolds, NIU Physics Dept., NIU College of Engineering and Engineering Technology, and F.N. Smith Corp. for all help in designing, manufacturing, testing, and funding required for the completion of this project.

## References

[1] "The CMS Detector Uses a Huge Solenoid Magnet to Bend the Paths of Particles from Collisions in the LHC." *CERN - Accelerating Science*, CERN, home.cern/science/experiments/cms.

[2] Chadeeva, M, et al. "Tests of Scintillator Tiles for the Technological Prototype of Highly Granular Hadron Calorimeter." *KnE Energy*, vol. 3, no. 1, 2018, p. 363., doi:10.18502/ken.v3i1.1768.

[3] Kumakura, K. "Film Suction Mechanism." U.S. Patent 9,808,937, issued April 29th, 2015

# *Development of a Heart Rate Monitoring System (Part II)*

Teef Alobaidan, Zachary Wagner, Jonathan Schrum, Jordan Drumgoole
Z1880321@students.niu.edu, Z1879445@students.niu.edu, Z1805114@students.niu.edu, Z1814460@students.niu.edu
Mechanical Engineering1, Electrical Engineering
Northern Illinois University
DeKalb, IL

***Abstract*—The respective Heart Rate Monitoring System is engineered to detect fear and anxiety levels in students undergoing engineering related activities. Dr. Pi-Sui Hsu is a staff member of Northern Illinois University's College of Education Program. Because anxiety toward math and science courses is prevalent, Dr. Hsu is conducting a study that will track these anxiety levels. The Heart Rate Monitoring System was carefully designed following each need and constraint from the client. This device uses a photodiode and LEDs to send a pulse signal to an Arduino. The signal is converted to a beats per minute (BPM) value and that data is sent wirelessly to an external computer in an excel file.**

## *I.* INTRODUCTION *(HEADING 1)*

School related anxiety is a growing pandemic for many young students. It is even more common when it comes to math and science related courses. Stress and anxiety are physical reactions that can be measured by a spike in one's heart rate. There are thousands of heart rate monitors on the market that can track heart rate, but most are extremely expensive or do not have the ability to transfer data to a computer for the sake of observing it. The main objective of this project was to design a heart rate monitoring device that was inexpensive and also capable of transferring its data in the form of an excel file to an external device. This data shows the user's beats per minute (BPM) in 15 second intervals. This data format is suitable for this setting because any spike in the data would be indicative of feelings of stress in the user.

The client of this project is Dr. Pi-Sui Hsu who is an associate professor for Northern Illinois University's College of Education. Dr. Hsu conducts an after-school program for middle school students that focuses on science and engineering. With years of experience, Hsu is well aware of the widespread anxiety students face when undergoing science and engineering related activities in school. As a result, she has been monitoring her student's heart rate during class with a product called Biodot. This product, which is worn around the user's wrist, is designed to measure the stress level of the wearer. Although inexpensive, this device gives feedback in the form of 3 different colors where the darker the color, the more stress the user is experiencing. It may give a general idea however; this is not a measurable amount and is therefore not appropriate for research. A better solution would be a heart rate monitor that gave numerical data which could also be transferred to a computer such that the data can be stored and analyzed. Additionally, having the ability to observe the user's heart rates as the activities are being held would be of importance because Dr. Hsu would be notified of a student's anxiety as it is happening.

With thousands of heart rate monitors on the market, there are many similar products to this one. The T31C Heart Rate Sensor created by Polar is relatively inexpensive and can transfer its data wirelessly [1]. Unfortunately, this data is sent to a very specific smartphone application and cannot be transferred or edited. One product that does transfer universal data to a computer is the Scosche Rythym24. This product, which uses the same sensors as the proposed design, has the same functions and even more [2]. Unfortunately, it is 3 times the cost as our design. The market offers many variations of heart rate monitors, but none that give live and editable data at a low cost.

## II. METHODS AND MATERIALS

Mainly, there are 4 methods to measure heartbeat rate which are, electrocardiogram, photoelectric pulse wave, blood pressure measurement, and phonocardiography [4]. The photoelectric pulse wave method is used for this project where infrared light (LED) emits through the skin, and the photodiode sense the reflected light from the body. The photodiode, then, sends the data to the Arduino to analyze the change in the blood volume based on the reflected light, measured by the photodiode, to determine the pulse rate and then it calculates the heartbeat rate per minute.

Below in Figure 1, is the schematic showing all the components and how they are connected. As shown, the heart rate monitoring device contains an Arduino Nano, IR LEDs, a Photodiode, a BTBEE Bluetooth Transmitter, and a Rechargeable Battery.

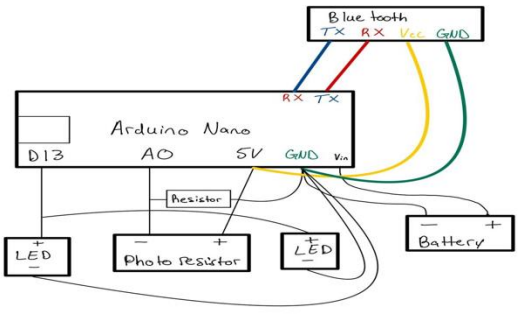


Figure 1: Heart Rate Monitoring Device Schematic

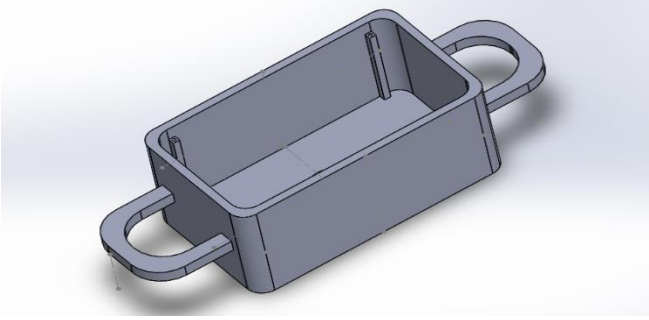

Figure 2: Housing Box

## III. Results and Discussion

Below in Figure 2, a waveform is shown. This wave was a result of the LEDs and photodiode working together to gain a signal from the user's pulse. By dividing the Samples by 100Hz, the duration in seconds is obtained. This is converted into duration in minutes by simply dividing by 60. From here, the beat count can be divided by the duration in minutes to obtain a beats per minute (BPM) value.

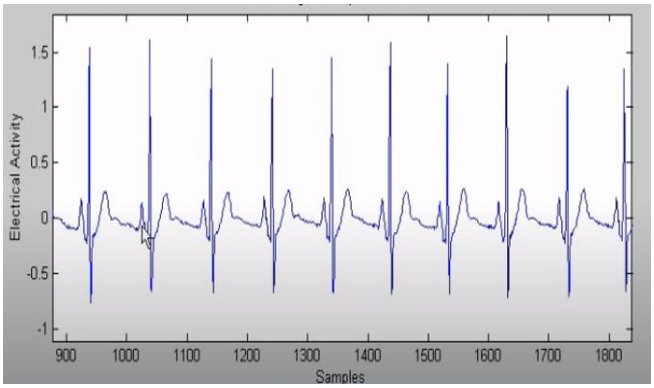


Figure 3: Pulse Waveform

All this is processed through the Arduino such that a BPM value is given every 15 seconds. With the aid of the BTBEE Bluetooth Transmitter, this data is transferred in live time to an excel file on a separate computer. Figure 3 shows an example of this.

| | A | B | C |
|---|---|---|---|
| 1 | Date | Time | BPM |
| 2 | 4/7/2021 | 4:32:07 | 84 |
| 3 | 4/7/2021 | 4:32:22 | 83 |
| 4 | 4/7/2021 | 4:32:37 | 82 |
| 5 | 4/7/2021 | 4:32:52 | 81 |
| 6 | 4/7/2021 | 4:33:07 | 81 |
| 7 | 4/7/2021 | 4:33:22 | 81 |
| 8 | 4/7/2021 | 4:33:37 | 81 |
| 9 | 4/7/2021 | 4:33:52 | 81 |
| 10 | 4/7/2021 | 4:34:07 | 80 |
| 11 | 4/7/2021 | 4:34:22 | 81 |
| 12 | 4/7/2021 | 4:34:37 | 81 |
| 13 | 4/7/2021 | 4:34:52 | 81 |
| 14 | 4/7/2021 | 4:35:07 | 82 |
| 15 | 4/7/2021 | 4:35:22 | 81 |
| 16 | 4/7/2021 | 4:35:37 | 81 |

Figure 4: BPM Data

As shown above, the user's heart rate is around a steady 81 BPM. When anxiety is induced, values will spike to around 140-180 BPM which will be obvious for the conductor to visualize [3].

## IV. Conclusion

Although the heart rate monitoring device wasn't able to be completed and tested through trials, the electronic circuit and programming have proven to have made appropriately so the device can record information through LED lights and transfer the given data to a computer via Bluetooth successfully. There have always been students who have struggled with staying calm and being patient in order to understand complicated courses like science and engineering.

*Acknowlegments*

The design team would like to thank Northern Illinois University for funding this project and giving the opportunity to be involved. Additionally, the team is very thankful for Dr. Lichuan Liu, Sandhya Chapagain, and Dr. Pi-Sui Hsu for offering support and encouragement.

## References

[1] T31C Heart Rate Sensor [online]. Available from: https://www.roguefitness.com/polar-t31c-heart-rate-sensor

[2] Scosche Rythym24 [online]. Available from: https://www.scosche.com/rhythm24-waterproof-armband-heart-rate-monitor

[3] "What's Considered a Dangerous Heart Rate?" *Healthline*, 19 Oct. 2018, https://www.healthline.com/health/dangerous-heart-rate#slow-beats

[4] Pulse sensor | Electronics Basics | ROHM. (2016). ROHM. https://www.rohm.com/electronics-basics/sensor/pulse-sensor

"Senior Design is the pinnacle learning experience of an engineering student's undergraduate education. It is a year-long process during which principles and theories gain substantive form and relevance to societal needs. Students learn and apply the principles of design; the complex interplay among engineering solutions and societal, environmental, economic, and ethical considerations; the language of industry; and the power of engineering to catalyze new solutions to entrenched problems."

**— Donald Peterson, Ph.D., Dean**


NORTHERN ILLINOIS UNIVERSITY

**College of Engineering and Engineering Technology**

590 Garden Road, DeKalb, IL 60115
815-753-1442
niu.edu/ceet
go.niu.edu/seniordesignday
ceet@niu.edu

@NIUengineering
#niuceet